Influence of Extremely-Low-Frequency Magnetic Fields on Epigenetic Programming and Cellular Differentiation

Inauguraldissertation

zur

Erlangung der Würde eines Doktors der Philosophie

vorgelegt der

Philosophisch-Naturwissenschaftlichen Fakultät

der Universität Basel

von

Melissa Manser

aus Appenzell (AI), Schweiz

Basel, 2017

Genehmigt von der Philosophisch-Naturwissenschaftlichen Fakultät
auf Antrag von

Prof. Dr. Primo Schär (Fakultätsverantwortlicher und Dissertationsleiter)
Prof. Dr. med. vet. Meike Mevissen (Korreferent)

Basel, den 18.10.2016

Prof. Dr. Jörg Schibler
Dekan der Philosophisch-Naturwissenschaftlichen Fakultät

Acknowledgments

First of all, I would like to thank Primo Schär for supervising my PhD thesis, for his guidance, contagious enthusiasm and motivating words during the whole study and for the times we had at the ARIMMORA congresses. I also thank Meike Mevissen for being part of my PhD committee and critical evaluation of my work.

Special thanks go to David Schürmann for his ongoing support and supervision of my study, his patience, readiness for help and open door policy, and all the times we had at different congresses. Additionally, I thank him for his supporting words, inputs and corrections during the ELF-MF manuscript writing and the critical reading of my thesis. I would like to thank Christoph Schmid and Mohamad Sater for performing the bioinformatic analysis of my ChIP-seq data and the times we had at the EU meetings. I thank Manuel Murbach for the maintenance of the exposure system and the ensured blinding of the exposure conditions.

I also would like to thank all the present and past members of the Schär lab for a good working atmosphere and all the nice times we had outside the lab. A special thank goes to Faiza Noreen for analysing my DNA methylation data, and to Stefan Weis, Emina Gyenge Besic and Zeinab Barekati for their support, critical reading of parts of my thesis and for being more than colleagues.

My heartfelt gratitude goes to Anna Frei, Julia Manzetti, Hannes Richter, David Berner and Petra Bernegger for their friendship and support during my entire studies. Last but not least I would like to thank my family and Fabian Dreier, for your unconditional support, for believing in me, your love and for everything you have done and still do for me.

"Nothing in life is to be feared, it is only to be understood.

Now is the time to understand more, so that we may fear less."

Marie Curie

Table of Content

1 Summary 9

2 Introduction 12

2.1 The genome and its epigenetic modifications 12

2.1.1 The genome and its organisation 12

2.1.2 Histone modifications and their regulation 16

2.1.3 DNA methylation and its regulation 19

2.1.4 Epigenetic programming during cell differentiation 23

2.2 Haematopoietic system 26

2.2.1 General overview of haematopoiesis 26

2.2.2 Neutrophils, their development and homeostasis 27

2.2.3 Epigenetics of the haematopoietic system 29

2.2.4 Leukaemia 31

2.3 Biological effects of extremely-low-frequency magnetic fields (ELF-MFs) 35

2.3.1 Basic physical background of electromagnetic fields 35

2.3.2 Association of ELF-MF exposure with the risk of childhood leukaemia 37

2.3.3 Effects of ELF-MF exposure on cell proliferation, cell cycle and cell viability 38

2.3.4 Effects of ELF-MF exposure on genomic integrity 42

2.3.5 Effects of ELF-MF exposure on cellular differentiation and development 44

3 Aims of the Thesis 46

4 Results 47

4.1 ELF-MF exposure affects robustness of epigenetic programming during granulopoiesis (Appendix I) 47

4.2 Dynamics of Histone Modifications and DNA Methylation during *in vitro* Granulopoiesis (Appendix II) 51

4.3 Extremely-Low-Frequency Magnetic Fields and Risk of Childhood Leukaemia: A Risk Assessment by the ARIMMORA Consortium (Appendix III) 55

4.4 Supplementary Results 58

4.4.1 ELF-MF exposure does not influence cell viability and cell cycle distribution in the leukaemic cell line REH 58

5 Concluding Discussion and Outlook 61

6 References 67

7 Appendix 81

Appendix

I. ELF-MF exposure affects the robustness of epigenetic programming during granulopoiesis

II. Dynamics of Histone Modifications and DNA Methylation during *in vitro* Granulopoiesis

III. Extremely Low-Frequency Magnetic Fields and Risk of Childhood Leukemia: A Risk Assessment by the ARIMMORA Consortium

Abbreviations

5caC	5-carboxylcytosine
5fC	5-formylcytosine
5hmC	5-hydroxymethylcytosine
5mC	5-methylacytosine
A	adenine
AC	alternating current
AID	activation-induced-deaminase
ALL	acute lymphocytic leukaemia
AML	acute myeloid leukaemia
ARIMMORA	Advanced Research on Interaction Mechanism of electromagnetic exposure with Organism for Risk Assessment
BER	base excision repair
C	cytosine
CD	cluster of differentiation
ChIP	chromatin immunoprecipitation
ChIP-seq	chromatin immunoprecipitation followed by next-generation sequencing
CLL	chronic lymphocytic leukaemia
CML	chronic myeloid leukaemia
CMP	common myeloid progenitor
CpG	cytosine-guanine
DC	direct current
DNA	deoxyribonucleic acid
DNMTs	DNA methyltransferases
ELF-MFs	extremely low frequency magnetic fields
EMFs	electromagnetic fields
ESCs	embryonic stem cells
FLT3	FMS-like tyrosine kinase 3
G phase	growth phase
G	guanine
G-CSF	granulocyte-colony stimulating factor
GMP	granulocyte-macrophage progenitor
H	histone
H3K27ac	histone 3 lysine 27 acetylation

H3K27me3	histone 3 lysine 27 trimethylation
H3K4me1	histone 3 lysine 4 monomethylation
H3K4me2	histone 3 lysine 4 dimethylation
H3K4me3	histone 3 lysine 4 trimethylation
H3K9me3	histone 3 lysine 9 trimethylation
HATs	histone acetyl-transferases
HDACs	histone deacetylases
HOX	homeobox
HSCs	haematopoietic stem cells
Hz	Hertz
IARC	International Agency for Research on Cancer
IL	Interleukin
K	lysine
KDMs	lysine demethylases
KMTs	lysine methyltransferases
M phase	mitotic phase
me1	monomethyl
me2	dimethyl
me3	trimethyl
MF	magnetic field
MLL	mixed lineage leukaemia
MLP	multipotent lymphoid progenitor
MPPs	Multipotent progenitors
PcG	polycomb-group
PGCs	primordial germ cells
PRCs	polycomb repressive complexes
R	arginine
S phase	synthesis phase
SAM	S-adenosylmethionine
T	Tesla
T	thymine
TDG	thymine DNA glycosylase
TET	ten-eleven translocation
trxG	trithorax-group
TSA	trichostatin A

1 Summary

Cellular homeostasis and function, including the controlled interaction with the environment, not only depends on the genetic code but also and primarily on the epigenetic information contained in histone tail modifications and DNA methylation. Histone modifications are most prominently acetylation or methylation of specific residues in the histone tails whereas cytosine on the DNA can be methylated to form 5-methylcytosine (5mC) (Bernstein et al., 2007; Kouzarides, 2007; Nicholson et al., 2015). Virtually all cells from a multicellular organism contain the same genetic code; the epigenetic system shapes the nuclear organisation of chromatin and DNA accessibility, determining gene expression programs in development to facilitate lineage commitment into specific tissue types. Thereby, patterns of epigenetic modifications change dramatically as cells undergo functional and morphological determination during differentiation and de-differentiation, including cancerous transformation (Bernstein et al., 2007; Cedar and Bergman, 2011; Dambacher et al., 2013). Genetic mutations as well as aberrations of epigenetic modifications are hallmarks of cancer, but may also be the driving force of cancerogenesis. Acute leukaemia is characterised by high abundance of progenitor cells and they often have alterations in genes encoding epigenetic modifiers (Greenblatt and Nimer, 2014; Ntziachristos et al., 2013). Hence, mutations in epigenetic modifiers in leukaemia and the blocked differentiation of progenitor cells may indicate a defect in the epigenetic control of differentiation. Additionally, epigenetic programming in differentiating cells is sensitive to disturbance by environmental factors (Feil and Fraga, 2011; Jaenisch and Bird, 2003; Mitchell et al., 2016). Extremely-low-frequency electromagnetic fields (ELF-MFs) have been considered as one of these environmental factors, caused by modern life style. The ever increasing use of electronic appliances generating electromagnetic fields in the ELF-MF range of 50 Hz has raised concerns regarding potential risks for human health. Due to epidemiological studies, indicating a correlation of ELF-MF exposure with an increased risk for childhood leukaemia, ELF-MF was evaluated as being possibly carcinogenic to humans (group 2B) by the International Agency for Research on Cancer (IARC) (IARC, 2002). However, the molecular mechanisms underlying this correlation have remained elusive. The energy transmitted by ELF-MF is not sufficient to directly damage DNA (Adair, 1998) and thereby unlikely to induce cancer-promoting mutations, but whether or not it has the potential to influence the epigenetic program of genomes has not been systematically addressed. The aim of my PhD thesis was to evaluate the influence of ELF-MF on the epigenetic code as a potential molecular explanation of the implicated leukaemogenic activity. Therefore, we analysed ELF-MF effects on the epigenetic stability in leukaemic cells and on the epigenetic reprogramming during an *in vitro* haematopoietic differentiation into the neutrophilic lineage. Additionally, I investigated the

epigenetic dynamics of histone modifications and DNA methylation during neutrophilic granulopoiesis in a second part.

Previous studies indicated a certain genotoxic potential of ELF-MF exposure (Duan et al., 2015; Focke et al., 2010; Mihai et al., 2014; Vijayalaxmi and Prihoda, 2009), although the energy content of ELF-MF is not high enough to induce structural damage to DNA. It is possible, however, that secondary effects such as changes in cell proliferation, cell cycle progression or apoptosis can account for the low levels of DNA breaks observed (Focke et al., 2010; Kim et al., 2010). On the other hand, the second layer of information superposed to the basic DNA sequence, the epigenetic code, has been hardly assessed with respect to ELF-MF exposure. There are a few studies indicating that the epigenome can be modified by ELF-MF exposure (Baek et al., 2014; Liu et al., 2015), but the potential of ELF-MF exposure to destabilize epigenetic modifications in general and in a cancer-relevant manner in particular has not been addressed systematically. We examined the influence of ELF-MF exposure on the chromatin landscape of the leukaemic Jurkat cell line by analysing the alterations of histone modifications. Furthermore, we studied the impact of ELF-MF exposure on the dynamics of histone modifications and DNA methylation during the epigenetic programming of human cord blood stem cells, differentiating into the neutrophilic lineage. We generated genomic profiles of the activating histone mark H3K4me2 and the repressive histone mark H3K27me3 as well as of DNA cytosine methylation. We report that ELF-MF exposure has no significant and consistent influence on epigenetic modifications in differentiated leukaemic cells as well as during haematopoietic differentiation. However, our data showed a consistent effect of ELF-MF exposure on the reproducibility of these histone and DNA modification profiles, indicating that ELF-MF may influence the robustness of histone modifications and DNA methylation most pronounced in the course of global reorganization of chromatin in the neutrophilic differentiation process. Moreover, our results indicate that ELF-MF exposure may stabilize the epigenetic features that are associated with open chromatin during differentiation as regions marked by H3K4me2, losing H3K27me3 or CpG demethylation. Our data suggest a stochastic effect of ELF-MF exposure on the chromatin landscape of individual cells.

Acute myeloid leukaemia (AML) is the most common leukaemia in adults (80%). It is characterized by high accumulation of progenitor stages mainly neutrophilic progenitors and alterations in modifiers of epigenetic modifications (Greenblatt and Nimer, 2014; Seiter, 2016; Zenhäusern et al., 2003). To understand the potential contribution of aberrant epigenetic programming in differentiation to carcinogenesis, it is important to understand the physiological epigenetic pattern established during the differentiation process. As the dynamic epigenetic programming during human neutrophilic granulopoiesis has not been addressed systematically, we investigated the reorganization of histone

modifications (H3K4me2 and H3K27me3) and DNA cytosine methylation during *in vitro* neutrophilic granulopoiesis at genome scale. The results show a fundamental reorganisation of the chromatin landscape most pronounced at lineage commitment at the transition of human cord blood stem cells into the neutrophilic lineage, shaping an overall more compact chromatin. We observed that epigenetic repression of pluripotency and developmental genes with a poised chromatin state in human cord blood stem cells occurred through a gain of H3K27me3 alone or with concomitant *de novo* DNA methylation, but rarely with DNA methylation alone. By contrast, our data indicate that epigenetic activation of neutrophil-specific genes preferentially appeared through DNA demethylation without simultaneous alterations in histone modifications. Our data suggest a specific regulatory role of DNA demethylation in lineage restriction of neutrophils.

This work was part of the European Commission funded project "Advanced Research on Interaction Mechanisms of electromagnetic exposure with Organisms for Risk Assessment" (ARIMMORA), evaluating possible pathways to explain the association between ELF-MF exposure and childhood leukaemia. I contributed to the final risk assessment applying an IARC Monograph evaluation scheme to hazard identification of ELF-MF. The ARIMMORA consortium concluded that the relationship between ELF-MF and childhood leukaemia remains consistent with the classification by IARC that ELF-MFs are possibly carcinogenic to humans (Group 2B). The risk assessment was published in a peer-reviewed comment (Schuz et al., 2016).

Taken together, in collaboration with others, I was able to elucidate and describe alterations of epigenetic modifications during an *in vitro* differentiation and induced by an environmental factor. As a proof-of-concept, I showed that ELF-MF, as an environmental factor, is able to influence the epigenetic code of histone modifications and DNA methylation. ELF-MF effects are subtle and stochastic rather than deterministic; the analysis of epigenetic patterns in cell populations showed altered reproducibility between replicate samples. These effects suggest that ELF-MF affects the robustness of epigenetic reprogramming by stabilizing epigenetic modifications associated with open chromatin. These observations will support further mechanistic studies analysing the contribution of ELF-MF exposure to cancerogenesis. Additionally, my data of the epigenetic programming during neutrophilic granulopoiesis provided novel insights into the regulatory role of DNA methylation and histone modifications in lineage restriction and cell plasticity, revealing a specific epigenetic pattern for activated and repressed genes during differentiation. These data may support further studies investigating chromatin epigenetic regulators as targets for leukaemia induced differentiation therapy.

2 Introduction

2.1 The genome and its epigenetic modifications

The genome and its genetic code are identical in virtually all cells of human body and stored in the DNA. The epigenetic code of each cell, however, can differ, contributing to distinct cell type-specific gene expression programs. The epigenome contains modifications of histone tails (e.g. acetylation or methylation) and DNA methylation of cytosine residues generating 5-methylcytosine (5mC) (Bernstein et al., 2007). Epigenetic features, once established, are relatively stable maintained, yet, they are flexible and capable to adapt to changing developmental or environmental conditions, resulting in reorganisation of the chromatin structure and DNA accessibility. Different enzymes are involved in the regulation of epigenetic modifications; they establish (writers), remove (erasers) or interpret and bind (readers) histone modifications or DNA methylation (Nicholson et al., 2015; Shen and Laird, 2013). The pattern of epigenetic modifications changes dramatically as cells undergo differentiation, establishing mainly three main classes of transcriptionally relevant chromatin states: transcriptionally active, repressed or poised chromatin. Active chromatin comprising highly expressed genes is occupied by histone 3 lysine 4 trimethylation (H3K4me3), histone 3 lysine 27 acetylation (H3K27ac) and non-methylated cytosine, whereas chromatin correlating with gene repression is characterized by trimethylated histone 3 lysine 27 (H3K27me3) and histone 3 lysine 9 trimethylation (H3K9me3) as well as 5mC. Transcriptionally poised chromatin is occupied by active as well as repressive epigenetic features including H3K4 di- and trimethylation and H3K27me3 modifications, and is preferentially located at developmental genes in stem cells (Boland et al., 2014). Thus, the epigenome represents a second dimension of genomic information, controlling a cell type-specific gene expression. Alterations in the epigenome are hallmarks of cancer (You and Jones, 2012) and may also be a driving force for cancerogenesis. The following chapters will introduce the genome and its epigenetic modifications

2.1.1 The genome and its organisation

Deoxyribonucleic acid (DNA) is the carrier of genetic information, which is transferred to each daughter cell and encodes the building blocks of all organisms. The DNA contains coding regions transcribed in mRNA and further translated into proteins fulfilling their function in each cell, but as well non-coding regions, including regulatory elements (e.g. promoter, enhancer), introns or repeat sequences. The DNA consists of four different nucleotides including a purine base adenine (A), guanine (G) or a pyrimidine base cytosine (C) or thymine (T) as well as a sugar-phosphate group. The

sequential arrangements of these four nucleotides build the genetic code. Methylation of cytosine at the C5 position (5-methylcytosine, 5mC), generating a fifth DNA base, adds an additional gene regulatory layer onto the DNA sequence, without changing the coding property. Two antiparallel DNA strands are built of nucleotides connected by the sugar-phosphate backbone that are complementary of each other and linked by hydrogen bonds according to the Watson-Crick base pairing model, connecting adenine to thymine and guanine to cytosine forming a right handed double-helical structure. The DNA structure facilitates replication, continued gene expression and packaging (Shabalina and Spiridonov, 2004; Travers and Muskhelishvili, 2015; Watson and Crick, 1953).

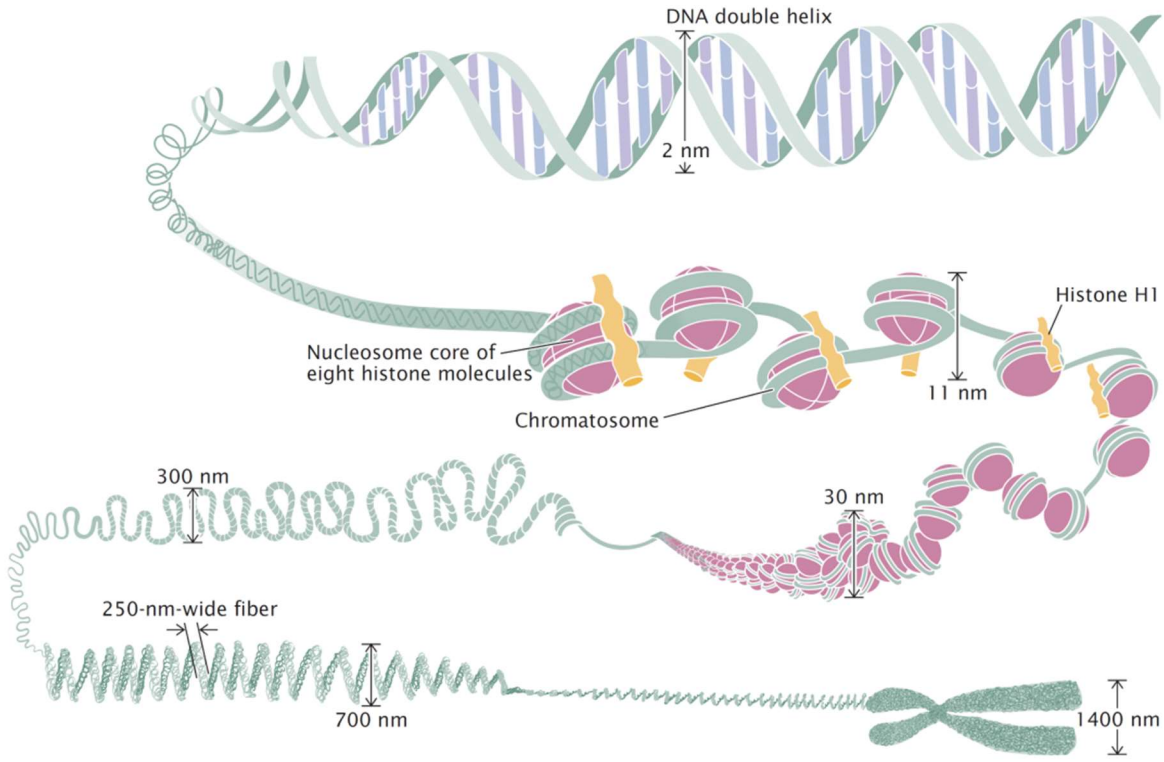

Figure 1: **DNA condensation into chromatin structures**. DNA double helix is wrapped around histones to form nucleosomes further compacted into chromatin fibers and coiled into chromatid of chromosome (adapted from Pierce, 2012).

Each cell of the human body has about 2 meters of DNA inside the nucleus, which is approximately 10 µm in diameter. Several steps of compaction are necessary to fit this amount of DNA inside this tiny space; still keeping it accessible for reading the genetic code (Figure 1). In total, the human genome is packed in 46 chromosomes. The primary structure of DNA is organized in nucleosomes where about 147 bp of the negatively charged DNA is wrapped 1.7 times around a core histone (H) octamer. These histone octamers consist of two H3-H4 and two H2A-H2B histone dimers. Nucleosome core particles are connected together by linker DNA (20 – 80 bp) forming a linear array

of repetitive 200 bp elements, also known as the 10 nm fiber, originally named 'beads on a string'. The linker DNA is occupied by the histone protein H1 (Maeshima et al., 2014). The 10 nm fiber, also bound by various non-histone proteins, forms the chromatin. The next compaction step is a 30 nm chromatin fiber, as indicated by *in vitro* studies from isolated nucleosomes, were the nucleosomes are folded in a higher order helical fiber in a solenoid or a zig-zag way (Finch and Klug, 1976; Woodcock et al., 1984). Beside these two favoured models, other ways of chromatin compactions in 30 nm fibers were suggested, but the precise structure of these fibers still remains elusive. However, recent *in vivo* studies using the chromosome conformation capture method do not support the existence of a stable 30 nm fiber in interphase cells, rather suggesting a more dynamic, highly disordered, interlinked chromatin state (Nishino et al., 2012). The chromatin fiber is further folded to finally form mitotic chromosomes from large interphase chromatin fibers (Hubner et al., 2013; Maeshima et al., 2010; Maeshima et al., 2016).

Chromatin state	H3K4me2/3	H3K27me3	H3K9me3	Transcription
Euchromatin	+	-	-	active
Euchromatin	+	+	-	poised
Facultative heterochromatin	-	+	+/-	silenced
Constitutive heterochromatin	-	-	+	permanently silenced

Table 1: Transcriptional activity of euchromatin and heterochromatin occupied by the histone modifications H3K4me2/3, H3K27me3 or H3K9me3.

Eukaryotic chromatin is not equally distributed in the nucleus; there are more compacted regions (heterochromatin) and open regions (euchromatin), inaccessible and accessible for transcription, respectively (Table 1). The compact heterochromatin comprising inactive genes is preferentially located at the nuclear periphery associated with the nuclear lamina. Two different heterochromatic regions are known: facultative and constitutive heterochromatin. Genes that become silent during development and differentiation are located in facultative heterochromatic regions and they are mainly occupied by H3K27me3 and H3K9me3 modifications (e.g. the X chromosome inactivation within mammalian female cells). Constitutive heterochromatin contains permanently silenced genes mainly occupied by H3K9me3 modifications and is mostly associated with centromeric and telomeric regions. By contrast, euchromatin regions are relaxed open environments that carry most of the active genes, undergo cyclic relaxation during cell cycle allowing transcription and fill the internal nucleoplasm. Regions of euchromatin are characterized by different compositions of histone modifications. Active enhancers are occupied by H3K4 monomethylation (H3K4me1) whereas active genes harbour H3K4me2/3 marks on their promoter (for more details on histone modifications see

2.1.2). Additionally, regions of euchromatin can be transcriptionally poised by co-occupancy of active and repressive histone marks H3K4me2/3 and H3K27me3, respectively, and they are located preferentially at developmental genes in stem cells (Boland et al., 2014). Regions in the chromatin, which are separating heterochromatin from euchromatin, are bound by specific 'boundary elements' like the insulator binding protein CTCF, preventing spreading of heterochromatin into neighbouring euchromatic regions (Bannister and Kouzarides, 2011; Felsenfeld and Groudine, 2003; Kouzarides, 2007; Pueschel et al., 2016).

Several processes such as DNA replication, DNA repair, and activation or silencing of transcription involve alterations of chromatin structures. In principle, there are three ways to change the chromatin organisation: (i) with the help of chromatin remodelling complexes, (ii) through exchange of core histones with histone variants and (iii) through alterations of epigenetic modifications. For instance to initiate transcription, specific transcription factors have to bind to their target sequence on the DNA. However, if the region is occupied by nucleosomes, transcription factors recruit chromatin-remodelling complexes to the DNA. They move the histone core complexes in a ATP-dependent manner over a short distance without disturbing the general chromatin structure, allowing the transcription factor to bind the DNA (Felsenfeld and Groudine, 2003). Additionally, core histones can be replaced by histone variants. For instance, an important histone variant of H2A is H2AX that has an important role in the DNA damage response as it gets phosphorylated following DNA repair. Moreover, histone variants of H3 are H3.3 and H3.2, where H3.3 was found to be associated with active chromatin, whereas H3.2 correlates with a repressive chromatin state (Hake and Allis, 2006; Kraushaar and Zhao, 2013; Snyers et al., 2014). The third way to induce chromatin reorganisation is through epigenetic modifications contained in histone modifications and DNA methylation (Figure 2). These epigenetic modifications shape the chromatin landscape and DNA accessibility by affecting directly the nucleosome structure, introducing chemical groups recognised by regulatory proteins or by disrupting directly the higher chromatin organisation (Felsenfeld and Groudine, 2003). Acetylation and methylation of specific residues in the histone tails are the most prominent histone modifications whereas the epigenetic modifications of DNA comprises methylated cytosine (5mC) mainly in a cytosine-guanine (CpG) context (Bernstein et al., 2007; Nicholson et al., 2015). In mammals, around 50% of all genes are transcriptionally repressed in a cell type-specific manner by epigenetic mechanism to assure heritability without changes of the DNA sequence (Cedar and Bergman, 2011; Sashida and Iwama, 2012). Therefore, epigenetic information undergoes fundamental changes during cellular differentiation, resulting in silencing of pluripotency genes through H3K27me3, H3K9me3 and stabilised by DNA methylation (5mC), and activation of lineage-specific genes through H3K4me3, leading to a cell type-specific gene expression pattern (Bernstein et

al., 2007). Dynamic epigenetic programming in differentiating cells is sensitive to disturbance by environmental factors. Several studies indicated that epigenetic features, particularly DNA methylation, can be altered through exposure to environmental factors (e.g. Aspirin, endocrine disruptive chemicals) (Damdimopoulou et al., 2012; Feil and Fraga, 2011; Noreen et al., 2014).

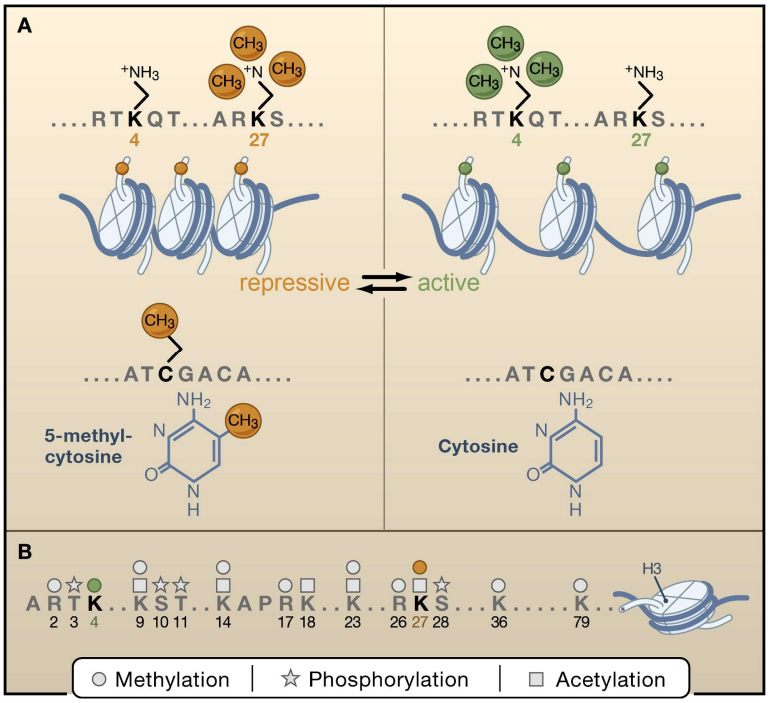

Figure 2: Cytosine methylation and histone modifications in mammals are part of the epigenetic code. (A) Methylation of the lysine at the fourth position (K4) of the N-terminal tail of histone H3 is associated with active genes (green), whereas H3K27 methylation is present in transcriptionally silenced regions (orange). In CpG rich regions, methylation of cytosine at the C5 position (5-methylcytosine, 5mC) is present in repressed regions, whereas non-methylated cytosine is enriched in transcriptionally active regions. (B) The N-terminal of histone H3 is subject to various post-translational modifications as methylations, phosphorylations and acetylations (adapted from Bernstein et al., 2007).

2.1.2 Histone modifications and their regulation

Important features of the epigenome are histone modifications of the amino-terminal histone tails as well as the octamer core histone body. More than 100 distinct posttranslational modifications of histones are known, including acetylation, methylation, phosphorylation, ubiquitination, sumoylation, ADP-ribosylation and deamination, mainly occurring at the histone tails of the four histone subunits (H2A, H2B, H3 and H4). The biological function of some of these modifications such as acetylation and methylation is well described. However, the role of other modifications is less clear (Bannister and Kouzarides, 2011; Bernstein et al., 2007; Kouzarides, 2007). Histone modifications can be dynamic, appearing and disappearing within minutes of external stimuli (Anink-

Groenen et al., 2014; Meagher, 2014; Waterborg, 2002), allowing for a rapid change of the epigenetic information. Two main functions of histone modifications are known; they can impact the setting up of the global chromatin organisation by altering the charge of the histone tail resulting in the separation into heterochromatin and euchromatin and, secondly, they are involved in the recruitment of non-histone proteins to the DNA (Kouzarides, 2007). Histone acetylation and methylation are described in more details, introducing the enzymes catalysing these modifications and the factors that recognise them.

Histone acetylation

Acetylation of lysine residues on histone tails neutralizes the positive charge of the lysine, indicating a potential to decrease the interactions between nucleosomes and the DNA, and resulting in a more open chromatin structure. However, there are different models explaining the correlation between histone acetylation and open chromatin, including that a decreased affinity of the lysine residue to the negatively charged DNA give rise to a more open chromatin structure or due to charge repulsion between nucleosomes and DNA, but it is not entirely clear how acetylation facilitates transcription. Hence, histone acetylation makes a locus more accessible for transcription factors and is associated with increased gene expression. Lysine acetylation marks are highly dynamic, the underlying histones are located mostly at promoters and enhancer of expressed genes (Nicholson et al., 2015). Acetylation of lysine residues appears in the tails of histone H3, H4, H2A and H2B and a few lysine residues can be either acetylated or methylated as for instance H3K9 (Rice and Allis, 2001). Several acetylation sites (e.g. H3K9ac, H3K56ac, H4K16ac) have been shown to be involved in DNA double-strand break repair (Gong and Miller, 2013). Lysine acetylation is controlled by two classes of proteins: the histone acetyl-transferases (HATs) and the histone deacetylases (HDACs). HATs catalyse the transfer of an acetyl group to the ε-amino group of lysine side chains and are divided in two main classes: type-A and type-B HATs. Newly synthesised cytoplasmic histones that are not yet incorporated into the chromatin are acetylated mainly by type-B HATs. Type-A HATs modify mainly N-terminal tails of histones assembled in nucleosomes. By contrast, HDACs remove the acetyl group and restores the positive charge of the lysine residue, resulting in chromatin compaction and transcriptional repression (Bannister and Kouzarides, 2011).

Histone methylation

Unlike acetylation, histone methylation does not alter the charge of the histone tails; therefore, it has no impact on the overall chromatin organisation on its own. However, it has an important role in the recruitment of non-histone proteins so-called readers to the chromatin, at least for the best known histone modifications, including methylation of H3K4, H3K27 or H3K9. Histone methylation

occurs preferentially on lysine and arginine residues of histone tails and depending on the position and number of the methyl groups, histone methylation has an activating or a repressing influence on gene transcription. Arginine (R) can be mono-, asymmetrically or symmetrically dimethylated, whereas lysine (K) can be modified with one (monomethyl; me1), two (dimethyl; me2) or three (trimethyl; me3) methyl groups. The target amino acid and the number of methyl groups correlate with the transcriptional activity at nearby genes. For instance, H3K4, H3K36 or H3K79 methylations are associated with active transcription, while H3K27, H3K9 or H4K27 methylation is linked to repressive chromatin (Nicholson et al., 2015).

As histone methylations at lysine residues, particularly H3K4me2 and H3K27me3, are a central part of my thesis, I will describe their regulation in details. Histone methylations at lysine residues are controlled by two classes of proteins: lysine methyltransferases (KMTs) and lysine demethylases (KDMs). KMTs methylate the ε-amino group of lysine residues in the histone tails, two major classes of KMTs are known, comprising or not having a SET domain. To date, there is only one KMT known not having a SET domain, which specifically modifies H3K79. In all other KMTs, the SET domain contains the enzymatic activity transferring a methyl group from S-adenosylmethionine (SAM) to the amino group of the lysine residue (Bannister and Kouzarides, 2011; Smith and Denu, 2009). By contrast, KDMs remove the methyl groups from lysine residues. Based on their catalytic activity, two types of KDMs can be distinguished. Members of the first group of KDMs, including LSD1 and LSD2, which demethylate mono- and dimethyl groups, contain a flavin adenine dinucleotide (FAD)-dependent amine oxidase domain. LSD1 can demethylate H3K4, repressing transcription and has demethylation activity on H3K9 in combination with the androgen receptor, mediating transcriptional activation. The second class of KDMs, including JHDM1, KDM2 or JARID1, have a Jumonji C domain and is capable of removing mono-, di- and trimethyl groups by oxidation of the methyl groups requiring iron Fe(II) and α-ketoglutarate as cofactors (Black et al., 2012; Nicholson et al., 2015). Different KMTs and KDMs fulfil their specificity only on certain lysine residues. Exemplified in detail for the best descripted key activating and repressing histone marks H3K4 and H3K27 methylation, respectively, as histone modifications are regulated by a complex interplay between many enzymes and protein complexes.

H3K4 methylation marks are generally found at active genes; H3K4me1 is associated with active and poised enhancers, H3K4 dimethylation (H3K4me2) is linked to active and poised genes, whereas trimethylation of H3K4 is linked to promoters of transcriptionally active genes (Eissenberg and Shilatifard, 2010; Hon et al., 2009; Nicholson et al., 2015). Moreover, during cellular differentiation such as haematopoiesis, H3K4me2 is not only present at active genes, but also at transcriptionally silent lineage-specific genes and is localized at enhancers of developmental genes (Orford et al.,

2008). Methylation of H3K4 is catalysed by trithorax-group (trxG) protein complexes containing not only KMTs but also HATs or HDACs. TrxG complexes are clearly associated with transcriptional activation. In mammals, several KMTs methylating H3K4 were identified, for example mixed lineage leukaemia (MLL) proteins (MLL1-4), hSET1A and B, and ASH1. MLL1, for instance, catalyses specifically H3K4 to H3K4me2, but is also able to trimethylate H3K4 with the help of association partners (RBBP5 and Ash2L) (Black et al., 2012; Dou et al., 2006; Hon et al., 2009; Lanzuolo and Orlando, 2012). KMTs from the trxG-MLL complex are associated with proteins having KDM activities in some genomic regions. For instance, MLL2 is present in a complex together with the H3K27me3-specific demethylase UTX. This suggests that methylation and demethylation of different lysine residues regulating transcription in specific genomic regions is highly coordinated (Pasini et al., 2008).

H3K27me2/3 marks, associated with gene repression, are catalysed by polycomb-group (PcG) proteins found in polycomb repressive complexes (PRCs). In mammals, two PRC complexes are known: PRC1 and PRC2. PRC2 consists of the subunits EED, SUZ12 and the histone methyltransferase EZH2, catalysing the H3K27 methylation. A variant form of the PRC2 complex exists, containing EZH1 instead of EZH2, which occupies active chromatin and promotes gene expression (Xu et al., 2015). PRC2-EZH1 is present in dividing as well as differentiated cells, while PRC2-EZH2 is found only in actively dividing cells. On the other side, PRC1 mediates gene repression by binding to methylated H3K27 and subsequent ubiquitylation of K119 on H2A leading to chromatin compaction (Bernstein et al., 2007; Lanzuolo and Orlando, 2012; Pasini et al., 2008). Jarid1 proteins (Rbp2/Jarid1a) catalyse demethylation of H3K4me2/3 marks that are present at sites of PRC2 complexes, important for the repression of target genes (Pasini et al., 2008).

2.1.3 DNA methylation and its regulation

DNA methylation is the second main feature of the epigenetic code, contributing to the distinct cell type-specific gene expression. Cytosine residues in DNA can be methylated at their C5 position, generating 5mC while not disturbing the base pairing properties of the nucleotides. Methylation of cytosine is the mechanistically best-understood epigenetic modification and evolutionary conserved among plants and animals. In the mammalian genome, DNA methylation mainly occurs at CpG dinucleotides, which are underrepresented in the bulk genome but enriched at specific genomic regions called CpG islands (Deaton and Bird, 2011; Illingworth and Bird, 2009). Non-CpG methylation is found in mammals, but to a much lower extend and its biological function is not yet clear. In the human genome, 60-80% of CpGs are methylated and less than 10% of CpGs are located in CpG islands (Du et al., 2015; Smith and Meissner, 2013). DNA methylation at CpG-rich promoters results

in gene silencing, whereas DNA methylation in gene bodies correlates with gene expression (Nicholson et al., 2015). DNA methylation patterns are dynamically regulated through DNA methylation and DNA demethylation during development to establish tissue- and cell type-specific methylation patterns.

DNA methylation is maintained and deposited by DNA methyltransferases (DNMTs). In mammals, three enzymatically active DNMTs are known: DNMT1, DNMT3a and DNMT3b. By flipping the cytosine residue out of the DNA helix, DNMTs catalyse and transfer a methyl group from the cofactor S-adenosyl-L-methionine (SAM) to the C5 position of cytosine, generating 5mC. Disruption of *DNMT1 or DNMT3b* genes in mice is embryonic lethal and DNMT3a deficient mice die shortly after birth, indicating that DNA methylation plays an important role during development. In mammals, DNMT3a and DNMT3b are probably responsible for *de novo* methylation in combination with a homologous protein DNMT3L which is catalytic inactive. DNMT3L is unable to bind the cofactor SAM but stimulates the enzymatic activity of the others. DNMT3a and DNMT3b are able to *de novo* methylate hemimethylated and unmethylated DNA (Jurkowska et al., 2011). In addition to *de novo* methylating in a CpG context, DNMT3a and DNMT3b can catalyse methylation of non-CpG cytosines (Arand et al., 2012). *De novo* methylation is important for the establishment of DNA methylation patterns in early development and in germ cells; *de novo* DNMTs are therefore highly expressed in embryonic stem cells (ESCs) and embryonic tissues, while downregulated in differentiated cells (Jurkowska et al., 2011). On the other side, DNMT1 is mainly responsible for DNA methylation maintenance, occurring during S phase of the cell cycle shortly after DNA replication. When cell enters S phase, DNMT1 is very abundant and recruited to replication fork through interactions with PCNA and UHRF1. By using the methylated parental strand as a template, DNMT1 converts hemimethylated CpG into a fully methylated double DNA strand, restoring the original methylation pattern (Du et al., 2015; Smith and Meissner, 2013). DNMT1 moves along with replication fork to methylate the newly synthesised DNA strand before chromatin is reassembled (Jurkowska et al., 2011). Biochemical assays showed that unmethylated DNA is not recognized by DNMT1 and its preferred substrate is hemimethylated DNA, indicating that DNMT1 contributes little to *de novo* methylation (Li and Zhang, 2014). DNMT1 alone is not sufficient in maintaining global DNA methylation; knock-out studies showed that the presence of DNMT3a and DNMT3b is required especially to maintain DNA methylation in heterochromatic regions (Jones, 2012; Jurkowska et al., 2011).

The mammalian genome is reprogrammed through active and passive demethylation processes. Passive demethylation occurs by diluting the 5mC mark during DNA replication due to inhibition of DNMT1 catalysed DNA maintenance methylation. In mammals, there is no DNA demethylase known yet. Active demethylation of 5mC is possible and occurs most likely through a family of DNA

hydroxylases called ten-eleven translocation (TET) proteins. The TET proteins TET1, TET2 and TET3 convert 5mC by oxidation to 5-hydroxymethylcytosine (5hmC) in a 2-oxoglutarate-dependent manner (Li and Zhang, 2014). 5hmC can be oxidised further by the TET enzymes, generating 5-formylcytosine (5fC) and 5-carboxylcytosine (5caC), both of which are substrates for the thymine DNA glycosylase (TDG) (He et al., 2011). TDG is able to excise 5fC and 5caC from the DNA and, through base excision repair (BER), the original cytosine residue is restored (Weber et al., 2016). Additionally, 5hmC, without further oxidation, can also be passively demethylated, as it is only poorly copied by DNMT1 (Ji et al., 2014; Shen and Zhang, 2013). Another protein shown to be involved in DNA demethylation during development is the activation-induced-deaminase (AID), able to deaminate 5mC to thymine that is recognised by DNA glycosylases and excised by the BER pathway (Seisenberger et al., 2013). Beside their important contribution in early development, DNA demethylation processes are also present and required in fully differentiated somatic cells, though to a lower extent. Site-specific DNA demethylation is involved in transcriptional responses to environmental changes, in oncogenic transformation or in aging, keeping the DNA methylation pattern dynamic through life (Li and Zhang, 2014).

DNA methylation dynamics during development

DNA methylation patterns are relatively stable throughout life and play an important role in determining cell fate. There are two points in the mammalian development where DNA methylation changes dramatically to allow nuclear reprogramming; during early embryogenesis as well as in primordial germ cells (PGCs) (Figure 3). During early development, the mammalian genome is reprogrammed through active and passive demethylation processes. After fertilization the DNA methylation pattern from the maternal and paternal genome is reprogrammed (Guo et al., 2014). The maternal genome is passively demethylated while the paternal genome undergoes a rapid, complete loss of DNA methylation through active enzymatic processes, before the first cell division. There is good evidence that TET3, the only TET protein present in early zygotes, oxidize 5mC residues generating 5hmC before DNA synthesis starts, and 5hmC is then serially diluted in each round of cell division. However, recent evidence also suggests that the early loss of paternal 5mC is independent of TET, and that 5hmC accumulation is uncoupled from the 5mC loss and dependent on *de novo* DNA methylation through DNMT3a and DNMT1 in the zygote (Amouroux et al., 2016). BER complexes including PARP1 and APE1 are as well enriched in zygotes and possibly involved in demethylation, but TDG seems to be absent (Hajkova et al., 2010). Further studies are necessary to determine the exact mechanism of the global demethylation during zygotic reprogramming. The global demethylation is followed by *de novo* methylation by DNMT3a and DNMT3b. The *de novo* methylation starts in the morula stage when cells located in the periphery separate to form the inner cell mass cells destined

to become the embryo. This separation results in the specific epigenetic features with low methylation levels in cells of the outer trophectoderm and re-establishing DNA methylation pattern of the inner cell mass cells (Schuermann et al., 2016; Seisenberger et al., 2013; Smith and Meissner, 2013).

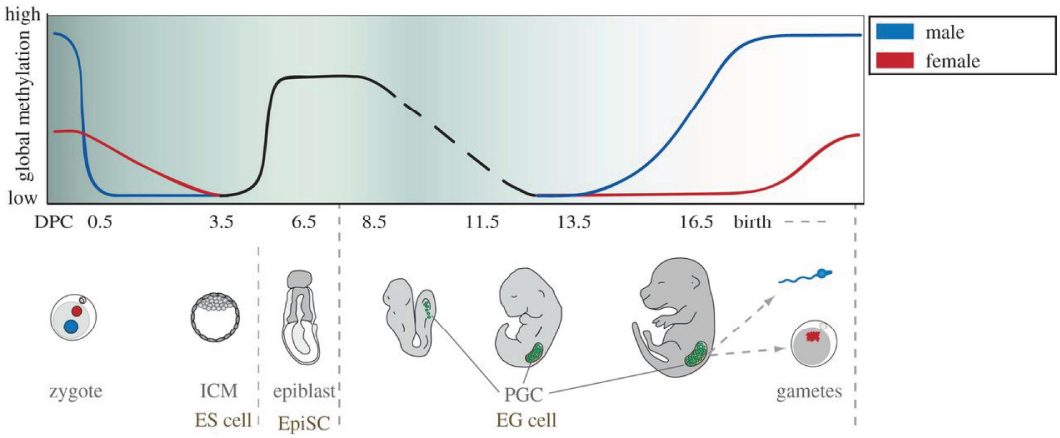

Figure 3: **DNA methylation dynamics during mammalian development.** DNA methylation is changed in a global scale two times during mammalian development by active or passive DNA demethylation processes followed by *de novo* DNA methylation and results in the reprogramming of the DNA methylation pattern. The first demethylation occurs during early embryogenesis affecting both the maternal (red) and the paternal (blue) genome. The second methylation change happens in primordial germ cells (PGCs) and *de novo* methylation is sex specific (adapted from Seisenberger et al., 2013).

The second demethylation step occurs in PGCs, the direct progenitors of sperm and oocytes, where the somatic epigenetic pattern of the epiblast state is changed into a germ cell state. This reprogramming step is important for the generation of gametes to erase the parental imprints before fertilisation and generating the next generation. In mice, most of the DNA methylation marks are reset in PGCs. Starting from embryonic day 8.5, DNA demethylation in PGCs consists of a passive demethylation processes through 5mC dilution followed by an actively regulated locus-specific DNA demethylation. Recent studies indicate that specific genomic regions as meiotic genes and imprints are demethylated by TET1 and the BER machinery (Kawasaki et al., 2014; Schuermann et al., 2016; Yamaguchi et al., 2013). After demethylation in early PGCs, the genome undergoes *de novo* methylation to achieve the higher methylation levels in mature gametes. In females, *de novo* methylation occurs in the growing oocyte after birth. By contrast, male PGCs gain their DNA methylation pattern between embryonic day 14.5 and 16.5. *De novo* DNMTs, DNMT3a and DNMT3b, with the help of DNMT3L catalyse the DNA methylation resulting in CpG methylation levels of about 85% and 30% in sperm and oocytes, respectively (Seisenberger et al., 2013).

2.1.4 Epigenetic programming during cell differentiation

Epigenetic modifications alter dramatically during a cell differentiation, shaping the nuclear organisation of chromatin and determining gene expression programs through development to facilitate lineage commitment into specific tissue types. Histone modifications in combination with DNA methylation change the overall chromatin structure during differentiation, establishing three main chromatin states at CpG rich regions: transcriptionally active, repressed and poised chromatin (Figure 4) (Boland et al., 2014).

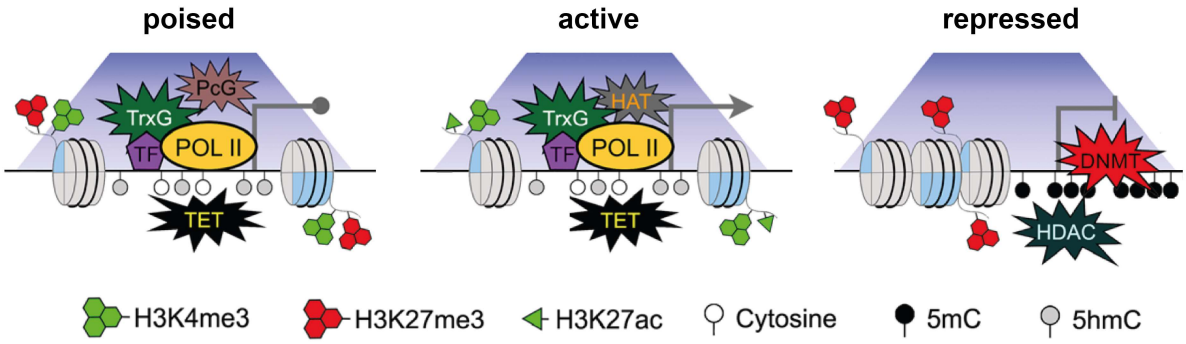

Figure 4: **Epigenetic control at promoters of poised, active and repressed transcript genes.** Involvement of histone tail modifications in the form of methylation and acetylation in combination with DNA methylation is illustrated. Contributions of the following chromatin associated proteins are indicated: DNMT (DNA methyltransferase), HAT (histone acetyltransferase), HDAC (histone deacetylase), PcG (polycomb group complex), POL II (RNA polymerase II), TET (ten eleven translocation dioxygenase), TF (transcription factor) and TrxG (trithorax group complex) (adapted from Boland et al., 2014).

Active open chromatin contains highly expressed genes and enhancers. Active promoters occupied by trxG, HATs, RNA polymerase II and TET proteins, are characterised by the presence of H3K4me3 and H3K27ac as well as non-methylated cytosine, but increased levels in 5hmC (Figure 4). Active enhancers are marked with H3K4me1, H3K27ac and are occupied by the mediator complex. Gene bodies of actively transcribed genes are defined by the presence of H3K36me3. Other modifications such as H3K79 methylation, H3K56 acetylation or H2B ubiquitination were also shown to be associated with active transcribed genes (Boland et al., 2014; Dambacher et al., 2013; Shilatifard, 2012). By contrast, the repressed chromatin features are present mainly at compact heterochromatic regions and associated with repressive genes. H3K27me3 modifications and 5mC are prominent at repressed promoters, which are as well occupied by DNMTs and HDACs (Figure 4). Genes that are occupied with H3K9me3 marks are completely repressed. Repressed enhancers lost their specific active enhancer features (H3K4me1 and H3K27ac) and are instead enriched for H3K27me3 and 5mC (Boland et al., 2014; Dambacher et al., 2013). In the poised chromatin state, promoter regions are marked with a bivalent histone modification profile including the activation mark H3K4me3 and the

repressive one H3K27me3 (Figure 4). The presence of the trxG and PcG proteins together with the poised RNA polymerase II allows a rapid transcriptional activation or repression upon initiation of cell differentiation (Aloia et al., 2013; Cui et al., 2009; Kouzarides, 2007). The DNA in poised chromatin contains little 5mC, but is enriched for 5hmC. Poised state correlates with an open chromatin structure, but the genes are silenced or lowly transcript (Bernstein et al., 2006; Meissner et al., 2008). Poised chromatin states at promoters are mainly present in pluripotent or multipotent stem cells such as ESCs or haematopoietic stem cells (HSCs) at genes that are important for development, morphogenesis and in cell signalling pathways. Poised enhancers are characterised by H3K4me1 and H3K27me3 and with the presence of the mediator complex as transcriptional coactivator and are associated with low transcription. The gene body of poised chromatin is covered with H3K27me3 and 5mC (Bernstein et al., 2006; Boland et al., 2014).

The rapid global change of chromatin and transcription during differentiation is resulting in stable silencing of pluripotency genes, activation of lineage-specific genes as well as the controlled activation and repression of progenitor-specific gene (Kraushaar and Zhao, 2013). There are on one site the pluripotent ESCs characterised by an open and highly dynamic chromatin landscape. Somatic cells, on the other hand, have more and larger genomic regions that are occupied by H3K27me3 (around 40% of total genome versus 8% in ESCs) resulting in a more defined, compact and closed chromatin structure with a higher content of heterochromatic regions. Comparison of histone modifications and DNA methylation pattern between ESCs and differentiated cells showed that around one-third of the genome differs in chromatin structure (Hawkins et al., 2010; Zhu et al., 2013). Extracellular signals (cytokines, growth factors or morphogens) and intracellular transcription factors drive the gene expression pattern required for cell differentiation and lineage specification (Kraushaar and Zhao, 2013). Differentiation in response to environmental cues activates chromatin marks through transcriptional responses. Additionally, chromatin stages can provide gene priming as a form of preparation for future needs and it is achieved by establishing bivalent or similar states (Dillon, 2012). Bivalent domains are preferentially present in stem cells (ESCs or adult stem cells) but as well at lineage-specific genes in more mature cell stages, at mature T-cells for instance. This poised chromatin state allows a fast transcriptional activation or repression by losing one of the histone modifications during differentiation into somatic cells (Bernstein et al., 2006; Cui et al., 2009; Kraushaar and Zhao, 2013). Beside the bivalent domains, other mechanisms of epigenetic priming have been suggested. For instance, regulatory elements for brain development are occupied by high levels of DNA methylation in ESCs; they get demethylated and associated with H3K4me1 during ectoderm formation, but kept methylated in other lineages. Additionally, it was suggested that CpG poor regions with high DNA methylation levels in ESCs, get demethylated and enriched with

H3K27me3 methylation during differentiation in a lineage-specific manner (Boland et al., 2014; Gifford et al., 2013). Other examples are the specific epigenetic priming of myeloid and lymphoid genes during haematopoietic differentiation. Myeloid-specific genes are occupied by DNA methylation whereas lymphoid-specific genes are associated with the H3K27me3 mark in ESCs, allowing a fast activation through DNA demethylation and loss of H3K27me3 during differentiation, respectively (Cedar and Bergman, 2011). These examples indicate that histone modifications as well as DNA methylation play an important role in cell-type specific epigenetic priming, illustrating their important role in lineage commitment and cell plasticity. For more details on epigenetic features during haematopoiesis see section 2.2.3.

2.2 Haematopoietic system

The haematopoietic system is the most regenerative tissue in humans and around two-thirds of its activity produces neutrophils, the most abundant white blood cell in the circulation. During haematopoiesis, alterations of histone modifications and DNA methylation generate lineage-specific gene expression patterns. Yet, aberrations in epigenetic modifications as well as genetic mutations are a hallmark of cancer and may also be a driving force of leukaemogenesis. The following chapters will introduce haematopoiesis especially neutrophilic granulopoiesis and specific epigenetic alterations during haematopoiesis and in leukaemic cells.

2.2.1 General overview of haematopoiesis

One trillion (10^{12}) new blood cells are generated every day in the adult human bone marrow, illustrating that blood is the most regenerative tissue in humans. Multipotent HSCs have the capacity of durable self-renewal and can differentiate into all mature blood cells. After differentiation, blood cells migrate out of the bone marrow and reside in tissues, lymph nodes or circulate in the blood stream (Murphy, 2008). HSCs are localized in specific niches generated by osteoblasts with little blood flow and low oxygen levels. The HSC niches are located in the endosteum near the interface between bone marrow and bone. This environment and the contact with osteoblast cells are important for HSC survival, self-renewal and contribution to long-term haematopoiesis (Borregaard, 2010; Winkler et al., 2010). HSCs differentiate into all different mature blood cells through several progenitor cell stages, which are categorized into lymphoid or myeloid cells (Doulatov et al., 2012) (Figure 5). T, B and natural killer cells belong to the lymphoid lineage, whereas the myeloid lineage comprises the megakaryocytes giving rise to platelets, erythrocytes (red blood cells), granulocytes and macrophages. According to the current model of human haematopoiesis, myeloid and lymphoid lineages are already separated at an early progenitor stage. The common myeloid progenitor (CMP) can differentiate into all myeloid cell types, whereas the lymphoid cells are generated by the multipotent lymphoid progenitor (MLP). However, recent studies indicated that human MLPs are not only restricted to the lymphoid lineage. They can give rise to myeloid cells, but do not have the potential to differentiate into erythroid and megakaryocytic cells. Dendritic cells are generated from either CMPs or MLPs and cannot be clearly grouped into a myeloid or lymphoid cell type (Doulatov et al., 2012; Kondo, 2010).

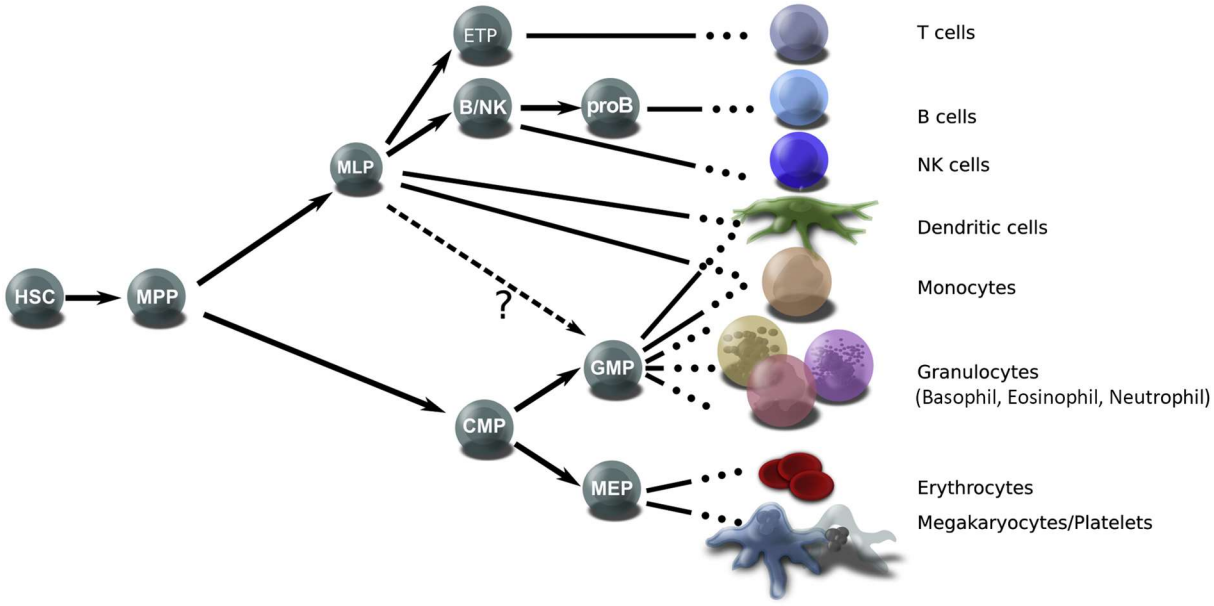

Figure 5: Lineage determination of human haematopoiesis. All the different types of human blood cells are derived from multipotent haematopoietic stem cells (HSCs) in the bone marrow. Differentiation gives rise to two common progenitor cells; the common myeloid (CMP) and the multipotent lymphoid progenitor (MLP). They are differentiating further into lineage-committed progenitor cells developing in multiple steps into distinct blood cells. All the different progenitor stages are indicated as following: ETP (earliest thymic progenitors), GMP (granulocyte–macrophage progenitor), MEP (megakaryocyte–erythrocyte progenitor), MPP (multipotent progenitor) (adapted from Doulatov et al., 2012).

2.2.2 Neutrophils, their development and homeostasis

Neutrophilic granulocytes are key players and the most abundant cell type of the innate immune system, arriving as the first immune cells at the site of infection. The immune system protects humans from disease-causing microorganism or pathogens and is divided into the innate and the adaptive immune system. Innate immunity is provided by macrophages, neutrophils and natural killer cells that constitute a fast but incomplete protection against microbes and generate a short-term memory. By contrast, the adaptive immunity is a specific immune response against a particular pathogen or their product, mediated by T and B lymphocytes, and evolves during exposure to the pathogen. Adaptive immunity is generating long-term memory (Murphy, 2008).

Granulocytes also known as polymorphonuclear leukocytes, they are derived from the CMP and are separated into three different cell types: neutrophils (~90%), eosinophils and basophils. As neutrophils are short-lived cells with a half-life between a few hours to a few days, they need to be constantly generated in the bone marrow. To maintain homeostasis, the daily production of neutrophils is around 1 to 2 x 10^{11} cells in humans (Amulic et al., 2012; Borregaard, 2010). Around

66% of the haematopoietic activity in the bone marrow produces monocytes/macrophages and granulocytes. Two types of neutrophilic granulopoiesis can be distinguished: the steady-state and the emergency granulopoiesis. The steady-state granulopoiesis occurs at normal no inflammatory conditions or when local infections are present without disseminations. After severe infections including disseminations, neutrophils are consumed in large numbers inducing the emergency granulopoiesis.

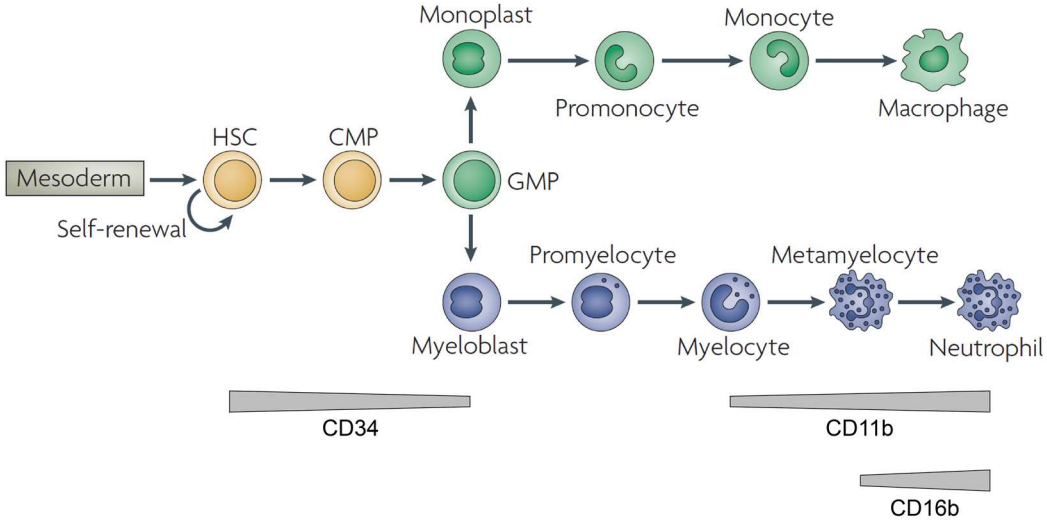

Figure 6: Lineage determination of neutrophilic granulopoiesis. Step-wise differentiation into neutrophilic lineage and its most related lineage, to macrophages. HSCs differentiate through the GMP stage into myeloblast cells, further through promyelocytes, myelocytes and metamyelocytes into neutrophils. The different neutrophilic stages can be distinguished by the expression of the surface markers CD34, CD11b and CD16b (adapted from Rosenbauer and Tenen, 2007).

Neutrophils are derived from HSCs through a regulated differentiation process generating the intermediate states of myeloblasts, promyelocytes, myelocytes and metamyelocytes. The different maturation stages are distinguishable by expression of different surface marker or by analysing the transcription profile. For instance, human HSCs and progenitors as such CMPs and granulocyte-macrophage progenitors (GMPs) express cluster of differentiation 34 (CD34), whereas CD11b and CD16b are upregulated in myelocytes and metamyelocytes, respectively (Figure 6). The production of neutrophils from progenitors is controlled by the key regulator of neutrophil development the granulocyte-colony stimulating factor (G-CSF), which is produced by bone marrow stroma cells in response to interleukin (IL)-17A. During steady-state conditions without infection, the release of G-CSF is regulated most likely by a feedback loop. Apoptotic neutrophils are phagocytosed in the tissue by macrophages and dendritic cells, which thereby reduce their IL-23 expression. In turn, reduction of IL-23 results in less IL-17A production by T cells and natural killer cells. As IL-17A is the main stimulus of G-CSF production in stroma cells of the bone marrow, neutrophilic granulopoiesis is

reduced (Borregaard, 2010; Bugl et al., 2012). G-CSF activates the major transcription factor C/EBPα through the STAT pathway, initiating the expression of several key genes of normal neutrophilic differentiation (Manz and Boettcher, 2014). Fully mature and non-mitotic neutrophils leave the bone marrow and enter the blood circulation. When no systemic infection is present, only 1-2% of mature neutrophils are circulating in the blood (Bugl et al., 2012).

During inflammation, neutrophils are recruited from the blood to the infected tissue, guided by endothelial cells (Borregaard, 2010; Carmona-Rivera and Kaplan, 2016). They are able to take up different types of microorganism by phagocytosis, destroying them in intracellular vesicles. Another mechanism neutrophils use to fight pathogens is netosis, which invokes the release of neutrophil extracellular traps formed by decondensed chromatin fibers decorated with antimicrobial factors, leading to cell death of neutrophils (Remijsen et al., 2011; Zawrotniak and Rapala-Kozik, 2013). After severe infections including disseminations, neutrophils are consumed in large numbers, inducing the emergency granulopoiesis. Emergency granulopoiesis is characterized by increased *de novo* production of neutrophils, accelerated cellular turnover and release of mature as well as immature neutrophils from the bone marrow into the blood. The levels of granulocytic cytokines as G-CSF or early cytokines like IL-3, IL-6 or FMS-like tyrosine kinase 3 (FLT3) ligand are up to 100 times higher during emergency granulopoiesis compared to steady-state conditions. The increased G-CSF receptor signalling through JAK and STAT3 activates the transcription factor C/EBPβ replacing C/EBPα and inducing enhanced myeloid progenitor proliferation and neutrophil generation (Bugl et al., 2012; Manz and Boettcher, 2014). In addition, there is some recent evidence that increased granulopoiesis can be induced independently of the presence of a microbial pathogen by chemical agents (e.g. thioglycollate or 5-fluoruracil), physical insults (e.g. trauma or ionizing radiation) or autoimmune disorders (e.g. rheumatoid arthritis). Further studies are needed to describe this 'reactive' granulopoiesis in more detail (Manz and Boettcher, 2014).

2.2.3 Epigenetics of the haematopoietic system

The cell-type specific gene expression pattern epigenetically established during haematopoiesis are not well understood and were investigated only recently by analysing different haematopoietic intermediates from the blood (Cedar and Bergman, 2011). Multipotent progenitors (MPPs) derived from HSCs differentiate into progenitor cells of the myeloid and the lymphoid lineage: CMPs and MLPs. There is evidence from mouse studies that different mechanisms of epigenetic priming are involved to mark specific genes required for myeloid and lymphoid development in HSCs and MPPs. Myeloid and lymphoid-specific genes are silent in HSCs but are activated cell type-specifically during

differentiation. Interestingly, the expression of myeloid- and lymphoid-specific genes is probably poised by two different mechanisms. Generally myeloid-specific genes are repressed by DNA methylation in HSCs and MPPs and undergo programmed active demethylation to initiate myeloid differentiation, especially in CMPs. *DNMT1* deletion in HSCs resulted in an increase of myeloid progenitor cells, whereas *TET2* depletion led to an impaired myeloid differentiation, illustrating the important role of DNA demethylation during myeloid differentiation (Cedar and Bergman, 2011; Ko et al., 2010; Trowbridge et al., 2009). By contrast, usually lymphoid-specific genes are marked by the polycomb (PRC2)-mediated, repressive H3K27me3 modification in HSCs and MPPs. Activation of lymphoid related genes is initiated by the removal of the polycomb complex. Deletion of *BMI1,* encoding a member of the polycomb repressive complex, resulted in an increase of lymphoid progenitors through the activation of *EBF1* and *Pax5* (Oguro et al., 2010). Hence two different epigenetic mechanisms regulate the process of haematopoietic gene priming and thereby proper lineage commitment and differentiation (Cedar and Bergman, 2011). In addition to those mechanisms, an H3K4me2-based process was described for a subset of lineage-specific genes. These genes are occupied by H3K4me2 and not by H3K4me3 marks at transcription start sites or regions important for transcription factor binding. They are not transcribed in HSCs, but can either be activated by methylating H3K4me2 to H3K4me3 in specific cell types or undergo H3K4 demethylation, eventually leading to silencing in other blood cell types. One example is *Gata1* which is an erythroid-specific gene occupied by H3K4me2 in HSCs. H3K4 trimethylation rises in erythrocytes whereas H3K4me2 is demethylated in other blood cell types (Orford et al., 2008).

Similar to ESCs, HSCs are characterized by a large number of bivalent chromatin domains. A small fraction of cell type-specific genes is losing the H3K27me3 modification during haematopoiesis and gets activated, but most of them lose H3K4me3 methylation and are silenced. The bivalent marks in HSCs maintain the activation potential for the genes necessary for cell type-specific activation (Cedar and Bergman, 2011). Bivalent domains in murine HSCs are enriched at promoters of genes encoding regulators of embryonic developmental, key transcription factors and growth factors for haematopoiesis (Weishaupt et al., 2010). The small fractions of bivalent domains that are activated during differentiation are characterized by the presence of the H3K4me1 and H3K9me1 marks as well as H2A.Z and RNA polymerase II occupancy, indicating a transcriptionally poised state. By contrast, bivalent regions concomitantly marked by H3K9me3 stay silent throughout differentiation (Cui et al., 2009). Notably, some bivalent domains are also present in later cell stages like mature T-cells, located at promoters of genes required for further differentiation into effector T-cells (Wei et al., 2009).

During differentiation, epigenetic modifications of stem cells change into cell type-specific modifications of somatic cells, resulting in a unique pattern in each lineage. Two-thirds of the haematopoietic activity produces neutrophils and neutrophilic granulopoiesis is an important subject in my PhD thesis, hence, exemplified the epigenetic alterations during human granulopoiesis. Global DNA methylation is decreasing during myeloid differentiation, but increasing upon lymphoid commitment comparing isolated HSCs with mature blood cells (Ji et al., 2010). Comparison of DNA methylation profiles of isolated CD34+ progenitor cells (including HSCs, CMPs, GMPs) with mature blood granulocytes indicated a global DNA demethylation during granulopoiesis (Bocker et al., 2011). However, an increase of genome-wide DNA methylation was observed between isolated CMPs and GMPs probably associated with the progressive loss of stemness. After global gain of DNA methylation, a loss of genome-wide methylation was observed between GMPs and promyelocytes, and to a lower extent between promyelocytes and blood neutrophils, reflecting the activation of neutrophil-specific genes (Alvarez-Errico et al., 2015; Ronnerblad et al., 2014). Therefore, DNA methylation is dynamically regulated, and levels and patterns depend on the stage of differentiation. Additionally, human blood neutrophils are characterized by a high amount of heterochromatin containing different repressive histone modifications, including H3K9me3, H3K27me3 or H3K20me3, and low amounts of active histone modifications (e.g. H3K4me3 and H3K4me2) (Navakauskiene et al., 2014; Olins and Olins, 2005). By contrast, ESCs are characterised by an open and highly dynamic chromatin state (Hawkins et al., 2010). However, the mechanism of progressive chromatin change during neutrophilic granulopoiesis is poorly understood. Global chromatin compaction takes place in non-dividing but shape-changing nuclei during granulopoiesis and is associated with stages beyond myelocytes (Olins and Olins, 2005). In contrast to this extensive chromatin mediated gene silencing, the neutrophil-specific genes *PU.1, MPO and CD11b*, which are kept in a poised state in human HSCs, are activated during an *in vitro* differentiation of 14 days into neutrophilic lineage, accompanied by high H3K4me3, low H3K27me3 and low H3K9me3 levels (Tang et al., 2014).

2.2.4 Leukaemia

Leukaemia is a haematopoietic malignancy also known as blood cancer, characterized by an accumulation of immature, non-functional malignant blood cells. According to the haematopoietic linage affected and mode of disease progression, four types of leukaemia are distinguished: acute myeloid (AML), chronic myeloid (CML), acute lymphocytic (ALL) and chronic lymphocytic (CLL) leukaemia. Acute leukaemia has a rapid progression with highly enriched immature cells, whereas chronic leukaemia is characterize by a slow progression in combination with high numbers of mature

cells. ALL is the most common type of leukaemia in children with around 80% of all acute cases in Switzerland (USA 75%), whereas AML is the most diagnosed type of acute leukaemia in adults (80% in Switzerland) (Florean et al., 2011; Krebsliga, 2016).

ALL is characterized by an accumulation of leukaemic lymphoblasts in the bone marrow and other tissues, displaying dysregulated proliferation and survival, as a consequence of genetic alterations in early B- and T-progenitor cells. The most common genetic alterations in ALL are chromosomal translocations, including t(9;22)/*BCR-ABL*, t(4;11)/*MLL-AF4*, t(12;21)/*TEL-AML1* and t(1;19)/*E2A-PBX* (chromosomes affected/fusion genes, Table 2) (Mrozek et al., 2009). In childhood lymphoblastic leukaemia for instance, the most common genetic alteration generated by a chromosomal translocation between chromosomes 12 and 21 results in the fusion protein TEL-AML1 (also known as ETV6-RUNX1). The translocations found in childhood leukaemia have foetal origin. Nevertheless, the development of childhood lymphoblastic leukaemia requires the postnatal accumulation of additional chromosomal or genetic aberrations as proposed in the 'two-hit' model of childhood leukaemia (Greaves, 2002). Several environmental factors were postulated promoting childhood leukaemia as a second hit after birth, including magnetic field exposure, infections or certain chemical (e.g. benzene) (Greaves, 2002; IARC, 2002; Martin-Lorenzo et al., 2015).

	chromosomal translocations	**mutations in epigenetic modifiers for**	
		DNA methylation	**histone modifications**
AML	t(15;17)/*PML–RARα* t(8;21)/*AML1–ETO* Inv(16)/*CBFb–MYH11* 11q23/*MLL-fusion protein*	DNMT3a IDH1 IDH2 TET2	ASXL1 EZH2 HAT domain of CBP MLL-fusion protein PRMTs UTX
ALL	t(9;22)/*BCR-ABL* t(4;11)/*MLL-AF4* t(12;21)/*TEL-AML1* t(1;19)/*E2A-PBX*	Dnmt3a	EZH2 HAT domain of CBP HDAC MLL-fusion protein UTX

Table 2: Acute leukaemia associated chromosomal translocations and epigenetic alterations. Genetic alterations and mutations in epigenetic modifiers are hallmarks of acute leukaemia, listed are the four most frequent chromosomal translocations and the best documented epigenetic modifiers with mutations in acute myeloid and lymphocytic leukaemia. The following epigenetic modifiers are indicated: DNMT3a (DNA methyltransferase 3a), IDH1/2 (isocitrate dehydrogenase 1/2), TET (ten eleven translocation dioxygenase), and ASXL1 (polycomb group protein additional sex comb like 1), EZH2 (polycomb group protein enhancer of zeste homolog 2), HAT (histone acetyltransferase), MLL (mixed lineage leukaemia protein a lysine methyltransferase), UTX (lysine-specific demethylase), and PRMTs (protein arginine methyltransferase). For chromosomal translocations: chromosomes affected/generated fusion genes (Florean et al., 2011; Greenblatt and Nimer, 2014; Martens and Stunnenberg, 2010; Mrozek et al., 2009; Xiao et al., 2016).

AML originates from blocked myeloid differentiation, resulting in rapid proliferation of immature myeloid progenitor cells in the bone marrow, which expand to other organs including liver and spleen (Mehdipour et al., 2015). The four most common AML associated chromosomal aberrations among more than 700 known ones are t(15;17)/*PML–RARα*, t(8;21)/*AML1–ETO*, Inv(16)/*CBFb–MYH11*, 11q23 and mixed lineage leukaemia (MLL)-fusion proteins (Table 2) (Florean et al., 2011; Martens and Stunnenberg, 2010). A simple 'two-hit' model of acute myeloid leukaemia was proposed as most of them have mutations or gene arrangements of two different classes. The first class (class I) of genetic alterations, resulting in a proliferation or survival advantage of haematopoietic progenitor cells, includes mutations that constitutively activate various signalling pathways like PI3K or RAS-MAPK (Shih et al., 2012). The second class (class II) alters the transcriptional regulation of haematopoietic differentiation and includes mutations in the core binding factor, retinoic acid receptor alpha or MLL protein (Conway O'Brien et al., 2014; Kelly and Gilliland, 2002).

Only about 60% of all AML patients have mutations in a signalling gene (class I mutation), indicating that not all AMLs can be explained by the two-hit model of AML (Cancer Genome Atlas Research, 2013). In addition, somatic mutations in genes involved in development or signalling were found in only 20% of early T-cell precursor-ALL (Zhang et al., 2012). This suggests at least a third class of mutations is involved in the development of leukaemia. A prominent candidate appears to be mutations in genes encoding epigenetic modifiers, as recent studies showed that in AML as well as in ALL somatic mutations are present in genes encoding epigenetic modifiers important for DNA methylation and histone modifications, pointing to a role of epigenetics in leukaemogenesis (Table 2) (Greenblatt and Nimer, 2014). As proper regulation of epigenetic mechanisms is critical for haematopoiesis, epigenetic modifications appear to constitute a class of genomic alterations with an important role in the development of leukaemia. Alterations in DNA methylation (5mC) patterns are found in various human cancers including leukaemia. For instance, tumour suppressor genes are transcriptionally silenced by methylation in different leukaemic subtypes. Additionally, gain of CpG methylation at promoters of the *homeobox (HOX) A4* and *HOXA5* genes was found in AML and ALL, correlating with poor prognosis and suggesting an important role of these HOX genes in the development of human leukaemia (Strathdee et al., 2007). By contrast, loss of DNA methylation was shown to activate proto-oncogenes in leukaemia. Moreover, epigenetic modifiers for DNA methylation, including DNMTs and TETs, are found in different types of leukaemia. 22% of patients with AML for instance, have a *DNMT3a* mutation, mainly including patients with repetitive *de-novo* AML having a poor prognosis. Additionally, expression of DNMT1, DNMT3a and DNMT3b is increased in some AML accompanied by a gain of DNA methylation at specific genomic regions. *IDH1* and *IDH2*

mutations disturbing function of TET2, amongst others, as well as *TET2* mutations themselves are frequently found in AML patients, linking epigenetic control of gene expression with cancer metabolism (Florean et al., 2011). Beside alterations at DNA methylation, mutations in genes encoding epigenetic modifiers of histone modifications were found in leukaemic cells, including subunits of the polycomb or trithorax-group. The most common mutation in T-ALL (16-19%) is found in the methyltransferase EZH2, a subunit of PRC2 (Ntziachristos et al., 2012). Other genetic alterations affecting PRC1 and PRC2 were found in different kind of leukaemia, including loss-of-function mutations, copy-number alterations or overexpression, indicating an important role of these complexes in the development of human leukaemia. Also, mutation in HATs, HDACs, HDMs and the trithorax *MLL* gene encoding the histone H3K4 methyltransferase occurs in leukaemia. Translocations of the *MLL* gene are found in AML (5-10%) and in ALL (70 % of childhood ALL), resulting in a poor prognosis for the patients (Greenblatt and Nimer, 2014). Moreover, the oncogenic character of some of the known fusion proteins is due to the recruitment of epigenetic partners to aberrant locations in the genome. This can result in silencing of tumour suppressor genes or activation of developmental genes promoting cancer development (Florean et al., 2011). In support of this notion, mutations in epigenetic modifiers of mice were shown to be critical for HSC self-renewal and differentiation, and to contribute but not to induce leukaemia. However, the early occurrence of epigenetic mutations in cancer and potentially reversibility of these modifications makes the usage of small inhibitory molecules able to target the epigenetic modifiers a promising strategy to add in leukaemic therapies (Greenblatt and Nimer, 2014).

2.3 Biological effects of extremely-low-frequency magnetic fields (ELF-MFs)

Over the last decades, there have been increasing concerns about potential health risks from the use of electronic appliances emitting magnetic (MF) and electromagnetic fields (EMF). Exposure to EMFs is not a new phenomenon, but man-made sources have simultaneously increased with advanced technologies and changed social behaviour. Main sources of EMFs start from household appliances and powerlines to telecommunications and wireless technologies. Human epidemiological studies as well as studies in animal and cellular models were used to investigate potential biological effects of ELF-MF exposure, but with inconclusive results (IARC, 2002; SCENIHR, 2015; WHO, 2007, 2016). On the grounds of epidemiological associations between ELF-MF exposure and increased risk of childhood leukaemia, ELF-MF were categorised as "possibly carcinogenic" to humans by the International Agency for Research on Cancer (IARC) (IARC, 2002). Mechanisms underlying this correlation, however, have remained elusive. Until now, there are hardly any reliable and reproducible data that would point to a universal mechanism. Contradictory results were generated analysing different endpoints relevant for cancer development, including cell cycle progression, apoptosis or genomic integrity. Due to the use of different cell types, exposure equipment, applied fields (static, dynamic, frequency, intensity etc.) and exposure times, it is difficult to compare and integrate reported positive and negative outcomes into consistent and plausible mechanistic concepts. The following chapters introduce electromagnetic fields, their observed correlation to human health and investigations into mechanism underlying its contribution to carcinogenesis.

2.3.1 Basic physical background of electromagnetic fields

Connected with our modern lifestyle, magnetic as well as electric fields are present wherever electricity is generated, transmitted or consumed, i.e. in power lines or electric applicants. EMFs are generated by electric charges and their motion. The energy is transported in the form of waves through space, consisting of an electric and a magnetic field perpendicular to each other (Figure 7). Electric fields are produced by the strength of electric charges and are indicated as volt per meter [V m^{-1}]. By contrast, magnetic fields result from the movement of the charge and are measured in Tesla [T]. The Maxwell's equation describes the fundamental law of electromagnetic fields: moving magnetic fields generate moving electric fields and vice versa. However at extremely-low frequency EMFs of 3-3000 Hz, the magnetic and the electric fields can be measured separately and are considered to be physically uncoupled (IARC, 2002). Most man-made sources of electromagnetic radiation emit EMF waves with field strengths that vary sinusoidally with time, produced by alternating current (AC) of electric systems. The current moves not unidirectional but back and forth

with a specific frequency; the number of cycles per seconds are quantified in Hertz [Hz] and the distance between peaks in the wave is indicated as wavelength [λ] (IARC, 2013; WHO, 2007). By contrast, static magnetic fields do not vary over time; the direct current (DC) is flowing constantly in one direction and DC is used in some rail or subway systems as well as in batteries or in magnetic resonance imaging (SCENIHR, 2009).

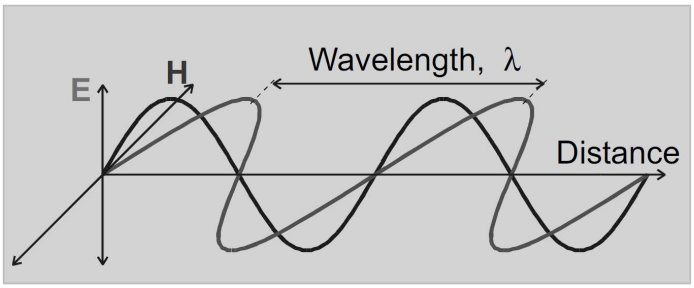

Figure 7: Schematic representation of an electromagnetic wave. Sinusoidally varying electromagnetic wave consisting of an electric (E) and a magnetic field (H) perpendicular to each other (IARC, 2013).

Electromagnetic fields are separated in two different classes: ionizing and non-ionizing radiation (Figure 8). High frequency EMFs are classified as ionizing radiation including X-rays and gamma rays, capable of transferring energy level that are high enough to break atomic bonds of molecules, i.e. to damage DNA directly. By contrast, non-ionizing radiations in the low- to mid-frequency range including EMFs from powerlines, radio waves, microwaves, infrared radiation as well as visible light are not able to damage DNA directly, they are not transferring enough energy required to affect chemical bonds. Extremely low frequency magnetic fields (ELF-MFs) such as emitted from powerlines (50 Hz in Switzerland) have frequencies between 1 and 3000 Hz, whereas radiofrequency EMFs used in communication technology like mobile phones range from 30 kHz to 300 GHz (Blank and Goodman, 2011). In homes, the main sources of ELF-MFs are in-house power installations, household appliances and powerlines, generating an average exposure level between 0.025 and 0.07 µT in Europe and 0.055 and 0.11 µT in the United States (SCENIHR, 2015; WHO, 2007). The International Commission on Non-Ionizing Radiation provides guidelines for ELF-MF exposure limitations to protect humans against EMF exposure in the low frequency range. These guidelines are based on scientific evidence on ELF-MF effects on human health (see 2.3.2). The most recent guideline, published in 2010, sets the emission threshold for general public areas to 200 µT for 50 Hz ELF-MFs (ICNIRP, 2010). Currently, Switzerland has one of the strictest regulations for 50 Hz magnetic fields worldwide; the threshold is set to 100 µT for public areas and even 1 µT for areas where people spend most of their time like in living rooms, bed rooms or at work places. As a comparison, Germany has only a fixed one at 100 µT (Swissgrid, 2015).

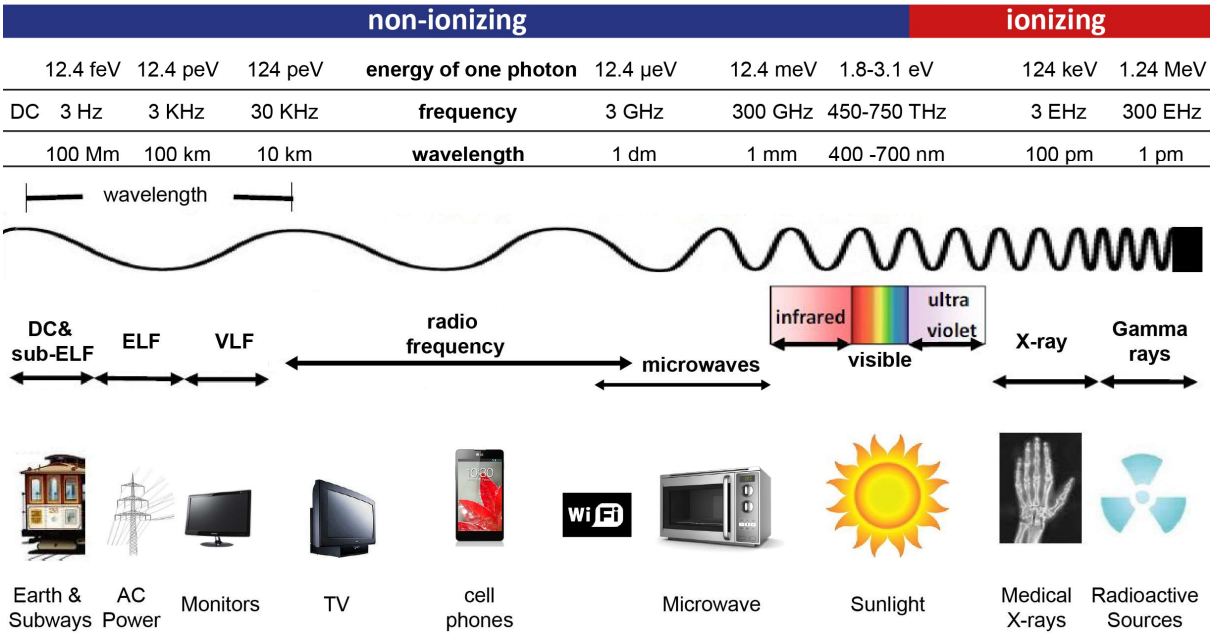

Figure 8: Electromagnetic spectrum. Electromagnetic fields are illustrated from non-ionizing radiation at low frequency to ionizing ration at high frequency ELFs and some examples of application of the different frequency ranges (adapted from Kumer, 2014).

2.3.2 Association of ELF-MF exposure with the risk of childhood leukaemia

Epidemiological studies over the last three decades repeatedly showed a positive association between ELF-MF exposure and the occurrence of childhood leukaemia, but no association with other types of cancer was observed. Based on the results of these epidemiological studies, ELF-MF was categorised as being possibly carcinogenic to humans (Group 2B) by IARC in 2002 (IARC, 2002). As the categorisation in this risk assessment was primarily based on the results of epidemiological studies, there was scientific debate on the validity of the assessment, yet, the potential risk of ELF-MFs was recently confirmed (SCENIHR, 2007, 2015; Schuz et al., 2016).

In Europe, a typical daily mean exposure level of children is below 0.1 µT, only 1-2% of children are exposed to ELF-MF daily means more than 0.3 µT. Latest epidemiological studies determined a 1.5 to 2-fold increase in risk for childhood leukaemia at average exposure levels for 24 hours above 0.3 - 0.4 µT, confirming the results from older studies. Yet, no significant correlation was determined at lower exposure levels (Ahlbom et al., 2000; Kheifets et al., 2010). Both studies were pooled analysis from several individual cohorts, including in total 3'247 cases of childhood leukaemia and 10'000 children in the control group analysed by Ahlbom et al. (2000) and 10'818 leukaemia patients vs 12'806 controls by Kheifets et al. (2010). Additionally, a recent study analysed childhood leukaemia data collected from 1962 until 2008 of 53'515 children together with matched controls, indicating an

association of leukaemia and ELF-MF exposure only before 1990 (Bunch et al., 2014). These suggest that changing population characteristics among those living near powerlines may play an additional role. Although despite the analysis of more than 20 epidemiological studies, the lack of supportive evidence of experimental studies and mechanistic data still raise concerns about the causality indicated by the results of the epidemiological studies. Due to participation bias for instance, as individual studies include small numbers of highly exposed children, different selection procedures of control children or low participation numbers in general. Additionally, methodological shortcomings of studies, including misclassifications of exposure levels, information bias, confounding or publication bias, are of concerns. Overall, the classification of ELF-MF as possibly carcinogenic remains valid. Hence, the current estimated risk of ELF-MF is that up to 2% of childhood leukaemia cases in Europa may be promoted by ELF-MF exposure (Schuz and Ahlbom, 2008).

2.3.3 Effects of ELF-MF exposure on cell proliferation, cell cycle and cell viability

Epidemiological studies determined a correlation of EMF and leukaemia, but the underlying cellular mechanisms are still elusive. The following three chapters will summarise results of *in vitro* studies dealing with possible EMF-induced effects, trying to explain the correlation of ELF-MF and increased risk for childhood leukaemia at the mechanistic level. However, the studies produced contradictory results, which is why it remains difficult to integrate all the reported negative and positive experimental outcomes into a global consistent mechanistic picture. Moreover, most animal studies failed to support evidence that magnetic fields can cause tumours, but a recent study indicated a significant carcinogenic effect in Spraque-Dawley rats exposed to sinusoidal 50 Hz magnetic field in combination with an acute low-dose γ-ray radiation (SCENIHR, 2015; Soffritti et al., 2016). Therefore, it is important to understand the ELF-MF induced cell damage or cell mis-programming and how it is related to cancer to be able to substantiate or decline the hypothesized causal relationship between exposure and leukaemia.

Impact of ELF-MF on cell cycle and cell proliferation

Cell cycle deregulation is a hallmark of tumour cells, contributing to unscheduled cell proliferation (Malumbres and Barbacid, 2009). Cell cycle is a regulated process controlled by cyclin-dependent kinases (CDKs), resulting in cell division and production of daughter cells. The mammalian cell cycle is separated into four phases: G1, S, G2 and M phase (Figure 9). Cellular growth takes place in growth phases G1 and G2. Non-cycling cells mostly rest in G1 phase, sometimes referred to as G0 phase. In the synthesis phase (S phase) the DNA is replicated and during mitotic phase (M phase) the

duplicated chromosomes are divided before the cellular division into daughter cells. Mitosis is separated in individual phases: prophase, prometaphase, metaphase, anaphase and telophase. During prophase, the duplicated chromosomes become decondensed and centrosomes are separated. The nuclear envelope disperses, and mitotic spindle are assembled and connected to the chromosomes during prometaphase. In metaphase, chromosomes are aligned at the spindle equator, while the centrosomes split, and chromatids separate and move towards the poles during anaphase. Reformation of nuclear envelope and DNA decondensation occurs during telophase followed by cell division into two daughter cells (Scholey et al., 2003; Verdaasdonk and Bloom, 2011; Walczak et al., 2010).

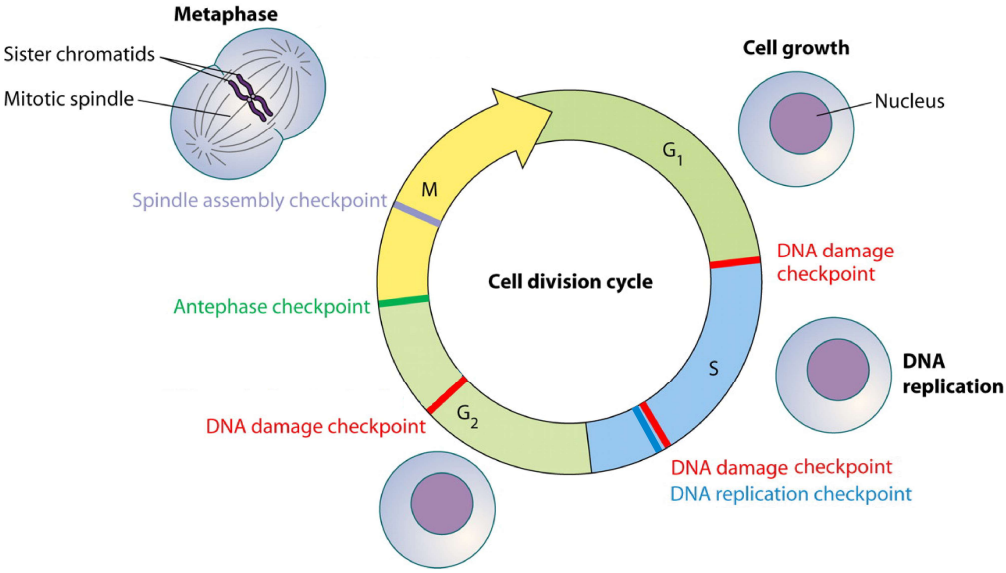

Figure 9: Mammalian cell cycle. DNA synthesis (S) phase, mitosis (M) phase including metaphase, and the two resting phases G1 and G2 are indicated. Checkpoint mechanisms control the cell cycle progression, including DNA damage, DNA replication, antephase and spindle assembly checkpoints (adapted from Chin and Yeong, 2010).

Checkpoint mechanisms ensure that cell cycle procedure occurs only by completion of all essential tasks in the processing cell phase. Activation of checkpoints induces cell cycle arrest allowing repair of the lesion. After successful repair, cells resume cell cycle progression, otherwise cells enter senescence or undergo apoptosis (Malumbres and Barbacid, 2009). Different checkpoints through the whole cell cycle coordinate DNA repair with chromosome metabolism and cell cycle transitions, including DNA damage, DNA replication, spindle damage and antephase checkpoints (Branzei and Foiani, 2008; Chin and Yeong, 2010). The DNA damage checkpoints detect and resolve DNA lesions during late G1, intro S and G2 phase, while the DNA replication checkpoint controls DNA damage in response to replication stress during S phase (Bertoli et al., 2013). The spindle assembly checkpoint controls the correct chromosome segregation and attachment of chromosomes to spindles during M

phase (Bertoli et al., 2013; Malumbres and Barbacid, 2009), and the antephase checkpoint prevents cell entering into M phase in the presence of stress conditions (Chin and Yeong, 2010). Notably, disturbed regulation of the cell cycle leads to altered cell proliferation and is often observed in cancerous cells (Bou Kheir and Lund, 2010; Gerard and Goldbeter, 2016; Santini et al., 2005).

Many studies investigated the impact of ELF-MF exposure on cell cycle progression and cell proliferation, yielding contradictory results. For instance, an increase of cell proliferation was observed by Zhang et al. (2013) in human epidermal stem cells exposed to ELF-MF (50 Hz, 5 mT, 30 min/day, 7 days), additionally they observed an increase of the percentage of cells in S phase and a decrease in G1 phase cells. Moreover, Mihai et al. (2014) found cell cycle effects of ELF-MF (100 Hz, 5.63 mT, continuous and discontinuous, 45 min) in Vero cells (kidney epithelial cell). Cell cycle profiles analysed 48 h after exposure illustrated an increase of the frequency of cells in S phase. Similarly, Martinez et al. (2012) reported an increase in cell number and in percentage of cells in S phase in NB69 cells (neuroblastoma) upon an intermitted ELF-MF (50 Hz, 0.1 mT, 5' on / 10' off, 63 h), effects which were absent when continuous ELF-MF exposure was applied. Further studies found increased cell proliferation upon ELF-MF (50 Hz, 0.1 mT, 3 h on and 3 h off, 45 h) in two human cell lines (neuroblastoma NB69 and hepatocarcinoma HepG2 cells), but decreased proliferation under MF exposure in the presence of all-trans-retinol (Martinez et al., 2016; Trillo et al., 2012; Trillo et al., 2013).

In addition, other studies observed a small cell cycle arrest upon ELF-MF exposure. For instance, ELF-MF exposure (50 Hz, 1 mT, 24-72 h, continuous) of all-trans-retinol-induced neuroblastoma BE(2)C cells resulted in an decreased cell number, seemingly, because of a higher proportion of cells in G0/G1 phase (Marcantonio et al., 2010). Additionally, Huang et al. (2014) observed an G1 arrest in human HaCaT cells (immortalized epidermal keratinocyte cell line) exposed to ELF-MF (60 Hz, 1.5 mT, 144 h) but no effect on cell growth, cell proliferation and cell cycle distribution in primary normal human epidermal keratinocytes, indicating a cell type-specific effect of ELF-MFs in this case.

There are many more studies describing effects of ELF-MF exposure on cell proliferation and cell cycle distribution, but with non-comparable results depending on cell type used and exposure conditions. One interesting observation is that several studies showed an effect upon ELF-MF exposure with an intermitted field, but no effect with continuous exposure (Focke et al., 2010; Ivancsits, 2002; Martinez et al., 2012). The dependency on intermitted ELF-MF remains elusive, but it may indicate a more complex biological response dependent on different processes in addition to cell cycle progression, including alteration of metabolic activity or induction of apoptotic cell death.

Impact of ELF-MF on cell viability

Another important hallmark of cancerous cells is that they can resist cell death, resulting in unlimited cell proliferation (Hanahan and Weinberg, 2011). There are two major types of controlled cell death in mammals: apoptosis and necrosis. Apoptosis is a mechanism of regulated cell death to eliminate abnormal, non-functional or harmful cells generated upon cell damage or stress but as well during normal development and morphogenesis. Caspase activation through death receptor ligands or release of apoptotic mediators from the mitochondria initiates mitochondrial membrane permeabilization, chromatin condensation, global mRNA decay, nuclear and DNA fragmentation (Nikoletopoulou et al., 2013; Thomas et al., 2015). These processes lead to the generation of apoptotic bodies (membrane-enclosed vesicles), which are removed by phagocytic cells such as neutrophils, macrophages or dendritic cells without inducing an immune response (Edinger and Thompson, 2004; Nikoletopoulou et al., 2013). By contrast, necrotic death is characterized by the alteration and degradation of organelles, resulting in cellular swelling followed by a rapid release of the whole cell content inducing an inflammatory response. Necrosis does not occur during normal development, but is important in inflammatory reactions or plays a role in cancer development. During inflammation for instance, necrosis can be triggered by biomolecules able to initiate an immune response, including the cytokine tumor necrosis factor or lipopolysaccharide present at pathogens (Nikoletopoulou et al., 2013; Wallach et al., 2016; Zong and Thompson, 2006).

Again, there are inconsistent results reported for the impact of ELF-MF exposure on induction of apoptosis, but also a great heterogeneity in the experimental conditions (cell type, ELF-MF field, exposure time, controls etc.) as well as the evaluation of apoptosis. A decrease of apoptotic cells upon ELF-MF exposure was observed in a study of Brisdelli et al. (2014). They investigated the effect of ELF-MF (50 Hz sinus, 1 mT) on apoptosis induced by different compounds (vinblastine, etoposide, quercetin and resveratrol) in human K562 chronic myeloid leukaemia cells. In quercetin treated cells after 48 h of ELF-MF exposure, they observed a significant reduction in the percentage of apoptotic cells as well as in caspase-3 activity. These effects were accompanied with an increased expression of the anti-apoptotic proteins Bcl-2 and Hsp70. The authors concluded that the ELF-MF exposure may modulate pro-survival mechanisms in K562 cells. Basile et al. (2011) observed no impact of ELF-MF exposure (50 Hz, 30 A/m, 6 h) on levels of stress-related Hsp70 protein and cell apoptosis but an increase in the anti-apoptotic protein BAG in two melanoma cell lines. On the other side, many other studies indicated either an induction of apoptosis or no effect by ELF-MF exposure. Garip and Akan (2010) reported that exposure of K562 human leukaemic cells with ELF-MF (50 Hz, 1 mT, 3 h) in combination with co-exposure to H_2O_2 increased the percentage of apoptotic cells compared to cell treated with H_2O_2 only. Moreover, human lymphoblast cells exposed for 72 h to ELF-MF (50 Hz, 60

μT) showed a two-fold increased rate of apoptosis (Mangiacasale et al., 2001). Tofani et al. (2001) described increased apoptosis after ELF-MF (50 Hz, 3 mT, 20 min) in two transformed cell lines (WiDr human colon adenocarcinoma and MCF-7 human breast adenocarcinoma) but no change in non-transformed cell line (MRC-5 embryonal lung fibroblast). Notably, no alteration in cell viability after ELF-MF exposure was reported in several additional studies (e.g. Giorgi et al., 2014; 2015).

2.3.4 Effects of ELF-MF exposure on genomic integrity

Based on elementary physical principles, the energy content of ELF-MFs is not high enough to directly alter chemical bonds of biomolecules, including DNA (Adair, 1998). ELF-MF is therefore unlikely to directly induce mutagenic DNA damage in cells, and increase the mutation rate in a way that could explain the putative cancerogenic effect. Yet, there are occasional reports indicating a genotoxic potential of ELF-MF exposure (e.g. Duan et al., 2015; Focke et al., 2010; Mihai et al., 2014; Vijayalaxmi and Prihoda, 2009). But, secondary effects that may give rise to DNA structural alterations such as changes in cell proliferation and cell cycle progression or apoptosis have in many cases not been excluded. Different studies evaluated the genotoxic potential of ELF-MF exposed cells by performing comet assays, sister chromatid exchange analysis and micronucleus formation, or by evaluating single- or double-strand break formation as well as chromosomal alterations.

A meta-data analysis compared 87 separate studies from 1990-2007 analysing genetic damage in mammalian somatic cells exposed to ELF-MF. The most prominently used condition was 50 Hz ELF-MF at a flux density of 1 mT (Vijayalaxmi and Prihoda, 2009). The analysis showed that in 46% of the studies no ELF-MF dependent increase in DNA damage were observed, whereas in 22% of them, a genotoxic potential was apparent and 32% had inconclusive results. The pooled analysis revealed a small significant increase in the genotoxic potential of ELF-MF exposure. More recent studies reported for instance, that ELF-MF exposure (100 Hz, 5.6 mT, continuous and discontinuous, 45 min) of the kidney epithelial cell line Vero resulted in an increase of cells with highly damaged DNA measured 48 hours after exposure (Mihai et al., 2014). Furthermore, primary human fibroblasts exposed to ELF-MF (50 Hz, 1 mT, 5’ on/10’ off) for 15 hours had a significant increase in DNA damage (Focke et al., 2010). Treatments with H_2O_2 indicated that these increased genotoxicity in fibroblasts upon ELF-MF exposure was unlikely to be due to increased levels of oxygen radical species. Disturbance of S phase associated DNA transactions and induction of apoptosis in a subpopulation of ELF-MF exposed cells was proposed as a possible explanation. Additionally, a genotoxic effect of ELF-MF (50 Hz, 5’ on/10’ off) was observed in mouse spermatocyte-derived GC-2 cells at a flux density of 3 mT but not at 1 mT or 2 mT (Duan et al., 2015). These results are in line with other

studies, which could not confirm the genotoxic effect of ELF-MF at lower flux densities. For instance, human blood cells exposed to ELF-MF (50 Hz, 1 mT) for 2 h showed no difference in DNA damage compared to control cells and co-exposure with ionizing radiation had no synergistic effect (Stronati et al., 2004).

Other studies investigated the potential of ELF-MF to induce nuclear foci of γH2AX. The phosphorylation of the histone variant H2AX generating γH2AX is a response to DNA strand interruptions and stress (Kuo and Yang, 2008). For instance, γH2AX levels as well as γH2AX foci formation was found to be increased in human lung fibroblasts and human lung epithelial L132 cells after ELF-MF exposure (60 Hz, 2 mT, 6 h). However, no difference was detected after exposure to a 50 Hz, 1 mT ELF-MF, consistent with a dose-dependent effect (Yoon et al., 2014). Furthermore, Giorgi et al. (2014) determined the γH2AX formation upon ELF-MF exposure (50 Hz, 1 mT, pulsed; 1 h, 24 h, 48 h or 72 h) in the presence of a genotoxic oxidative agent (H_2O_2) in human neuroblastoma and did not observe alteration of the DNA damage response following magnetic field exposure. Burdak-Rothkamm et al. (2009) found no significant change in DNA or chromosomal damage in ELF-MF (50 Hz, 0.5-1 mT, 5'on/10'off, 15 h) exposed fibroblasts, analysed by γH2AX formation, comet assay, sister chromatid exchange and micronuclei detection.

Several studies investigated the potential of ELF-MF exposure to affect DNA damage levels initiated by other genotoxic reagents, such as ionising radiation, H_2O_2 or menadione. Indeed, some authors reported increased genotoxicity of the carcinogen after co-exposure with ELF-MF, whereas others found no such effects. Luukkonen et al. (2014) found that human SH-SYSY neuroblastoma cells exposed to ELF-MF (50 Hz, 0.1 mT, 24 h) followed by a 3 hours menadione treatment have an increase in micronuclei formation 8 and 15 days after exposure. Additionally, they observed an increase in levels of reactive oxygen species directly after exposure as well as 15 days later. Moreover, DNA strand break and micronuclei induction were analysed in human peripheral blood lymphocytes by Cho et al. (2014) after. Cells were exposure to ELF-MF (60 Hz, 0.8 mT, 48 h) in combination with gadolinium, a contrast agent used for magnetic resonance imaging, reporting an increased genotoxic effect of gadolinium when exposed with ELF-MF. In another study, human fibroblasts and two epithelial cell lines exposed to ELF-MF (60 Hz, 1 mT, 4 h or 16 h) in the presence, or absence of different carcinogens (ionising radiation, H_2O_2), showed no difference in DNA damage formation when ELF-MF exposed (Jin et al., 2014). All in all, ELF-MF exposure was associated with increase DNA single- and double-strand break formations in some studies but not in others. This may indicate that the genotoxicity of ELF-MF is cell type-specific.

2.3.5 Effects of ELF-MF exposure on cellular differentiation and development

During differentiation, cell specialisation is accompanied by changes in gene expression and stabilised by epigenetic modifications. These processes are triggered by developmental and environmental cues and are therefore particularly sensitive to environmental conditions. Recently, several studies investigated the influence of ELF-MF exposure on cell differentiation, mainly in the context of neuronal development. For instance, Jung et al. (2014) differentiated the rat neuroblastic cell line PC12 *in vitro* for 5 days under ELF-MF exposure (50 Hz sinus, 1 mT, continuous). They observed an increased percentage of cells with neuronal outgrowth as well as longer neurites after ELF-MF exposure concomitant with an overall reduction of cell proliferation, presumably due to more differentiated cells. In another study, embryonic neural stem cells induced to differentiate under ELF-MF (50 Hz, 1 - 2 mT, 5' on / 10' off, 72 h) by Ma et al. (2014) showed altered expression of specific key regulators of early neuronal development; without, however, affecting the differentiation into neurons and astrocytes notably. Yet, the same group found in a more recent study that embryonic neuronal stem cells exposed to ELF-MF (50 Hz, 1 mT, 4 h per 24 h for 72 h) enhance cell proliferation, neuronal differentiation and the neurite outgrowth (Ma et al., 2016). Also, Marcantonio et al. (2010) measured increased expression of several differentiation markers during all-trans-retinol induced differentiation of neuroblastoma BE(2) cells when exposed to ELF-MF (50 Hz, 1 mT, 24 -72 h). Additionally, four independent studies illustrated that ELF-MF (50 Hz, 1-5 mT, 192 – 288 h) exposure of bone marrow-mesenchymal stem cells induces neuronal differentiation without the addition of a growth factor, resulting in the appearance of specific cellular structures and also electrophysiological properties of neurons (Bai et al., 2013; Cho et al., 2012; Kim et al., 2013; Seong et al., 2014). Early growth response protein 1 was described as one of the key transcription factors of ELF-MF induced neuronal differentiation (Seong et al., 2014). These reported ELF-MF effects on neuronal differentiation could suggest that ELF-MF indeed can influence the dynamics and efficiency of cellular differentiation processes.

The epigenetic code is reorganized during cellular differentiation and prone to be affected by environmental factors. Whether or not ELF-MF exposure has the potential to alter epigenetic patterns in a way that could drive cancerogenesis has not been assessed. There is evidence, however, that ELF-MF exposure (50 Hz, 1, 2 or 3 mT, 5'on/10' off, 72 h) may alter genome-wide DNA methylation (Liu et al., 2015). The observation that ELF-MF exposure at a flux density of 1 mT (50 Hz, 5'on/10' off, 72 h) a decreased global methylation levels along with the expression of DNMT1 and DNMT3b, whereas DNA methylation as well as DNMT1 and DNMT3b expression was increased following ELF-MF at a flux density of 3 mT (50 Hz, 5'on/10' off, 72 h). Another study investigated the chromatin conformation changes after low dose ELF-MF exposure (50 Hz, 20 μT, 1 h) of human

lymphocytes (Sarimov et al., 2011). Analysing the viscosity of chromatin, the authors found that relaxed chromatin becomes more condensed and compact chromatin more open, suggesting a convergence of chromatin states in response to ELF-MF exposure. Moreover, a paper was published recently by Baek et al. (2014), reporting that ELF-MF exposure (50 Hz sinus, 1 mT, 360 h) increases the reprogramming efficiency of somatic cells, involving the upregulation of the histone lysine methyltransferase Mll2, which triggers an enrichment of H3K4me3 in pluripotency genes.

3 Aims of the Thesis

Aberrations of the epigenome are a hallmark of human cancers including leukaemia, and indicate a loss of cellular identity (Bernstein et al., 2007). An overrepresentation of haematopoietic progenitor cells harbouring genetic aberrations in epigenetic modifiers is often observed in leukaemia, suggesting that defect in epigenetic mechanism contribute to leukaemogenesis (Greenblatt and Nimer, 2014). ELF-MF exposure was associated with an increased risk of childhood leukaemia, and therefore classified as "possibly carcinogenic" to humans (group 2B) (IARC, 2002). However, the underlying biophysical mechanisms have been remaining elusive. ELF-MF is unlikely to directly damage DNA (Adair, 1998; Focke et al., 2010) and thereby to induce cancer-promoting genetic aberrations. Yet, epigenetic stability can be affected by environmental factors, especially during differentiation-associated dynamic epigenetic programming (Feil and Fraga, 2011). Whether or not, ELF-MF can cause alterations of the epigenome has not been addressed. The **first aim** of my PhD thesis was to evaluate the influence of ELF-MF exposure on the establishment and the stability of key epigenetic modifications in haematopoietic cells. I - in collaboration with others, investigated the impact of exposure on the stability of key active (H3K4me2) and repressive (H3K27me3) histone modifications at genome scale in the leukaemic cell line Jurkat as well as on the cell type-specific genome-wide H3K4me2, H3K27me3 and DNA methylation pattern in *in vitro* differentiating human cord blood cells into the neutrophilic lineage. The results and expertise from this work were brought into a risk assessment workshop, which took place at the IARC in Lyon, France and confirmed the classification of ELF-MF as "possibly carcinogenic" to humans.

Acute myeloid leukaemia, the most common leukaemia in adults is characterized by an overrepresentation of neutrophilic progenitors and mutations in genes encoding epigenetic modifiers (Florean et al., 2011; Greenblatt and Nimer, 2014). To understand the underlying disturbance in cell differentiation and its contribution to leukaemogenesis, it is important to understand the physiological epigenetic changes established during differentiation. Previous studies investigated histone modifications and DNA methylation in isolated mature neutrophils and neutrophilic progenitors, respectively (Olins and Olins, 2005; Ronnerblad et al., 2014), and therefore did not provide information on the dynamics of these epigenetic modifications in the differentiating cell population. A **second aim** of my PhD thesis was to evaluate alterations of the epigenome during *in vitro* neutrophilic granulopoiesis. To this end, I - in collaboration with others, determined the regulatory role of alterations in DNA methylation and histone modifications at genome scale during lineage restriction of human neutrophils.

4 Results

The following section summarizes the results presented in the manuscripts provided in the appendix as well as supplementary results not included in the manuscripts.

4.1 ELF-MF exposure affects robustness of epigenetic programming during granulopoiesis (Appendix I)

ELF-MF is a widespread man-made environmental agent, brought forth by the increasing use of electronic appliances emitting MF at frequency around 50 Hz. Addressing public concerns about possible health effects, epidemiological studies pointed to a correlation between ELF-MF exposure and an increased risk of childhood leukaemia. This evidence lead to classification of ELF-MF as being "possibly carcinogenic" to humans (group 2B) (IARC, 2002). Studies in animal and cellular models were used to investigate the biological effects of ELF-MF exposure, but with inconclusive outcome (IARC, 2002; SCENIHR, 2015). Hence, the mechanism underlying a potential cancerogenic effect remained elusive. A number of studies indicated a genotoxic potential of ELF-MF exposure (Duan et al., 2015; Focke et al., 2010; Mihai et al., 2014), although based on theoretical consideration, the energy content of ELF-MF is not high enough to directly damage the DNA (Adair, 1998). As epigenetic alterations are known to be sensitive to environmental conditions (Feil, 2006; Feil and Fraga, 2011), we reasoned that ELF-MF exposure may affect the epigenome, rather than the genome, and thereby induce cancer promoting alterations.

To address whether ELF-MF influences the chromatin landscape of cancerous cells, we exposed the T cell lymphoma cell line Jurkat in exponential growth to ELF-MF (50 Hz sinus, 1 mT, 5’ on/10’ off) or a sham control (< 7 µT residual field) for 72 h and performed chromatin immunoprecipitation (ChIP) followed by next generation sequencing (ChIP-seq) of the histone modifications H3K4me2 and H3K27me3 (Appendix I, Supplementary Figure S1a). Additionally, we analysed the histone profiles of Jurkat cells treated with a low, sub-toxic dose of the histone deacetylase trichostatin A (10 nM TSA) for 72 h to assess the impact of a known epigenetic modulator. The results with low dose TSA provided a proof of concept that histone modifications H3K4me2 and H3K27me3 can be altered (Appendix I, Figure 1a, b). By contrast, we observed no significant difference when comparing ELF-MF and sham-exposed Jurkat cells, indicating that the genome-wide profiles of H3K4me2 and H3K27me3 marks is not significantly altered upon ELF-MF exposure in this leukaemic cell line (Appendix I, Figure 1c). In parallel and as a control we monitored health parameters of the cells as previous studies indicated an effect of ELF-MF exposure on cellular growth rates, cell cycle and cell viability (Brisdelli

et al., 2014; Focke et al., 2010; Santini et al., 2005), which may themselves affect histone modifications. However, ELF-MF exposure did not alter any of these parameters in the Jurkat cell line exposed for 72 h (Appendix I, Supplementary Figure 2).

The dynamic epigenetic changes occurring during cellular differentiation are likely to be particularly sensitive to disturbance by environmental factors (Feil and Fraga, 2011; Jaenisch and Bird, 2003; Noreen et al., 2014), and interference with the proper shaping of the chromatin landscape in this situation may lead to the loss of cell identity and development of cancer. To investigate whether ELF-MF influences the establishment of histone modifications and DNA methylation during the chromatin reorganisation in differentiating cells, we *in vitro* differentiated CD34+ cord blood cells into the neutrophilic linage under ELF-MF (50 Hz powerline, 1 mT, 5' on/10' off), parallel sham or no exposure (Appendix I, Supplementary Figure S1b). During this process, CD34+ cells differentiate into promyelocyes and later on into myelocytes and metamyelocytes. We found that neither the differentiation efficiency nor the cell proliferation was affected by ELF-MF exposure (Appendix I, Supplementary Figure 6). We noticed in ELF-MF exposed neutrophilic progenitors after 4 days a small but significant increase of apoptotic cells and a trend for a reduction of G1 and an increase of S phase cells, indicating a minor positive selection effect of the ELF-MF exposure (Appendix I, Figure 2a,b). We performed ChIP-seq for H3K4me2 and H3K27me3 before and after five days of differentiation, which produced high quality datasets clearly separating epigenetic pattern of different maturation stages (Appendix I, Figure 2c, Supplementary Figure S9 and S10). Yet, although the cells underwent a global epigenetic reorganisation in the differentiation process, we were not able to identify a single genomic region, showing a statistically significant alteration in the patterns of H3K4me2 or H3K27me3 during ELF-MF exposure (Appendix I, Figure 2d,e). Additionally, we addressed weather ELF-MF exposure alters the pattern of DNA cytosine methylation during haematopoietic differentiation by analysing the genome-wide DNA methylation at single CpGs using an Illumina Infinium HumanMethylation 450 array. Again, we observed an excellent correlation between all biological replicas and a clear separation of the different maturation stages (Appendix I: Figure 3a, Supplementary Figure S12). Like the histone modifications, DNA methylation patterns dramatically changed during differentiation from CD34+ cells into the neutrophilic lineage, but no single CpG was differently methylated after ELF-MF exposure (Appendix I, Figure 3b,c). From these results, we conclude that ELF-MF exposure does not influence the formation of cell type-specific DNA methylation patterns.

Although we did not observe genomic regions with significantly altered histone modifications or DNA methylation, we identified some genomic locations with up to 16-fold differential occupancy by H3K4me2, H3K27me3 marks or DNA methylation between ELF-MF and sham exposed cell

populations. We elaborated that these genomic locations did not reach statistical significance due to high variation in replicate samples. This variation occurred in the background of an overall good correlation between replicates in an apparently non-random manner. H3K4me2 and H3K27me3 read counts in all tiles revealed exposure condition-dependent effects on the variability of replicate samples, both in Jurkat cells and neutrophilic progenitors (Appendix I, Figure 4a,b). In Jurkat cells, we observed the highest increased replicate variability of H3K4me2 and H3K27me3 following low dose TSA, indicating that epigenetic disturbance can be measured at the level of variance between replicate populations (Appendix I, Figure 4c). In ELF-MF exposed Jurkat cells, we observed an increased replicate variability of H3K27me3 but a decreased variability of the H3K4me2 modification. On the other hand, in the epigenetically more plastic differentiating neutrophilic progenitors, the variability of both histone modifications was decreased in the ELF-MF exposed population (Appendix I, Figure 4d,e). Additionally, the variability of DNA methylation was also decreased in neutrophilic progenitors upon ELF-MF exposure (Appendix I, Figure 4f). These results suggest that ELF-MF exposure can affect the robustness of the establishment and/or maintenance of key epigenetic modifications, particularly in differentiating cell populations.

We further investigated whether the variability of the epigenetic features is randomly distributed over the genome or located in specific genomic regions such as gene promoters, exons, introns and intergenic regions or bivalent domains identified by co-occupancy of H3K4me2 and H3K27me3 marks in our ChIP-seq data. In ELF-MF exposed Jurkat cells, the H3K4me2 marks were more robust while the H3K27me3 modifications were more variable, irrespective of the context (Appendix I, Figure 5a,b). By contrast, H3K27me3 was clearly more variable in TSA treated Jurkat cells at promoters and bivalent domains, consistent with the preferential location of histone acetylation at promoters or enhancers (Nicholson et al., 2015). In neutrophilic progenitors, we observed the highest reproducibility of H3K4me2 and H3K27me3 at promoters and bivalent domains and the pronounced replicate variability at introns and intergenic regions. ELF-MF exposure decreased replicate variability of H3K4me2 at all genomic features except at bivalent domains, whereas the variability of H3K27me3 was reduced without much preference for any of the genomic sites assessed (Appendix I, Figure 5c-f). Additionally, we found that the variability of DNA methylation is reduced at all genomic features upon ELF-MF exposure (Appendix I, Figure 5g). These results indicate that ELF-MF affects the robustness of epigenetic marks in a partially genomic context-dependent manner, with the most distinctive feature being the H3K4me2 modification at bivalent domains.

Bivalent domains are associated with transcriptionally poised chromatin and are present at regulatory elements of developmental genes that will be activated or repressed during differentiation (Bernstein et al., 2006; Boland et al., 2014). Hence, bivalent domains are highly

dynamic but seemingly more protected from ELF-MF impact during differentiation. Therefore, we investigated whether the reorganisation of the chromatin during differentiation affects the robustness of the epigenetic features in ELF-MF exposed neutrophilic progenitors. Upon ELF-MF exposure, the H3K4me2 modification was more robust at genomic locations with only the active mark present but not at bivalent domains, regardless of their dynamics during differentiation (Appendix I, Figure 6a). By contrast, we observed the most pronounced decrease of the replicate variability of H3K27me3 in genomic regions losing the repressive histone mark during differentiation, regardless of bivalency. We then examined the relationship between the differentiation dynamics of the histone modifications and the ELF-MF effect on their relative enrichment. We found the highest difference in H3K4me2 occupancy in non-bivalent tiles gaining H3K4me2, while we observed the highest exposure effect on H3K27me3 occupancy in tiles lost the modification during differentiation (Appendix I, Figure 6b). In addition to this differentiation-dependent pattern of histone modification, we also observed that the variability of DNA methylation of ELF-MF exposed cells is significantly reduced at sites losing mC during differentiation but not changed at CpGs gaining methylation (Appendix I, Figure 6c).

In conclusion, our data suggest that ELF-MF exposure does not globally and deterministically influence epigenetic modifications of differentiated leukaemic and differentiating haematopoietic cells. Nevertheless, we noticed that ELF-MF may affect the robustness of epigenetic programming of histone modifications and DNA methylation in the course of chromatin reorganisation during neutrophilic granulopoiesis. Our data suggest that ELF-MF stabilizes mainly epigenetic features associated with open chromatin marked by H3K4me2 or in chromatin changing from a repressive to an active state during differentiation marked by losing H3K27me3 and/or undergoes DNA demethylation.

Contribution: I conceived, performed and analysed the *in vitro* exposure experiments of leukaemic cells as well as during the neutrophilic differentiation. I analysed the cell cycle, amount of apoptotic cells and the different maturation stages by flow cytometry. I determined the histone modifications by ChIP, prepared the ChIP samples for next-generation sequencing and contributed to the bioinformatic analysis of the ChIP-seq data. I prepared the DNA samples for the DNA methylation array, did the variance analysis of the histone modifications and DNA methylation and wrote the manuscript in the Appendix I.

4.2 Dynamics of Histone Modifications and DNA Methylation during *in vitro* Granulopoiesis (Appendix II)

During cellular differentiation, epigenetic modifications shape the chromatin structure and the DNA accessibility, determining the gene expression pattern required for cell lineage commitment. Active epigenetic features present at pluripotency genes change to a repressed state and repressed or poised epigenetic features of lineage-specific genes are converted to transcriptionally permitted states, altogether resulting in a global reorganisation of the epigenome (Boland et al., 2014; Hawkins et al., 2010; Kraushaar and Zhao, 2013). Regulatory epigenetic modifications include the acetylation and methylation of histone tails and the methylation of DNA cytosine bases (Bernstein et al., 2007; Cedar and Bergman, 2011), altogether establishing three main classes of chromatin; active, repressed and chromatin poised for gene expression. Active chromatin is marked by H3K4me2, H3K4me3 and H3K27 acetylation, whereas chromatin correlating with gene repression is characterized by H3K27me3 and H3K9me3. Poised chromatin is occupied by active as well as repressive marks and is preferentially located at regulatory elements of developmental genes in stem cells (Boland et al., 2014; Hawkins et al., 2010; Kraushaar and Zhao, 2013). In gene regulatory regions with intermediate to high CpG content, DNA methylation negatively regulates gene expression; cytosine methylation is associated with chromatin compaction, absence of methylation with open chromatin (Bernstein et al., 2007; Nicholson et al., 2015). Epigenetic aberrations are a hallmark of cancers such as leukaemia. The most common leukaemia in adults is acute myeloid leukaemia, characterized by an accumulation of cells in progenitor stages especially neutrophilic progenitors (Krebsliga, 2016; Mehdipour et al., 2015; Zenhäusern et al., 2003). The blocked differentiation of progenitor cells together with alterations in epigenetic modifiers for DNA methylation and histone modifications found in leukaemic cells, indicating a defect in the epigenetic control during differentiation. To understand the driving force of epigenetic aberration in cancerogenesis, it is important to determine the normal shaping of the chromatin landscape during a normal cellular differentiation. The epigenetic programming during human neutrophilic granulopoiesis has not been investigated systematically, although few studies analysed histone modifications and DNA methylation in isolated mature neutrophils and neutrophilic progenitors, respectively (Olins and Olins, 2005; Ronnerblad et al., 2014). Therefore, we set out to monitor the dynamics of histone modifications and DNA methylation during an *in vitro* neutrophilic differentiation, using a well-defined *in vitro* system. We differentiated human CD34+ cord blood cells into the neutrophilic lineage for 14 days. Cells differentiated from the CD34+ progenitor stage mainly to a promyelocytes state within five days and into myelocytes and metamyelocytes within nine days of differentiation (Appendix II, Figure 1a and Supplementary Figure 1).

We addressed the dynamic pattern of DNA cytosine methylation during haematopoietic differentiation by analysing the genome-wide DNA methylation at single CpGs using an Illumina Infinium HumanMethylation 450 array (Appendix II, Figure 1). The pattern of DNA cytosine methylation was dramatically altered during neutrophilic granulopoiesis, with the highest changes at lineage commitment between CD34+ cells and neutrophilic progenitors after five days of differentiation. In total, we observed more CpG loci losing than gaining (FDR-adjusted *P* value < 0.05, log2 fold change [FC] > ±0.6) DNA methylation especially at lineage commitment with 3'882 and 2'977 CpGs, respectively; only at the latest stage of differentiation comparing progenitors after nine and 14 days more CpGs are gaining DNA methylation (17 and 419, respectively, Appendix II, Figure 1b). The majority of sites with DNA methylation changes are either consistently gaining or losing methylation during the entire differentiation (Appendix II, Figure 1c,d). At lineage commitment, CpGs losing DNA methylation are preferentially located at introns and outside of CpG islands (CGI) at CGI shelfs, whereas CpGs gaining DNA methylation are enriched at promoters and CGI (Appendix II, Figure 1e,f). In addition, we found that CpGs losing methylation were preferentially associated with genes that become activated in neutrophils, while methylation gain was observed in genes important in other blood lineages (Appendix II, Figure 1g). Our data therefore suggest an important regulatory role of DNA demethylation in neutrophilic lineage restriction. These results are in line with previous reports indicating a genome-wide loss of DNA methylation between GMPs and promyelocytes, and that myeloid-specific genes are repressed through DNA methylation in HSCs and become activated by DNA demethylation (Ko et al., 2010; Ronnerblad et al., 2014; Trowbridge et al., 2009).

HSCs are characterized by a high number of bivalent domains co-occupied by active H3K4me2 and H3K4me3 as well as repressive H3K27me3 marks, while mature neutrophils have a high amount of heterochromatin containing repressive histone modifications (Cui et al., 2009; Navakauskiene et al., 2014; Olins and Olins, 2005). During *in vitro* neutrophilic differentiation, we investigated the dynamic reorganisation of the H3K4me2 and H3K27me3 modifications by ChIP-sequencing (Appendix II, Figure 2). We observed a fundamental and widespread reorganisation of both histone modifications at the transition of CD34+ cells into neutrophilic progenitors after five days, but as well later on in the differentiation between progenitors after five and nine days (Appendix II, Figure 2a,b,d). Overall, we found in both time periods of differentiation more genomic locations that are losing (log2 FC < -0.6, FDR-adjusted *P* value < 0.05) than gaining (log2 FC > 0.6, FDR-adjusted *P* value < 0.05) H3K4me2 modifications (t5/t0: 11'260 and 8'358; t9/t5: 12'186 and 6'438, respectively, Appendix II, Figure 2a). In contrast, we revealed a higher number of regions gaining than losing H3K27me3 modifications (log2 FC >± 0.6, FDR-adjusted *P* value < 0.05) in both time periods during differentiation (t5/t0: 7'914 and 6'260, t9/t5: 9'563 and 7'204, respectively, Appendix II, Figure 2b). Generally, at genomic

locations undergoing differentiation associated alterations in both histone modifications, H3K4me2 marks were preferentially lost and H3K27me3 gained during differentiation (Appendix II, Figure 2c). Genomic locations showing H3K4me2 changes are enriched at introns, those showing H3K27me3 changes at intergenic regions and promoters, while genomic regions with alterations in both histone modifications are preferentially located at gene promoters (Appendix II, Figure 2f). Also, alterations in H3K4me2, H3K27me3 or both histone modifications occur predominantly at genes important in other lineages than neutrophils (Appendix II, Figure 2g). Overall, we conclude that the majority of the observed histone modification changes point to an overall converting chromatin into a more compact state during differentiation, leaving lineage-specific genes in an active state.

We found the highest alterations of DNA methylation and histone modifications at lineage commitment. To address the correlation of the different epigenetic features to each other, we analysed genomic locations undergoing differentiation associated changes in DNA methylation and histone modifications (Appendix II, Figure 3a). We determined that genomic regions with histone modification and DNA methylation changes are enriched at gene promoters and active enhancers, and they are located closer to the transcription start site than regions with only alterations of histone modifications (Appendix II, Figure 3b-d). During lineage commitment, moreover, genomic locations with changes in H3K4me2 and DNA methylation showed either loss of H3K4me2 and gain of DNA methylation at CpGs or gain of the active mark and loss of DNA methylation, indicating the negative correlation of these epigenetic marks (Appendix II, Figure 4a). By contrast, genomic locations undergoing H3K27me3 and DNA methylation changes at lineage commitment are predominantly characterized by a gain of the repressive histone mark as well as of DNA methylation. Genomic regions with concomitant changes in all three epigenetic features lose preferentially the active H3K4me2 mark and gain H3K27me3 as well as DNA methylation, indicating a general transition towards a more repressed chromatin state (Appendix II, Figure 4a,b). Additionally, such regions are located at genes important in cellular development of other lineages, including erythroid cells, leukocytes or natural killer cells (Appendix II, Figure 4c). We observed only two neutrophil-specific genes activated through a concomitant increase of H3K4me2, loss of H3K27me3 and CpG methylation during differentiation (Appendix II, Figure 4b,c). From these results, we conclude that genomic regions dynamically regulated through histone modifications and DNA methylation lose predominantly the active mark and increase the repressive marks, leading to gene silencing. Important pluripotency and developmental genes are associated with a poised chromatin state in HSCs, allowing a fast epigenetic adaptation during differentiation and a rapid activation or repression of the gene (Boland et al., 2014). To investigate the time-dependency of the epigenetic repression in genomic regions occupied by poised chromatin in HSCs, we analysed genomic regions repressed

through alterations in H3K4me2, H3K27me3 and *de novo* DNA methylation in both time periods of neutrophilic granulopoiesis (Appendix II, Figure 5). We determined that the loss of H3K4me2 occurred to equal parts in both time periods during differentiation, whereas *de novo* DNA methylation and gain of the H3K27me3 modification occurs preferentially at lineage commitment. The majority of genomic regions with a poised chromatin state in CD34+ cells were preferentially repressed at lineage commitment through gaining of the H3K27me3 mark alone or in combination with *de novo* DNA methylation, and occasionally only by DNA methylation alone.

Overall, our study provides novel insight into the genome-wide dynamics of histone modifications and DNA methylation during human granulopoiesis. We report a fundamental reorganisation of the chromatin landscape during granulopoiesis most pronounced at the transition of CD34+ cells into the neutrophilic lineage, shaping an overall more compact chromatin. The global perspective does not reveal context specific local chromatin dynamics that seems to be relevant for the establishment of cell type-specific gene expression. Directed for local pattern changes, the data suggest a regulatory role of DNA demethylation in the establishment of neutrophil-specific gene expression. By contrast, our data indicate that epigenetic repression of pluripotency and developmental genes marked by a poised chromatin state in CD34+ cells occurred preferentially through gaining of H3K27me3 alone or concomitant with *de novo* DNA methylation. These results suggest a role of *de novo* DNA methylation in stabilizing gene repression or subsequent long term silencing, rather than in initiating gene silencing. Our results are in line with previous studies indicating that myeloid-specific genes are poised through DNA methylation in HSCs and activated by DNA demethylation, while lymphoid-specific genes are keep in a poised state in HSCs through H3K27me3, leading to activation by histone modification changes rather than DNA methylation alterations (Cedar and Bergman, 2011; Ko et al., 2010; Oguro et al., 2010; Trowbridge et al., 2009).

Contribution: I conceived, performed and analysed the *in vitro* neutrophilic granulopoiesis. I analysed the different maturation stages by flow cytometry. I determined the histone modifications by ChIP, prepared the ChIP samples for next-generation sequencing and contributed to the bioinformatic analysis of the ChIP-seq data. I prepared the DNA samples for the DNA methylation array, and did all the analysis on the observed alterations of histone modifications and DNA methylation and wrote the manuscript in the Appendix II.

4.3 Extremely-Low-Frequency Magnetic Fields and Risk of Childhood Leukaemia: A Risk Assessment by the ARIMMORA Consortium (Appendix III)

ELF-MF exposure has been classified as being “possibly carcinogenic” to humans (group 2B) due to an association with an increased risk of childhood leukaemia in epidemiological studies, but in the absence of a plausible scientific rationale for an underlying mechanism (IARC, 2002). The ARIMMORA project funded by the European Commission aimed to explore the underlying biophysical mechanism by developing and applying novel experimental and computational techniques. Our investigations in the field of epigenetics (Appendix I), together with experts in the fields of ERK signalling, leukaemic *in vivo* models, *in vivo* toxicology and EMF-sensitive animal models as well as specialists in exposure assessment and biophysical modelling were contributing to this long collaborative project. Based on the results on the individual partners, the consortium performed a re-evaluation of the potential carcinogenicity of ELF-MF; according to IARC rules (published commentary of risk assessment in appendix III).

The evaluation was based on the results of the ARIMMORA project and on recent work performed outside the consortiums, published until March 2015. The standardised IARC evaluation scheme was applied, assessing the evidence of carcinogenicity in human and in experimental animals (*in vivo* studies) separately, and classifying the cumulative evidence as sufficient, limited, inadequate or lacking. Additionally, mechanistic data obtained from *in vitro* experimentations were categorised in weak, moderate or strong. The combination of evidence in the three groups defines the classification of agent into group 1 (carcinogenic to humans), group 2A (probably carcinogenic to humans), group 2B (possibly carcinogenic to humans), group 3 (not classifiable as to its carcinogenicity to humans) or group 4 (probably not carcinogenic to humans).

The daily mean exposure levels of children is below 0.1 µT, only a small fraction of children (1-2%) is exposed to ELF-MF with a daily average of 3 µT or more. Recent studies established an association between ELF-MF and childhood leukaemia (two fold increased risk) at average exposure levels for 24 h above 0.3 -0.4 µT, whereas no significant correlation could be found for lower exposure levels (Ahlbom et al., 2000; Kheifets et al., 2010; Schuz, 2011). Measurements within ARIMMORA confirmed these typical daily exposure levels and highlighted the importance of child’s behaviour around powerlines (Struchen et al., 2015). Additionally, simulation of exposure with ELF-MF of pregnant women revealed the highest electromagnetic field to be on the skin, fat, and subcutaneous adipose tissue of the foetus during all gestational ages and increased continuously with gestational age (Liorni et al., 2014). Within ARIMMORA, no additional epidemiological studies were performed. However, most recent epidemiological studies indicated a possible carcinogenicity of ELF-MF (IARC,

2002; SCENIHR, 2007, 2009, 2015; WHO, 2007), but doubts about methodological limitations cannot be ruled out. Therefore, the evaluation of the evidence of carcinogenicity was considered “limited” in humans by the ARIMMORA consortium.

One goal of the ARIMMORA project was the generation of a novel mouse model for B-cell acute lymphoblastic leukaemia (B-ALL), the most common human childhood leukaemia. This was achieved by constitutively expression of the fusion gene *ETV6-RUNX1 (*also known as *TEL-AML1)* in the haematopoietic stem/progenitors compartment of mice (Martin-Lorenzo et al., 2015). In these transgenic mice, the influence of ELF-MF exposure in the development of B-ALL was analysed, by exposing mice throughout embryonic life and after birth until three month of age. From a total of 30 transgenic mice exposed to ELF-MF (50 Hz, 1.5 mT, 10’ on/5’off, 20 h/day), one mouse developed ETV6-RUNX1-positive precursor B-ALL at 14 month of age compared to none of the 65 control animals. Despite these findings the consortium concluded that more studies are necessary to substantiate the possible adverse impact of exposure. Therefore, in combination with the published literature, the evidence of carcinogenicity in experimental animals was considered by the ARIMMORA consortium as “inadequate”.

The weakness of previous risk assessments was the lack of support from mechanistic evidence (IARC, 2002; SCENIHR, 2007, 2009, 2015; WHO, 2007). For many years of research, it remains difficult to integrate all reported effects and non-effects of ELF-MF exposure into a consistent chain of causality, without the identification of the underlying mechanism. Therefore, ARIMMORA intended to elucidate possible biological mechanism. Animal studies within ARIMMORA showed transient reduction of CD8+ T-cells in ELF-MF exposed (50 Hz; 10 µT, 1 mT or 10 mT) CD-1 and B6CBA mice, after 28 days. These observations were corroborated by findings in ELF-MF exposed *ETV6-RUNX1* transgenic mice, showing a consistent decrease in total numbers of CD8+ T-cells at 2 month of age. These results suggest that levels of CD8+ T-cells could serve as a biomarker for ELF-MF exposure. Furthermore, experiments in Lewis and Fischer rats indicated that cytokines altered by ELF-MF exposure (50 Hz, 0.1 mT) were involved in T-cell functions or influenced the number of T-cells. *In vitro* studies within ARIMMORA investigated the ERK signalling cascades and epigenetic regulation (our part). Surprisingly, ELF-MF exposure induced ERK1/2 activation in cell types at intensities as low as 0.15 µT and was detectable within minutes of exposure. Furthermore, ERK1/2 activation was decreased by co-exposure with blue light, suggesting that ELF-MF induced ERK activation could be controlled by the photoreceptor cytochrome. Analysis of activating and repressing histone modifications in exposed (50 Hz, 1 mT, 5’ on/10’ off) and sham exposed Jurkat cells did not indicate a consistent influence on the epigenome of ELF-MF on fully differentiated cells. Minor epigenetic changes were observed on activating and repressing histone marks upon ELF-MF exposure (50 Hz

powerline, 1 mT, 5’ on/10’ off) in differentiating haematopoietic stem cells, suggesting that ELF-MF exposure is able to influence the epigenome to a small extent (final results see Appendix I). As the functional relevance and association to carcinogenesis of the observed mechanistic data in the *in vivo* and *in vitro* studies within ARIMMORA remains to be clarified and no mechanism was meanwhile identified outside ARIMMORA, the overall mechanistic evidence can be considered moderate while the contribution to carcinogenesis remains weak.

The combination of the limited evidence of carcinogenicity in humans and the inadequate evidence of carcinogenicity in experimental animal with only weak evidence from mechanistic studies resulted in the classification of ELF-MF as “IARC Group 2B” (possible carcinogenic to humans) (Appendix III, Figure 1).

Contribution: I planned and performed the *in vitro* exposure experiments in leukaemic cells as well as during a haematopoietic differentiation, determined histone modifications (H3K4me2 and H3K27me3) by ChIP, prepared the ChIP samples for next-generation sequencing and contributed to the bioinformatic analysis of the ChIP-seq data. Furthermore, participated at the ARIMMORA risk assessment meeting at IARC and was involved in the writing of the risk assessment.

4.4 Supplementary Results

4.4.1 ELF-MF exposure does not influence cell viability and cell cycle distribution in the leukaemic cell line REH

Epidemiological studies determined an association between ELF-MF and leukaemia, but the underlying cellular mechanisms are not clear. Studies in animal and cellular models were used to investigate biological effects of ELF-MF exposure, yielding inconclusive information. Previous studies described effects of ELF-MF exposure on cellular growth rates and apoptosis (Brisdelli et al., 2014; Focke et al., 2010; Santini et al., 2005), but not consistently and depending on cell type or exposure conditions. We observed (Appendix I) that ELF-MF exposure has no influence on cell proliferation, cell cycle distribution and the amount of apoptotic cells when the T cell lymphoma cell line Jurkat was exposed for the duration of 3.5 cell cycles (50 Hz sinus, 1 mT, 5’ on/10’ off). To address a potential cell type dependency, we exposed another leukaemic cell line, the B cell precursor leukaemia REH, in the exponential growth phase to a sinusoidal intermitted ELF-MF (50 Hz sinus, 1 mT, 5’ on/10’ off) or a sham control (< 7 µT residual field) for 144 h, corresponding to again 3.5 cell cycles (Figure 10a). As in all experiments, the exposure settings were blinded for the experimenter.

REH cells proliferated exponentially during the 144 h analysed (Figure 10b). Before the exposure, 25% and 10% of the cells in the population were in S and G2 phase, respectively (Figure 10c). After 72 h of exposure a transient alteration of the cell cycle progression with a decrease of G1 and an increase of S and G2 phase cells occurred in all conditions. We measured around 95% living cells after 72 h of ELF-MF or sham exposure, whereas after 144 h the apoptotic and dead cells increased to 9%. Exposure of REH cells for 3.5 cell cycles (144 h) did not significantly affect either the overall proliferation of the cell culture, the proportion of apoptotic cells nor the cell cycle distribution at all assessed time-points (Figure 10b-d).

Together with the results in the Jurkat cells (Appendix I), we conclude that ELF-MF exposure in a highly controlled experimental setup, does not affect viability and proliferation of leukaemic cells. The discrepancy of our results to previous studies might be explained by cancer cell-specific features, cell type-specific sensitivity to ELF-MF intensities, different magnetic field characteristics used (static, dynamic, frequency and intensity) or limited exposure times (Juutilainen et al., 2006; Mangiacasale et al., 2001; SCENIHR, 2015; Yoon et al., 2014)

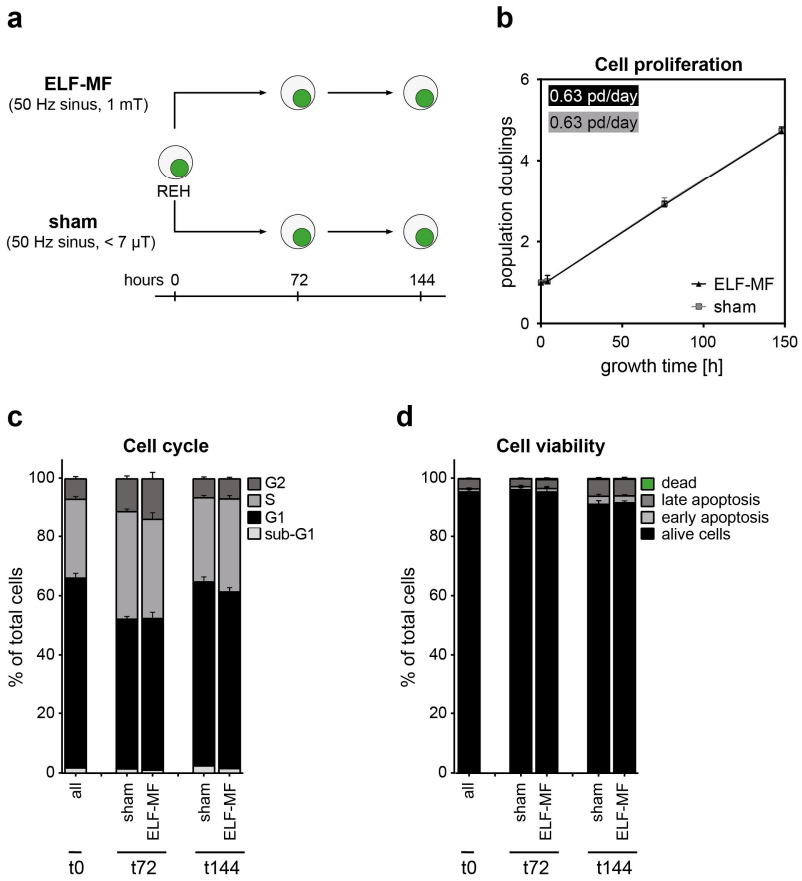

Figure 10: ELF-MF exposure does not alter proliferation and viability of cultured REH cells (a) Blinded for the operator, the leukaemic cell line REH cells was exposed to ELF-MF (50 Hz sinus, 1 mT, 5' on/10' off), sham (< 7 µT residual field) for 144 h. (b) Starting with $3x10^5$ cells/mL, the proliferation was monitored by cell counting at the indicated time-points. Average population doublings of independent biological replicates (n=4) in function of culture time were calculated and statistically analysed by ANOVA (*P < 0.05) and Student's t-test. Error bars indicate SEM. (c) Cell cycle profiles were assessed by flow cytometry, before (t0) and after exposure to ELF-MF, or sham at the indicated time-points. Data represent the mean proportion of cells in the different cell cycle phases with SEM (n=4). (d) Analysis of apoptosis by flow cytometry at the indicated time-points of exposure by Annexin-V/PI staining, discriminating alive, apoptotic and dead/necrotic cells. Data represent mean percentage of cells in different states of cell viability with SEM (n=4). Flow cytometry data were analysed by FlowJo software and statistically analysed by χ^2 test for each replica (* P < 0.05) and Student's t-test.

Methods

Cell culture and ELF-MF exposure

REH cells (B cell precursor leukaemia) were cultured in RPMI-1640 medium supplemented with 2 mM L-glutamine, 1 mM Na-pyruvate, 10% FCS and 0.6x penicillin/streptomycin (Sigma-Aldrich) at 37°C in a humidified atmosphere with 5% CO_2. Fresh medium was supplied every 48 h. For ELF-MF exposure experiments, cells were seeded at a density of $3x10^5$ cells/mL and grown for the indicated time without addition of fresh medium. The exposure system sXc-ELF (IT'IS, Zurich, Switzerland) allows for a well-controlled exposure with ELF-MF (Schuderer et al., 2004). The selected exposure for the

leukaemic cell line was sinusoidal ELF-MF (50 Hz, 1 mT, 5' on/10' off) or sham for approximately 3.5 cell cycles (144 h). The electric field caused by the coil was shielded and the magnetic field uniformity was better than 1% (SD). Each coil was place inside a µ-metallic box and the boxes placed side by side in the same incubator to decouple the coils, to shield the electric and magnetic fields generated by the incubator and to ensure the same environmental conditions (temperature, humidity and CO_2). The field attenuation between the coils was at least a factor of 150, i.e., the shame exposure was anywhere less than 7 µT compared to the uniform exposure of 1 mT. The exposure system meets the general criteria established in Kuster and Schoenborn (2000). Randomized assignment of ELF-MF and sham exposure conditions to the two chambers allows experiments blinded for the observer. Continuous temperature monitoring confirmed that the temperature difference between the exposure chambers was less than 0.1°C.

Cell cycle analysis and apoptosis measurement by flow cytometry

For the cell cycle analysis, 20-50x10^3 cells were fixed with cold 70% ethanol overnight. Cells were collected by centrifugation, resuspended in 1 mg/mL RNase A (in 200 mM Tris-HCl pH 7.5 and 200 mM NaCl) and incubated at 37°C for 30 min. After addition of 0.5 mg/mL pepsin (in 0.2% HCl) and incubation for another 15 min at 37°C, the cells were stained with propidium iodide (100 µg/mL in PBS, pH 7.5) and incubated on ice for at least 30 min. The number of apoptotic cells in the population was estimated by the Annexin-V Alexa488/PI kit (Invitrogen) according to the provider's recommendations. 20-50x10^3 cells were blocked on ice in Annexin-binding solution supplemented with 1% bovine serum albumin for 15 min before staining with the FITC-anti-Annexin V antibody for 20 min at RT, followed by washing three times with Annexin-binding solution. PI (Invitrogen) or DAPI was added before analysing the cells. All samples were measured using a FACS cytometer (Beckton Dickinson) and analysed by FlowJo Software. Data were statistically analysed by χ^2 test for each replica as well as pairwise comparison by Student's t-test using Graphpad Prism.

5 Concluding Discussion and Outlook

Cancerous tissues are characterized by genetic and epigenetic alterations. Histone modification and DNA methylation changes shape the chromatin structure during differentiation in a cell type-specific manner. Environmental factors can exert influence on this process, perturb the establishment and/or maintenance of cell identity, which can promote the development of cancer (Feil and Fraga, 2011; Shen and Laird, 2013). During my PhD studies, I investigated the effect of ELF-MF exposure, as an environmental factor, on epigenetic modifications in differentiating haematopoietic stem cells as well as in leukaemic cells.

Exposure to ELF-MF, which represents a common situation due to electric power supply, has been increasingly associated with an increased risk of childhood leukaemia (IARC, 2002). However, the mechanisms remain elusive. As the energy content of ELF-MFs is orders of magnitudes below of what would be required to affect chemical bonds in DNA (Adair, 1998), we proposed that ELF-MF may affect the epigenome, instead of the genome, and thereby promotes cancerous transformation. Together with collaborators, I analysed alterations in the active H3K4me2 and repressive H3K27me3 histone marks as well as in DNA methylation at genome scale during a well-controlled *in vitro* neutrophilic differentiation. In addition, activating and repressive histone marks were analysed in leukaemic Jurkat cells. We observed that after ELF-MF exposure of 3 days, the pattern of H3K4me2 and H3K27me3 of terminally differentiated leukaemic cells is not significantly altered. The suitability and sensitivity of our approach was confirmed by non-toxic treatment with the histone deacetylase inhibitor trichostatin A, which dramatically altered the histone methylation pattern. During neutrophilic differentiation, ELF-MF exposure did not significantly impact histone modifications and DNA methylation, although the chromatin landscape undergoes a fundamental reorganisation during haematopoietic differentiation. These results indicate an absence of a global effect of ELF-MF exposure on epigenetic modifications of leukaemic cells and differentiating CD34+ cells, at least in our experimental setup. A previous study proposed that ELF-MF exposure can alter the genome-wide DNA methylation in mouse spermatocytes (Liu et al., 2015). This discrepancy to our results can be explained by the two different cell systems or cell type-specific responses to ELF-MF. In addition, ELF-MF exposure might induce spontaneous and random spermatogenesis, which is accompanied by extensive differentiation-dependent DNA methylation changes. It was previously reported that ELF-MF exposure enhances differentiation efficiency in neurons, correlating with a gain of H3K9 acetylation at specific neuronal genes (Jung et al., 2014; Leone et al., 2014; Ma et al., 2014). In addition, the reprogramming efficiency of somatic cells is mediated by the histone methyltransferase Mll2 (Baek et al., 2014). Our haematopoietic differentiation system was controlled by the growth

factor G-CSF and the cytokines SCF and Flt-3 ligand, allowing a reproducible differentiation towards the neutrophilic lineage. We did not observe any significant alterations in the differentiation efficiency following ELF-MF exposure measured by the distribution of different maturation stages. However, at lineage commitment, we found an increase of apoptotic cells and a slight transient non-significant alteration of cell cycle progression with an increase in S phase and a decrease in G1 phase cells upon ELF-MF exposure. Our *in vitro* differentiation starts with a heterogeneous CD34+ stem cell population, including haematopoietic stem cells as well as the earlier progenitor types MPP, MLP, CMP, GMP and MEP (Seita and Weissman, 2010). However, MLPs and MEPs are no longer committed to differentiate into the neutrophilic lineage and undergo apoptosis through stimulation with only the neutrophilic growth factor G-CSF (Doulatov et al., 2012). Therefore, the increase of apoptotic cells upon ELF-MF exposure could indicate a small positive selection of neutrophilic cells due to a weak synchronisation effect of the cell population as more non-neutrophilic precursor cells are removed by apoptosis. In addition, the slight accumulation of ELF-MF exposed cells in S phase may suggest a disturbance of S phase progression and an accumulation of cells at the intra S phase DNA damage checkpoint, indicating a correlation to the ELF-MF induced increase of apoptotic cells due to cell death induction after an incomplete DNA repair during S phase (Bertoli et al., 2013; Malumbres and Barbacid, 2009). This small positive selection of neutrophilic cells, however, did not notably affect the overall dynamics and efficiency of granulopoiesis, and the underlying global reorganisation of epigenetic modifications.

Although, we did not observe any global effect of ELF-MF exposure on the epigenetic modifications, we observed genomic loci showing differential occupancy by H3K4me2, H3K27me3 or DNA methylation upon ELF-MF exposure. Hence, we found that ELF-MF exposure had an influence on the variability of the epigenetic modifications in the replicate samples. Treatment with TSA resulted in a dramatic replicate variability of the histone modifications in Jurkat cells, especially at promoters and bivalent domains. These variability pattern correlate with the preferred localisation of histone acetylation at gene promoters (Nicholson et al., 2015) and indicates that epigenetic perturbation can be measured at the level of sample variance. In Jurkat cells, we noticed a decreased replicate variability of H3K4me2 and an increased variability of H3K27me3, regardless of the genomic location. During neutrophilic differentiation, we observed an overall decreased replicate variability of histone modifications as well as DNA methylation after ELF-MF exposure. The discrepancy of the increased replicate variability of H3K27me3 in ELF-MF exposed Jurkat cells to the decreased variability of H3K4me2 in ELF-MF exposure Jurkat cells or of epigenetic modifications during differentiation could be explained by cancer cell-specific features (Mangiacasale et al., 2001), cell type-specific sensitivity to ELF-MF strength (Juutilainen et al., 2006; Yoon et al., 2014) or the different epigenetic plasticity in

terminal differentiated cells compared to differentiating cells. We observed a variability pattern depending on the chromatin state during the reorganisation of the epigenome in differentiating cells: epigenetic modifications of open chromatin or chromatin opening such as regions marked by H3K4me2, losing H3K27me3 and *de novo* DNA methylation during differentiation appear to be less variable upon ELF-MF exposure. The decreased replicate variability of histone modifications and DNA methylation preferential located at open chromatin or chromatin activated during differentiation may indicate an influence of the exposure on the establishment and/or maintenance of the epigenetic modifications, resulting in a stabilisation of epigenetic programming at sites of transcriptional activity and/or chromatin opening during differentiation. As we did not observe genomic locations with significantly altered histone modifications or DNA methylation analysed in a cell population, but observed that ELF-MF exposure can stabilise epigenetic features at open chromatin detected by sample variance between the replicates, we conclude that ELF-MF exposure has an effect on the robustness of the epigenetic modification in a stochastic manner, in only a small fraction of differentiating neutrophilic cells. Previous work indicated that ionizing radiation, induced five to 50 fold more DNA double strand breaks in decondensed than condensed chromatin (Takata et al., 2013; Yoshikawa et al., 2008). ELF-MFs are unlikely to directly damage DNA, but our results indicate as well that open or opening chromatin is more affected by ELF-MF exposure than compact chromatin. Another study showed that chromatin changes upon ELF-MF exposure depend on the initial chromatin state, meaning that relaxed chromatin becomes more compact and compact chromatin more open (Sarimov et al., 2011). Our haematopoietic differentiation starts with a heterogeneous population of expanded CD34+ cord blood cells (D'Arena et al., 1996; Engelhardt et al., 2002; Jobin et al., 2015) and a high replicate variance of epigenetic features, suggesting a slightly different initial chromatin state. ELF-MF exposure may result in the homogenisation of the epigenetic pattern by reducing heterogeneity in the cell population. Taken together, our results indicate that ELF-MF may affect the robustness of histone modifications and DNA methylation associated with transcriptional activity and/or chromatin opening during differentiation in a stochastic manner at individual cells.

However, our methodological approach of ChIP-seq and 450k Infinium array is limited in sensitivity and does not allow a detection of small differences between individual cells in a heterogeneous cell population. By analysing the variance between the replicates, we were able to avoid these limitations and determine the stochastic effect of ELF-MF on individual subpopulation of cells. Nevertheless, variance determination is in general highly sensitive to experimental variations (Altman and Krzywinski, 2014), especially with small amount of replicates. In order to limit this problem, we reduced the technical variations as much as possible, as documented in a good correlation of the

read counts in genomic regions between the replicates. Also, we observed a reduced replicate variability upon ELF-MF exposure on histone modifications and DNA methylation analysed by two different methodologies, and therefore we believe that the reduced variability is biologically relevant. To further investigate the stochastic effect of ELF-MF exposure on the robustness of epigenetic modifications in individual cells in a heterogeneous cell populations, epigenetic features could be analysed in a single cell approach together with ChIP-seq (Hyun et al., 2015; Rotem et al., 2015) and reduced representation bisulfite sequencing (Guo et al., 2015; Hu et al., 2016; Wang et al., 2015).

In summary, my data provide a proof-of-concept that ELF-MF exposure can potentially affect the patterns of the epigenetic code. The effect on the robustness of epigenetic modifications, appeared to be on a stochastic nature on individual cells, not globally detectable, are particularly notable in differentiating haematopoietic cells undergoing epigenetic programming. This epigenetic footprint of ELF-MF exposure, especially on open chromatin, is important information for further mechanistic studies investigating the potential mechanism underlying leukaemogenic effects of ELF-MF. In future studies, it will be interesting to address the epigenetic alteration of ELF-MF exposure in another cellular system, for instance during neuronal differentiation as previous studies investigated an enhanced differentiation efficiency and alterations in epigenetic features following ELF-MF exposure (Cheng et al., 2015; Jung et al., 2014; Ma et al., 2016; Ma et al., 2014).

A new risk assessment in 2015 by the ARIMMORA consortium evaluated the evidence for the contribution of ELF-MF exposure to carcinogenesis. We were part of the ARIMMORA consortium and our data provided a novel insight into a possible molecular aspect of ELF-MF exposure; however, the functional relevance remains to be determined. Therefore, the overall conclusion of the mechanistic data, including all publicly available data and the data generated in the ARIMMORA project was that evidence of ELF-MF contribution to carcinogenesis at this point is weak. Together with the evaluation of the epidemiological studies (limited evidence) and studies in animal models (inadequate evidence) the classification of ELF-MF as possibly carcinogenic to humans was not adjusted. So far most animal studies included in risk assessments do not suggest that ELF-MF exposure induces tumour development. However, a recent study from 2016 indicated a significant co-carcinogenic effect in rats exposed to sinusoidal 50 Hz magnetic field in combination with an acute low-dose γ radiation (SCENIHR, 2015; Soffritti et al., 2016). The increasing knowledge about possible effects of ELF-MF exposure and their molecular mechanism, will hopefully lead to a clear evaluation of the risk to public health in near future.

Epigenetic alterations are a hallmark of cancer including acute myeloid leukaemia (AML), the most common leukaemia in adults. AML is characterized by an increase in progenitor cell stages, particularly neutrophilic progenitors (50-60%), indicating an involvement of defects in control mechanisms of differentiation. However, dynamic epigenetic changes during neutrophilic granulopoiesis that could serve as a base line for the identification of cancerous abnormalities have not been discussed yet. In a second part of my studies, I investigated the dynamic alterations of the histone modifications H3K4me2 and H3K27me3 as well as of DNA cytosine methylation during the *in vitro* neutrophilic granulopoiesis. We showed a dynamic pattern of DNA methylation during *in vitro* granulopoiesis, with more CpGs gaining methylation at the beginning, in progenitor cells after five and nine days, and more CpGs losing methylation in progenitors after 14 days compared to the earlier progenitor stages. In total, we observed more CpGs losing than gaining DNA methylation, most pronounced at the transition of CD34+ cells into the neutrophilic lineage. These results are in line with previous studies reporting predominant loss of DNA methylation in human promyelocytes compared to GMPs and between mature neutrophils and promyelocytes (Bocker et al., 2011; Hodges et al., 2011; Ronnerblad et al., 2014). Further, we found that the patterns of active and repressive histone modifications H3K4me2 and H3K27me3, respectively, are dramatically altered during granulopoiesis. In general, we observed more genomic regions gaining H3K27me3 than losing it, while the H3K4me2 modification is preferentially lost. Moreover, genomic regions with alterations in both histone modifications mainly lost the H3K4me2 modification and gained H3K27me3. These results indicate a general compaction and silencing of chromatin during neutrophilic differentiation. In line with our results, human blood neutrophils were described to be enriched for heterochromatic regions containing repressive histone marks and low amounts of active marks (Navakauskiene et al., 2014; Olins and Olins, 2005). Genomic locations with changes in histone modifications and DNA methylation at lineage commitment were enriched at regulatory regions as promoters and active enhancers. We observed a dynamic regulation of the modifications at the same sites where a gain in H3K4me2 was generally associated with a loss in H3K27me3 and DNA demethylation, indicating a transcriptional activation, whereas a loss in H3K4me2 correlated with a gain in H3K27me3 and *de novo* DNA methylation, indicating transcriptional repression. We investigated that genomic locations with changes in all three epigenetic features investigated preferentially guide the chromatin towards a more repressed state and are present at genes important in other blood lineages, indicating an important role of concomitant alteration of histone modifications and DNA methylation in epigenetic repression. Additionally, we noticed that epigenetic repression of poised chromatin domains in CD34+ cells occurred preferentially at the point of lineage commitment between CD34+ cells and neutrophilic progenitors after 5 days of differentiation through a gain of H3K27me3 alone or in combination with *de novo* DNA methylation, but rarely with DNA methylation alone. These results

suggest that epigenetic repression of importent pluripotency genes was mainly initiated by H3K27me3 modifications before *de novo* DNA methylation and could indicate that DNA methylation stabilised gene repression or was involved in long-term silencing. By contrast, we observed a high amount of CpGs with DNA demethylation at lineage commitment present at neutrophil-specific genes and without simultaneous alterations at histone modifications. Therefore, our data indicate an important regulatory role of DNA demethylation in lineage restriction. These results are in line with previous studies showing that myeloid specific genes are poised through DNA methylation in HSCs and activated with DNA demethylation, indicated as *Dnmt1* deletion in HSCs resulted in an increase of myeloid progenitor cells, whereas *Tet2* depletion led to an impaired myeloid differentiation. On the other side, lymphoid specific genes are poised through H3K27me3 and activated through changes in histone modifications (Cedar and Bergman, 2011; Ko et al., 2010; Trowbridge et al., 2009). Overall our data provide an insight into the interplay between DNA methylation and histone modifications during neutrophilic differentiation, indicating their specific role in lineage restrictions and cell plasticity. In future studies it will be interesting to address the time-dependency of epigenetic alterations and gene expression, the correlation to heterochromatin marks like H3K9me3 and the role of individual epigenetic modifications in the course of carcinogenesis.

In conclusion, my studies provided novel insight into the landscape of histone modifications and DNA methylation in the course of a neutrophilic differentiation and how these patterns can be modified by ELF-MF. We observed a stochastic effect of ELF-MF exposure on the stability of epigenetic features, predominantly at open chromatin. These data may serve as a basis for further studies investigating the mechanism for ELF-MF induced leukaemogenic effects as well as for the establishment of biomarker panels for ELF-MF exposure assessment. Additionally, we investigated the regulatory role of DNA methylation and histone modifications during neutrophilic granulopoiesis. These data may provide information for further studies investigating chromatin epigenetic regulators as targets for leukaemia induced differentiation therapy, initiating the differentiation of cancerous cells into mature cells finally leading to cell death.

6 References

Adair, R.K. (1998). Extremely Low Frequency Electromagnetic Fields Do Not Interact Directly With DNA. Bioelectromagnetics, 136–137.

Ahlbom, A., Day, N., Feychting, M., Roman, E., Skinner, J., Dockerty, J., Linet, M., McBride, M., Michaelis, J., Olsen, J.H*., et al.* (2000). A pooled analysis of magnetic fields and childhood leukaemia. Br J Cancer *83*, 692-698.

Aloia, L., Di Stefano, B., and Di Croce, L. (2013). Polycomb complexes in stem cells and embryonic development. Development *140*, 2525-2534.

Altman, N., and Krzywinski, M. (2014). Points of significance: Sources of variation. Nature Methods *12*, 5-6.

Alvarez-Errico, D., Vento-Tormo, R., Sieweke, M., and Ballestar, E. (2015). Epigenetic control of myeloid cell differentiation, identity and function. Nat Rev Immunol *15*, 7-17.

Amouroux, R., Nashun, B., Shirane, K., Nakagawa, S., Hill, P.W., D'Souza, Z., Nakayama, M., Matsuda, M., Turp, A., Ndjetehe, E*., et al.* (2016). De novo DNA methylation drives 5hmC accumulation in mouse zygotes. Nat Cell Biol *18*, 225-233.

Amulic, B., Cazalet, C., Hayes, G.L., Metzler, K.D., and Zychlinsky, A. (2012). Neutrophil function: from mechanisms to disease. Annu Rev Immunol *30*, 459-489.

Anink-Groenen, L.C., Maarleveld, T.R., Verschure, P.J., and Bruggeman, F.J. (2014). Mechanistic stochastic model of histone modification pattern formation. Epigenetics Chromatin *7*, 30.

Arand, J., Spieler, D., Karius, T., Branco, M.R., Meilinger, D., Meissner, A., Jenuwein, T., Xu, G., Leonhardt, H., Wolf, V*., et al.* (2012). In vivo control of CpG and non-CpG DNA methylation by DNA methyltransferases. PLoS Genet *8*, e1002750.

Baek, S., Quan, X., Kim, S., Lengner, C., Park, J.K., and Kim, J. (2014). Electromagnetic Fields Mediate Efficient Cell Reprogramming into a Pluripotent State. Acs Nano *8*, 10125-10138.

Bai, W.F., Xu, W.C., Feng, Y., Huang, H., Li, X.P., Deng, C.Y., and Zhang, M.S. (2013). Fifty-Hertz electromagnetic fields facilitate the induction of rat bone mesenchymal stromal cells to differentiate into functional neurons. Cytotherapy *15*, 961-970.

Bannister, A.J., and Kouzarides, T. (2011). Regulation of chromatin by histone modifications. Cell Res *21*, 381-395.

Basile, A., Zeppa, R., Pasquino, N., Arra, C., Ammirante, M., Festa, M., Barbieri, A., Giudice, A., Pascale, M., Turco, M.C*., et al.* (2011). Exposure to 50 Hz electromagnetic field raises the levels of the anti-apoptotic protein BAG3 in melanoma cells. J Cell Physiol *226*, 2901-2907.

Bernstein, B.E., Meissner, A., and Lander, E.S. (2007). The mammalian epigenome. Cell *128*, 669-681.

Bernstein, B.E., Mikkelsen, T.S., Xie, X., Kamal, M., Huebert, D.J., Cuff, J., Fry, B., Meissner, A., Wernig, M., Plath, K*., et al.* (2006). A bivalent chromatin structure marks key developmental genes in embryonic stem cells. Cell *125*, 315-326.

Bertoli, C., Skotheim, J.M., and de Bruin, R.A. (2013). Control of cell cycle transcription during G1 and S phases. Nat Rev Mol Cell Biol *14*, 518-528.

Black, J.C., Van Rechem, C., and Whetstine, J.R. (2012). Histone lysine methylation dynamics: establishment, regulation, and biological impact. Mol Cell *48*, 491-507.

Blank, M., and Goodman, R. (2011). DNA is a fractal antenna in electromagnetic fields. Int J Radiat Biol *87*, 409-415.

Bocker, M.T., Hellwig, I., Breiling, A., Eckstein, V., Ho, A.D., and Lyko, F. (2011). Genome-wide promoter DNA methylation dynamics of human hematopoietic progenitor cells during differentiation and aging. Blood *117*, e182-189.

Boland, M.J., Nazor, K.L., and Loring, J.F. (2014). Epigenetic regulation of pluripotency and differentiation. Circ Res *115*, 311-324.

Borregaard, N. (2010). Neutrophils, from marrow to microbes. Immunity *33*, 657-670.

Bou Kheir, T., and Lund, A.H. (2010). Epigenetic dynamics across the cell cycle. Essays Biochem *48*, 107-120.

Branzei, D., and Foiani, M. (2008). Regulation of DNA repair throughout the cell cycle. Nat Rev Mol Cell Biol *9*, 297-308.

Brisdelli, F., Bennato, F., Bozzi, A., Cinque, B., Mancini, F., and Iorio, R. (2014). ELF-MF attenuates quercetin-induced apoptosis in K562 cells through modulating the expression of Bcl-2 family proteins. Mol Cell Biochem *397*, 33-43.

Bugl, S., Wirths, S., Muller, M.R., Radsak, M.P., and Kopp, H.G. (2012). Current insights into neutrophil homeostasis. Ann N Y Acad Sci *1266*, 171-178.

Bunch, K.J., Keegan, T.J., Swanson, J., Vincent, T.J., and Murphy, M.F. (2014). Residential distance at birth from overhead high-voltage powerlines: childhood cancer risk in Britain 1962-2008. Br J Cancer *110*, 1402-1408.

Burdak-Rothkamm, S., Rothkamm, K., Folkard, M., Patel, G., Hone, P., Lloyd, D., Ainsbury, L., and Prise, K.M. (2009). DNA and chromosomal damage in response to intermittent extremely low-frequency magnetic fields. Mutat Res *672*, 82-89.

Cancer Genome Atlas Research, N. (2013). Genomic and epigenomic landscapes of adult de novo acute myeloid leukemia. N Engl J Med *368*, 2059-2074.

Carmona-Rivera, C., and Kaplan, M.J. (2016). Neutrophil Biology. 750-758.

Cedar, H., and Bergman, Y. (2011). Epigenetics of haematopoietic cell development. Nat Rev Immunol *11*, 478-488.

Cheng, Y., Dai, Y., Zhu, X., Xu, H., Cai, P., Xia, R., Mao, L., Zhao, B.Q., and Fan, W. (2015). Extremely low-frequency electromagnetic fields enhance the proliferation and differentiation of neural progenitor cells cultured from ischemic brains. Neuroreport *26*, 896-902.

Chin, C.F., and Yeong, F.M. (2010). Safeguarding entry into mitosis: the antephase checkpoint. Mol Cell Biol *30*, 22-32.

Cho, H., Seo, Y.K., Yoon, H.H., Kim, S.C., Kim, S.M., Song, K.Y., and Park, J.K. (2012). Neural stimulation on human bone marrow-derived mesenchymal stem cells by extremely low frequency electromagnetic fields. Biotechnol Prog *28*, 1329-1335.

Cho, S., Lee, Y., Lee, S., Choi, Y.J., and Chung, H.W. (2014). Enhanced cytotoxic and genotoxic effects of gadolinium following ELF-EMF irradiation in human lymphocytes. Drug Chem Toxicol *37*, 440-447.

Conway O'Brien, E., Prideaux, S., and Chevassut, T. (2014). The epigenetic landscape of acute myeloid leukemia. Adv Hematol *2014*, 103175.

Cui, K., Zang, C., Roh, T.Y., Schones, D.E., Childs, R.W., Peng, W., and Zhao, K. (2009). Chromatin signatures in multipotent human hematopoietic stem cells indicate the fate of bivalent genes during differentiation. Cell Stem Cell *4*, 80-93.

D'Arena, G., Musto, P., Cascavilla, N., Di Giorgio, G., Zendoli, F., and Carotenuto, M. (1996). Human umbilical cord blood: immunophenotypic heterogeneity of CD34+ hematopoietic progenitor cells. Haematologica *81*, 404-409.

Dambacher, S., de Almeida, G.P., and Schotta, G. (2013). Dynamic changes of the epigenetic landscape during cellular differentiation. Epigenomics *5*, 701-713.

Damdimopoulou, P., Weis, S., Nalvarte, I., and Ruegg, J. (2012). Marked For Life: How Environmental Factors Affect the Epigenome. Issues Toxicol, 44-69.

Deaton, A.M., and Bird, A. (2011). CpG islands and the regulation of transcription. Genes Dev *25*, 1010-1022.

Dillon, N. (2012). Factor mediated gene priming in pluripotent stem cells sets the stage for lineage specification. Bioessays *34*, 194-204.

Dou, Y., Milne, T.A., Ruthenburg, A.J., Lee, S., Lee, J.W., Verdine, G.L., Allis, C.D., and Roeder, R.G. (2006). Regulation of MLL1 H3K4 methyltransferase activity by its core components. Nat Struct Mol Biol *13*, 713-719.

Doulatov, S., Notta, F., Laurenti, E., and Dick, J.E. (2012). Hematopoiesis: a human perspective. Cell Stem Cell *10*, 120-136.

Du, J., Johnson, L.M., Jacobsen, S.E., and Patel, D.J. (2015). DNA methylation pathways and their crosstalk with histone methylation. Nat Rev Mol Cell Biol *16*, 519-532.

Duan, W., Liu, C., Zhang, L., He, M., Xu, S., Chen, C., Pi, H., Gao, P., Zhang, Y., Zhong, M.*, et al.* (2015). Comparison of the genotoxic effects induced by 50 Hz extremely low-frequency electromagnetic fields and 1800 MHz radiofrequency electromagnetic fields in GC-2 cells. Radiat Res *183*, 305-314.

Edinger, A.L., and Thompson, C.B. (2004). Death by design: apoptosis, necrosis and autophagy. Curr Opin Cell Biol *16*, 663-669.

Eissenberg, J.C., and Shilatifard, A. (2010). Histone H3 lysine 4 (H3K4) methylation in development and differentiation. Dev Biol *339*, 240-249.

Engelhardt, M., Lubbert, M., and Guo, Y. (2002). CD34(+) or CD34(-): which is the more primitive? Leukemia *16*, 1603-1608.

Feil, R. (2006). Environmental and nutritional effects on the epigenetic regulation of genes. Mutat Res *600*, 46-57.

Feil, R., and Fraga, M.F. (2011). Epigenetics and the environment: emerging patterns and implications. Nat Rev Genet *13*, 97-109.

Felsenfeld, G., and Groudine, M. (2003). Controlling the double helix. Nature *421*, 448-453.

Finch, J.T., and Klug, A. (1976). Solenoidal model for superstructure in chromatin. Proc Natl Acad Sci U S A *73*, 1897-1901.

Florean, C., Schnekenburger, M., Grandjenette, C., Dicato, M., and Diederich, M. (2011). Epigenomics of leukemia: from mechanisms to therapeutic applications. Epigenomics *3*, 581-609.

Focke, F., Schuermann, D., Kuster, N., and Schar, P. (2010). DNA fragmentation in human fibroblasts under extremely low frequency electromagnetic field exposure. Mutat Res *683*, 74-83.

Garip, A.I., and Akan, Z. (2010). Effect of ELF-EMF on number of apoptotic cells; correlation with reactive oxygen species and HSP. Acta Biol Hung *61*, 158-167.

Gerard, C., and Goldbeter, A. (2016). Dynamics of the mammalian cell cycle in physiological and pathological conditions. Wiley Interdiscip Rev Syst Biol Med *8*, 140-156.

Gifford, C.A., Ziller, M.J., Gu, H., Trapnell, C., Donaghey, J., Tsankov, A., Shalek, A.K., Kelley, D.R., Shishkin, A.A., Issner, R.*, et al.* (2013). Transcriptional and epigenetic dynamics during specification of human embryonic stem cells. Cell *153*, 1149-1163.

Giorgi, G., Lecciso, M., Capri, M., Lukas Yani, S., Virelli, A., Bersani, F., and Del Re, B. (2014). An evaluation of genotoxicity in human neuronal-type cells subjected to oxidative stress under an extremely low frequency pulsed magnetic field. Mutat Res Genet Toxicol Environ Mutagen *775-776*, 31-37.

Gong, F., and Miller, K.M. (2013). Mammalian DNA repair: HATs and HDACs make their mark through histone acetylation. Mutat Res *750*, 23-30.

Greaves, M. (2002). Childhood leukaemia. BMJ *324*, 283-287.

Greenblatt, S.M., and Nimer, S.D. (2014). Chromatin modifiers and the promise of epigenetic therapy in acute leukemia. Leukemia *28*, 1396-1406.

Guo, H., Zhu, P., Guo, F., Li, X., Wu, X., Fan, X., Wen, L., and Tang, F. (2015). Profiling DNA methylome landscapes of mammalian cells with single-cell reduced-representation bisulfite sequencing. Nat Protoc *10*, 645-659.

Guo, H., Zhu, P., Yan, L., Li, R., Hu, B., Lian, Y., Yan, J., Ren, X., Lin, S., Li, J.*, et al.* (2014). The DNA methylation landscape of human early embryos. Nature *511*, 606-610.

Hajkova, P., Jeffries, S.J., Lee, C., Miller, N., Jackson, S.P., and Surani, M.A. (2010). Genome-wide reprogramming in the mouse germ line entails the base excision repair pathway. Science *329*, 78-82.

Hake, S.B., and Allis, C.D. (2006). Histone H3 variants and their potential role in indexing mammalian genomes: the "H3 barcode hypothesis". Proc Natl Acad Sci U S A *103*, 6428-6435.

Hanahan, D., and Weinberg, R.A. (2011). Hallmarks of cancer: the next generation. Cell *144*, 646-674.

Hawkins, R.D., Hon, G.C., Lee, L.K., Ngo, Q., Lister, R., Pelizzola, M., Edsall, L.E., Kuan, S., Luu, Y., Klugman, S.*, et al.* (2010). Distinct epigenomic landscapes of pluripotent and lineage-committed human cells. Cell Stem Cell *6*, 479-491.

He, Y.F., Li, B.Z., Li, Z., Liu, P., Wang, Y., Tang, Q., Ding, J., Jia, Y., Chen, Z., Li, L.*, et al.* (2011). Tet-mediated formation of 5-carboxylcytosine and its excision by TDG in mammalian DNA. Science *333*, 1303-1307.

Hodges, E., Molaro, A., Dos Santos, C.O., Thekkat, P., Song, Q., Uren, P.J., Park, J., Butler, J., Rafii, S., McCombie, W.R.*, et al.* (2011). Directional DNA methylation changes and complex intermediate states accompany lineage specificity in the adult hematopoietic compartment. Mol Cell *44*, 17-28.

Hon, G.C., Hawkins, R.D., and Ren, B. (2009). Predictive chromatin signatures in the mammalian genome. Hum Mol Genet *18*, R195-201.

Hu, Y., Huang, K., An, Q., Du, G., Hu, G., Xue, J., Zhu, X., Wang, C.Y., Xue, Z., and Fan, G. (2016). Simultaneous profiling of transcriptome and DNA methylome from a single cell. Genome Biol *17*, 88.

Huang, C.Y., Chang, C.W., Chen, C.R., Chuang, C.Y., Chiang, C.S., Shu, W.Y., Fan, T.C., and Hsu, I.C. (2014). Extremely low-frequency electromagnetic fields cause G1 phase arrest through the activation of the ATM-Chk2-p21 pathway. PLoS One *9*, e104732.

Hubner, M.R., Eckersley-Maslin, M.A., and Spector, D.L. (2013). Chromatin organization and transcriptional regulation. Curr Opin Genet Dev *23*, 89-95.

Hyun, B.R., McElwee, J.L., and Soloway, P.D. (2015). Single molecule and single cell epigenomics. Methods *72*, 41-50.

IARC (2002). Evaluation of carcinogenic risks to humans: Non-ionizing radiation, Part 1:static and extremely low-frequency (elf) electro and magnetic fields. WHO.

IARC (2013). Non-ionizing radiation, Part 2: radiofrequency electromagnetic fields WHO.

ICNIRP (2010). Guidelines for limiting exposure to time-varying electric and magnetic fields (1 Hz to 100 kHz). Health Phys *99*, 818-836.

Illingworth, R.S., and Bird, A.P. (2009). CpG islands--'a rough guide'. FEBS Lett *583*, 1713-1720.

Ivancsits (2002). Induction of DNA strand breaks by intermittent exposure to extremely-low-frequency electromagnetic fields in human diploid fibroblast.

Jaenisch, R., and Bird, A. (2003). Epigenetic regulation of gene expression: how the genome integrates intrinsic and environmental signals. Nat Genet *33 Suppl*, 245-254.

Ji, D., Lin, K., Song, J., and Wang, Y. (2014). Effects of Tet-induced oxidation products of 5-methylcytosine on Dnmt1- and DNMT3a-mediated cytosine methylation. Mol Biosyst *10*, 1749-1752.

Ji, H., Ehrlich, L.I., Seita, J., Murakami, P., Doi, A., Lindau, P., Lee, H., Aryee, M.J., Irizarry, R.A., Kim, K.*, et al.* (2010). Comprehensive methylome map of lineage commitment from haematopoietic progenitors. Nature *467*, 338-342.

Jin, Y.B., Choi, S.H., Lee, J.S., Kim, J.K., Lee, J.W., Hong, S.C., Myung, S.H., and Lee, Y.S. (2014). Absence of DNA damage after 60-Hz electromagnetic field exposure combined with ionizing radiation, hydrogen peroxide, or c-Myc overexpression. Radiat Environ Biophys *53*, 93-101.

Jobin, C., Cloutier, M., Simard, C., and Neron, S. (2015). Heterogeneity of in vitro-cultured CD34+ cells isolated from peripheral blood. Cytotherapy *17*, 1472-1484.

Jones, P.A. (2012). Functions of DNA methylation: islands, start sites, gene bodies and beyond. Nat Rev Genet *13*, 484-492.

Jung, I.S., Kim, H.J., Noh, R., Kim, S.C., and Kim, C.W. (2014). Effects of extremely low frequency magnetic fields on NGF induced neuronal differentiation of PC12 cells. Bioelectromagnetics *35*, 459-469.

Jurkowska, R.Z., Jurkowski, T.P., and Jeltsch, A. (2011). Structure and function of mammalian DNA methyltransferases. Chembiochem *12*, 206-222.

Juutilainen, J., Kumlin, T., and Naarala, J. (2006). Do extremely low frequency magnetic fields enhance the effects of environmental carcinogens? A meta-analysis of experimental studies. Int J Radiat Biol *82*, 1-12.

Kawasaki, Y., Lee, J., Matsuzawa, A., Kohda, T., Kaneko-Ishino, T., and Ishino, F. (2014). Active DNA demethylation is required for complete imprint erasure in primordial germ cells. Sci Rep *4*, 3658.

Kelly, L.M., and Gilliland, D.G. (2002). Genetics of myeloid leukemias. Annu Rev Genomics Hum Genet *3*, 179-198.

Kheifets, L., Ahlbom, A., Crespi, C.M., Draper, G., Hagihara, J., Lowenthal, R.M., Mezei, G., Oksuzyan, S., Schuz, J., Swanson, J*., et al.* (2010). Pooled analysis of recent studies on magnetic fields and childhood leukaemia. Br J Cancer *103*, 1128-1135.

Kim, H.J., Jung, J., Park, J.H., Kim, J.H., Ko, K.N., and Kim, C.W. (2013). Extremely low-frequency electromagnetic fields induce neural differentiation in bone marrow derived mesenchymal stem cells. Exp Biol Med (Maywood) *238*, 923-931.

Kim, J., Ha, C.S., Lee, H.J., and Song, K. (2010). Repetitive exposure to a 60-Hz time-varying magnetic field induces DNA double-strand breaks and apoptosis in human cells. Biochem Biophys Res Commun *400*, 739-744.

Ko, M., Huang, Y., Jankowska, A.M., Pape, U.J., Tahiliani, M., Bandukwala, H.S., An, J., Lamperti, E.D., Koh, K.P., Ganetzky, R*., et al.* (2010). Impaired hydroxylation of 5-methylcytosine in myeloid cancers with mutant TET2. Nature *468*, 839-843.

Kondo, M. (2010). Lymphoid and myeloid lineage commitment in multipotent hematopoietic progenitors. Immunol Rev *238*, 37-46.

Kouzarides, T. (2007). Chromatin modifications and their function. Cell *128*, 693-705.

Kraushaar, D.C., and Zhao, K. (2013). The epigenomics of embryonic stem cell differentiation. Int J Biol Sci *9*, 1134-1144.

Krebsliga (2016). Leukämien - Gemeinsam gegen Krebs. retrieved August 28, 2016, from https://wwwkrebsligach/de/uber_krebs/krebsarten/leukamien/.

Kumer, G. (2014). Are Cell Phones Carcinogenic retrieved August 28, 2016, from https://seshusophywordpresscom/2014/05/24/are-cell-phones-carcinogenic/.

Kuo, L.J., and Yang, L.X. (2008). Gamma-H2AX - a novel biomarker for DNA double-strand breaks. In Vivo *22*, 305-309.

Kuster, N., and Schoenborn, F. (2000). Recommended Minimal Requirements and Development Guidelines for Exposure Setup of Bio-Experiments Addressing the Health Risk Concern of Wireless Communications. Bioelectromagnetics.

Lanzuolo, C., and Orlando, V. (2012). Memories from the polycomb group proteins. Annu Rev Genet *46*, 561-589.

Lee, H.C., Hong, M.N., Jung, S.H., Kim, B.C., Suh, Y.J., Ko, Y.G., Lee, Y.S., Lee, B.Y., Cho, Y.G., Myung, S.H*., et al.* (2015). Effect of extremely low frequency magnetic fields on cell proliferation and gene expression. Bioelectromagnetics.

Leone, L., Fusco, S., Mastrodonato, A., Piacentini, R., Barbati, S.A., Zaffina, S., Pani, G., Podda, M.V., and Grassi, C. (2014). Epigenetic modulation of adult hippocampal neurogenesis by extremely low-frequency electromagnetic fields. Mol Neurobiol *49*, 1472-1486.

Li, E., and Zhang, Y. (2014). DNA methylation in mammals. Cold Spring Harb Perspect Biol *6*, a019133.

Liorni, I., Parazzini, M., Fiocchi, S., Douglas, M., Capstick, M., Gosselin, M.C., Kuster, N., and Ravazzani, P. (2014). Dosimetric study of fetal exposure to uniform magnetic fields at 50 Hz. Bioelectromagnetics *35*, 580-597.

Liu, Y., Liu, W.B., Liu, K.J., Ao, L., Zhong, J.L., Cao, J., and Liu, J.Y. (2015). Effect of 50 Hz Extremely Low-Frequency Electromagnetic Fields on the DNA Methylation and DNA Methyltransferases in Mouse Spermatocyte-Derived Cell Line GC-2. Biomed Res Int *2015*, 237183.

Luukkonen, J., Liimatainen, A., Juutilainen, J., and Naarala, J. (2014). Induction of genomic instability, oxidative processes, and mitochondrial activity by 50Hz magnetic fields in human SH-SY5Y neuroblastoma cells. Mutat Res *760*, 33-41.

Ma, Q., Chen, C., Deng, P., Zhu, G., Lin, M., Zhang, L., Xu, S., He, M., Lu, Y., Duan, W*., et al.* (2016). Extremely Low-Frequency Electromagnetic Fields Promote In Vitro Neuronal Differentiation and Neurite Outgrowth of Embryonic Neural Stem Cells via Up-Regulating TRPC1. PLoS One *11*, e0150923.

Ma, Q., Deng, P., Zhu, G., Liu, C., Zhang, L., Zhou, Z., Luo, X., Li, M., Zhong, M., Yu, Z*., et al.* (2014). Extremely low-frequency electromagnetic fields affect transcript levels of neuronal differentiation-related genes in embryonic neural stem cells. PLoS One *9*, e90041.

Maeshima, K., Hihara, S., and Eltsov, M. (2010). Chromatin structure: does the 30-nm fibre exist in vivo? Curr Opin Cell Biol *22*, 291-297.

Maeshima, K., Ide, S., Hibino, K., and Sasai, M. (2016). Liquid-like behavior of chromatin. Curr Opin Genet Dev *37*, 36-45.

Maeshima, K., Imai, R., Tamura, S., and Nozaki, T. (2014). Chromatin as dynamic 10-nm fibers. Chromosoma *123*, 225-237.

Malumbres, M., and Barbacid, M. (2009). Cell cycle, CDKs and cancer: a changing paradigm. Nat Rev Cancer *9*, 153-166.

Mangiacasale, R., Tritarelli, A., Sciamanna, I., Cannone, M., Lavia, P., Barberis, M.C., Lorenzini, R., and Cundari, E. (2001). Normal and cancer-prone human cells respond differently to extremely low frequency magnetic fields. FEBS Lett *487*, 397-403.

Manz, M.G., and Boettcher, S. (2014). Emergency granulopoiesis. Nat Rev Immunol *14*, 302-314.

Marcantonio, P., Del Re, B., Franceschini, A., Capri, M., Lukas, S., Bersani, F., and Giorgi, G. (2010). Synergic effect of retinoic acid and extremely low frequency magnetic field exposure on human neuroblastoma cell line BE(2)C. Bioelectromagnetics *31*, 425-433.

Martens, J.H., and Stunnenberg, H.G. (2010). The molecular signature of oncofusion proteins in acute myeloid leukemia. FEBS Lett *584*, 2662-2669.

Martin-Lorenzo, A., Hauer, J., Vicente-Duenas, C., Auer, F., Gonzalez-Herrero, I., Garcia-Ramirez, I., Ginzel, S., Thiele, R., Constantinescu, S.N.P., Bartenhagen, C*., et al.* (2015). Infection exposure is a causal factor in B-precursor acute lymphoblastic leukemia as a result of Pax5 inherited susceptibility. Cancer Discov.

Martinez, M.A., Ubeda, A., Cid, M.A., and Trillo, M.A. (2012). The Proliferative Response of NB69 Human Neuroblastoma Cells to a 50 Hz Magnetic Field is mediated by ERK1/2 Signaling. Cellular Physiology and Biochemistry *29*, 675-686.

Martinez, M.A., Ubeda, A., Moreno, J., and Trillo, M.A. (2016). Power Frequency Magnetic Fields Affect the p38 MAPK-Mediated Regulation of NB69 Cell Proliferation Implication of Free Radicals. Int J Mol Sci *17*.

Meagher, R.B. (2014). 'Memory and molecular turnover,' 30 years after inception. Epigenetics Chromatin *7*, 37.

Mehdipour, P., Santoro, F., and Minucci, S. (2015). Epigenetic alterations in acute myeloid leukemias. FEBS J *282*, 1786-1800.

Meissner, A., Mikkelsen, T.S., Gu, H., Wernig, M., Hanna, J., Sivachenko, A., Zhang, X., Bernstein, B.E., Nusbaum, C., Jaffe, D.B*., et al.* (2008). Genome-scale DNA methylation maps of pluripotent and differentiated cells. Nature *454*, 766-770.

Mihai, C.T., Rotinberg, P., Brinza, F., and Vochita, G. (2014). Extremely low-frequency electromagnetic fields cause DNA strand breaks in normal cells. J Environ Health Sci Eng *12*, 15.

Mitchell, C., Schneper, L.M., and Notterman, D.A. (2016). DNA methylation, early life environment, and health outcomes. Pediatr Res *79*, 212-219.

Mrozek, K., Harper, D.P., and Aplan, P.D. (2009). Cytogenetics and molecular genetics of acute lymphoblastic leukemia. Hematol Oncol Clin North Am *23*, 991-1010, v.

Murphy, K. (2008). Janeway's Immunobiology: seventh edition. Garland Science, Taylor & Francis Group, LLC.

Navakauskiene, R., Borutinskaite, V.V., Treigyte, G., Savickiene, J., Matuzevicius, D., Navakauskas, D., and Magnusson, K.E. (2014). Epigenetic changes during hematopoietic cell granulocytic

differentiation--comparative analysis of primary CD34+ cells, KG1 myeloid cells and mature neutrophils. BMC Cell Biol *15*, 4.

Nicholson, T.B., Veland, N., and Chen, T. (2015). Writers, Readers, and Erasers of Epigenetic Marks. 31-66.

Nikoletopoulou, V., Markaki, M., Palikaras, K., and Tavernarakis, N. (2013). Crosstalk between apoptosis, necrosis and autophagy. Biochim Biophys Acta *1833*, 3448-3459.

Nishino, Y., Eltsov, M., Joti, Y., Ito, K., Takata, H., Takahashi, Y., Hihara, S., Frangakis, A.S., Imamoto, N., Ishikawa, T.*, et al.* (2012). Human mitotic chromosomes consist predominantly of irregularly folded nucleosome fibres without a 30-nm chromatin structure. EMBO J *31*, 1644-1653.

Noreen, F., Roosli, M., Gaj, P., Pietrzak, J., Weis, S., Urfer, P., Regula, J., Schar, P., and Truninger, K. (2014). Modulation of age- and cancer-associated DNA methylation change in the healthy colon by aspirin and lifestyle. J Natl Cancer Inst *106*.

Ntziachristos, P., Mullenders, J., Trimarchi, T., and Aifantis, I. (2013). Mechanisms of epigenetic regulation of leukemia onset and progression. Adv Immunol *117*, 1-38.

Ntziachristos, P., Tsirigos, A., Van Vlierberghe, P., Nedjic, J., Trimarchi, T., Flaherty, M.S., Ferres-Marco, D., da Ros, V., Tang, Z., Siegle, J.*, et al.* (2012). Genetic inactivation of the polycomb repressive complex 2 in T cell acute lymphoblastic leukemia. Nat Med *18*, 298-301.

Oguro, H., Yuan, J., Ichikawa, H., Ikawa, T., Yamazaki, S., Kawamoto, H., Nakauchi, H., and Iwama, A. (2010). Poised lineage specification in multipotential hematopoietic stem and progenitor cells by the polycomb protein Bmi1. Cell Stem Cell *6*, 279-286.

Olins, D.E., and Olins, A.L. (2005). Granulocyte heterochromatin: defining the epigenome. BMC Cell Biol *6*, 39.

Orford, K., Kharchenko, P., Lai, W., Dao, M.C., Worhunsky, D.J., Ferro, A., Janzen, V., Park, P.J., and Scadden, D.T. (2008). Differential H3K4 methylation identifies developmentally poised hematopoietic genes. Dev Cell *14*, 798-809.

Pasini, D., Bracken, A.P., Agger, K., Christensen, J., Hansen, K., Cloos, P.A., and Helin, K. (2008). Regulation of stem cell differentiation by histone methyltransferases and demethylases. Cold Spring Harb Symp Quant Biol *73*, 253-263.

Pierce, B.A. (2012). Genetics: A Conceptual Approach, fourth edition. New York: W H Freeman and Company.

Pueschel, R., Coraggio, F., and Meister, P. (2016). From single genes to entire genomes: the search for a function of nuclear organization. Development *143*, 910-923.

Remijsen, Q., Kuijpers, T.W., Wirawan, E., Lippens, S., Vandenabeele, P., and Vanden Berghe, T. (2011). Dying for a cause: NETosis, mechanisms behind an antimicrobial cell death modality. Cell Death Differ *18*, 581-588.

Rice, J.C., and Allis, C.D. (2001). Histone methylation versus histone acetylation: new insights into epigenetic regulation. Current Opinion in Cell Biology *13*, 263-273.

Ronnerblad, M., Andersson, R., Olofsson, T., Douagi, I., Karimi, M., Lehmann, S., Hoof, I., de Hoon, M., Itoh, M., Nagao-Sato, S.*, et al.* (2014). Analysis of the DNA methylome and transcriptome in granulopoiesis reveals timed changes and dynamic enhancer methylation. Blood *123*, e79-89.

Rosenbauer, F., and Tenen, D.G. (2007). Transcription factors in myeloid development: balancing differentiation with transformation. Nat Rev Immunol *7*, 105-117.

Rotem, A., Ram, O., Shoresh, N., Sperling, R.A., Goren, A., Weitz, D.A., and Bernstein, B.E. (2015). Single-cell ChIP-seq reveals cell subpopulations defined by chromatin state. Nat Biotechnol *33*, 1165-1172.

Santini, M.T., Ferrante, A., Rainaldi, G., Indovina, P., and Indovina, P.L. (2005). Extremely low frequency (ELF) magnetic fields and apoptosis: a review. Int J Radiat Biol *81*, 1-11.

Sarimov, R., Alipov, E.D., and Belyaev, I.Y. (2011). Fifty hertz magnetic fields individually affect chromatin conformation in human lymphocytes: dependence on amplitude, temperature, and initial chromatin state. Bioelectromagnetics *32*, 570-579.

Sashida, G., and Iwama, A. (2012). Epigenetic regulation of hematopoiesis. Int J Hematol *96*, 405-412.

SCENIHR (2007). Possible effects of Electromagnetic Fields (EMF) on Human Health. European Commission.

SCENIHR (2009). Health Effects of Exposure to EMF. European Commission.

SCENIHR (2015). Potential health effects of exposure to electromagnetic fields (EMF). European Commission.

Scholey, J.M., Brust-Mascher, I., and Mogilner, A. (2003). Cell division. Nature *422*, 746-752.

Schuderer, J., Oesch, W., Felber, N., Spat, D., and Kuster, N. (2004). In vitro exposure apparatus for ELF magnetic fields. Bioelectromagnetics *25*, 582-591.

Schuermann, D., Weber, A.R., and Schar, P. (2016). Active DNA demethylation by DNA repair: Facts and uncertainties. DNA Repair (Amst).

Schuz, J. (2011). Exposure to extremely low-frequency magnetic fields and the risk of childhood cancer: update of the epidemiological evidence. Prog Biophys Mol Biol *107*, 339-342.

Schuz, J., and Ahlbom, A. (2008). Exposure to electromagnetic fields and the risk of childhood leukaemia: a review. Radiat Prot Dosimetry *132*, 202-211.

Schuz, J., Dasenbrock, C., Ravazzani, P., Roosli, M., Schar, P., Bounds, P.L., Erdmann, F., Borkhardt, A., Cobaleda, C., Fedrowitz, M.*, et al.* (2016). Extremely low-frequency magnetic fields and risk of childhood leukemia: A risk assessment by the ARIMMORA consortium. Bioelectromagnetics.

Seisenberger, S., Peat, J.R., Hore, T.A., Santos, F., Dean, W., and Reik, W. (2013). Reprogramming DNA methylation in the mammalian life cycle: building and breaking epigenetic barriers. Philos Trans R Soc Lond B Biol Sci *368*, 20110330.

Seita, J., and Weissman, I.L. (2010). Hematopoietic stem cell: self-renewal versus differentiation. Wiley Interdiscip Rev Syst Biol Med *2*, 640-653.

Seiter, K. (2016). Acute Myeloid Leukemia Staging retrieved July 31, 2016, from http://emedicinemedscapecom/article/2006750-overview.

Seong, Y., Moon, J., and Kim, J. (2014). Egr1 mediated the neuronal differentiation induced by extremely low-frequency electromagnetic fields. Life Sci *102*, 16-27.

Shabalina, S.A., and Spiridonov, N.A. (2004). The mammalian transcriptome and the function of non-coding DNA sequences. Genome Biol *5*, 105.

Shen, H., and Laird, P.W. (2013). Interplay between the cancer genome and epigenome. Cell *153*, 38-55.

Shen, L., and Zhang, Y. (2013). 5-Hydroxymethylcytosine: generation, fate, and genomic distribution. Curr Opin Cell Biol *25*, 289-296.

Shih, A.H., Abdel-Wahab, O., Patel, J.P., and Levine, R.L. (2012). The role of mutations in epigenetic regulators in myeloid malignancies. Nat Rev Cancer *12*, 599-612.

Shilatifard, A. (2012). The COMPASS family of histone H3K4 methylases: mechanisms of regulation in development and disease pathogenesis. Annu Rev Biochem *81*, 65-95.

Smith, B.C., and Denu, J.M. (2009). Chemical mechanisms of histone lysine and arginine modifications. Biochim Biophys Acta *1789*, 45-57.

Smith, Z.D., and Meissner, A. (2013). DNA methylation: roles in mammalian development. Nat Rev Genet *14*, 204-220.

Snyers, L., Zupkovitz, G., Almeder, M., Fliesser, M., Stoisser, A., Weipoltshammer, K., and Schofer, C. (2014). Distinct chromatin signature of histone H3 variant H3.3 in human cells. Nucleus *5*, 449-461.

Soffritti, M., Tibaldi, E., Padovani, M., Hoel, D.G., Giuliani, L., Bua, L., Lauriola, M., Falcioni, L., Manservigi, M., Manservisi, F*., et al.* (2016). Life-span exposure to sinusoidal-50 Hz magnetic field and acute low-dose gamma radiation induce carcinogenic effects in Sprague-Dawley rats. Int J Radiat Biol *92*, 202-214.

Strathdee, G., Holyoake, T.L., Sim, A., Parker, A., Oscier, D.G., Melo, J.V., Meyer, S., Eden, T., Dickinson, A.M., Mountford, J.C*., et al.* (2007). Inactivation of HOXA genes by hypermethylation in myeloid and lymphoid malignancy is frequent and associated with poor prognosis. Clin Cancer Res *13*, 5048-5055.

Stronati, L., Testa, A., Villani, P., Marino, C., Lovisolo, G.A., Conti, D., Russo, F., Fresegna, A.M., and Cordelli, E. (2004). Absence of genotoxicity in human blood cells exposed to 50 Hz magnetic fields as assessed by comet assay, chromosome aberration, micronucleus, and sister chromatid exchange analyses. Bioelectromagnetics *25*, 41-48.

Struchen, B., Liorni, I., Parazzini, M., Gangler, S., Ravazzani, P., and Roosli, M. (2015). Analysis of personal and bedroom exposure to ELF-MFs in children in Italy and Switzerland. J Expo Sci Environ Epidemiol.

Swissgrid (2015). Elektrische und magnetische Felder: Ständige Begleiter unseres Lebens.

Takata, H., Hanafusa, T., Mori, T., Shimura, M., Iida, Y., Ishikawa, K., Yoshikawa, K., Yoshikawa, Y., and Maeshima, K. (2013). Chromatin compaction protects genomic DNA from radiation damage. PLoS One *8*, e75622.

Tang, H., An, S., Zhen, H., and Chen, F. (2014). Characterization of combinatorial histone modifications on lineage-affiliated genes during hematopoietic stem cell myeloid commitment. Acta Biochim Biophys Sin (Shanghai) *46*, 894-901.

Thomas, M.P., Liu, X., Whangbo, J., McCrossan, G., Sanborn, K.B., Basar, E., Walch, M., and Lieberman, J. (2015). Apoptosis Triggers Specific, Rapid, and Global mRNA Decay with 3' Uridylated Intermediates Degraded by DIS3L2. Cell Rep *11*, 1079-1089.

Tofani, S., Barone, D., Cintorino, M., de Santi, M.M., Ferrara, A., Orlassino, R., Ossola, P., Peroglio, F., Rolfo, K., and Ronchetto, F. (2001). Static and ELF magnetic fields induce tumor growth inhibition and apoptosis. Bioelectromagnetics *22*, 419-428.

Travers, A., and Muskhelishvili, G. (2015). DNA structure and function. FEBS J *282*, 2279-2295.

Trillo, M.A., Martinez, M.A., Cid, M.A., Leal, J., and Ubeda, A. (2012). Influence of a 50 Hz magnetic field and of all-transretinol on the proliferation of human cancer cell lines. Int J Oncol *40*, 1405-1413.

Trillo, M.A., Martinez, M.A., Cid, M.A., and Ubeda, A. (2013). Retinoic acid inhibits the cytoproliferative response to weak 50Hz magnetic fields in neuroblastoma cells. Oncol Rep *29*, 885-894.

Trowbridge, J.J., Snow, J.W., Kim, J., and Orkin, S.H. (2009). DNA methyltransferase 1 is essential for and uniquely regulates hematopoietic stem and progenitor cells. Cell Stem Cell *5*, 442-449.

Verdaasdonk, J.S., and Bloom, K. (2011). Centromeres: unique chromatin structures that drive chromosome segregation. Nat Rev Mol Cell Biol *12*, 320-332.

Vijayalaxmi, and Prihoda, T.J. (2009). Genetic damage in mammalian somatic cells exposed to extremely low frequency electro-magnetic fields: a meta-analysis of data from 87 publications (1990-2007). Int J Radiat Biol *85*, 196-213.

Walczak, C.E., Cai, S., and Khodjakov, A. (2010). Mechanisms of chromosome behaviour during mitosis. Nat Rev Mol Cell Biol *11*, 91-102.

Wallach, D., Kang, T.B., Dillon, C.P., and Green, D.R. (2016). Programmed necrosis in inflammation: Toward identification of the effector molecules. Science *352*, aaf2154.

Wang, K., Li, X., Dong, S., Liang, J., Mao, F., Zeng, C., Wu, H., Wu, J., Cai, W., and Sun, Z.S. (2015). Q-RRBS: a quantitative reduced representation bisulfite sequencing method for single-cell methylome analyses. Epigenetics *10*, 775-783.

Waterborg, J.H. (2002). Dynamics of histone acetylation in vivo. A function for acetylation turnover? Biochemistry and Cell Biology *80*, 363-378.

Watson, J.D., and Crick, F.H. (1953). Molecular structure of nucleic acids; a structure for deoxyribose nucleic acid. Nature *171*, 737-738.

Weber, A.R., Krawczyk, C., Robertson, A.B., Kusnierczyk, A., Vagbo, C.B., Schuermann, D., Klungland, A., and Schar, P. (2016). Biochemical reconstitution of TET1-TDG-BER-dependent active DNA demethylation reveals a highly coordinated mechanism. Nat Commun *7*, 10806.

Wei, G., Wei, L., Zhu, J., Zang, C., Hu-Li, J., Yao, Z., Cui, K., Kanno, Y., Roh, T.Y., Watford, W.T.*, et al.* (2009). Global mapping of H3K4me3 and H3K27me3 reveals specificity and plasticity in lineage fate determination of differentiating CD4+ T cells. Immunity *30*, 155-167.

Weishaupt, H., Sigvardsson, M., and Attema, J.L. (2010). Epigenetic chromatin states uniquely define the developmental plasticity of murine hematopoietic stem cells. Blood *115*, 247-256.

WHO (2007). Environmental Health Criteria 238, Extremely low frequency fields World Health Organization.

WHO (2016). Retrieved 13.5.2016, http://www.who.int/peh-emf/about/WhatisEMF/en/index1.html.

Winkler, I.G., Barbier, V., Wadley, R., Zannettino, A.C., Williams, S., and Levesque, J.P. (2010). Positioning of bone marrow hematopoietic and stromal cells relative to blood flow in vivo: serially reconstituting hematopoietic stem cells reside in distinct nonperfused niches. Blood *116*, 375-385.

Woodcock, C.L., Frado, L.L., and Rattner, J.B. (1984). The higher-order structure of chromatin: evidence for a helical ribbon arrangement. J Cell Biol *99*, 42-52.

Xiao, H., Wang, L.M., Luo, Y., Lai, X., Li, C., Shi, J., Tan, Y., Fu, S., Wang, Y., Zhu, N.*, et al.* (2016). Mutations in epigenetic regulators are involved in acute lymphoblastic leukemia relapse following allogeneic hematopoietic stem cell transplantation. Oncotarget *7*, 2696-2708.

Xu, J., Shao, Z., Li, D., Xie, H., Kim, W., Huang, J., Taylor, J.E., Pinello, L., Glass, K., Jaffe, J.D.*, et al.* (2015). Developmental control of polycomb subunit composition by GATA factors mediates a switch to non-canonical functions. Mol Cell *57*, 304-316.

Yamaguchi, S., Shen, L., Liu, Y., Sendler, D., and Zhang, Y. (2013). Role of Tet1 in erasure of genomic imprinting. Nature *504*, 460-464.

Yoon, H.E., Lee, J.S., Myung, S.H., and Lee, Y.S. (2014). Increased gamma-H2AX by exposure to a 60-Hz magnetic fields combined with ionizing radiation, but not hydrogen peroxide, in non-tumorigenic human cell lines. Int J Radiat Biol *90*, 291-298.

Yoshikawa, Y., Mori, T., Magome, N., Hibino, K., and Yoshikawa, K. (2008). DNA compaction plays a key role in radioprotection against double-strand breaks as revealed by single-molecule observation. Chemical Physics Letters *456*, 80-83.

You, J.S., and Jones, P.A. (2012). Cancer genetics and epigenetics: two sides of the same coin? Cancer Cell *22*, 9-20.

Zawrotniak, M., and Rapala-Kozik, M. (2013). Neutrophil extracellular traps (NETs) - formation and implications. Acta Biochim Pol *60*, 277-284.

Zenhäusern, R., Zwicky, C., Solenthaler, M., Fey, M.F., and A., T. (2003). Akute Leukämien beim Erwachsenen. Schweiz Med Forum.

Zhang, J., Ding, L., Holmfeldt, L., Wu, G., Heatley, S.L., Payne-Turner, D., Easton, J., Chen, X., Wang, J., Rusch, M.*, et al.* (2012). The genetic basis of early T-cell precursor acute lymphoblastic leukaemia. Nature *481*, 157-163.

Zhang, M., Li, X., Bai, L., Uchida, K., Bai, W., Wu, B., Xu, W., Zhu, H., and Huang, H. (2013). Effects of low frequency electromagnetic field on proliferation of human epidermal stem cells: An in vitro study. Bioelectromagnetics *34*, 74-80.

Zhu, J., Adli, M., Zou, J.Y., Verstappen, G., Coyne, M., Zhang, X., Durham, T., Miri, M., Deshpande, V., De Jager, P.L.*, et al.* (2013). Genome-wide chromatin state transitions associated with developmental and environmental cues. Cell *152*, 642-654.

Zong, W.X., and Thompson, C.B. (2006). Necrotic death as a cell fate. Genes & Development *20*, 1-15.

7 Appendix

I. ELF-MF exposure affects the robustness of epigenetic programming during granulopoiesis

II. Dynamics of Histone Modifications and DNA Methylation during *in vitro* Granulopoiesis

III. Extremely Low-Frequency Magnetic Fields and Risk of Childhood Leukemia: A Risk Assessment by the ARIMMORA Consortium

ELF-MF exposure affects the robustness of epigenetic programming during granulopoiesis

Melissa Manser[1], Mohamad R. Abdul Sater[2,3,#], Christoph D. Schmid[2,3], Faiza Noreen[1], Manuel Murbach[4], Niels Kuster[4,5], David Schuermann[1,*], Primo Schär[1]

[1] Department of Biomedicine, University of Basel, Mattenstrasse 28, Basel, CH-4058, Switzerland

[2] Swiss Tropical and Public Health Institute, Socinstrasse 57, Basel, CH-4002, Switzerland

[3] University of Basel, Petersplatz 1, Basel, CH-4001, Switzerland

[4] IT'IS Foundation, Zeughausstrasse 43, Zürich, CH-8004, Switzerland

[5] Swiss Federal Institute of Technology (ETH), Zürich, CH-8006, Switzerland

[#]Present address: Department of Immunology and Infectious disease, Harvard T.H. Chan School of Public Health, Boston, MA 02115, United States of America

[*]Correspondence and requests for materials should be addressed to D.S. (david.schuermann@unibas.ch)

Keywords: Extremely low frequency magnetic fields, ELF-MF, epigenetics, histone modification, DNA methylation, leukaemic cells, human haematopoietic stem cells, differentiation, granulopoiesis

Contribution: I planned, performed and analysed the *in vitro* exposure experiments of leukaemic cells as well as during the neutrophilic differentiation. I analysed the cell cycle, amount of apoptotic cells and the different maturation stages by flow cytometry. I determined the histone modifications by ChIP, prepared the ChIP samples for next-generation sequencing and contributed to the bioinformatic analysis of the ChIP-seq data. Then, I prepared the DNA samples for the DNA methylation array, did the variance analysis of the histone modifications and DNA methylation by RStudio/Bioconductor and wrote the manuscript.

Abstract

Extremely-low-frequency magnetic fields (ELF-MF) have been classified as "possibly carcinogenic" to humans on the grounds of an epidemiological association of ELF-MF exposure with an increased risk of childhood leukaemia. Underlying mechanisms, however, have remained obscure. Genome instability seems an unlikely reason as the energy transmitted by ELF-MF is not sufficient to damage DNA and induce cancer-promoting mutations. ELF-MF, however, may perturb the epigenetic code of genomes, which is well-known to be sensitive to environmental factors and generally deranged in cancers, including leukaemia. We examined the potential of ELF-MF to influence key epigenetic modifications in leukaemic Jurkat cells and in human CD34+ hematopoietic stem cells undergoing *in vitro* differentiation into the neutrophilic lineage. Sensitive genome-wide profiling revealed no statistically significant, ELF-MF dependent alterations in the patterns of active (H3K4me2) and repressive (H3K27me3) histone marks, nor in the formation DNA methylation patterns during granulopoiesis. However, ELF-MF exposure showed consistent effects on the reproducibility of these histone and DNA modification profiles, which appear to be of a stochastic nature but show a genomic context preference. The data indicate that ELF-MF exposure may stabilize H3K4me2 modifications in chromatin that changes from a repressive to an active state during cell differentiation.

Introduction

The increasing use of electronic appliances generating electromagnetic fields in the extremely-low-frequency range of 50 or 60 Hz (ELF-MF) has raised concerns about potential health risks. The main sources of ELF-MFs are in-house installations, household appliances and powerlines, resulting in average indoors exposure levels between 0.025 and 0.07 µT in Europe[1,2]. Based on epidemiological studies, associating ELF-MF exposure with an increased risk for childhood leukaemia, ELF-MF exposure was evaluated as being possibly carcinogenic to humans (group 2B) by the International Agency for Research on Cancer (IARC)[3,4]. Animal and cellular studies, performed to address biological effects of ELF-MF exposure and pinpoint mechanisms underlying potential health impacts, however, failed to come up with a consistent mechanistic explanation of these epidemiological observations[1,3]. Most animal studies failed to support evidence that magnetic fields can cause tumours, an exception being a recent study indicating a co-carcinogenic effect in rats exposed to sinusoidal 50 Hz ELF-MF in combination with an acute low-dose γ-ray iradiation[1,5].

Acute lymphoblastic leukaemia (ALL) is the most common type of childhood leukaemia, characterized by high accumulation of T or B lymphocytes in progenitor stages, unable to terminally differentiate[6,7]. Many ALLs arise from foetal genetic lesions or translocations like TEL-AML1 (ETV6-RUNX1) or MLL-TET1 fusions in blood progenitor cells, resulting in unlimited self-renewal and failure in stage-specific developmental arrest[8]. Besides the foetal genetic events, the classical 'two-hit' model of childhood ALL postulates a requirement of a second hit after birth in the form of additional chromosomal or genetic alteration[9]. Prominent amongst these appear to be mutations in genes encoding epigenetic modifiers like in the methyltransferase EZH2, a subunit of the polycomb repressive complex 2, or the DNA methyltransferase DNMT3a[10-12]. This selection for mutations in epigenetic modifiers indicates that defects in the control of cell differentiation associated changes in gene expression and chromatin landscapes contribute to the establishment of ALL.

Cancers generally emerge as a consequence of progressive change in genome structure and function, including mutation of the DNA sequence and alteration of chromatin structure and gene expression[13]. Genomic instability is therefore a hallmark of tumor progression[14,15]. Whether or not ELF-MFs have the power to induce genetic mutations is questionable as the energy deposited by ELF-MFs is orders of magnitudes below of what would be required to affect chemical bonds in DNA[16]. Therefore, notwithstanding occasional reports of a genotoxic potential of ELF-MFs[17-20], it seems unlikely that ELF-MF-induced genetic mutations contribute significantly to the mutagenesis in cancer. Another hallmark of cancers are aberrations in the cell type-specific patterns of epigenetic modifications. Epigenetic modifications to histone proteins and the DNA, established mainly during

cell differentiation, guide and stabilize cell-type-specific gene expression. This "programming" of genomes in differentiating cells is instructed by environmental cues and, hence, is also likely to be sensitive to disturbance by environmental factors[21,22], such as MFs. Consistent with a possible impact of ELF-MFs exposure on epigenetic cell programming, it has been reported that ELF-MFs are able to alter neural differentiation[23-26]. Regulatory epigenetic modifications include the acetylation and methylation of histone tails and the methylation of DNA cytosine bases[27,28], altogether establishing three main classes of chromatin; i.e. active, repressed and poised chromatin. Active chromatin, comprising highly expressed genes, is marked by trimethylation of histone 3 lysine 4 (H3K4me3), acetylation of histone 3 lysine 27 (H3K27ac) and unmethylated DNA cytosine, whereas chromatin correlating with gene repression is characterized by histone 3 trimethylated at lysine 27 (H3K27me3) and lysine 9 (H3K9me3) and DNA cytosine methylation (5-methylcytosine, 5mC). Transcriptionally poised chromatin is co-occupied by the active and repressive marks H3K4me2/3 and H3K27me3 and is located preferentially at developmental genes in stem cells[29]. The potential of ELF-MF exposure to destabilize epigenetic modifications in general and in a cancer-relevant manner has not been addressed systematically. Yet, it was reported to alter global levels of 5mC and the expression of DNA methyltransferases DNMT1 and DNMT3b in mouse spermatocytes[30], and to increase the reprogramming efficiency of somatic cells by upregulation of the histone lysine methyltransferase Mll2, which appears to enrich H3K4me3 at pluripotent genes[31].

To investigate whether ELF-MFs have a potential to alter the epigenome, we analysed under highly controlled and standardized conditions the impact of exposure on the stability of key active (H3K4me2) and repressive (H3K27me3) histone modifications in a leukaemic cell line, as well as on the formation of cell-type-specific H3K4me2 and H3K27me3 and DNA methylation patterns in *in vitro* differentiating human cord blood cells. We profiled these modifications genome-wide and found that ELF-MF exposure has no specific and reproducible effects on the stability of histone and DNA modifications in leukaemic cells nor on the establishment of cell type-specific modifications during haematopoietic differentiation. Yet, the ELF-MF exposure appeared affected the reproducibility, i.e. the robustness, of the epigenetic marks in replicate cell populations.

Results

ELF-MF exposure does not reproducibly induce alterations in histone modifications in Jurkat cells.

To determine if ELF-MF exposure affects the epigenetic stability of leukaemic cells, we profiled the genome-wide patterns of the key histone marks H3K4me2 and H3K27me3 (Figure 1) in the T cell

lymphoma cell line Jurkat exposed intermittently (5' on/10' off) to a 50 Hz sine ELF-MF at a flux density of 1 mT, or to a sham control (< 7 µT residual field) for 72 h (Supplementary Figure S1). Exposure settings were blinded throughout the experiments. We also included a treatment with the histone deacetylation inhibitor trichostatin A (TSA) at a sub-toxic dose of 10 nM to assess the impact of a known epigenetic modulator (Supplementary Figure S2). Previous studies – although not consistently – described effects of ELF-MF exposure on cell proliferation and apoptosis[17,32,33], parameters that on their own may influence epigenetic modifications. We therefore assessed exposure effects on proliferation, cell cycle progression and apoptosis in our exponentially growing Jurkat cells. These controls showed no significant exposure effect on either of these parameters throughout the 3.5 cell cycle duration (72 h) of the experiment (Supplementary Figure S2). By contrast, TSA treatment (10 nM) resulted in a transient increase of G1 and a decrease of S and G2 phase cells 24 hours after treatment start without, however, affecting overall cell proliferation or the proportion of apoptotic cells. We therefore conclude that the ELF-MF exposure condition applied did not affect cell viability and proliferation in our experiment.

We then combined chromatin immunoprecipitation (ChIP) with next generation sequencing (ChIP-seq) to quantitatively map H3K4me2 and H3K27me3 occurrence in chromatin isolated from Jurkat cells before exposure (t0), following ELF-MF/sham exposure for 72 h, or treated with TSA. Two ChIP-seq replicates were generated from six biological replicates for each condition by pooling three samples each. About 51 million reads per Chip-seq sample were mapped to the hg19 human genome. H3K4me2 and H3K27me3 profiles in 500 bp genomic tiles showed a high reproducibility between the replica of all condition (Supplementary Figures S3 and S4). Principal component analysis of the data clearly separated TSA treated Jurkat cells from exposed cells. ELF-MF and sham-exposed cells, however, clustered together, indicating that the exposure has no global effect on H3K4me2 and H3K27me3 patterns (Figure 1a). Consistently, we observed a large number of 500 bp tiles showing significantly different enrichment in H3K4me2 and H3K27me3 modifications in TSA treated cells (FDR-adjusted P value < 0.05, log2 fold change [FC] > ±0.6) (Figure 1b, 1e), but no significant differences were apparent when comparing ELF-MF- and sham-exposed Jurkat cells (Figure 1c, Supplementary Figure S5). Several loci, however, showed up to three-fold differential H3K4me2 and H3K27me3 occupancy upon ELF-MF exposure, as illustrated for two regions within the *RPTOR* and *CEP170* genes (Figure 1d). These differences, however, did not reach statistical significance. These results indicate that the landscape of H3K4me2 and H3K27me3 modifications in leukemic cells is largely unaffected by ELF-MF exposure.

ELF-MF exposure does not reproducibly affect global patterning of histone marks in granulopoiesis. As epigenetic processes are highly dynamic and likely to be sensitive to disturbance by environmental factors during cellular differentiation[22,34,35], we addressed whether ELF-MF exposure affects differentiation-associated patterning of H3K4me2 and H3K27me3 marks. Under exposure to a powerline-simulating ELF-MF (50 Hz, 1 mT, 5' on/10' off) with parallel sham and no ELF-MF controls (Supplementary Figure S1), we differentiated *in vitro* CD34+ haematopoietic stem cells from human cord blood into the neutrophilic lineage by an established protocol[36]. The differentiation process was monitored by flow cytometry by analysing granulocytic maturation stages. 90% of cells differentiated from the CD34+ progenitor state to a promyelocyte (75%) or myelocyte (15%) stage within five days irrespective of the exposure condition (Supplementary Figure S6). By day 10, more than 50% of cells matured into myelocytes and metamyelocytes/neutrophils, again without notable differences between ELF-MF- and sham-exposed populations. Also, cell proliferation was not affected by ELF-MF exposure (Supplementary Figure S6). Throughout exponential growth, around 25% and 10% of cells in all populations were in S and G2 phase of the cell cycle, respectively (Figure 2a; Supplementary Figure S7). At days four and five (neutrophilic progenitor cell stage), ELF-MF exposed cultures showed a small reduction of G1 and a compensating increase of S phase cells when compared to sham and unexposed controls. Investigating potentially associated effects of the ELF-MF exposure on cell viability as observed previously[32,33,37,38], we quantified the proportion of alive cells, early apoptotic, late apoptotic and dead cells by flow cytometry. Expansion cultures of CD34+ cells (t0) were highly proliferating and composed of around 95% living cells (Figure 2b; Supplementary Figure S8). Following induction of differentiation, the fraction of apoptotic cells increased, establishing a significant difference between exposure conditions at day four, where 24% of cells were apoptotic or dead in ELF-MF exposed cultures and 19% in sham exposed cultures (Figure 2b). Although small, these differences indicate that ELF-MF has the potential to induce apoptosis directly or indirectly in a small fraction of differentiating neutrophilic cells. The concomitant slight accumulation of ELF-MF exposed cells in S-phase suggest that this may be related to an ELF-MF-induced disturbance of S-phase progression.

To determine whether ELF-MF exposure influences the patterning of H3K4me2 and H3K27me3 modifications, we performed ChIP-seq with chromatin of cells harvested before (t0) and after five days (t5) of differentiation. Two ChIP-seq replicates were generated from three independent differentiation experiments by pooling experiments two and three into ChIP-seq replicate two. 26 million reads per ChIP-seq sample were mapped to the human genome and read numbers in 500 and 1,000 bp genomic tiles were analysed. The comparison of reads per tile between samples confirmed a good reproducibility and clearly separated samples of CD34+ cells and neutrophilic progenitors in a

principal component analysis (Figure 2c, Supplementary Figures S9, S10). We first analysed the ChIP-seq data by a likelihood-ratio test assuming fixed standard deviations to compare ELF-MF with sham- and non-exposed cells after five days of differentiation. This identified only few genomic regions with differential (FDR-adjusted *P* value < 0.05, log2 FC > ±0.6) H3K4me2 or H3K27me3 enrichments (Supplementary Figure S11), most pronounced in the comparison of ELF-MF-exposed with non-exposed cells. Nine and 19 genomic regions showed significant differences in H3K4me2 and H3K27me3 enrichment, respectively, between ELF-MF and sham exposed neutrophilic progenitors. To address potential false positives due the statistical reasons, we adjusted the analysis by allowing for variable standard deviations between samples. Analyzed this way, the differences in H3K4me2 or H3K27me3 occupancy between ELF-MF or sham exposed cells disappeared (FDR-adjusted *P* value < 0.05, log2 FC > ±0.6) (Figure 2d). By contrast, comparing cells prior to and five days into differentiation yielded large numbers of tiles with significant differences in H3K4me2 and H3K27me3 occupancy (Figure 2e), including loci like *ELANE* and *CD34* with 3.8- and 11-fold differential enrichments, respectively (Figure 2f), and documenting the epigenetic reorganization occurring throughout neutrophilic differentiation. Notably, however, despite the lack of significant differences between ELF-MF and sham-exposed cells, many genomic loci showed substantial differential enrichments for either of the histone marks (up to 8-12 fold) (Figure 2d), as illustrated in the respective profiles at the *UBAP2* and *CLF5* loci (Figure 2g). These results show that, while the epigenetic landscape undergoes major alterations during neutrophilic differentiation, ELF-MF exposure does not reproducibly impair the global patterning of the two key histone modifications examined.

Genome-wide formation of DNA methylation patterns is not affected by ELF MF exposure.

Environmental conditions modulate epigenetic modifications not only at histones but also at the level of DNA[39,40]. To address whether ELF-MF affects DNA cytosine methylation during neutrophilic differentiation, we performed genome-wide methylation analysis at single CpG sites of CD34+ (t0) and day five progenitor (t5) cells, using the Illumina Infinium HumanMethylation 450 platform. We analysed 412,940 CpGs and observed a high correlation between all biological replicas and a clear separation of samples from CD34+ and neutrophilic progenitor cells in a principal component analysis (Figure 3a; Supplementary Figure S12). As expected, the pattern of DNA methylation dramatically changed during differentiation, resulting in 3,882 hypo- (log2 FC < -0.6) and 2,977 hypermethylated (log2 FC > 0.6) sites (FDR-adjusted *P* value < 0.05) (Figure 3b). Yet, no CpGs were differentially methylated with statistical significance when ELF-MF exposed progenitor cells were compared with control conditions (Figure 3c; Supplementary Figure S12). These results indicate that,

although DNA methylation undergoes major changes during neutrophilic granulopoiesis, ELF-MF exposure does not influence the formation of cell-type-specific DNA methylation patterns.

ELF-MF exposure affects the variability of epigenetic modifications between replicate experiments. Although we did not identify consistent alterations of histone modifications or DNA methylation upon ELF-MF exposure both in leukaemic cells and in differentiating neutrophilic cells, we observed a number of genomic loci showing up to 16-fold differential occupancy by H3K4me2 and H3K27me3 or DNA methylation (Figures 1c, 2d, and 3c). These differences did not reach statistical significance (FDR-adjusted *P* value < 0.05) due to a considerable variance between the data sets. Although the overall correlation of the ChIP-seq data was high (Supplementary Figures S3, S4, S9, and S10), a closer examination of the H3K4me2 and H3K27me3 read counts in all tiles revealed exposure condition-dependent effects on the variability of replicate samples, both in Jurkat cells and neutrophilic progenitors (Figure 4a, 4b). We reasoned that this differences in replicate variability may reflect an influence of the exposure on the establishment and/or maintenance of H3K4me2 and H3K27me3 modification patterns, resulting in a stochastic perturbation of epigenetic programming. The dramatic replicate variability of H3K4me2 and H3K27me3 marks also observed in Jurkat cells treated low-dose TSA, a known epigenetic modulator (Figure 4c), corroborated that epigenetic perturbation is indeed detectable at the level of sample variance. ELF-MF exposure, when compared to sham-exposed or un-exposed (t0) conditions, significantly increased the replicate variability of H3K27me3 modifications while reducing the variability of H3K4me2 modifications in Jurkat cell (Figure 4c). Consistent with the higher epigenetic plasticity of stem- and tissue progenitor cells, replicate variabilities of H3K4me2 and H3K27me3 modifications were more pronounced in populations of CD34+ hematopoietic stem cells and neutrophilic progenitors (t5) than in populations of Jurkat cells (Figure 4c, 4d). Here, ELF-MF exposure significantly reduced the replicate variability of both H3K4me2 and H3K27me3 modifications in neutrophilic progenitors (Figure 4d), and the same was apparent in the DNA methylation data (Figure 4f). Notably, the decrease in replicate variability in ELF-MF exposed cells correlated well with a more robustly directed differentiation into the neutrophilic lineage, as indicated by a reduced median variability of the maturation stages (Supplementary Figure S13). Together, these observations indicate that ELF-MF exposure can affect the robustness of the establishment and/or maintenance of key epigenetic modifications, particularly in differentiating cell populations.

The stabilizing effect of ELF-MF on epigenetic modifications partially depends on chromatin state. Next, we investigate whether the variability in epigenetic modifications is randomly distributed across the genome or preferentially associated with certain genomic features. We intersected the

profiles of histone and DNA modifications with annotated gene promoters, exons, introns and intergenic regions and also correlated them with bivalent chromatin domains identified by co-occupancy of active H3K4me2 and repressive H3K27me3 marks in our ChIP-seq data. In TSA treated Jurkat cells, H3K4me2 variability showed little dependency on genomic context while H3K27me3 was clearly most variable at gene promoters and in bivalent chromatin (Figure 5b), consistent with the preferential localisation of histone acetylation at gene promoters and enhancers[41]. ELF-MF exposure, however, reduced replicate variability of H3K4me2 modifications and increased variability of H3K27me3 modifications irrespective of the genomic context (Figure 5a,b). In neutrophilic progenitors, H3K4me2 and H3K27me3 modifications generally showed the highest reproducibility at promoters and in bivalent chromatin domains and a pronounced replicate variability particularly in introns and intergenic regions (Figure 5c). ELF-MF exposure decreased replicate variability of H3K4me2 marks at all genomic locations except in bivalent chromatin domains (Figure 5c,e; Supplementary Figure S13). Consistently, active gene promoters, devoid of H3K27me3, were significantly more stabilized by exposure than bivalent promoters, co-occupied by H3K4me2 and H3K27me3 modifications (Supplementary Figure S13). ELF-MF exposure also reduced the variability of H3K27me3 modifications, although less pronounced and without much preference for any of the genomic sites assessed (Figure 5d,f; Supplementary Figure S13). The variability of DNA methylation was also significantly decreased upon ELF-MF exposure, although without much preference for a particular genomic context (Figure 5g). These results indicate that ELF-MF affects the robustness of epigenetic marks in a partially genomic context-dependent manner, with the most distinctive feature being the H3K4me2 modification in active and bivalent gene promoters of differentiating cells.

Bivalent chromatin is associated with transcriptionally poised states and often present at regulatory elements of developmental genes that will be activated or repressed in the course of cell differentiation[29,42]. As bivalent chromatin is highly dynamic but seemingly less variable and more protected from ELF-MF impact in differentiating neutrophilic progenitors, we investigated whether the robustness of H3K4me2 and H3K27me3 marks correlates with differentiation associated changes in chromatin status. We identified genomic tiles changing H3K4me2 or H3K27me3 modification (FDR-adjusted P value < 0.05) during neutrophilic differentiation and categorized them into upregulated (log2 FC > +0.6), downregulated (log2 FC < -0.6) or not changed for either of the histone modifications. Then, we intersected tiles with H3K4me2 and/or H3K27me3 occupancy in neutrophilic progenitors with the tiles in the three categories of differentiation associated change (Figure 6a) Analysing these categories confirmed that ELF-MF exposure generally reduced H3K4me2 variability in active (H3K4me2) but not in bivalent chromatin (H3K4me2 and H3K27me3), and this effect was independent of the differentiation dynamics in either of the modifications (Figure 6a). By contrast,

ELF-MF exposure reduced the variability of H3K27me3 modification with a clear dependency on chromatin dynamics; it was most pronounced in tiles losing the repressive histone mark during differentiation, regardless the status of bivalency (Figure 6a). We then examined the relationship between the differentiation dynamics of the histone modifications and the ELF-MF effect on their relative enrichment (Figure 6b). The ELF-MF effect on H3K4me2 occupancy was strongest in tiles representing active chromatin (H3K4me2 only) that gained H3K4me2 during differentiation, while the exposure effect on H3K27me3 occupancy was highest in tiles that lost the modification during differentiation. To address whether effects of ELF-MF exposure on DNA methylation follow the same pattern, we analysed replicate variability of DNA methylation data from neutrophilic progenitors in CpG sites significantly hypo- (log2 FC < -0.6, FDR-adjusted *P* value < 0.05) or hypermethylated (log2 FC > +0.6, FDR-adjusted *P* value < 0.05) or unchanged in the course of differentiation. Consistent with the data on H3K27me3, the ELF-MF exposure was associated with a significantly reduced variability of CpG methylation at sites losing 5mC during differentiation but had no effect as sites gaining 5mC. We also observed that the ELF-MF impact on DNA methylation levels in neutrophilic progenitors was less pronounced at sites that change CpG methylation during differentiation that at sites that show no changes (Figure 6d). These observations suggest that ELF-MF exposure stabilizes epigenetic modifications in regions marked by H3K4me2 that lose H3K27me3 and/or undergo DNA demethylation during differentiation, i.e. in chromatin that changes from a repressive to an active state during differentiation.

Discussion

Epidemiological studies have associated the exposure to ELF-MF with an increased risk of childhood leukaemia but underlying biological mechanisms have remaining elusive. The concept of cancer promotion through DNA damage-induced genetic mutation is widely accepted for ionizing ration but appears, on the basis of energetic considerations, not applicable to ELF-MF. We reasoned that ELF-MF exposure may affect the epigenome rather than the genome, thereby promoting cancerous changes in cell identity and behaviour. Our aim was to explore the possibility that ELF-MF exposure influences the stability and programming of key epigenetic modifications in leukemic cells and in differentiating hematopoietic stem cells in a way that may explain enhanced leukaemogenesis.

The epigenome is well-known to be susceptible to environmental influences of all kinds, including the exposure to non-mutagenic carcinogens[21,22,34]. We showed here that the treatment of leukaemic Jurkat cells with a very low, sub-toxic dose of TSA, not affecting cell behaviour or phenotype in any notable way, destabilizes and alters patterns of the key epigenetic modifications (H3K4me2 and

H3K27me3) in a way readily detectable by genome-wide profiling, hence documenting the feasibility and sensitivity of our approach to measure subtle epigenetic aberrations. Yet, the evaluation of the impact of ELF-MF exposure on the profile of these marks in Jurkat cells did not reveal any specific and reproducible exposure-dependent alterations. We therefore conclude that in the well-controlled experimental setup of this study, ELF-MF exposure does not cause perturbations on the epigenetic landscape in a leukaemic cell line. Likewise, we observed no statistically significant alterations of epigenetic modifications in neutrophilic progenitors after five days of *in vitro* differentiation under ELF-MF exposure. Neither H3K4me2, nor H3K27me3, nor DNA methylation marks were influenced by the exposure, although extensive differentiation-associated changes in these modifications were clearly evident. The absence of an impact of the ELF-MF on CpG methylation levels and patterning during neutrophilic granulopoiesis is in contrast to a previous report, indicating changes in global cytosine methylation of a murine spermatocytes-derived cell line when exposed to a comparable ELF-MF (50 Hz, 1 mT or 3 mT, intermitted, 72 h)[30]. This discrepancy could be explained by cell type-specific susceptibilities of the DNA methylation system to ELF-MF exposure or by a different permissiveness of the culture systems for the establishment of epigenetic variation in subpopulations of cells. Our *in vitro* differentiation system was tightly controlled by the growth factor G-CSF and cytokines, allowing specifically for growth and development of cells of the neutrophilic lineage while restricting the establishment of other cell-types. The minor exposure-dependent, transient differences in cell cycle progression and apoptosis early in the differentiating cell populations may indeed reflect an underlying positive selection for neutrophilic cells, which overall supported the formation of homogenous populations of promyelocytes and myelocytes, irrespective of the ELF-MF exposure. So, selection may have masked epigenetic divergence in our experiments, which may have been picked up more easily by the less stringent conditions in the experiments with spermatocyte-derived cells. ELF-MF exposure of these cells might have triggered spontaneous differentiation responses that were tolerated in the culture and, ultimately, gave rise to detectable epigenetic change. Enhancement of differentiation upon ELF-MF exposure was reported in neuronal cells[23,24,43], where it correlated with a gain of H3K9 acetylation at specific neuronal genes, promoting their activation[44].

Our data thus suggests that ELF-MF exposure has no specific and reproducible effect on key epigenetic modifications in leukaemic cells and differentiating haematopoietic cells. We cannot rule out potential effects on histone modifications that were not studied here or under different experimental conditions, .e.g. under prolonged duration or a different mode of ELF-MF exposure or with different cell-lines or differentiation cell culture conditions. A closer examination of the data, however, revealed a potential impact ELF-MF exposure on the robustness of the epigenetic

programming. ELF-MF exposure was generally associated with a reduced variability in ChIP-seq and DNA methylation data between replicate samples, the exception being H3K27me3 in Jurkat cells, showing increased variability upon ELF-MF exposure. Notably, the treatment of Jurkat cells with TSA, a known epigenetic modulator, generated similar effects on replicate variability for both histone modifications, suggesting that the variance in replicate data sets can be a measure for epigenetic robustness, which in the case of ELF-MF exposure appears to be perturbed in a stochastic manner. The impact of ELF-MF exposure on the reproducibility of histone and DNA modification patterns is likely to depend on cell-type specific epigenetic states and plasticity, as well as differential sensitivities to ELF-MFs[45,46,47]. For instance, it was reported that chromatin conformation changes following low dose ELF-MF exposure of human lymphocytes depend on the initial chromatin state[48]. Investigating the viscosity of chromatin, these authors found that relaxed chromatin becomes more condensed and compact chromatin more open upon ELF-MF exposure; i.e. that chromatin perturbance by ELF-MFs is context dependent. Our *in vitro* differentiation starts with an epigenetically dynamic and heterogeneous stem cell population[49-51], as also indicated by a high replicate variability for H3K4me2 and H3K27me3 modifications in CD34+ cells. ELF-MF exposure then appears to exert a homogenizing effect on the initially variable chromatin states in the early differentiating cell population, hence reducing the replicate variability at later time points in differentiation. We found ELF-MF exposure to increase the robustness of histone modifications as well as DNA methylation, particularly in genomic regions marked by H3K4me2 and losing H3K27me3 and/or DNA methylation in the course of differentiation. As H3K4me2 and unmethylated CpGs are associated with transcriptionally active chromatin, allowing for binding of transcription factors, the locus-specific pattern of reduced replicate variability upon ELF-MF exposure coincides with sites of transcriptional activity and/or chromatin opening during differentiation. These results therefore suggest that open and active chromatin is more affected by MF exposure than condensed chromatin.

Notably, to monitor the status of our cell cultures and assess the comparability of the genomic data produced, we systematically measures a variety of cell growth parameters throughout all experiments. Previous studies reported ELF-MF exposure-dependent alterations in cell proliferation, cell cycle progression and apoptosis in various cancerous and non-cancerous cells[19,32,38,52,53]. We observed no alterations in cell proliferation in Jurkat cells and during granulopoiesis upon ELF-MF exposure and neither did we notice any effects on apoptosis or cell cycle progression in Jurkat cells. During granulopoiesis, we found small differences in cell cycle progression concomitant with an increased induction of apoptosis in ELF-MF exposed cultures at day four, which may have had a synchronizing effect on exposed cell populations and thereby contributed to the reduced replicate variability observed of these cultures.

In conclusion, we report that ELF-MF exposure has no significant effect on the epigenetic landscapes of leukaemic and differentiating haematopoietic cells. However, our data indicate that ELF-MF exposure may influence the robustness of histone modification and DNA methylation patterning in the course of the global chromatin reorganization associated with neutrophilic differentiation. This, however, did not notably affect the overall dynamics and efficiency of granulopoiesis.

Methods

Cell culture and neutrophilic differentiation.

Culturing of cells was routinely performed at 37°C in a humidified atmosphere with 5% CO_2. Jurkat cells (acute T cell leukaemia) were cultured in RPMI-1640 medium supplemented with 2 mM L-glutamine, 1 mM Na-pyruvate, 10% FCS and 0.6x penicillin/streptomycin (Sigma-Aldrich). Fresh medium was supplied every 48 h. For ELF-MF exposure experiments, cells were seeded at a density of 10^5 cells/mL and grown for the indicated time without addition of fresh medium. As positive control, cells were treated with 10 nM trichostatin A (TSA). CD34-positive cells isolated from human cord blood of mixed donors were obtained from AllCells (Alabama, United States). CD34+ cells were propagated in Stemline II medium expansion medium (Stemcell technology) supplemented with 100 ng/mL thrombopoietin, 100 ng/mL stem cell factor, 10 ng/mL Flt3-ligand (Peprotech), 5000 U/mL Penicillin and 5 mg/mL Streptomycin (Sigma-Aldrich) for four days (De Bruyn et al., 2003). For the neutrophilic differentiation, expanded CD34+ cord blood cells were seeded at cell densities of 10^5 cells/mL in Stemline II medium supplemented with 100 ng/mL stem cell factor, 10 ng/mL Flt3-ligand, 100 ng/mL G-CSF (Peprotech), 5000 U/mL Penicillin and 5 mg/mL Streptomycin (Sigma-Aldrich) and cultured for 10 days. Every second day, fresh cell culture medium was added (1:2 dilution).

Exposure to ELF-MF.

The exposure system sXc-ELF (IT'IS, Zurich, Switzerland) allows for a well-controlled exposure with ELF-MF (Supplementary Figure S1)[54]. The selected exposure for the leukaemic cell line was sinusoidal ELF-MF (50 Hz, 1 mT, 5' on/10' off) or sham for approximately 3.5 cell cycles (72 h). The electric field caused by the coil was shielded and the magnetic field uniformity was better than 1% (SD). Each coil was place inside a μ-metallic box and the boxes placed side by side in the same incubator to decouple the coils, to shield the electric and magnetic fields generated by the incubator and to ensure the same environmental conditions (temperature, humidity and CO_2). The field attenuation between the coils was at least a factor of 150, i.e., the shame exposure was anywhere less than 7 μT

compared to the uniform exposure of 1 mT. The exposure system meets the general criteria established in [Recommended Minimal Requirements and Development Guidelines for Exposure Setup of Bio-Experiments Addressing the Health Risk Concern of Wireless Communications]. Intermittent exposure is often chosen as it reflects in situ better than continuous exposures and it has also been demonstrated to enhance the response, i.e. showed the largest ELF-MF response on comet assay tail factors with 5'on/10'off cycles. Control exposures were done in parallel, either in a μ-metal shielded compartment inside the exposure incubator or in different incubator. Randomized assignment of ELF-MF and sham exposure conditions to the two chambers allows experiments blinded for the observer. Continuous temperature monitoring confirmed that the temperature difference between the exposure chambers was less than 0.1°C.

Cell cycle, apoptosis measurement and identification of cell differentiation state by flow cytometry.

Cell cycle profiles were analysed by propidium iodide staining as described in detail elsewhere[17]. The number of apoptotic cells in the population was estimated by the Annexin-V Alexa488/PI kit (Invitrogen) according to the provider's recommendations. Maturation status of the differentiating neutrophilic cell population was analysed by immuno-detection of cell surface markers. The following combination of antibodies were used: PE mouse anti-human CD16b, APC mouse anti-human CD34, APC-Cy7 mouse anti-human CD11b, PE-Cy7 mouse anti-human CD14 (all from BD Biosciences) and FITC-anti-Annexin V (Invitrogen). Neutrophilic differentiation stages were identified by gating on subpopulations according to the expression of surface markers (Supplementary Figure S6)[55]: CD34+ cells (CD34+, CD11b-, CD16b-), promyelocytes (CD34-, CD11b-, CD16b-), myelocytes (CD34-, CD11b+, CD16b-) and metamyelocytes (CD36-, CD11b+, CD16b+). Monocytes were identified according to the expression of CD14+. All samples were measured using a FACS cytometer (Beckton Dickinson) and analysed by FlowJo Software. Data were statistically analysed by χ^2 test for each replica as well as pairwise comparison by Student's *t*-test using GraphPad Prism. Full methodical details are given in the Supplementary information.

Base resolution DNA methylation analysis by Illumina Infinium HumanMethylation 450 array.

Genomic DNA was extracted from frozen cell pellets by QIAamp DNA mini kit (Qiagen) according to the manufacturer's instructions including an RNase-treatment step. 500 ng of genomic DNA was bisulfide converted using the EZ-96 DNA Methylation Kit (Zymo Research Corporation). Genome-wide assessment of DNA methylation was done on Illumina Infinium HumanMethylation 450 Beadchip arrays, interrogating methylation at 485,577 sites[56]. Raw signal intensities were extracted by the Illumina GenomeStudio software and imported into R as a methylumi object using the

methylumi package. Data normalization was performed applying the dasen method as described previously[57]. Briefly, probe-level signals for individual CpG sites were subjected to background adjustment, followed by quantile normalization of both typeI and typeII probes separately. Probes for CpG sites with signal intensities not significantly different ($P < 0.05$) from background measurements in any data sets or mapping to regions with known germline polymorphisms, to multiple genomic loci[58], or to either sex chromosome were removed, yielding a total of 412,940 CpG after filtering. All computational and statistical analyses were performed using R and Bioconductor[59]. All analyses for differential methylation were performed on M-values (M = log2 (methylated/unmethylated) as recommended[60]. Empirical Bayes methodology utilizing a moderated t-statistic available in limma was used to test for significant differences between the groups (Smyth, 2004). False-discovery rate (FDR)-adjusted *P* values for multiple comparisons were calculated using the Benjamini and Hochberg approach. Differentially methylated CpGs were defined as those with both a false discovery rate (FDR) adjusted *P* value < 0.05 and log2 fold change > 0.6. Variance was calculated based on M-values[60].

Whole-genome analysis of histone modifications.

The ChIP protocol using ChIP-validated antibodies for the H3K4 dimethylation and H3K27 trimethylation histone modifications (Millipore) of 20-30 µg chromatin was performed as described previously[61] and in the Supplementary information in detail. Single-end 50 bp reads sequencing of ChIP was performed at the Quantitative Genomics Facility in Basel and at Genome Technology Access Center (GTAC) in St. Louis (Missouri, USA), using standard protocols for library generation for the Illumina HiSeq platform. To maintain the blinding of ELF-MF exposure conditions during ChIP-seq and bioinformatics analyses, sample pooling was guided by the IT'IS foundation. In total 16 libraries were sequenced from H3K4me2 and H3K27me3 ChIP samples of Jurkat cells: 2 sample pools of 3 independent exposure replicates for each condition (before exposure, sham-, ELF-MF-exposure and TSA treatment) and both histone modifications, resulting in around 200 Mio reads for the exposure conditions and 50 Mio reads for the TSA treated samples. For the analysis of primary cells during neutrophilic differentiation, 14 libraries were generated from H3K4me2 and H3K27me3 ChIP samples: one independent exposure replicate as well as one pool of two independent exposure replicates for each exposure condition (ELF-MF and sham) for CD34+ cells and neutrophilic progenitors at day°5. For the control differentiation, ChIPs of two independent replicates of progenitor cells were pooled. Additionally, two input controls were included, one each for CD34+ and progenitors cells.

The analysis of ChIP-seq data was performed at the scientific computing core facility (sciCORE) of the University of Basel. For each library, sequence reads were aligned to the human reference genome assembly (hg19) using the Sequence Mapping and Alignment Tool (SMALT v 0.6.2). High quality alignments (bamtools filter-mapQuality ">30") were extracted. Center positions of ChIPped DNA fragments were approximated based on average fragment lengths and orientations of read alignments (http://ccg.vital-it.ch/chipseq/chip_center.php). Fragment center-positions of each library were used to call genomic domains for H3K4me2 or H3K27me3 with increased read densities applying the program "chippart" (http://ccg.vital-it.ch/chipseq/). Global domain sets were assembled by combining domains less than 1 kb apart with the merge function of bedtools and being present in at least one of the samples. Merged domain sets were subdivided into tiles of uniform lengths of 500 and 1,000 bp. After random downsampling of high quality alignments (51 Mio and 26 Mio for Jurkat and HSC, respectively), the number of reads mapping within tiles (fragment center-positions) were extracted for each library. Tiles were further filtered for read counts above an arbitrary threshold above background (50 reads for H3K4me2, 30 for H3K27me3 per 500 bp tile and 100 reads for H3K4me2, 60 for H3K27me3 per 1,000 bp tile length) in at least one sample. In the differentiation experiment an additional filtering criteria of 7 read counts above the corresponding input was applied. Read counts within genomic tiles were tested for differences between groups of samples applying a generalized linear model (GLM) likelihood ratio test as implemented in the EdgeR package, originally developed for differential gene expression data[62]. In brief, the dispersion parameter of the negative binomial model was estimated for each genomic interval. Tables with read counts resulting from the merging, normalization and filtering were used and the log2-fold changes and *P* values of the GLM likelihood ratio test were computed under the null hypothesis that the fitted coefficients of negative binomial GLMs of the compared groups are equal. Domains (500 bp and 1,000 bp) with significant alterations were defined as those with both a false discovery rate (FDR) adjusted *P* value < 0.05 and log2 fold change > ±0.6. If overlaying 500 and 1,000 bp tiles had significant alteration 500 bp tile was selected.

The integrative genomics viewer was used to visualize ChIP-seq reads[63,64]. Coefficient of variation and the principal component coefficients were calculated based on the normalized read counts from EdgeR comparisons of 500 bp domain of Chip-seq datasets and analysed by R/Bioconductor. Intersections between H3K4me2 and H3K27me3 ChIP-seq data in 500 bp tiles indicate bivalent domains. Promoter, exons, introns, intergenic regions and transcription start side were defined using the Bioconductor package TxDb.Hsapiens.UCSC.hg19.knownGene and analysed by R/Bioconductor[59].

References

1 SCENIHR. Potential health effects of exposure to electromagnetic fields (EMF). *European Commission* (2015).

2 WHO. Environmental Health Criteria 238, Extremely low frequency fields *World Health Organization* (2007).

3 IARC. Evaluation of carcinogenic risks to humans: Non-ionizing radiation, Part 1:static and extremely low-frequency (elf) electro and magnetic fields. *WHO* (2002).

4 Schuz, J. *et al.* Extremely low-frequency magnetic fields and risk of childhood leukemia: A risk assessment by the ARIMMORA consortium. *Bioelectromagnetics*, doi:10.1002/bem.21963 (2016).

5 Soffritti, M. *et al.* Life-span exposure to sinusoidal-50 Hz magnetic field and acute low-dose gamma radiation induce carcinogenic effects in Sprague-Dawley rats. *Int J Radiat Biol* **92**, 202-214, doi:10.3109/09553002.2016.1144942 (2016).

6 Pui, C. H., Robison, L. L. & Look, A. T. Acute lymphoblastic leukaemia. *Lancet* **371**, 1030-1043, doi:10.1016/S0140-6736(08)60457-2 (2008).

7 Bhojwani, D., Yang, J. J. & Pui, C. H. Biology of childhood acute lymphoblastic leukemia. *Pediatr Clin North Am* **62**, 47-60, doi:10.1016/j.pcl.2014.09.004 (2015).

8 Armstrong, S. A. & Look, A. T. Molecular genetics of acute lymphoblastic leukemia. *J Clin Oncol* **23**, 6306-6315, doi:10.1200/JCO.2005.05.047 (2005).

9 Greaves, M. Childhood leukaemia. *BMJ* **324**, 283-287 (2002).

10 Greenblatt, S. M. & Nimer, S. D. Chromatin modifiers and the promise of epigenetic therapy in acute leukemia. *Leukemia* **28**, 1396-1406, doi:10.1038/leu.2014.94 (2014).

11 Grossmann, V. *et al.* The molecular profile of adult T-cell acute lymphoblastic leukemia: mutations in RUNX1 and DNMT3A are associated with poor prognosis in T-ALL. *Genes Chromosomes Cancer* **52**, 410-422, doi:10.1002/gcc.22039 (2013).

12 Ntziachristos, P. *et al.* Genetic inactivation of the polycomb repressive complex 2 in T cell acute lymphoblastic leukemia. *Nat Med* **18**, 298-301, doi:10.1038/nm.2651 (2012).

13 Hanahan, D. & Weinberg, R. A. Hallmarks of cancer: the next generation. *Cell* **144**, 646-674, doi:10.1016/j.cell.2011.02.013 (2011).

14 Mathews, C. K. Deoxyribonucleotide metabolism, mutagenesis and cancer. *Nat Rev Cancer* **15**, 528-539, doi:10.1038/nrc3981 (2015).

15 Negrini, S., Gorgoulis, V. G. & Halazonetis, T. D. Genomic instability--an evolving hallmark of cancer. *Nat Rev Mol Cell Biol* **11**, 220-228, doi:10.1038/nrm2858 (2010).

16 Adair, R. K. Extremely Low Frequency Electromagnetic Fields Do Not Interact Directly With DNA. *Bioelectromagnetics*, 136–137 (1998).

17 Focke, F., Schuermann, D., Kuster, N. & Schar, P. DNA fragmentation in human fibroblasts under extremely low frequency electromagnetic field exposure. *Mutat Res* **683**, 74-83, doi:10.1016/j.mrfmmm.2009.10.012 (2010).

18 Vijayalaxmi & Prihoda, T. J. Genetic damage in mammalian somatic cells exposed to extremely low frequency electro-magnetic fields: a meta-analysis of data from 87 publications (1990-2007). *Int J Radiat Biol* **85**, 196-213, doi:10.1080/09553000902748575 (2009).

19 Mihai, C. T., Rotinberg, P., Brinza, F. & Vochita, G. Extremely low-frequency electromagnetic fields cause DNA strand breaks in normal cells. *J Environ Health Sci Eng* **12**, 15, doi:10.1186/2052-336X-12-15 (2014).

20 Duan, W. *et al.* Comparison of the genotoxic effects induced by 50 Hz extremely low-frequency electromagnetic fields and 1800 MHz radiofrequency electromagnetic fields in GC-2 cells. *Radiat Res* **183**, 305-314, doi:10.1667/RR13851.1 (2015).

21 Feil, R. Environmental and nutritional effects on the epigenetic regulation of genes. *Mutat Res* **600**, 46-57, doi:10.1016/j.mrfmmm.2006.05.029 (2006).

22 Feil, R. & Fraga, M. F. Epigenetics and the environment: emerging patterns and implications. *Nat Rev Genet* **13**, 97-109, doi:10.1038/nrg3142 (2011).

23 Ma, Q. *et al.* Extremely low-frequency electromagnetic fields affect transcript levels of neuronal differentiation-related genes in embryonic neural stem cells. *PLoS One* **9**, e90041, doi:10.1371/journal.pone.0090041 (2014).

24 Jung, I. S., Kim, H. J., Noh, R., Kim, S. C. & Kim, C. W. Effects of extremely low frequency magnetic fields on NGF induced neuronal differentiation of PC12 cells. *Bioelectromagnetics* **35**, 459-469, doi:10.1002/bem.21861 (2014).

25 Cheng, Y. *et al.* Extremely low-frequency electromagnetic fields enhance the proliferation and differentiation of neural progenitor cells cultured from ischemic brains. *Neuroreport* **26**, 896-902, doi:10.1097/WNR.0000000000000450 (2015).

26 Ma, Q. *et al.* Extremely Low-Frequency Electromagnetic Fields Promote In Vitro Neuronal Differentiation and Neurite Outgrowth of Embryonic Neural Stem Cells via Up-Regulating TRPC1. *PLoS One* **11**, e0150923, doi:10.1371/journal.pone.0150923 (2016).

27 Bernstein, B. E., Meissner, A. & Lander, E. S. The mammalian epigenome. *Cell* **128**, 669-681, doi:10.1016/j.cell.2007.01.033 (2007).

28 Cedar, H. & Bergman, Y. Epigenetics of haematopoietic cell development. *Nat Rev Immunol* **11**, 478-488, doi:10.1038/nri2991 (2011).

29 Boland, M. J., Nazor, K. L. & Loring, J. F. Epigenetic regulation of pluripotency and differentiation. *Circ Res* **115**, 311-324, doi:10.1161/CIRCRESAHA.115.301517 (2014).

30 Liu, Y. *et al.* Effect of 50 Hz Extremely Low-Frequency Electromagnetic Fields on the DNA Methylation and DNA Methyltransferases in Mouse Spermatocyte-Derived Cell Line GC-2. *Biomed Res Int* **2015**, 237183, doi:10.1155/2015/237183 (2015).

31 Baek, S. *et al.* Electromagnetic Fields Mediate Efficient Cell Reprogramming into a Pluripotent State. *Acs Nano* **8**, 10125-10138, doi:10.1021/nn502923s (2014).

32 Brisdelli, F. *et al.* ELF-MF attenuates quercetin-induced apoptosis in K562 cells through modulating the expression of Bcl-2 family proteins. *Mol Cell Biochem* **397**, 33-43, doi:10.1007/s11010-014-2169-1 (2014).

33 Santini, M. T., Ferrante, A., Rainaldi, G., Indovina, P. & Indovina, P. L. Extremely low frequency (ELF) magnetic fields and apoptosis: a review. *Int J Radiat Biol* **81**, 1-11, doi:10.1080/09553000400029502 (2005).

34 Damdimopoulou, P., Weis, S., Nalvarte, I. & Ruegg, J. Marked For Life: How Environmental Factors Affect the Epigenome. *Issues Toxicol*, 44-69, doi:10.1039/9781849732970-00044 (2012).

35 Jaenisch, R. & Bird, A. Epigenetic regulation of gene expression: how the genome integrates intrinsic and environmental signals. *Nat Genet* **33 Suppl**, 245-254, doi:10.1038/ng1089 (2003).

36 Tura, O., Barclay, G. R., Roddie, H., Davies, J. & Turner, M. L. Optimal ex vivo expansion of neutrophils from PBSC CD34+ cells by a combination of SCF, Flt3-L and G-CSF and its inhibition by further addition of TPO. *J Transl Med* **5**, 53, doi:10.1186/1479-5876-5-53 (2007).

37 Tofani, S. *et al.* Static and ELF magnetic fields induce tumor growth inhibition and apoptosis. *Bioelectromagnetics* **22**, 419-428 (2001).

38 Garip, A. I. & Akan, Z. Effect of ELF-EMF on number of apoptotic cells; correlation with reactive oxygen species and HSP. *Acta Biol Hung* **61**, 158-167, doi:10.1556/ABiol.61.2010.2.4 (2010).

39 Noreen, F. *et al.* Modulation of age- and cancer-associated DNA methylation change in the healthy colon by aspirin and lifestyle. *J Natl Cancer Inst* **106**, doi:10.1093/jnci/dju161 (2014).

40 Mitchell, C., Schneper, L. M. & Notterman, D. A. DNA methylation, early life environment, and health outcomes. *Pediatr Res* **79**, 212-219, doi:10.1038/pr.2015.193 (2016).

41 Nicholson, T. B., Veland, N. & Chen, T. Writers, Readers, and Erasers of Epigenetic Marks. 31-66, doi:10.1016/b978-0-12-800206-3.00003-3 (2015).

42 Bernstein, B. E. *et al.* A bivalent chromatin structure marks key developmental genes in embryonic stem cells. *Cell* **125**, 315-326, doi:10.1016/j.cell.2006.02.041 (2006).

43 Marcantonio, P. *et al.* Synergic effect of retinoic acid and extremely low frequency magnetic field exposure on human neuroblastoma cell line BE(2)C. *Bioelectromagnetics* **31**, 425-433, doi:10.1002/bem.20581 (2010).

44 Leone, L. *et al.* Epigenetic modulation of adult hippocampal neurogenesis by extremely low-frequency electromagnetic fields. *Mol Neurobiol* **49**, 1472-1486, doi:10.1007/s12035-014-8650-8 (2014).

45 Mangiacasale, R. *et al.* Normal and cancer-prone human cells respond differently to extremely low frequency magnetic fields. *FEBS Lett* **487**, 397-403 (2001).

46 Yoon, H. E., Lee, J. S., Myung, S. H. & Lee, Y. S. Increased gamma-H2AX by exposure to a 60-Hz magnetic fields combined with ionizing radiation, but not hydrogen peroxide, in non-tumorigenic human cell lines. *Int J Radiat Biol* **90**, 291-298, doi:10.3109/09553002.2014.887866 (2014).

47 Juutilainen, J., Kumlin, T. & Naarala, J. Do extremely low frequency magnetic fields enhance the effects of environmental carcinogens? A meta-analysis of experimental studies. *Int J Radiat Biol* **82**, 1-12, doi:10.1080/09553000600577839 (2006).

48 Sarimov, R., Alipov, E. D. & Belyaev, I. Y. Fifty hertz magnetic fields individually affect chromatin conformation in human lymphocytes: dependence on amplitude, temperature, and initial chromatin state. *Bioelectromagnetics* **32**, 570-579, doi:10.1002/bem.20674 (2011).

49 Engelhardt, M., Lubbert, M. & Guo, Y. CD34(+) or CD34(-): which is the more primitive? *Leukemia* **16**, 1603-1608, doi:10.1038/sj.leu.2402620 (2002).

50 Jobin, C., Cloutier, M., Simard, C. & Neron, S. Heterogeneity of in vitro-cultured CD34+ cells isolated from peripheral blood. *Cytotherapy* **17**, 1472-1484, doi:10.1016/j.jcyt.2015.05.006 (2015).

51 D'Arena, G. *et al.* Human umbilical cord blood: immunophenotypic heterogeneity of CD34+ hematopoietic progenitor cells. *Haematologica* **81**, 404-409 (1996).

52 Trillo, M. A., Martinez, M. A., Cid, M. A., Leal, J. & Ubeda, A. Influence of a 50 Hz magnetic field and of all-transretinol on the proliferation of human cancer cell lines. *Int J Oncol* **40**, 1405-1413, doi:10.3892/ijo.2012.1347 (2012).

53 Zhang, M. *et al.* Effects of low frequency electromagnetic field on proliferation of human epidermal stem cells: An in vitro study. *Bioelectromagnetics* **34**, 74-80, doi:10.1002/bem.21747 (2013).

54 Schuderer, J., Oesch, W., Felber, N., Spat, D. & Kuster, N. In vitro exposure apparatus for ELF magnetic fields. *Bioelectromagnetics* **25**, 582-591, doi:10.1002/bem.20037 (2004).

55 Elghetany, M. T. Surface antigen changes during normal neutrophilic development: a critical review. *Blood Cells Mol Dis* **28**, 260-274, doi:10.1006/bcmd.2002.0513 (2002).

56 Sandoval, J. *et al.* Validation of a DNA methylation microarray for 450,000 CpG sites in the human genome. *Epigenetics* **6**, 692-702, doi:10.4161/epi.6.6.16196 (2014).

57 Touleimat, N. Complete pipeline for Infinium®Human Methylation 450K BeadChip data processing using subset quantile normalization for accurate DNA methylation estimation. *Epigenomics* (2012).

58 Price, M. E. *et al.* Additional annotation enhances potential for biologically-relevant analysis of the Illumina Infinium HumanMethylation450 BeadChip array. *Epigenetics Chromatin* **6**, 4, doi:10.1186/1756-8935-6-4 (2013).

59 Gentleman, R. C. *et al.* Bioconductor: open software development for computational biology and bioinformatics. *Genome Biol* **5**, R80, doi:10.1186/gb-2004-5-10-r80 (2004).

60 Du, P. *et al.* Comparison of Beta-value and M-value methods for quantifying methylation levels by microarray analysis. *BMC Bioinformatics* **11**, 587, doi:10.1186/1471-2105-11-587 (2010).

61 Cortazar, D. *et al.* Embryonic lethal phenotype reveals a function of TDG in maintaining epigenetic stability. *Nature* **470**, 419-423, doi:10.1038/nature09672 (2011).

62 Robinson, M. D., McCarthy, D. J. & Smyth, G. K. edgeR: a Bioconductor package for differential expression analysis of digital gene expression data. *Bioinformatics* **26**, 139-140, doi:10.1093/bioinformatics/btp616 (2010).

63 Robinson, J. T. *et al.* Integrative genomics viewer. *Nat Biotechnol* **29**, 24-26, doi:10.1038/nbt.1754 (2011).

64 Thorvaldsdottir, H., Robinson, J. T. & Mesirov, J. P. Integrative Genomics Viewer (IGV): high-performance genomics data visualization and exploration. *Brief Bioinform* **14**, 178-192, doi:10.1093/bib/bbs017 (2013).

65 Barrett, T. *et al.* NCBI GEO: archive for functional genomics data sets--update. *Nucleic Acids Res.* **41**, D991-995, doi:10.1093/nar/gks1193 (2013).

Acknowledgements

We thank all members of the Schär laboratory and the ARIMMORA consortium for critical and helpful discussions. The research leading to these results has received funding from the European Union's Seventh Framework Programme (FP7/2007-2013) under grant agreement no. 282891.

Author contributions

M.Ma. conceived, performed and analyzed the experiments, and also contributed to the bioinformatic analyses and the writing of the manuscript. M.R.S., C.D.S. and F.N. performed bioinformatics analyses of the genome-wide data sets. M.Mu. and N.K. provided and serviced the exposure system, and ensured experimental blinding. D.S. and P.S. designed and supervised the project, and contributed to the writing of the paper. All authors have read and reviewed the manuscript.

Additional information

Accession codes: Raw and processed data of ChIP-seq and DNA methylation analyses have been deposited in NCBI's Gene Expression Omnibus (GEO) database[65] and are accessible through the GEO accession numbers GSE85392 (DNA methylation), GSE85562 and GSE85601 (histone modifications).

Geo reviewer links:

http://www.ncbi.nlm.nih.gov/geo/query/acc.cgi?token=aruzoaykfvkttil&acc=GSE85392

http://www.ncbi.nlm.nih.gov/geo/query/acc.cgi?token=gpcvmokmrhyrvul&acc=GSE85601

http://www.ncbi.nlm.nih.gov/geo/query/acc.cgi?token=cngxgwuezpklvqr&acc=GSE85562

Supplementary information accompanies this paper at http://www.nature.com/srep

Competing financial interests: The authors declare no competing financial interests.

Figures

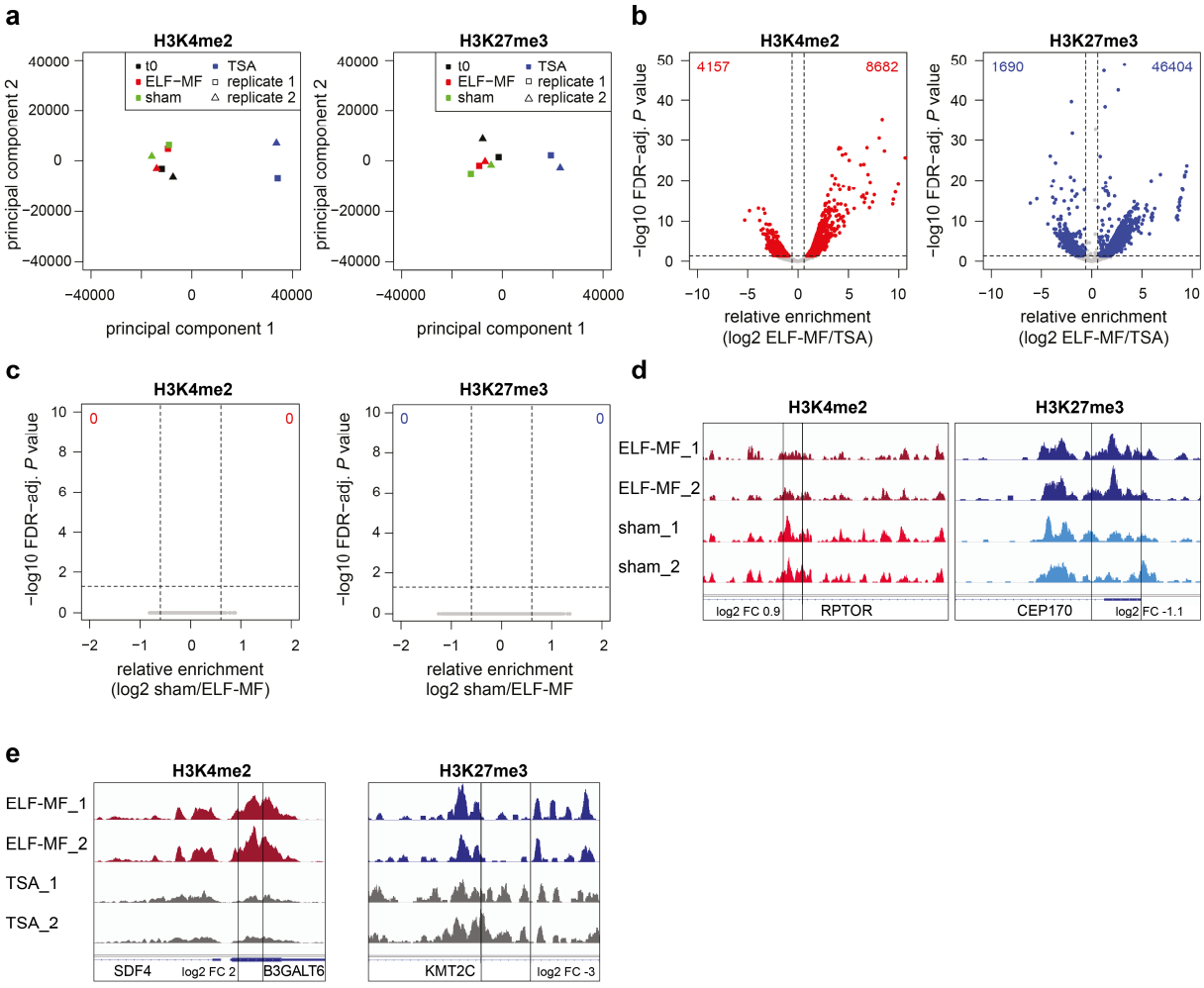

Figure 1. ELF-MF exposure does not alter global patterns of histone modifications in Jurkat cells. Jurcat cells were ELF-MF (50 Hz sinus, 1 mT, 5' on/10' off), sham exposed or treated with 10 nM Trichostatin A (TSA) for 72 h. Profiles of H3K4me2 and H3K27me3 modification were generated by ChIP-sequencing of two replica (representing pools of three biological replicates). (a) Principal component analysis of H3K4me2 and H3K27me3 ChIP-seq data from non-exposed (t0), ELF-MF and sham exposed or TSA treated cells, comparing read counts in 500 bp genomic tiles. (b,c) Comparison of H3K4me2 and H3K27me3 read counts within 500 bp genomic tiles between TSA treated and ELF-MF exposed (b) or ELF-MF and sham exposed (c) cells. Shown are differences in relative enrichments as log2-fold change (FC) (x-axis) against the false discovery rate (FDR)-adjusted *P* value (likelihood ratio test) (y-axis). Statistically significant tiles (FC > ±0.6, FDR-adjusted $P < 0.05$) are highlighted in red (H3K4me2) or blue (H3K27me3). (d) Exemplary profiles of H3K4me2 and H3K27me3 modifications at the *RPTOR* and *CEP170* loci with FCs between sham and ELF-MF exposed cells of 1.8 and 2.1, respectively, but not reaching statistical significance. (e) H3K4me2 and H3K27me3 profiles at the *B3GALT6* and *KMT2C* locus, significantly different in ELF-MF and TSA treated cells.

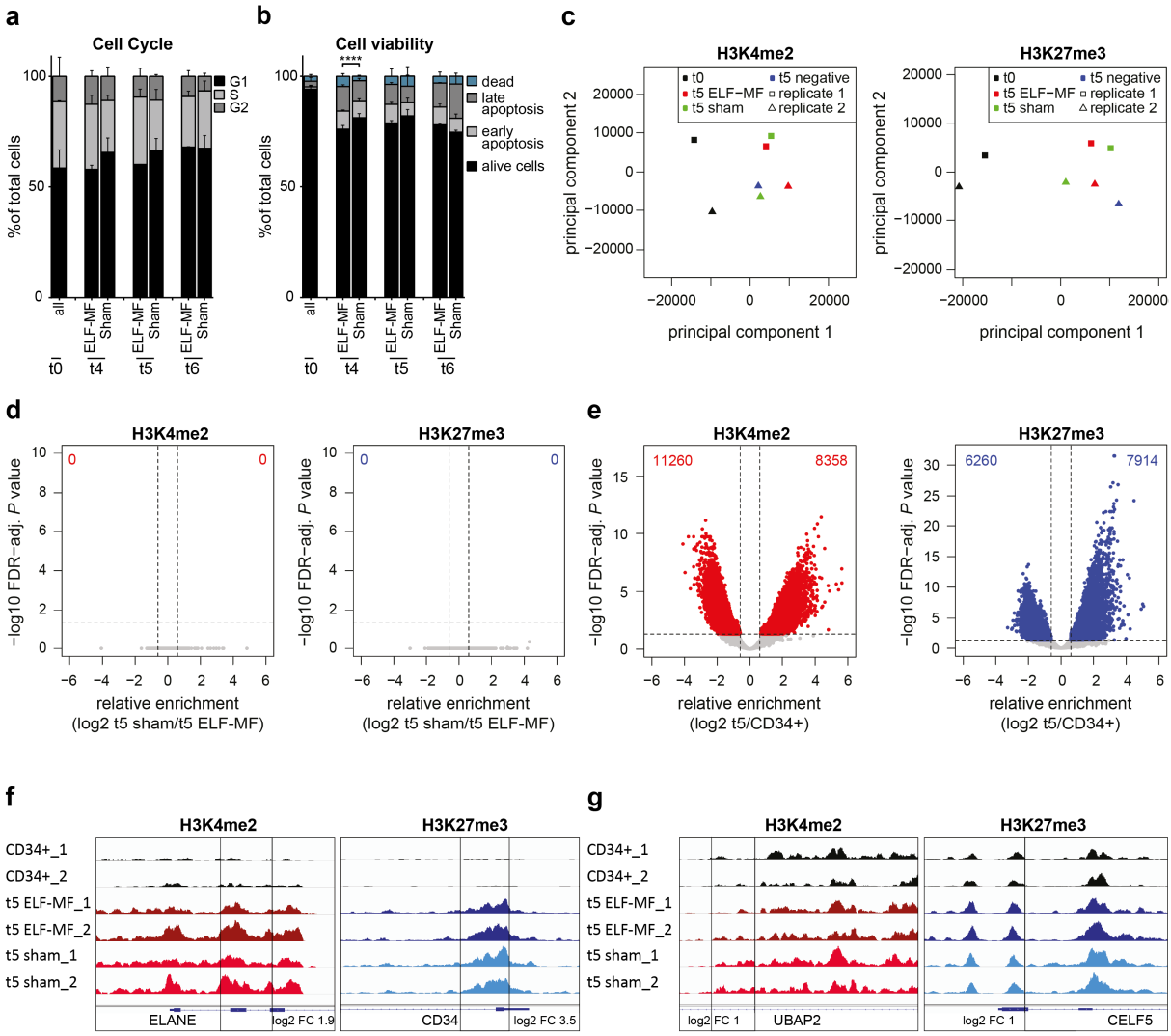

Figure 2. Patterning of histone modifications during granulopoiesis is not affected by ELF-MF. Human CD34+ cord blood cells were differentiated *in vitro* to neutrophilic progenitors under ELF-MF (50 Hz powerline signal, 1 mT, 5' on/10' off) or sham exposure for 5 days. (a,b) Cell cycle profiles and apoptosis were assessed by flow cytometry before and at days 4, 5 and 6 of neutrophilic differentiation and statistically analysed by χ^2 test on each replica (**** $P < 0.001$) and pairwise comparison by Student's *t*-test. Shown are the mean percentages of cells in the G1, S, and G2 phase of the cell cycle (a) and of alive, early apoptotic, late apoptotic and dead/necrotic cells (b). Error bars; SEM of n≥2 and n=3 biological replicates, respectively. (c-g) H3K4me2 and H3K27me3 profiles of CD34+ cells (t0) and neutrophilic progenitors (t5) were obtained by ChIP-seq and two replicates were statistically analysed. (c) Principal component analysis of ChIP-seq data. (d,e) Comparison of ELF-MF and sham exposed neutrophilic progenitors (d) or of CD34+ and combined neutrophilic progenitor cells (e). Shown are differences in relative enrichments of ChIP-seq reads within 500 and 1,000 bp genomic tiles as log2-fold change (FC) (x-axis) against the false discovery rate (FDR)-adjusted *P* value (likelihood ratio test with variable dispersion) (y-axis). Statistically significant (FC > ±0.6, FDR-adjusted

P < 0.05) tiles differentially occupied by H3K4me2 and H3K27me3 are highlighted in red and blue, respectively. (f,g) Exemplary profiles of H3K4me2 and H3K27me3 marks at genomic loci, identified by a 500 bp tile (black box) with significant differences in neutrophilic progenitors and CD34+ cells (f) or more than 2-fold enrichment between ELF-MF and sham exposed progenitor cells (g).

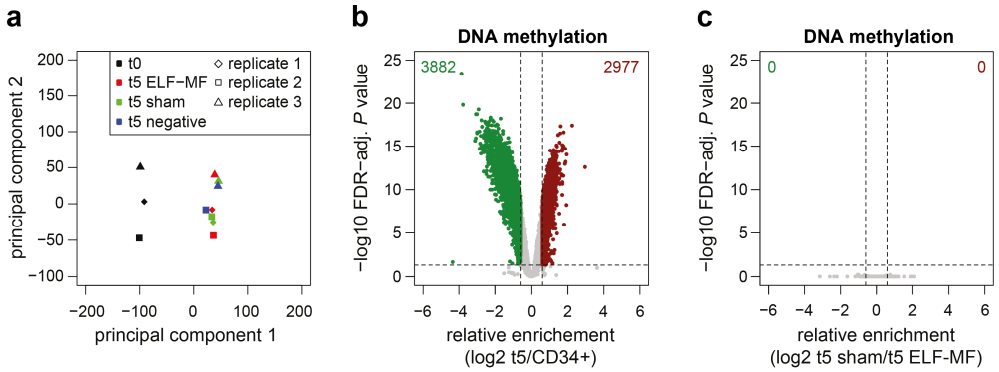

Figure 3. The DNA methylation pattern does not change upon ELF MF exposure. DNA methylation of CD34+ human cord blood cells (t0) and neutrophilic progenitors (t5), *in vitro* differentiated under ELF-MF (50 Hz powerline signal, 1 mT, 5' on/10' off), sham or no exposure condition for five days, was analysed by Illumina Infinium HumanMethylation 450 array. (a) Principal component analysis of all samples (M-values). (b,c) Differences in elative DNA methylation levels as log2-fold change (FC) (x-axis) are plotted against the false discovery rate (FDR)-adjusted *P* value (calculated by moderated *t*-statistic) (y-axis) for the comparison of (b) neutrophilic progenitors at t5 (combined exposed progenitors) and CD34+ cells and (c) ELF-MF and sham exposed day 5 neutrophilic progenitors. CpGs statistically significantly (FDR-adjusted $P < 0.05$) hypomethylated (FC < -0.6) and hypermethylated (FC > 0.6) are indicated in green and dark red, respectively.

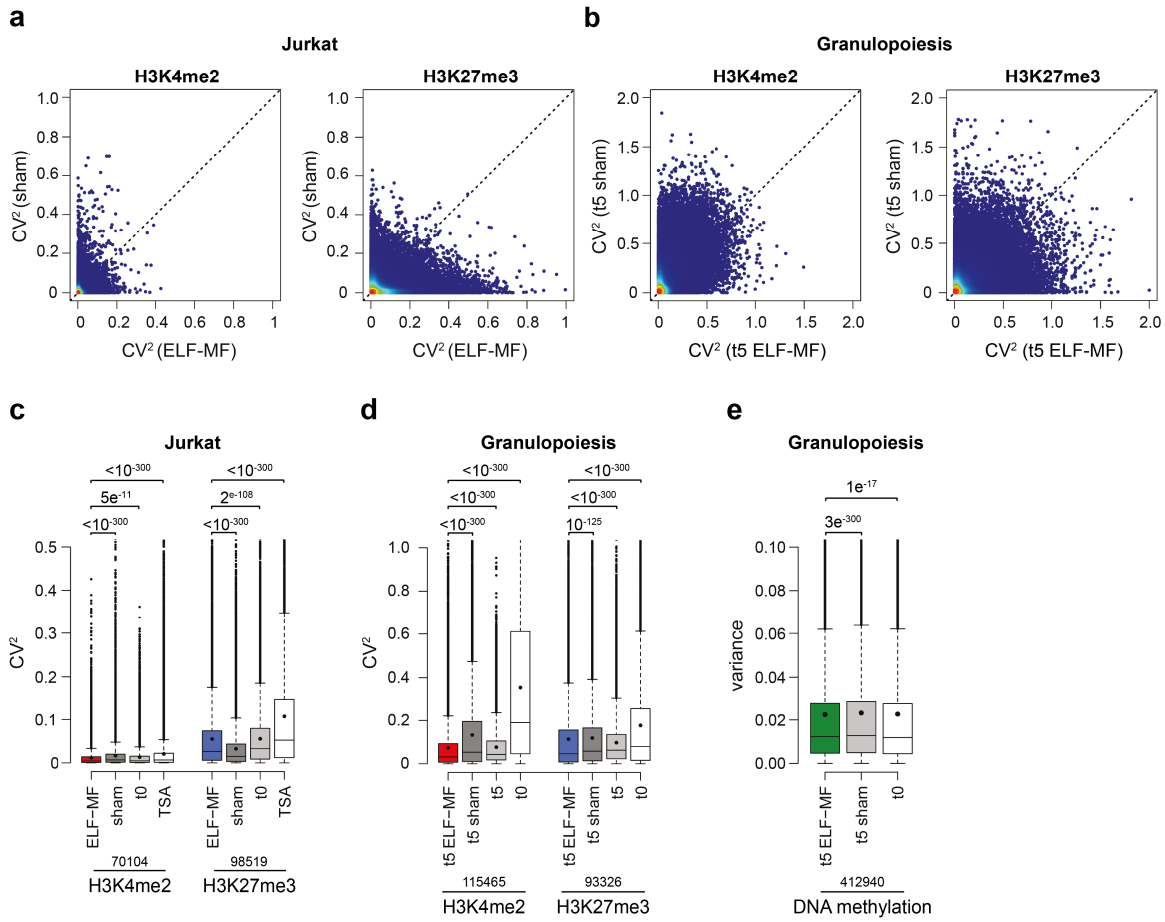

Figure 4. ELF-MF exposure impacts the variability of the epigenetic landscape. The squared coefficient of variation (CV2) of ChIP-seq read counts within 500 bp genomic tiles was determined based on the two replicate datasets for H3K4me2 and H3K27me3, generated from non-exposed (t0), ELF‑MF exposed (50 Hz sinus, 1 mT, 5’ on/10’ off, 72 h), sham exposed or Trichostatin A (10 nM, 72 h) treated Jurkat cells, and from neutrophilic progenitors after five days of in vitro differentiation under ELF‑MF (50 Hz powerline, 1 mT, 5’ on/10’ off) or sham exposure. Linear comparison of CV2 values of ELF‑MF (x-axis) and sham exposed (y-axis) Jurkat cells (a) and neutrophilic progenitor cells (b) for H3K4me2 and H3K27me3 marks. Global replicate variability of the two replicate ChIP-seq datasets for H3K4me2 and H3K27me3 in Jurkat cells (c) and in neutrophilic progenitors (d). (e) Variance in DNA methylation levels (M value) of the three biological replicates for CD34+ human cord blood cells (t0), ELF-MF and sham exposed neutrophilic progenitors after five days of in vitro differentiation. (c,d,e) Box-and-whisker plots illustrate median (lines) and mean (black circles) CV2 values with interquartile ranges (boxes), 1.5x interquartile ranges (whiskers) and outliers. Data were statistically analysed by Wilcox rank sum test (**** $P < 0.001$).

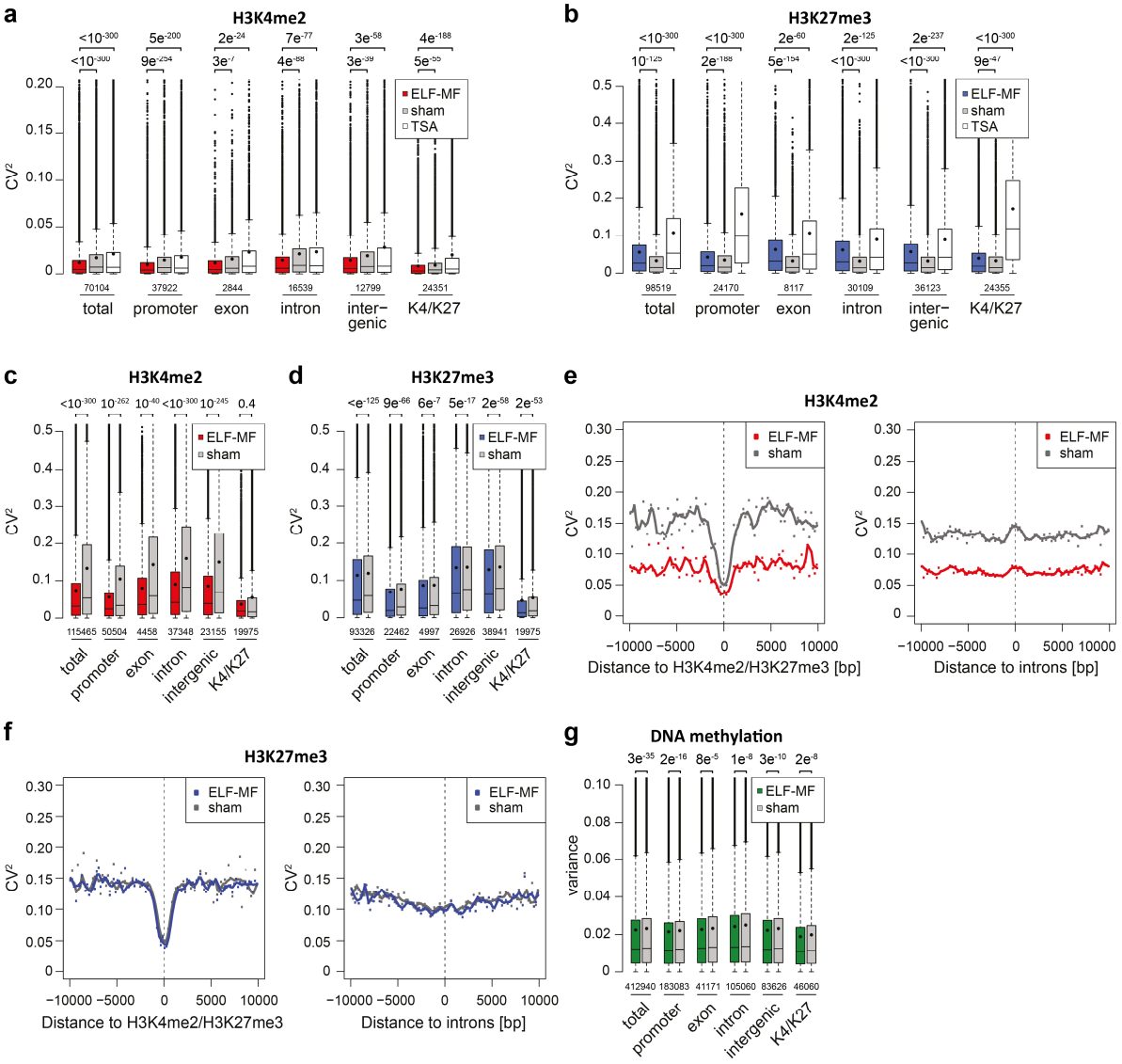

Figure 5. Genomic context dependent effect of ELF-MF exposure on the robustness of epigenetic modifications. (a, b) Assessment of the variability of epigenetic modifications in ELF-MF- (50 Hz sinus, 1 mT, 5' on/10' off, 72 h) and sham-exposed or TSA (10 nM, 72 h) treated Jurkat with respect to genomic features indicated. (c, d) As in (a, b) but with data from neutrophilic progenitors after five days of *in vitro* differentiation under ELF-MF (50 Hz powerline, 1 mT, 5' on/10' off) or sham exposure. (a-d) The squared coefficient of variation (CV^2) of reads in 500 bp tiles of two H3K4me2 and H3K27me3 ChIP-seq replicates was analysed for promoters (± 1,000 bp of TSS), exons, introns, intergenic regions (UCSC hg19) or bivalent domains in our data set (H3K4me2 and H3K27me3 occupancy). Box-and-whisker plots illustrate median (lines) and mean (black circles) CV^2 values with interquartile ranges (boxes), 1.5x interquartile ranges (whiskers) and outliers. *P* values of the Wilcoxon rank sum test are indicated. (e,f) Comparison of the mean variabilities of ChIP-seq reads of H3K4me2 and H3K27me3 tiles (CV^2 values on y-axis) between ELF-MF and sham-exposed samples of neutrophilic progenitors, plotted as a function of distance to the nearest bivalent domain or intron.

(g) Variability of three replicates of DNA methylation assessed with respect to genomic features, comparing ELF-MF and sham-exposed neutrophilic progenitors. Box-and-whisker plots illustrate median (lines) and mean (black circles) variance with interquartile ranges (boxes), 1.5x interquartile ranges (whiskers) and outliers. The *P* values are according to Wilcoxon rank sum test.

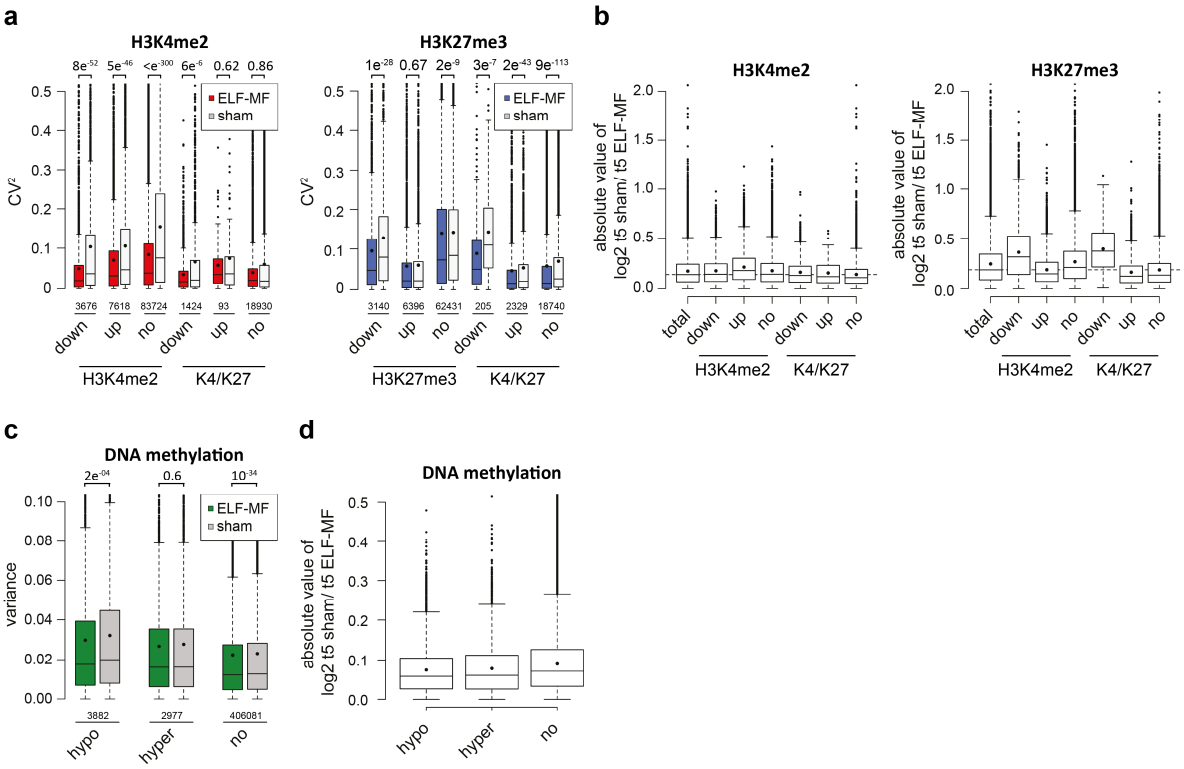

Figure 6. The chromatin state defines the stability of epigenetic features under ELF-MF exposure. Variability of epigenetic marks in sham and ELF-MF exposed neutrophilic progenitors, intersected with tiles/sites significantly (FDR-adjusted $P < 0.05$) changing modifications during differentiation of CD34+ cells to day five progenitors. (a) Median (lines) and mean (black circles) CV^2 values (a) and with interquartile ranges (boxes), 1.5x interquartile ranges (whiskers) and outliers categorized according to tiles enriched in H3K4me2, H3K27me3 or both that either significantly change (up, log2 fold change > 0.6; down, log2 fold change < -0.6) or remain stable (no) during differentiation. (b) As in (a) but for differential enrichments of histone modifications between ELF-MF and sham exposed samples. (c,d) Variability of DNA methylation of sham and ELF-MF exposed neutrophilic progenitors, intersected with CpGs significantly changing methylation (hypo, FDR-adjusted $P < 0.05$, log2 fold change < -0.6; hyper, FDR-adjusted $P < 0.05$, log2 fold change > 0.6) or not (no) during neutrophilic differentiation. Shown are median (lines) and mean (black circles) with interquartile ranges (boxes), 1.5x interquartile ranges (whiskers) and outliers of variance (c) and log fold changes between ELF-MF and sham exposed samples (d). (a,c) *P* values indicate statistical significance level by the Wilcoxon rank sum test.

Supplementary Information

ELF-MF exposure affects the robustness of epigenetic programming during granulopoiesis

Melissa Manser[1], Mohamad R. Abdul Sater[2,3,#], Christoph D. Schmid[2,3], Faiza Noreen[1], Manuel Murbach[4], Niels Kuster[4,5], David Schuermann[1,*], Primo Schär[1]

[1] Department of Biomedicine, University of Basel, Mattenstrasse 28, Basel CH-4058, Switzerland

[2] Swiss Tropical and Public Health Institute, Socinstrasse 57, Basel CH-4002, Switzerland

[3] University of Basel, Petersplatz 1, Basel, CH-4001, Switzerland

[4] IT'IS Foundation, Zeughausstrasse 43, Zürich, CH-8004, Switzerland

[5] Swiss Federal Institute of Technology (ETH), Zürich, CH-8006, Switzerland

[#]Present address: Department of Immunology and Infectious Disease, Harvard T.H. Chan School of Public Health, Boston, MA 02115, United States of America

[*]Correspondence and requests for materials should be addressed to D.S. (david.schuermann@unibas.ch)

Supplementary Figures

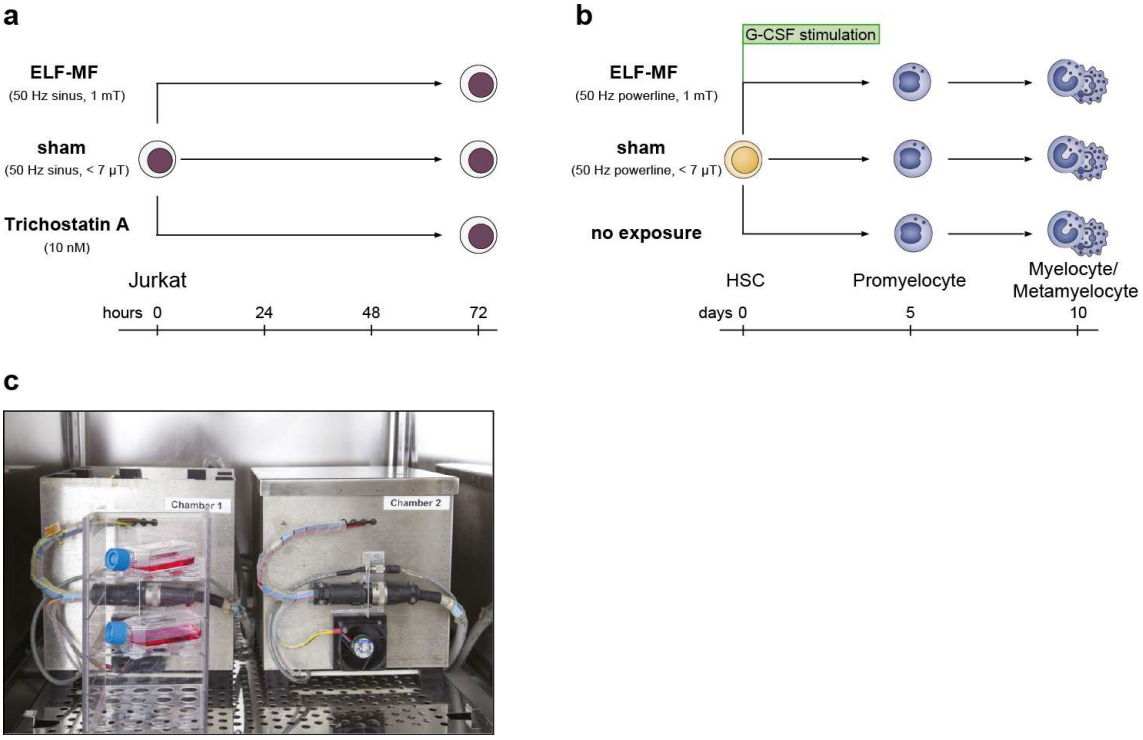

Supplementary Figure S1. Schematic overview of ELF-MF exposure experiments. (a) Blinded for the operator, the leukaemic cell line Jurkat was exposed to ELF-MF (50 Hz sinus, 1 mT, 5’ on/10’ off) and sham for 72 h, or treated with 10 nM trichostatin A for 72 h. (b) After the expansion of CD34+ human cord blood cells for 4 days, the hematopoietic stem cells (HSC) population was split into three experimental groups before initiating the *in vitro* differentiation into neutrophilic lineage for 10 days by the addition of G-CSF. Blinded for the experimenter, ELF-MF (50 Hz powerline, 1 mT, 5’ on/10’ off) or sham exposure was carried out throughout the differentiation. Control differentiations without ELF-MF exposure were done either in a µ-metal shielded box inside the exposure incubator or in an independent incubator. (c) sXcELF exposure system provided and serviced by the IT’IS foundation (http://www.itis.ethz.ch/services/exposure-systems/in-vitro-sxc/sxcelf/).

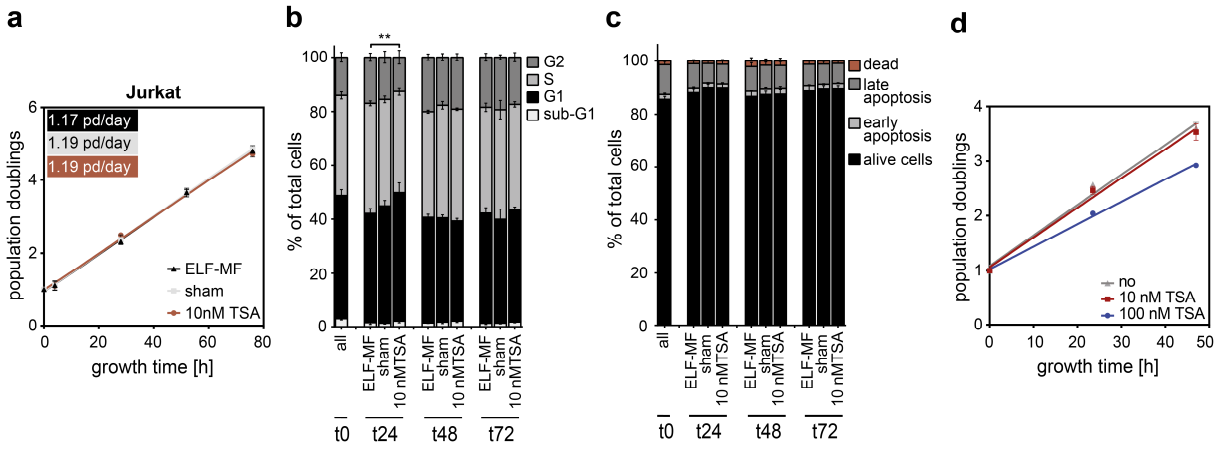

Supplementary Figure S2. ELF-MF exposure does not alter proliferation and survival of Jurkat cells. Cells were ELF-MF exposed (50 Hz sinus, 1 mT, 5' on/10' off), sham exposed or treated with 10 nM Trichostatin A (TSA) for 72 h. (a) Starting with $1x10^5$ cells/mL, the proliferation was monitored by cell counting at the indicated time points. Average population doublings of independent biological replicates (n=6) as a function of time were calculated and statistically analysed by ANOVA (*$P < 0.05$) and Student's *t*-test. Error bars indicate SEM. (b) Cell cycle profiles were assessed by flow cytometry, before (t0) and after exposure to ELF-MF, sham or TSA at the indicated time points. Data represent the mean proportion of cells in the different cell cycle phases with SEM (n=5). (c) Analysis of apoptosis by flow cytometry of cells at the indicated time points of exposure. Annexin-V/PI staining was used to discriminate living, apoptotic and dead/necrotic cells. Data represent mean percentages of cells in different states of cell viability with SEM (n=6). Flow cytometry data were analysed by FlowJo software and statistically analysed by χ^2 test for each replica (* $P < 0.05$) and Student's *t*-test. (d) Average population doublings of Jurkat cells treated with 10 nM or 100 nM Trichostatin A (TSA) for 48 h compared to untreated cells. Indicated are error bars and SEM from two biological replicates.

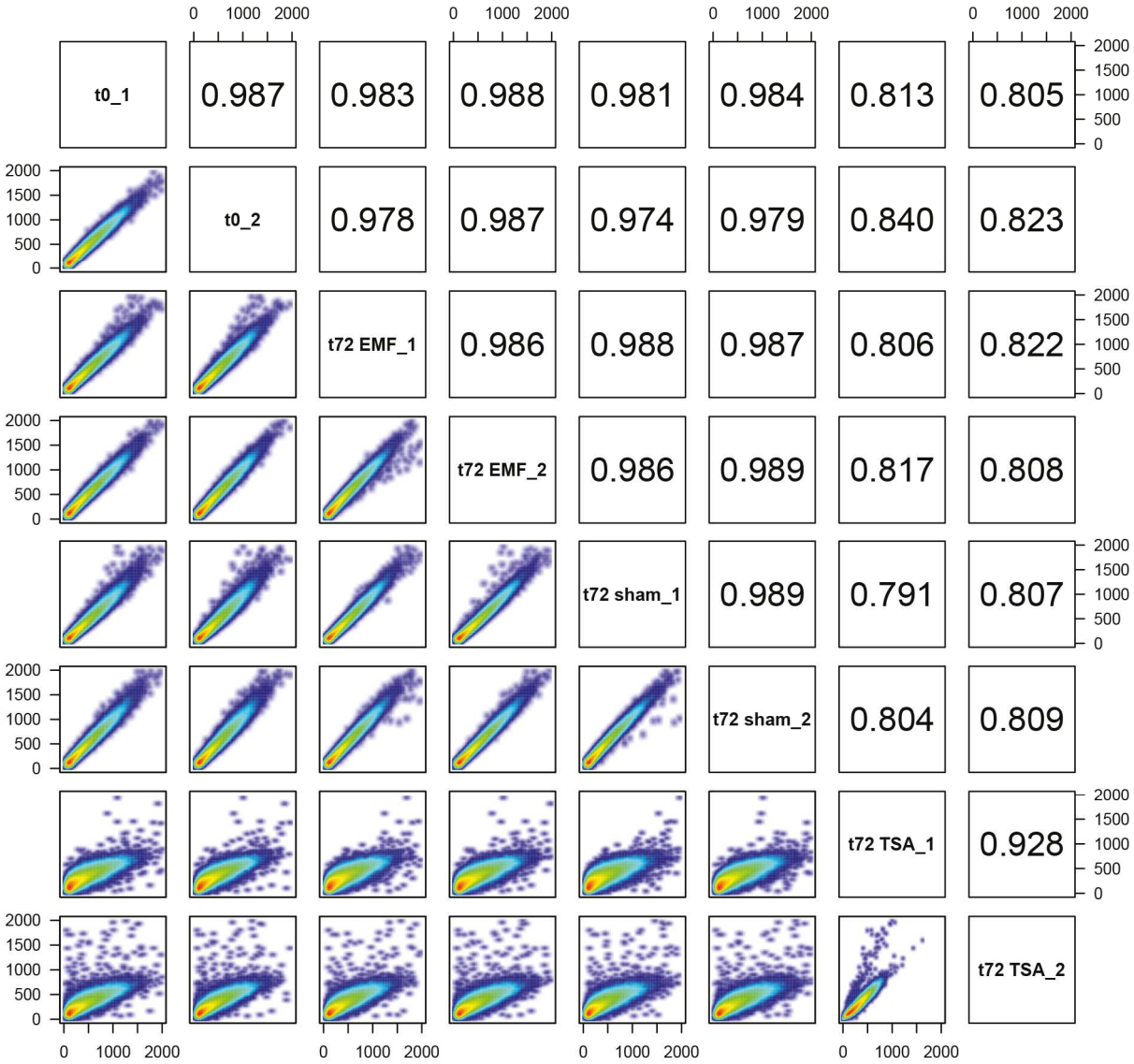

Supplementary Figure S3: Correlation between H3K4me2 ChIP-seq data from Jurkat cells. Global profiles of H3K4me2 histone modification of Jurkat cells prior to treatment (t0), exposed to ELF-MF (t72 EMF; 50 Hz sinus, 1 mT, 5' on/10' off) and sham, or treated with 10 nM trichostatin A (TSA) for 72 h were generated by ChIP-sequencing. For each condition, two ChIP-seq replicates were generated by pooling three biological replicates each. The correlation of ChIP-seq reads in 500 bp genomic tiles between all H3K4me2 ChIP-seq samples is illustrated by density plots (lower left) and correlation coefficients (R values; upper right).

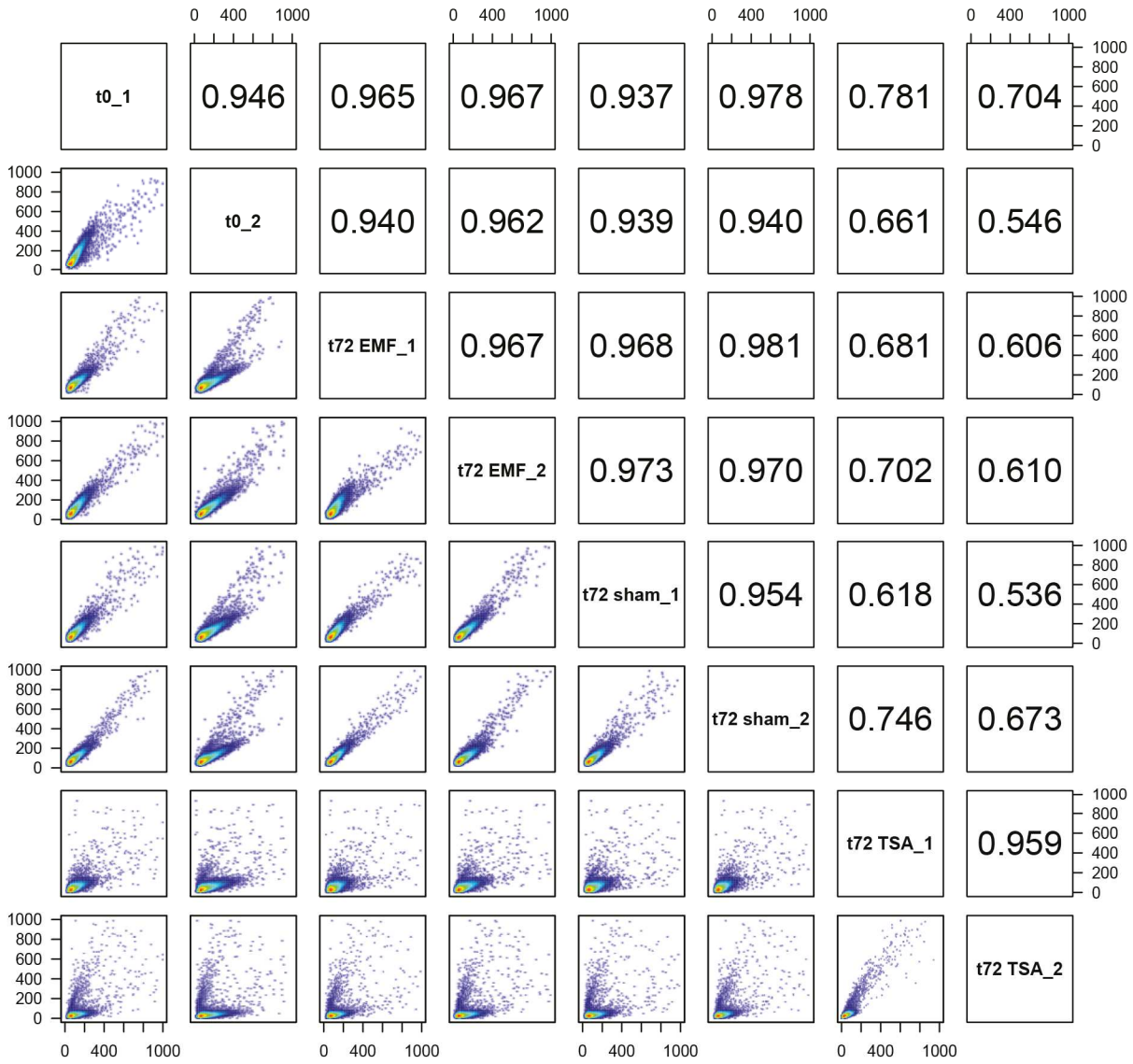

Supplementary Figure S4. Correlation between H3K27me3 ChIP-seq data from Jurkat cells. Global profiles of H3K27me3 histone modification of Jurkat cells prior to treatment (t0), exposed to ELF-MF (t72 EMF; 50 Hz sinus, 1 mT, 5' on/10' off) and sham, or treated with 10 nM trichostatin A (TSA) for 72 h were generated by ChIP-sequencing. For each condition, two ChIP-seq replicates were generated by pooling three biological replicates each. The correlation of ChIP-seq reads in 500 bp genomic tiles between all H3K27me3 Chip-seq samples is illustrated by density plots (lower left) and correlation coefficients (R values; upper right).

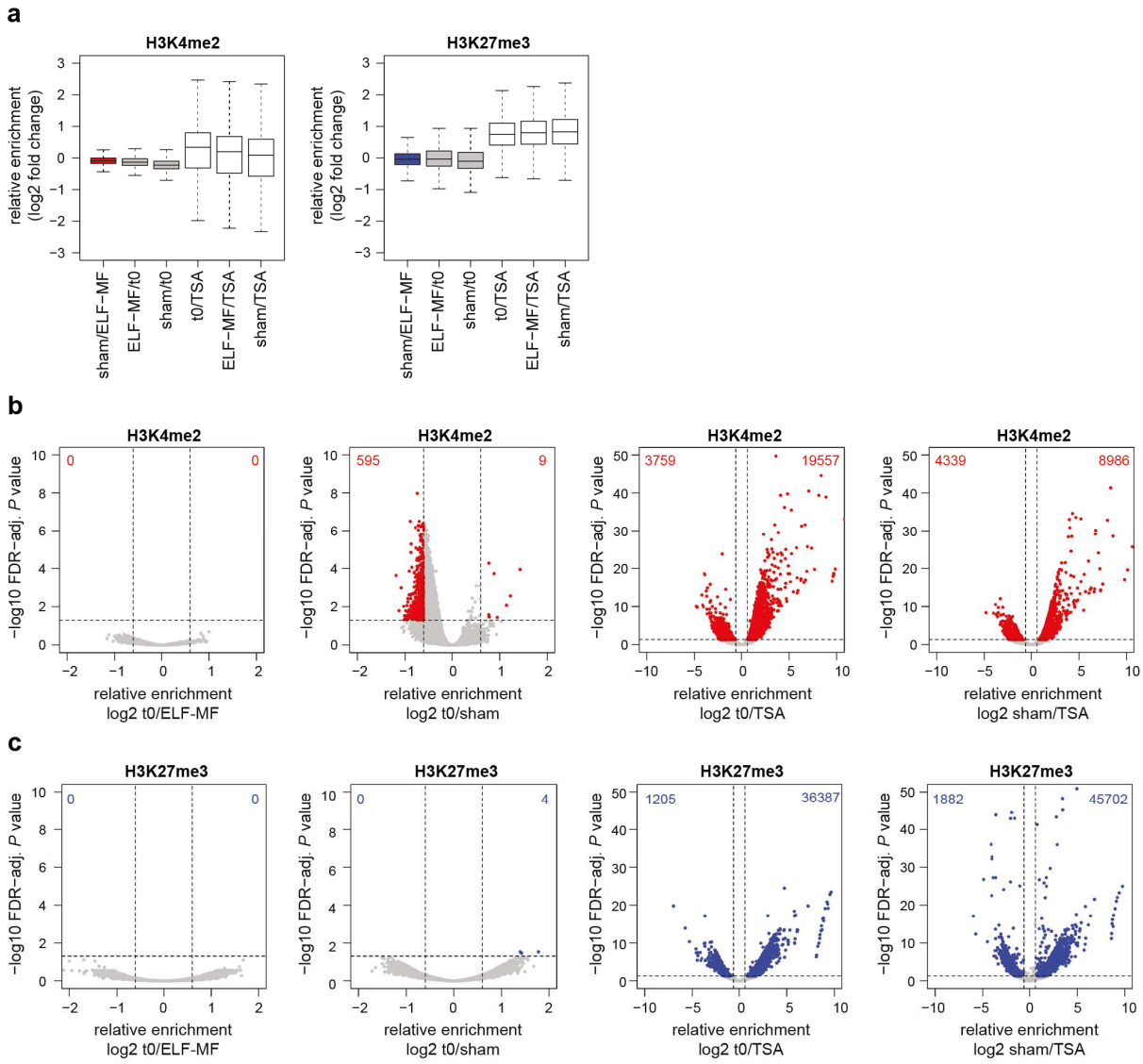

Supplementary Figure S5. Differences of H3K4me2 and H3K27me3 enrichment in Jurkat ChIP-seq samples. Jurkat cells were ELF-MF (50 Hz sinus, 1 mT, 5' on/10' off), sham exposed, or treated with 10 nM Trichostatin A (TSA) for 72 h. Profiles of histone H3K4me2 and H3K27me3 modification were generated by ChIP-sequencing and two replica (pools of three biological replicates) were statistically analysed. Pairwise comparison of histone modification profiles of cells before exposure (t0), exposed to ELF-MF or sham, or treated with TSA. (a) Box-and-whisker plots illustrate the median values (line) of log2 fold changes of H3K4me2 or H3K27me3 ChIP-seq read counts within 500 bp tiles with interquartile ranges (boxes), 1.5x interquartile ranges (whiskers) and outliers. Differences in relative enrichments of H3K4me2 (b) and H3K27me3 (c) are shown as log2-fold change (FC) (x-axis) and plotted against the false discovery rate (FDR)-adjusted *P* value (calculated by likelihood ratio test) on the y-axis. Statistically significant tiles (FC > ±0.6, FDR-adjusted $P < 0.05$) are highlighted in red (H3K4me2) or blue (H3K27me3).

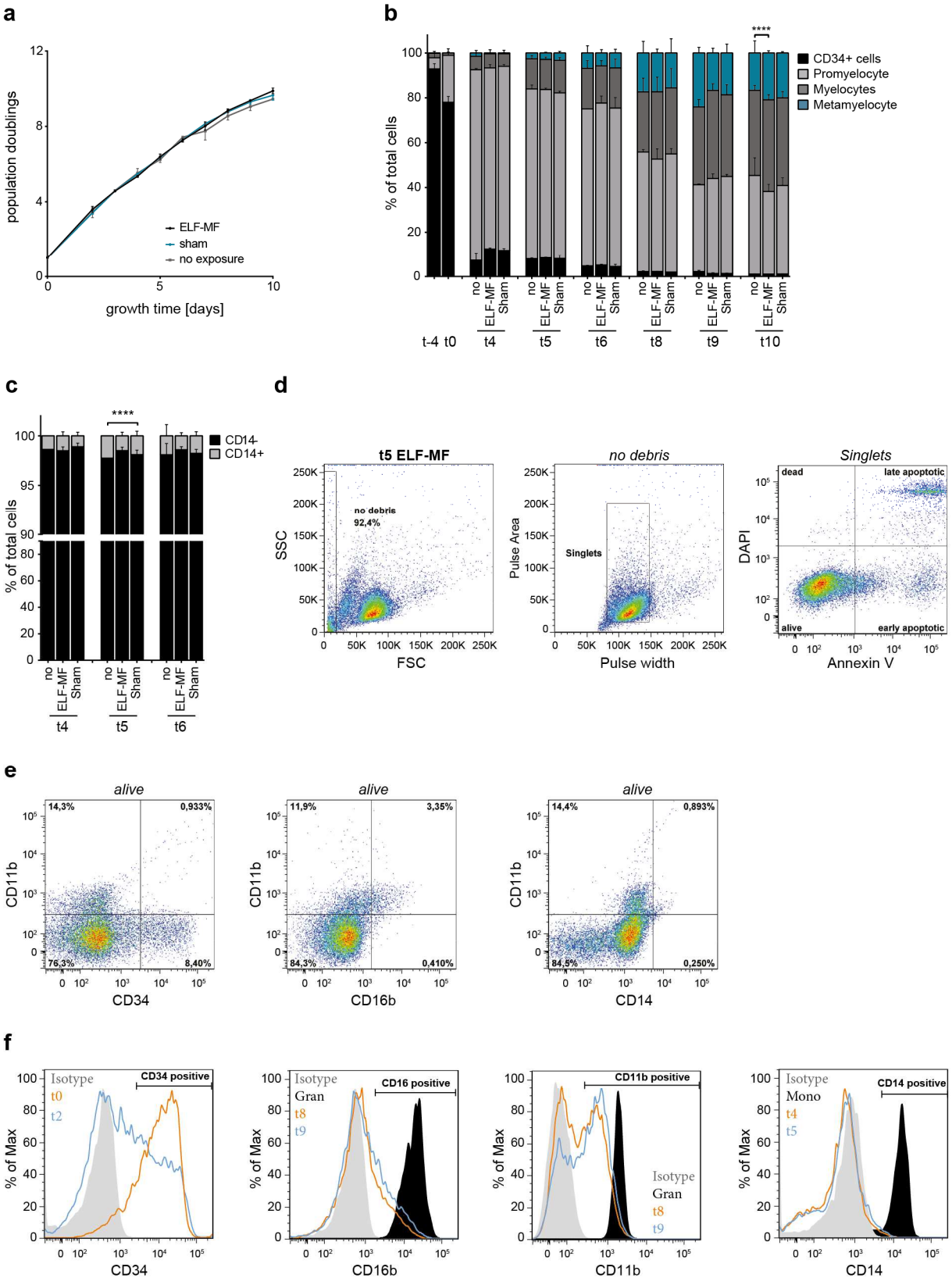

Supplementary Figure S6: ELF-MF exposure has no impact on lineage commitment. Exposed either to ELF-MF (50 Hz powerline signal, 1 mT, 5' on/10' off) and sham or non-exposed negative control, CD34+ cord blood cells were differentiated *in vitro* into neutrophilic lineage for 10 days. (a) Cell

proliferation of the differentiating cell population monitored daily by counting. Average of population doublings of three independent biological replica are shown as function of time and statistically analysed by ANOVA and Student's *t*-test. (b) Proportion of living cells in neutrophilic differentiation stages was analysed at the time-points indicated by flow cytometry using the stem cell marker CD34 and the two neutrophilic markers CD11b and CD16b. Using the FlowJo software, the expression of these markers was used to discriminate between CD34+ cells (CD34+, CD11b-, CD16b-), promyelocytes (CD34-, CD11b-, CD16b-), myelocytes (CD34-, CD11b+, CD16b-) and metamyelocytes/neutrophils (CD36-, CD11b+, CD16b+). (c) Flow cytometric analysis of the population for cells differentiating into granulocytic or monocytic lineage after 4 to 6 days, characterized by CD14 expression. (b,c) Shown are the means of three independent replicates (two for the negative control) with SEM , statistically analysed by χ^2 test for each replica ($P < 0.05$) and pairwise comparison by Student's *t*-test. (d,e) Gating strategy combining the analysis of apoptosis and discrimination of neutrophilic differentiation stages in the alive cell fraction. (d) To obtain intact and single (singlet) cells, cell debris and clusters were excluded by gating on forward scatter (FSC)/side scatter (SSC) and on pulse-width, respectively. Single cells were separated in alive, early apoptotic, late apoptotic and dead/necrotic cells according to Annexin V and DAPI stainings. (e) Alive cells (Annexin V negative/ DAPI negative) were then analysed for CD34, CD11b, CD16b and CD14 expression. (f) Isotype controls (grey) for each antibody used. Freshly isolated human blood granulocytes and monocytes were used as positive controls (black). Expressions of indicated marker of neutrophilic progenitor at two time-points were illustrated as examples (orange/blue).

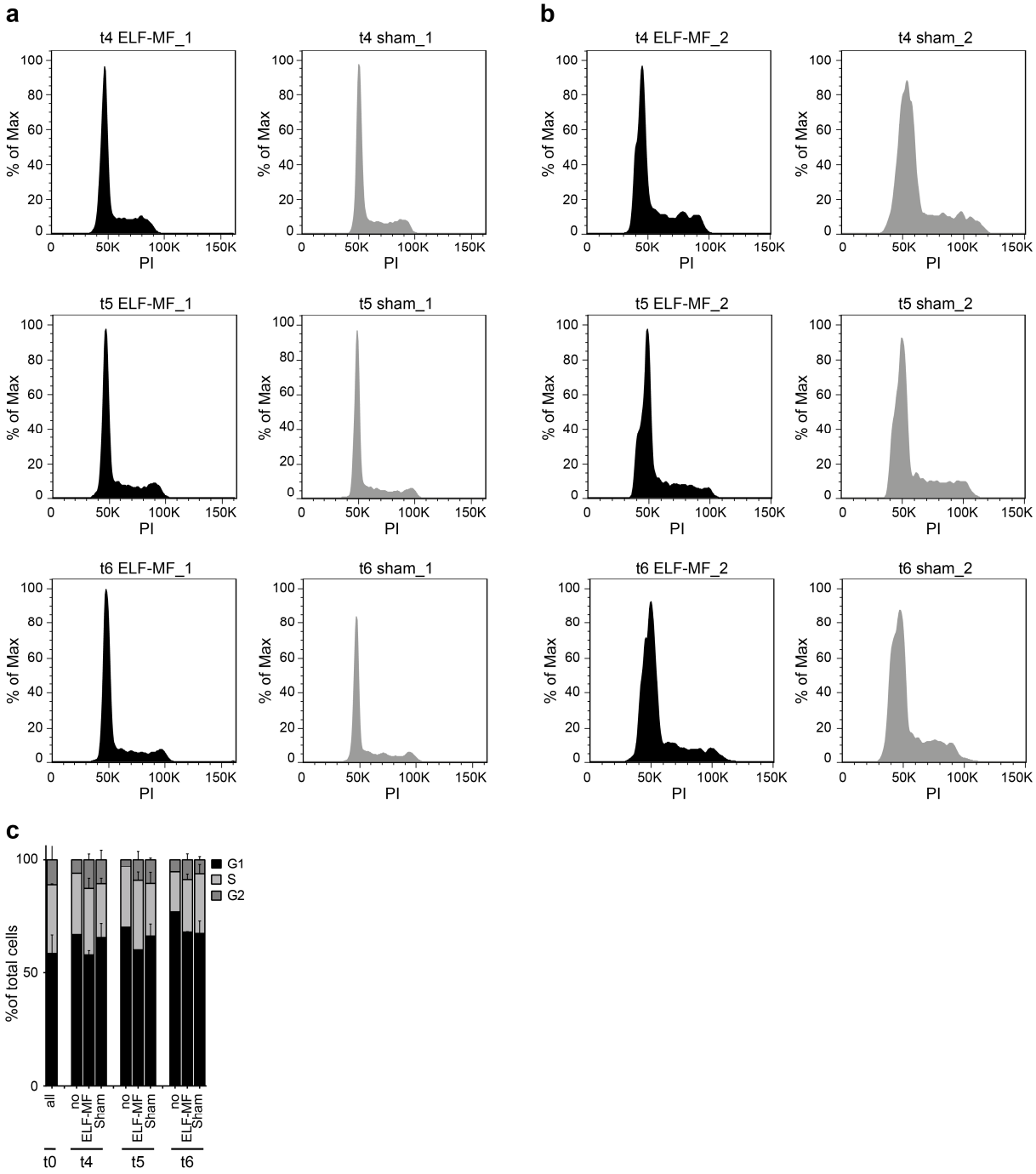

Supplementary Figure S7. Analysis of the cell cycle profiles of differentiating neutrophilic cells. Cell cycle profiles of two independent biological replicates (a,b) from neutrophilic progenitors, sham or ELF-MF (50 Hz powerline signal, 1 mT, 5' on/10' off) exposed, were analysed by flow cytometry 4, 5 and 6 days (t4, t5, t6) after induction of differentiation. (c) Summary and statistical analysis of cell cycle profiles. Mean percentage of cells in different cell cycle phases with SEM are shown. Data represent two biological replicates for ELF-MF and sham exposure, and one replica for the control differentiation. They were statistically analysed by χ^2 test for each replica (*$P < 0.05$).

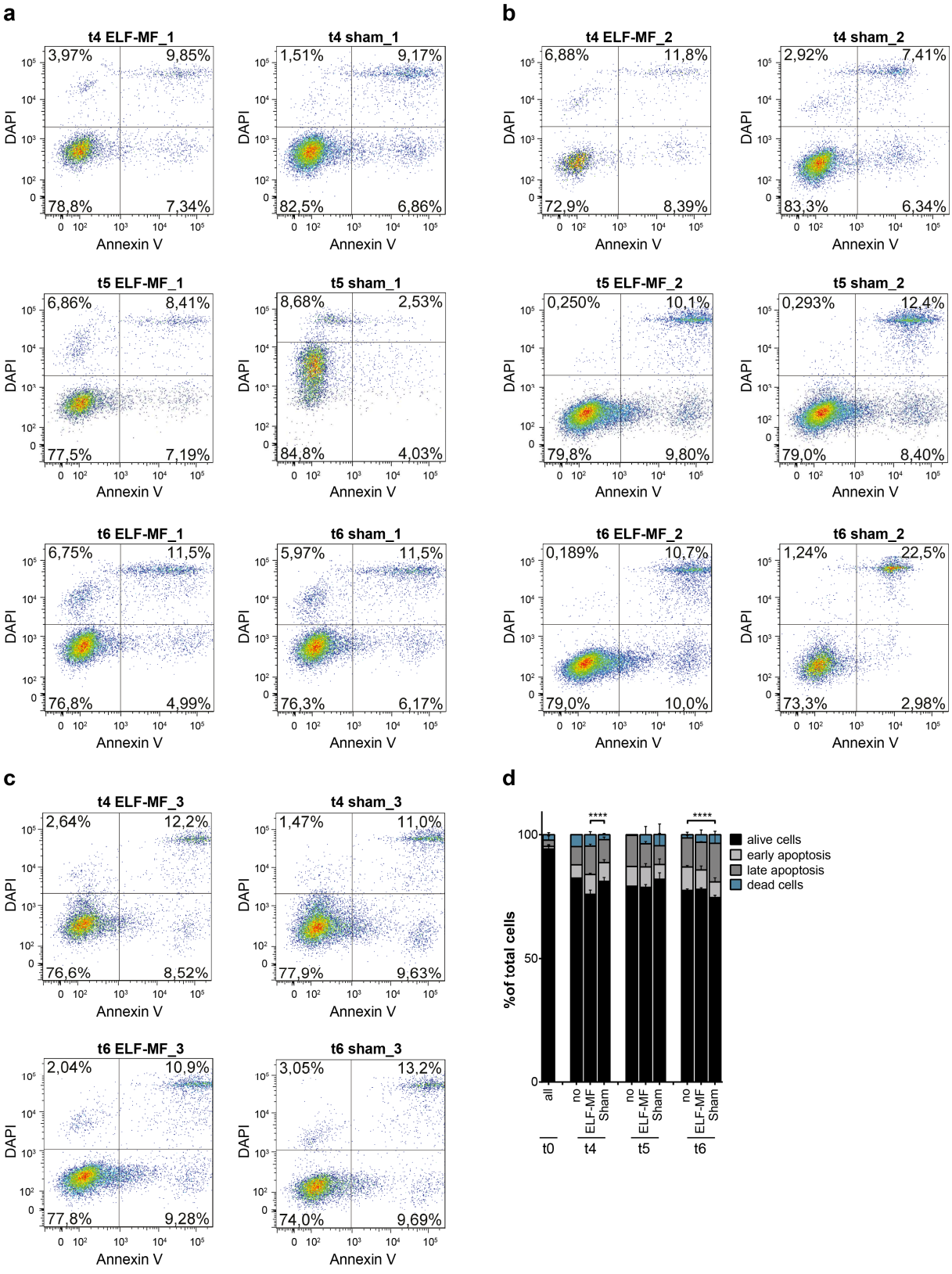

Supplementary Figure S8. Analysis of apoptosis in differentiating neutrophilic progenitors. Apoptosis in the haematopoietic cell population was analysed by flow cytometry before and at days 4 to 6 of the differentiation into neutrophilic lineage for non-exposed, ELF-MF (50 Hz powerline signal, 1 mT, 5' on/10' off) and sham exposed cultures. (a) Density plots with Annexin V expression

on the x-axis and DAPI permeability on the y-axis indicating alive cells (Annexin V/DAPI double negative), early apoptotic (Annexin V+/DAPI-), late apoptotic (double positive) and dead/necrotic (Annexin V-/DAPI+) cells are shown. (b) Summary and statistical analysis of the apoptosis, showing the mean percentage and SEM of cells in the different cell viability state at the indicated time-points. Data of three biological replicates (only two negative control and t5) were statistically analysed by χ^2 test by pairwise comparison (*P < 0.05), considering significance only when observed in every replicate.

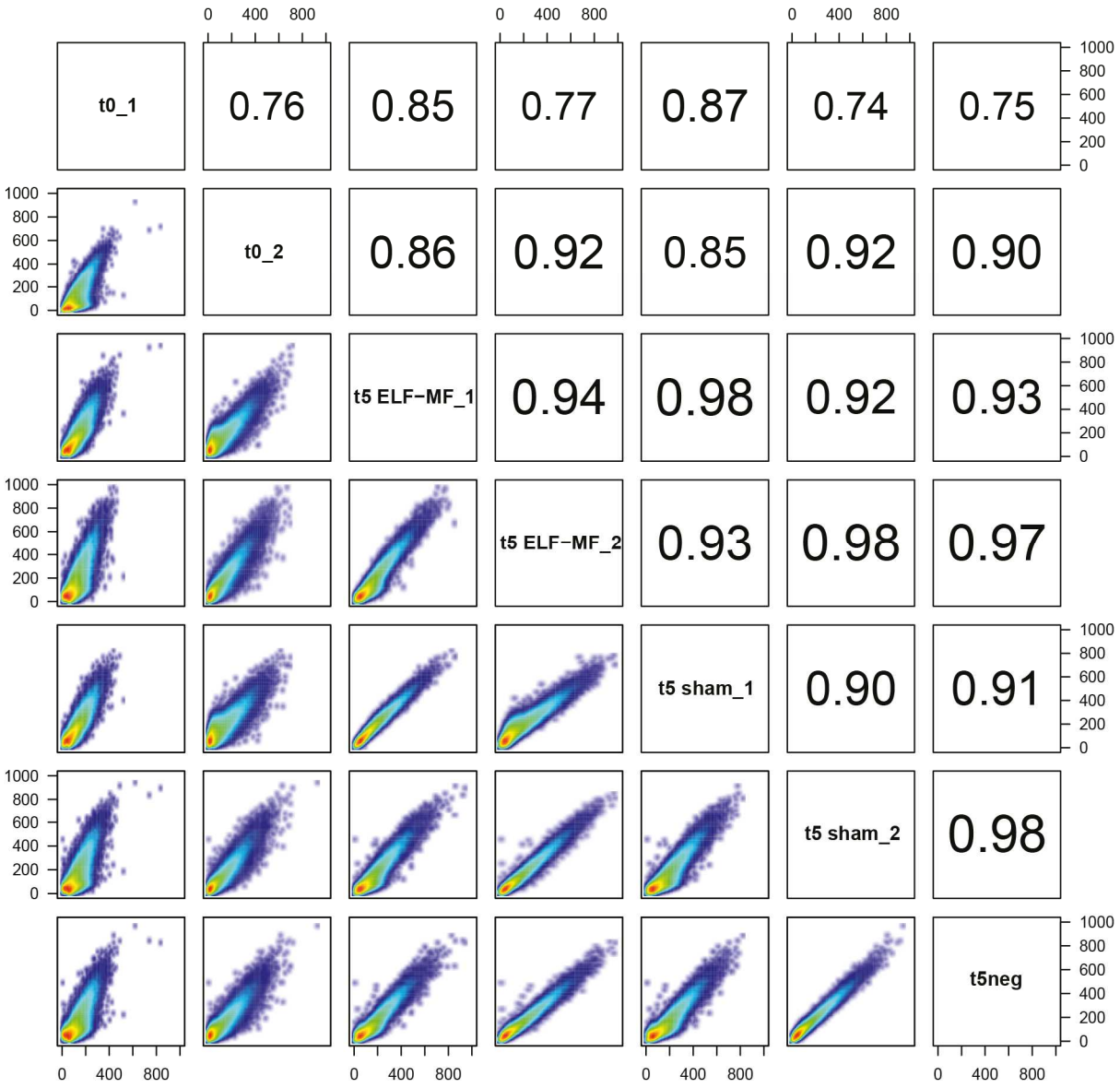

Supplementary Figure S9. Correlation between H3K4me2 ChIP data of neutrophilic granulopoiesis. Global profiles of H3K4me2 histone modification of CD34+ cord blood cells (t0), ELF-MF (50 Hz powerline signal, 1 mT, 5' on/10' off), sham or not exposed neutrophilic progenitor cells (t5) after 5 days of differentiation were generated by ChIP-sequencing. Two ChIP-seq replicates were generated for each condition, except only one replicate for the non-exposed neutrophilic progenitors (a pool of two independent biological replicates). The correlation of ChIP-seq reads in 500 bp genomic tiles between all H3K4me2 ChIP-seq samples is illustrated by density plots (lower left) and correlation coefficients (R values; upper right).

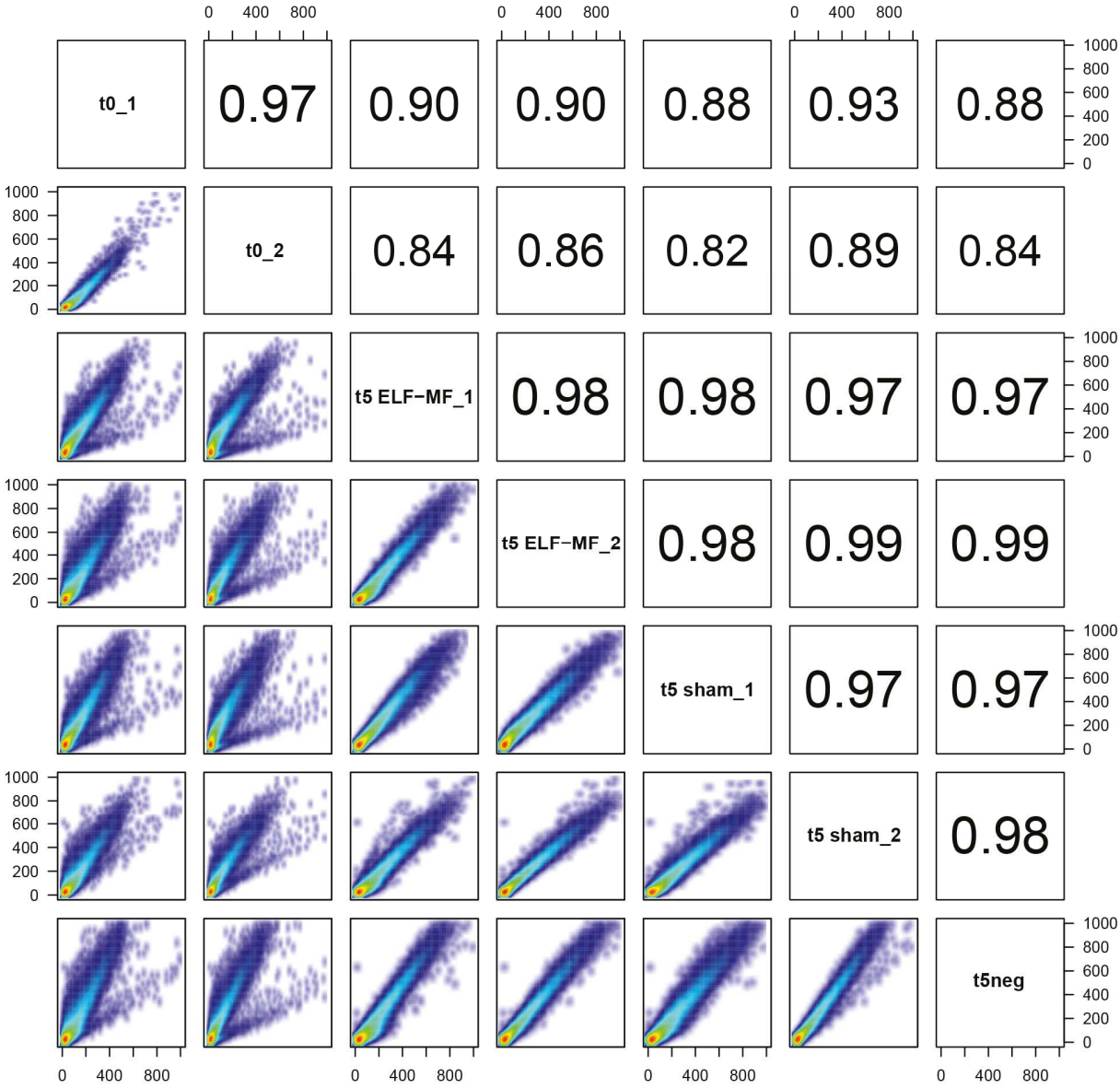

Supplementary Figure S10. Correlation between H3K27me3 ChIP data of neutrophilic granulopoiesis. Global profiles of H3K27me3 histone modification of CD34+ cord blood cells (t0), ELF-MF (50 Hz powerline signal, 1 mT, 5' on/10' off), sham or not exposed neutrophilic progenitor cells (t5) after 5 days of differentiation were generated by ChIP-sequencing. Two ChIP-seq replicates were generated for each condition, except only one replicate for the non-exposed neutrophilic progenitors (a pool of two independent biological replicates). The correlation of ChIP-seq reads in 500 bp genomic tiles between all H3K27me3 ChIP-seq samples is illustrated by density plots (lower left) and correlation coefficients (R values; upper right).

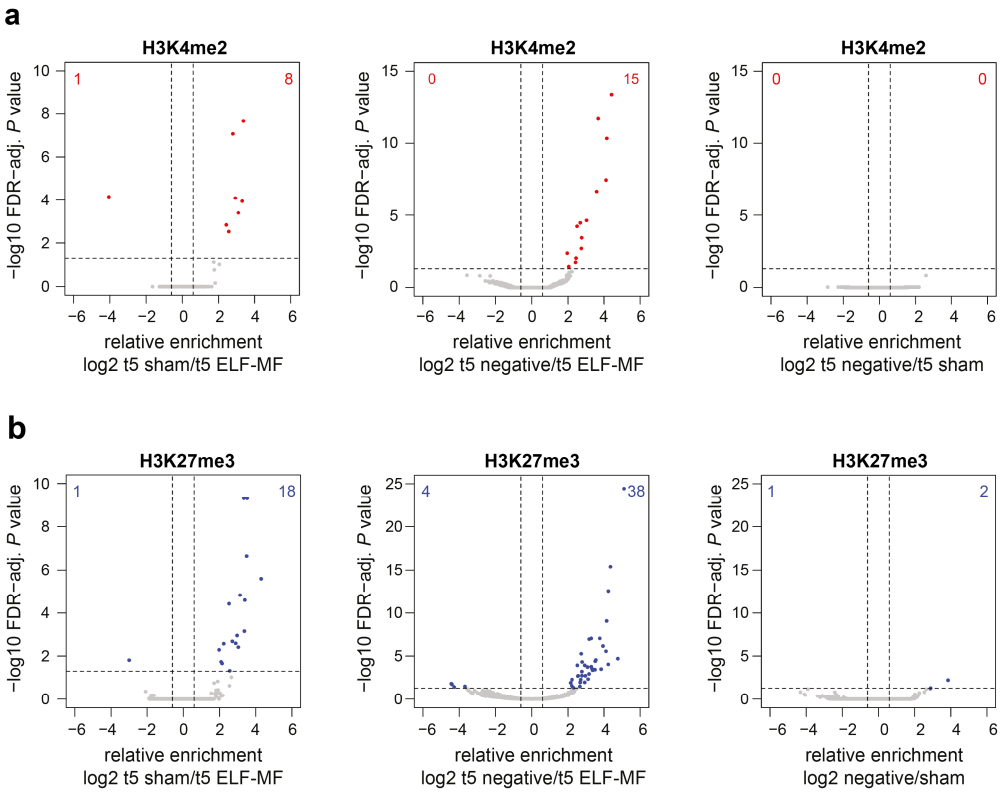

Supplementary Figure S11. Pairwise comparison of histone modifications in neutrophilic progenitors results in a few statistically significant alterations depending on the ELF-MF exposure condition. Human CD34+ cord blood cells were differentiated *in vitro* into the neutrophilic progenitor cells under ELF-MF (50 Hz powerline signal, 1 mT, 5' on/10' off), sham or no exposure for five days. H3K4me2 and H3K27me3 enrichment profiles for CD34+ cells and neutrophilic progenitors were generated by ChIP-seq and two replicates (one independent and a pool of two independent biological replicates, only one replicate for non-exposed neutrophilic progenitors) were statistically analysed. Shown are differences in relative enrichment of ChIP-seq reads for H3K4me2 (a) and H3K27me3 (b) modifications within 500 bp genomic tiles as log2-fold change (FC) (x-axis) between ELF-MF, sham or non-exposed neutrophilic progenitors plotted against false discovery rate (FDR)-adjusted *P* value (calculated by likelihood ratio test with fixed dispersion) (Y-axis). Statistically significant (FC > ±0.6, FDR-adjusted $P < 0.05$) tiles (500 bp or additional in 1,000 bp tiles) differentially occupied by H3K4me2 and H3K27me3 are highlighted in red and blue, respectively.

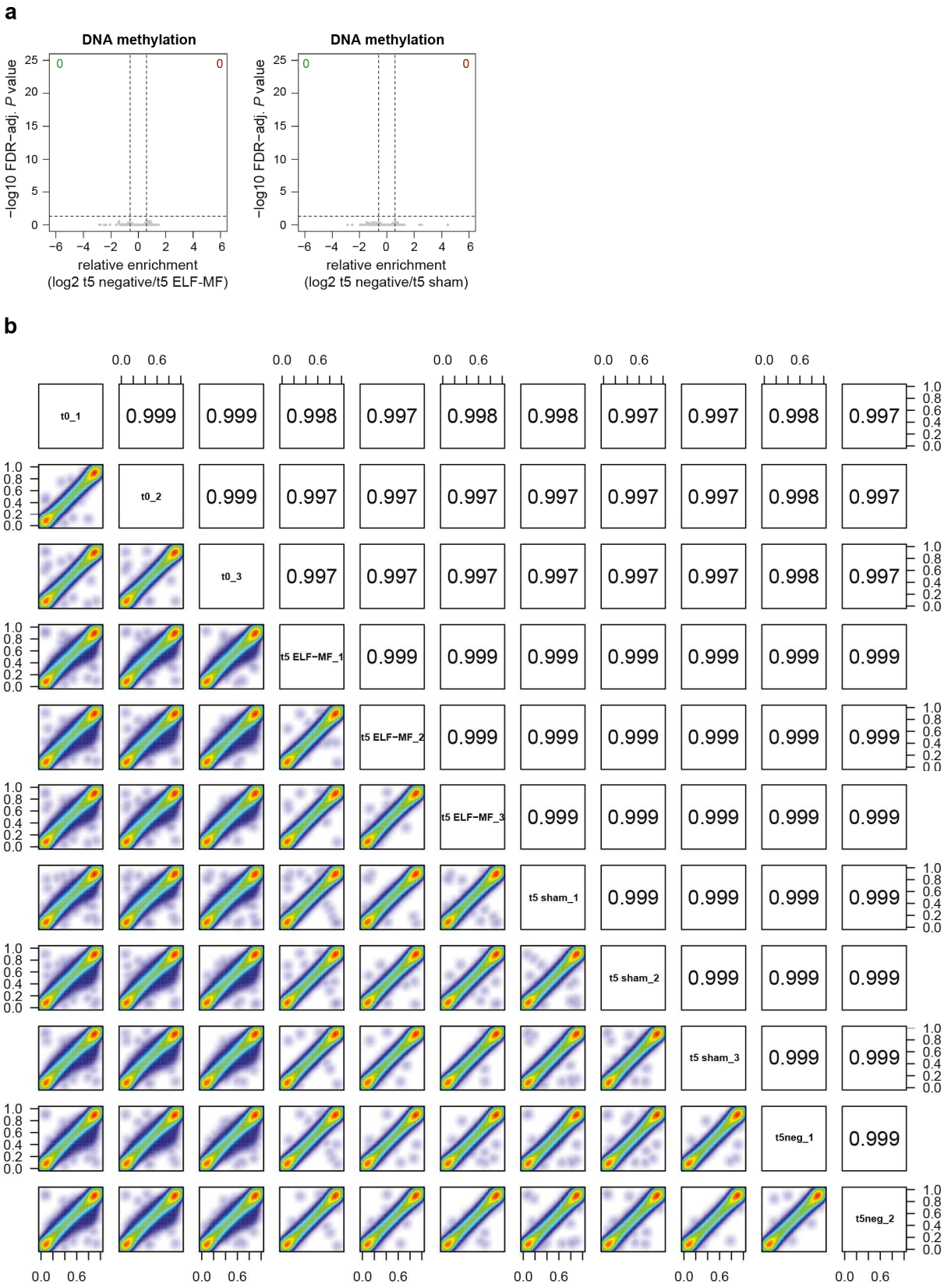

Supplementary Figure S12. Analysis of cytosine methylation data from neutrophilic differentiation. CD34+ cord blood cells were *in vitro* differentiated into the neutrophilic lineage for five days, while exposing them to ELF-MF (50 Hz powerline signal, 1 mT, 5' on/10' off) and sham or not exposed

negative control conditions. DNA methylation of CD34+ cells (t0) and ELF-MF-, sham or not exposed neutrophil progenitor cells at day five (t5) was analysed by Illumina Infinium HumanMethylation 450 array. (a) Comparison of DNA methylation levels of negative controls with ELF-MF and sham exposed progenitor cells at day five, plotting relative differences in log2-fold change (FC) (x-axis) against false discovery rate (FDR)-adjusted *P* value (moderated *t*-statistic; n=3, n=2 for negative control) (y-axis). (b) The correlation of DNA methylation levels (β-values) between all replicates and experimental conditions is illustrated by density plots and correlation coefficients (R values).

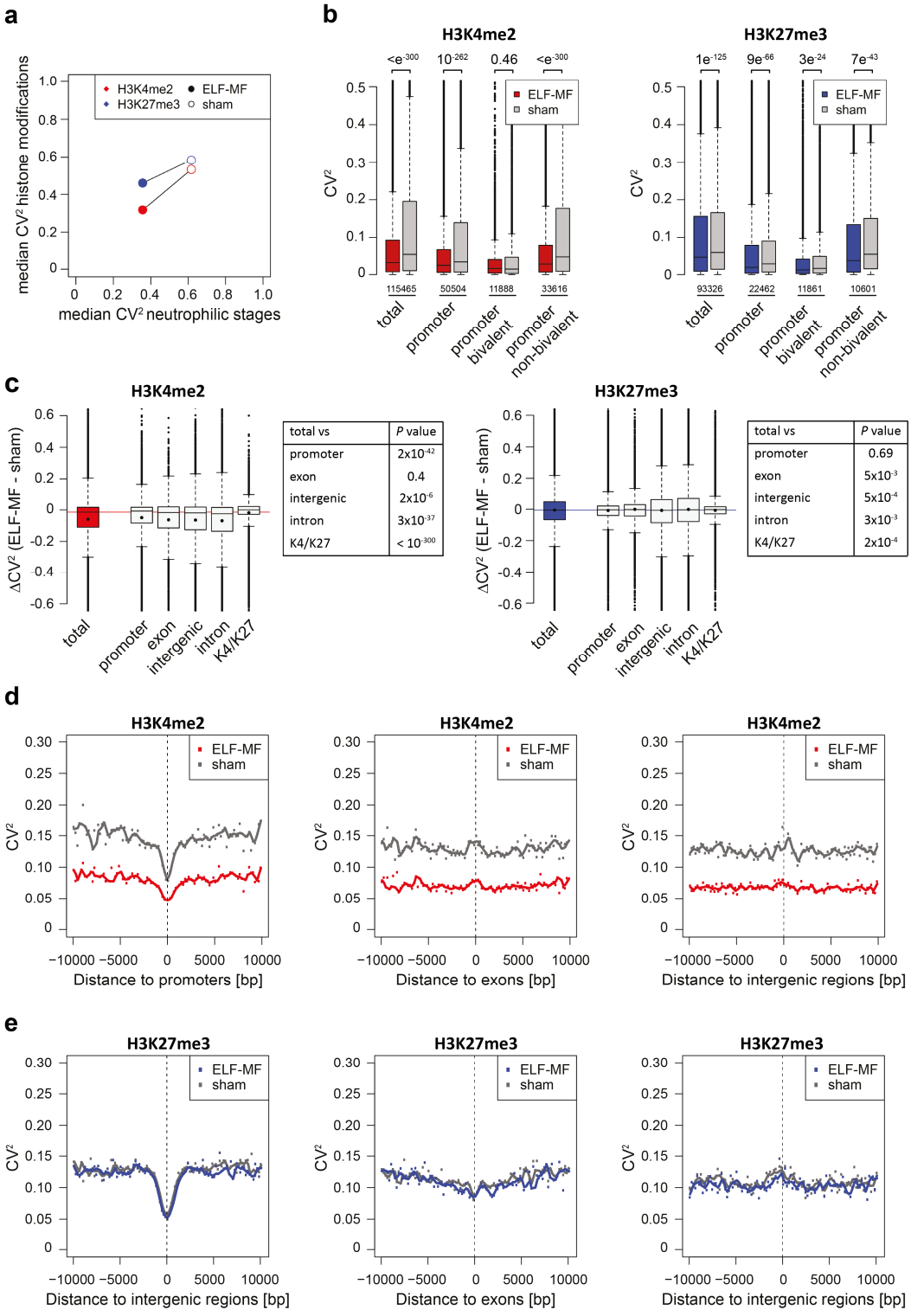

Supplementary Figure S13. Replicate variability of H3K4me2 and H3K27me3 marks in neutrophilic progenitors are locus-specific. Variability of ChIP-seq replicates for H3K4me2 and H3K27me3 modifications of ELF-MF (50 Hz powerline, 1 mT, 5' on/10' off) and sham-exposed neutrophilic progenitors at day five of in vitro differentiation was assessed. (a) Median of the squared coefficient of variation (CV^2) of reads in 500 bp tiles of two H3K4me2 and H3K27me3 ChIP-seq replicates (x-axis)

was correlated with the median variance of neutrophilic stages (three replicates, y-axis) in ELF-MF and sham exposed neutrophilic progenitors. Neutrophilic stages were analysed by flow cytometry discriminating CD34+ cells (CD34+, CD11b-, CD16b-), promyelocytes (CD34-, CD11b-, CD16b-), myelocytes (CD34-, CD11b+, CD16b-) and metamyelocytes/neutrophils (CD36-, CD11b+, CD16b+). (b-e) The squared coefficient of variation (CV^2) of reads in 500 bp tiles of two H3K4me2 and H3K27me3 ChIP-seq replicates was assessed with respect to genomic features: promoters (± 1,000 bp of TSS), exons, introns, intergenic regions (UCSC hg19) or bivalent domains. (b) Box-and-whisker plots illustrate median (lines) and mean (black circles) CV^2 values of H3K4me2 and H3K27me3 modification at non-bivalent (non-bi) and bivalent (bi) promoters. *P* values above indicate significance levels by Wilcoxon rank sum test. (c) Box-and-whisker plots illustrate median (lines) and mean (black circles) delta CV^2 values (CV^2 ELF-MF – CV^2 sham) and horizontal lines indicate the median of all H3K4me2 or H3K27me3 tiles. P values of the Wilcoxon rank sum test indicate significant differences between delta CV^2 values of all tiles and delta CV^2 values of tiles at corresponding genomic feature. (d,e) Comparing ELF-MF and sham exposed samples, mean variability of ChIP-seq reads of H3K4me2 (d) and H3K27me3 (e) tiles (CV^2 values on y-axis) were plotted as function of distance to the nearest corresponding genomic feature.

Supplementary Methods

Cell cycle analysis by propidium iodide staining

20-50x10^3 cells were fixed with cold 70% ethanol overnight. Cells were collected by centrifugation, resuspended in 1 mg/mL RNase A (in 200 mM Tris-HCl pH 7.5 and 200 mM NaCl) and incubated at 37°C for 30 min. After addition of 0.5 mg/mL pepsin (in 0.2% HCl) and incubation for another 15 min at 37°C, the cells were stained with propidium iodide (100 µg/mL in PBS, pH 7.5) and incubated on ice for at least 30 min. The DNA content was measured using a FACS cytometer (Beckton Dickinson) in FL2 channel (emission at 575 nm). Raw data were analysed with FlowJo software (TreeStar). Data were statistically analysed by χ^2 test for each replica as well as pairwise comparison by Student's *t*-test using GraphPad Prism.

Apoptosis measurement by Annexin V staining

The number of apoptotic cells in the population was estimated by the Annexin-V Alexa488/PI kit (Invitrogen) according to the provider's recommendations. 20-50x10^3 cells were blocked on ice in Annexin-binding solution supplemented with 1% bovine serum albumin for 15 min before staining with the FITC-anti-Annexin V antibody for 20 min at RT, followed by washing three times with Annexin-binding solution. PI (Invitrogen) or DAPI was added before analysing the cells. Samples were measured using a FACS cytometer (Beckton Dickinson) and analysed by FlowJo Software. Data were statistically analysed by χ^2 test for each replica as well as pairwise comparison by Student's *t*-test using GraphPad Prism.

Identification of cell differentiation state by flow cytometry

Maturation status of the differentiating neutrophilic cell population was analysed by flow cytometry detecting cell surface markers (CD34, CD11b, CD16b) by antibodies. After blocking the cells in Annexin-binding solution (Invitrogen) with 1% BSA on ice for 20 min, the cells were stained in 50 µL blocking buffer on ice for 20 min with the following combination of antibodies: PE mouse anti-human CD16b, APC mouse anti-human CD34, APC-Cy7 mouse anti-human CD11b, PE-Cy7 mouse anti-human CD14 (all from BD Biosciences) and FITC-anti-Annexin V (Invitrogen) and washed three times with blocking buffer. As negative control, samples were stained with an unrelated isotype-matched antibody (BD Biosciences, Supplementary Figure S6f). Freshly isolated monocytes and granulocytes from human blood, separated by a Ficoll-plaque-plus density gradient (GE Healthcare), were used as positive controls. Cell samples were analysed by a FACSCanto II (BD Biosciences) (Supplementary Figure S6d) and Flow cytometry data were determined with FlowJo software (TreeStar), with gating to exclude doublets and nonviable cells on the basis of pulse width and incorporation of DAPI in combination with Annexin V. The neutrophilic differentiation stages were identified by gating on

subpopulations according to the expression of surface markers (Supplementary Figure S6e)[1]: CD34+ cells (CD34+, CD11b-, CD16b-), Promyelocytes (CD34-, CD11b-, CD16b-), Myelocytes (CD34-, CD11b+, CD16b-) and Metamyelocytes (CD36-, CD11b+, CD16b+). Monocytes were identified according to the expression of CD14+.

Chromatin-Immunoprecipitation (ChIP)

Proteins bound to DNA were crosslinked by incubating cells with freshly prepared 1% methanol-free formaldehyde in PBS, pH 7.4 at room temperature under slow agitation for 10 min. Crosslinking was stopped by the addition of glycine to a final concentration of 125 mM. Cells were washed three times with ice-cold PBS, pelleted and snap-frozen. Cells were lysed in cold lysis buffer (1% SDS, 10 mM EDTA, 50 mM Tris-HCl pH 8 and 0.5% Triton-X100, 1 mM PMSF, 1x cOmplete™ Protease Inhibitor Cocktail [Roche]) on ice for 20 min while vortexing several times. To produce random chromatin fragments ranging from 250-400 base pairs in length, cell lysates were sonicated for 30 min (30 sec on, 30 sec off, power high) using a Bioruptor sonicator with a cooling system (diagenode) and cleared by centrifugation at 14,000 g at 4°C for 10 min. Chromatin concentration was estimated by measuring absorbance at 260 nm on a Nanodrop 1000 (Witec AG). For histone ChIPs, 20-30 µg chromatin were diluted 10-fold in ChIP dilution buffer (0.01% SDS, 16.7 mM Tris-HCl pH 8.0, 1.2 mM EDTA, 167 mM NaCl, 1.055% Triton X-100, 1 mM PMSF, 1x cOmplete™), saving 1% of the volume for input analysis. Diluted chromatin was pre-cleared with 20 µL of magnetic Protein G beads (Invitrogen) and pre-blocked with 1 mg/mL BSA and 1 mg/mL tRNA or single-stranded salmon sperm DNA at 4°C for 1 h, prior to incubation with 1-2 µg of the respective antibody (H3K4me2: 07-030 Millipore; H3K27me3: 07-449 Millipore) overnight at 4°C under slow rotation. Histone-antibody-complexes were pulled down by incubation with 40 µL of pre-blocked magnetic Protein G beads at 4°C for 2 h, followed by serial washing with 500 µL ChIP wash buffer I (150 mM NaCl, 20 mM Tris-HCl pH 8.0, 2 mM EDTA, 0.1% SDS, 1% Triton X-100, 1 mM PMSF), 500 µL ChIP wash buffer II (500 mM NaCl, 20 mM Tris-HCl pH 8.0, 2 mM EDTA, 0.1% SDS, 1% TritonX-100, 1 mM PMSF) and 500 µL ChIP wash buffer III (250 mM LiCl, 1% NP40, 10 mM Tris-HCl pH 8.0, 1 mM EDTA, 1% sodium deoxycholate, 1 mM PMSF) at 4°C under rotation. After two additional washes with 500 µL TE buffer (10 mM Tris-HCl pH 8, 1 mM EDTA), bound complexes were eluted by two sequential incubations with 250 µL elution buffer (1% SDS, 0.1 M $NaHCO_3$) at 65°C for 10 min while shaking at 1,400 rpm. Reversal of crosslinking in eluates and input samples was done by incubation at 65°C for 4 h in the presence of 200 mM NaCl. After proteinase K digestion (50 µg/mL) in the presence of 10 mM EDTA and 40 mM Tris-HCl pH 6.5 at 45°C for 1 h, DNA was purified by phenol/chloroform extraction and NaCl/ethanol precipitation and resuspended in 10 mM Tris-HCl pH 8.0.

Supplementary References

1 Elghetany, M. T. Surface antigen changes during normal neutrophilic development: a critical review. *Blood Cells Mol Dis* **28**, 260-274, doi:10.1006/bcmd.2002.0513 (2002).

Dynamics of Histone Modifications and DNA Methylation during *in vitro* Granulopoiesis

Melissa Manser[1], Mohamad R. Abdul Sater[2,3], Christoph D. Schmid[2,3], Faiza Noreen[1], David Schuermann[1], Primo Schär[1*]

[1] Department of Biomedicine, University of Basel, Mattenstrasse 28, Basel, CH-4058, Switzerland

[2] Swiss Tropical and Public Health Institute, Socinstrasse 57, Basel, CH-4002, Switzerland

[3] University of Basel, Petersplatz 1, Basel, CH-4001, Switzerland

Correspondence and requests for materials should be addressed to P.S.
(email: primo.schaer@unibas.ch).

Key words: epigenetics, DNA methylation, histone modification, H3K4me2, H3K27me3, granulopoiesis, differentiation, human haematopoietic progenitor cells

Contribution: I conceived, performed and analysed the *in vitro* neutrophilic granulopoiesis. I analysed the different maturation stages by flow cytometry. I determined the histone modifications by ChIP, prepared the ChIP samples for next-generation sequencing and contributed to the bioinformatic analysis of the ChIP-seq data. I prepared the DNA samples for the DNA methylation array, and did all the analysis on the observed alterations of histone modifications and DNA methylation and wrote the manuscript.

Abstract

The epigenetic information contained in histone tail modifications and DNA methylation is crucial for the establishment and maintenance of the cell type-specific gene expression pattern. The dramatic shaping of the chromatin landscape during a cellular differentiation reflects the transcriptional programming of a stem cell into a functional, terminally differentiated cell. Aberrations of epigenetic modifications are a hallmark of cancer including leukaemia and indicate a loss of cellular identity. Characteristics of acute myeloid leukaemia (AML) are defects in genes encoding epigenetic modifiers, indicating a role of dysregulated epigenetic programming in the development of cancer. To understand the potential perturbance of epigenetic programming during differentiation and its contribution to carcinogenesis, it is important to understand the physiological epigenetic pattern established during the differentiation process. We investigated the changes in DNA cytosine methylation, the activating histone mark H3K4me2 and the repressive histone mark H3K27me3 at genome scale in human CD34+ cord blood cells, differentiating into the neutrophilic lineage. We report that DNA cytosine methylation as well as histone modifications undergo fundamental changes during granulopoiesis especially at the transition of CD34+ cells into the neutrophilic lineage. Epigenetic repression of key pluripotency and developmental genes occurs through a gain of H3K27me3, a loss of H3K4me2 and gain of DNA methylation. Epigenetic activation of neutrophil-specific genes preferentially occurs through DNA demethylation without coincidental alterations at histone modifications. Overall, our data provide insight into the dynamics of the landscape of epigenetic histone modifications and DNA methylation in the human myeloid system, illustrating their regulatory role in lineage restrictions and cell plasticity.

Introduction

Cellular homeostasis and function, including the controlled interaction with the environment, not only depends on the genetic code but also and primarily on the epigenetic information contained in histone tail modifications and DNA methylation. While virtually all cells of a multicellular organism contain the same genetic code, epigenetic modifications shape the chromatin landscape and DNA accessibility, determining the gene expression pattern required for cell lineage commitment (Bernstein et al., 2007; Cedar and Bergman, 2011). Acetylation and methylation of specific residues in the histone tails are the most prominent histone modifications whereas the epigenetic modification of DNA comprises the methylation of cytosine (5mC) at CpG sequences (Bernstein et al., 2007; Kouzarides, 2007; Nicholson et al., 2015). The pattern of epigenetic modification changes as genomes undergo functional adaptation during differentiation (Dambacher et al., 2013). The epigenetic control mechanisms establish three main classes of chromatin: active, repressed and chromatin poised for gene expression. Active chromatin, containing highly expressed genes is occupied by histone 3 lysine 4 tri-methylation (H3K4me3), H3K4me2 and H3K27 acetylation, while chromatin associated with gene repression is marked by H3K27me3 and H3K9me3. Chromatin poised for gene expression is occupied by active as well as repressive epigenetic features including H3K4me2, H3K4me3 and H3K27me3 modifications and is preferentially located at developmental genes in stem cells (Boland et al., 2014; Cantone and Fisher, 2013; Dambacher et al., 2013). In gene regulatory regions with intermediate to high CpG content, DNA methylation negatively regulates gene expression; cytosine methylation is associated with chromatin compaction, absence of methylation with open chromatin (Bernstein et al., 2007; Nicholson et al., 2015). Hence, in organismal development, epigenetic mechanisms establish chromatin stages allowing cell type-specific gene expression and cell lineage restrictions.

Aberrations in the epigenetic information as well as genetic mutations are hallmarks of cancer, but may also be a driving force of cancerogenesis. Acute myeloid leukaemia (AML) is the most common leukaemia in adults and is characterised by a high accumulation of myeloid progenitor cells, among them about 50-60% being neutrophilic progenitors (Seiter, 2016; Zenhäusern et al., 2003). Many AMLs arise from foetal genetic lesions or chromosomal translocations generating fusion proteins such as *PML–RARα*, *AML1–ETO and* mixed lineage leukaemia (*MLL*) (Florean et al., 2011; Kelly and Gilliland, 2002; Martens and Stunnenberg, 2010). Additionally, recent studies on AML uncovered the presence of somatic mutations in genes encoding modifier of DNA methylation (e.g. DNMTs, TET2) and histone modifications (e.g. EZH2, MLL), illustrating a significant epigenetic contribution to leukaemogenesis (Conway O'Brien et al., 2014; Dohner, 2002; Ernst et al., 2010; Figueroa et al., 2010; Greenblatt and Nimer, 2014; Ley et al., 2010; Mizuno, 2001; Nicholson et al., 2015). As cellular

differentiation is based on activation or repression of specific genes, accompanied by global rearrangement of chromatin and epigenetic modifications, the blocked differentiation of progenitor cells and mutations in epigenetic modifiers in AML may indicate a defect in the epigenetic control mechanism of differentiation.

Maintaining the blood system, human haematopoiesis occurs in the bone marrow where multipotent haematopoietic stem cells (HSCs) differentiate into all different types of blood cells. Around two-thirds of the haematopoietic activity in the bone marrow produces monocytes and granulocytes, especially neutrophilic granulocytes with a daily production of 10^{11} cells (Borregaard, 2010). Neutrophils are the most abundant white blood cell in the circulation and key players in the innate immune system. Stimulation of HSCs with the granulocyte-colony stimulating factor (G-CSF) results in the production of neutrophils through a regulated differentiation process with distinct intermediate states: myeloblasts, promyelocytes, myelocytes and metamyelocytes (Amulic et al., 2012; Borregaard, 2010). Neutrophilic granulopoiesis is disturbed and blocked in 50-60% of AML, resulting in the accumulation of progenitors, which suggests a defect in control mechanisms of granulopoiesis as cause for leukaemogenesis. Yet, no study investigated the dynamic epigenetic transitions occurring during human neutrophilic granulopoiesis. It was shown in isolated cells, however, a gain of DNA methylation in neutrophils when compared to HSCs, dynamically regulated throughout differentiation with the most pronounced changes occurring at points of lineage restrictions. Myeloid-specific genes were shown to be repressed by DNA methylation in HSCs and undergo programmed active demethylation upon myeloid differentiation, apparent at common myeloid progenitor states (CMPs) (Cedar and Bergman, 2011; Ko et al., 2010; Trowbridge et al., 2009). This demethylation is followed by an increase of genome-wide DNA methylation in granulocyte-macrophage progenitors (GMPs) compared to CMPs, and again a decrease of methylation in promyelocytes and further neutrophilic differentiation states (Alvarez-Errico et al., 2015; Ronnerblad et al., 2014). Concomitantly, chromatin of neutrophils was shown to be characterized by a high amount of heterochromatin containing different repressive histone modifications like H3K9me3, H3K27me3 or H3K20me3 and low amounts of active histone modifications such as H3K4me3 and H3K4me2 (Navakauskiene et al., 2014; Olins and Olins, 2005).

To investigate the programming of epigenetic modifications during neutrophilic granulopoiesis, we studied the changes of active and repressive histone modifications as well as DNA methylation during an *in vitro* differentiation of human neutrophilic granulocytes. We generated genome-wide profiles of histone modifications (H3K4me2 and H3K27me3) and DNA cytosine methylation. We report that the epigenetic code undergoes fundamental changes during granulopoiesis most pronounced at the stage of lineage commitment, shaping an overall more compact chromatin. Our data show that the

activation of neutrophil-specific genes preferentially occurs through DNA demethylation without coincident alterations at histone modifications. By contrast, the epigenetic repression of important pluripotency and developmental genes occurs through a gain of H3K27me3 with concomitant loss of H3K4me2 and *de novo* DNA methylation.

Results

CpG methylation changes are most pronounced at the beginning of *in vitro* neutrophilic granulopoiesis.

To analyse the changes of the epigenetic modifications during granulopoiesis, CD34+ cells isolated from human cord blood were *in vitro* differentiated into the neutrophilic lineage by the addition of the growth factor G-CSF and the cytokines stem cell factor and Flt3-ligand (Tura et al., 2007) (Figure 1a). We performed three differentiation experiments to address whether extremely-low-frequency magnetic field (ELF-MF) exposure affects cell differentiation associated chromatin reorganisation (Supplementary Figure S1) (Manser et al., in preparation). As ELF-MF exposure did not impact the programming of DNA methylation and histone modifications during granulopoiesis, we used the data of the different exposure conditions as replicates for the analysis of differentiation dependent epigenetic reorganisation. After five days of differentiation, 90% of the cells differentiated to the promyelocyte (75%) or myelocyte (15%) state (Supplementary Figure S1b). By day nine, 60% of cells matured into myelocytes (40%) and metamyelocytes/neutrophils (20%), while 50% of cells differentiated into myelocytes and 25% into metamyelocytes/neutrophils within 14 days of differentiation. To address the dynamic changes of cytosine methylation during granulopoiesis, we performed genome-wide methylation analysis of single CpG sites in CD34+ cells (t0) and neutrophilic progenitors after five (day 5 progenitors, t5), nine (t9) and 14 (t14) days of differentiation, using the Illumina Infinium HumanMethylation 450 platform (Figure 1). The hierarchical clustering of the 412'940 CpGs analysed in all samples (three replicates for CD34+ cells, eight replicates each for neutrophilic progenitors) documented the high reproducibility of the biological replicates (Supplementary Figure S2a). Principal component analysis revealed a clear separation of the maturation stages (Supplementary Figure S2b). Specific genes expressed in neutrophilic granulocytes (*MPO, ELANE, PRTN3*) lost DNA methylation at CpG sites, whereas stem cell genes (*GATA2, CD34*) gained DNA methylation at CpG sites during differentiation (Supplementary Figure S3), consistent with previous results (Ronnerblad et al., 2014). The pattern of cytosine DNA methylation was dramatically altered during differentiation from CD34+ cells (t0) into day 5 progenitors, resulting in

3'882 and 2'977 significantly changed (FDR-adjusted $P < 0.05$) CpG sites losing (log2 FC < -0.6) and gaining (log2 FC > 0.6) methylation, respectively (Figure 1b). Comparing neutrophilic progenitors with the preceding time-point, we observed 1'800 sites losing and 267 sites gaining methylation in day nine progenitors, whereas in progenitors after 14 days of differentiation 17 CpGs gained and 419 CpGs lost methylation (Figure 1b). Investigating the dynamics of changes of DNA methylation throughout the *in vitro* differentiation, we observed that CpGs with DNA methylation changes consistently either loss or gain methylation throughout the entire differentiation process (Figure 1c). The majority of CpGs hypomethylated in neutrophilic progenitors after nine and 14 days (80% and 100%) already lost methylation in early progenitors, while a majority of sites gaining methylation did so during the first five days of differentiation (Figure 1d). Loss of DNA methylation in early progenitors after 5 days occurs at CpG sites with a high DNA methylation content, while gain of DNA methylation occurs preferentially at CpG sites with low or median DNA methylation levels (Supplementary Figure S3d). To evaluate the findings of our *in vitro* differentiation with previous data showing a genome-wide loss of DNA methylation between CMPs and promyelocytes isolated from the bone marrow (Ronnerblad et al., 2014), we compared sites with DNA methylation changes between *in vitro* generated progenitors after five days of differentiation (75% promyelocytes) and CD34+ cells with those of isolated promyelocytes compared to CMPs. We observed an overlap of 46% in CpGs losing and 7% in CpGs gaining DNA methylation (Supplementary Figure S3a). These results indicate a good reproducibility of DNA methylation alterations at sites losing methylation in our *in vitro* differentiation.

During cellular differentiation, changes in DNA methylation are preferentially observed at CpG rich gene regulatory regions, including promoters, CpG islands (CGI) and CGI shores (Boland et al., 2014; Doi et al., 2009; Irizarry et al., 2009; Smith and Meissner, 2013). To investigate whether *de novo* methylation or methylation loss observed in neutrophilic progenitors are preferentially associated with certain genomic features, we intersected sites of methylation changes with annotated gene promoters (1'000 bp up- and downstream of transcription start site [TSS]), exons, introns and intergenic regions as well as with CpG islands, CGI shores (0-2 kb outside CGI), CGI shelf (2-4 kb outside CGI) and open sea (> 4 kb outside CGI, Figure 1e,f). In day 5 progenitors, CpGs lost methylation were often present at introns (40%) and intergenic regions (28%) but less frequently at promoters (23%), while CpGs gained methylation were preferentially found at promoters (44%, Figure 1e). CpGs changing methylation in progenitor cells after nine days of differentiation compared to progenitors after five days, were most prominently located at intron (39% loss and 45% gain) and promoter (29% loss and 27% gain) regions. Analysing all CpGs, we observed that CGIs are enriched for non-methylated CpGs, CGI shores show methylated and non-methylated CpGs, while CGI shelf

and open sea are preferentially methylated, irrespective of the differentiation states (Supplementary Figure S4). During five days of differentiation, gain of DNA methylation occurred preferentially at CpGs in CGIs whereas CGI shelves showed a clear trend for methylation loss, while CGI shores and open sea showed both gains and losses of methylation (Figure 1f). By contrast, at nine days of differentiation methylation gain is observed only at CGI, whereas CpGs outside of CGI are enriched for methylation loss. Notably, we observed the highest numbers of sites with DNA methylation changes outside of CGIs at open sea (t5/t0: 3'643 and t9/t5: 1'311 sites) or CGI shores (t5/t0: 1'304 and t9/t5: 350 sites). To investigate a possible regulatory role of these genomic sites, we intersected sites with DNA methylation changes of day five progenitors with the location of genes in the human genome and analysed the respective ontology (Figure 1g). CpGs lost methylation correlated with genes important in neutrophils (e.g. *ELANE, CTSG*), while CpGs gained methylation occurred mainly at genes important in other blood lineages as neutrophils (e.g. *TNF, IL1B, SELL*).

Overall, these results indicate that changes of the DNA methylation pattern during *in vitro* neutrophilic differentiation occur most widespread at the transition of multipotent cells into the neutrophilic lineage, at lineage commitment. Methylation loss is more pronounced than methylation gain and occurs preferentially at neutrophil-specific genes, indicating a role of DNA demethylation in the regulation of cell plasticity of neutrophils.

H3K4me2 and H3K27me3 modifications undergo fundamental changes during *in vitro* neutrophilic granulopoiesis.

Terminally differentiated human blood neutrophils are characterized by a high amount of transcriptionally non-permissive chromatin containing repressive histone modifications such as H3K9me3, H3K27me3 or H3K20me3 and a low amounts of active histone modifications such as H3K4me2 and H3K4me3 (Navakauskiene et al., 2014; Olins and Olins, 2005). By contrast, HSCs contain typically a relatively large fraction of bivalent chromatin marked by active H3K4me2, H3K4me3 and repressive H3K27me3 (Cedar and Bergman, 2011; Cui et al., 2009). To investigate the dynamic alterations of histone modifications during neutrophilic differentiation, we performed chromatin immunoprecipitation (ChIP) for the histone modifications H3K4me2 and H3K27me3, combined with next generation sequencing (ChIP-seq), in chromatin isolated from CD34+ cells and neutrophilic progenitors after five and nine days of differentiation (Figure 2). For all these points, we generated biological and technical replicates (CD34+: two, t5: five and t9: three). Reads mapped to the hg19 human genome were randomly downsampled to generate 26 million mapped reads per Chip-seq sample that were then analysed in 500 bp and 1'000 bp genomic tiles. The comparison of H3K4me2 and H3K27me3 profiles of all samples showed a good reproducibility in the replicates and a

clear separation and clustering of samples of the different maturation stages (Supplementary Figure S5). Comparing early day five progenitors with CD34+ cells, we observed a total of 19'618 tiles significantly (FDR-adjusted *P* value < 0.05, log2 FC > ± 0.6) changed levels of H3K4me2, while 18'624 tiles were significantly altered in H3K4me2 between progenitors after 5 and 9 days (Figure 2a). The profile of H3K27me3 revealed significant changes (FDR-adjusted *P* value < 0.05, log2 FC > ± 0.6) in 14'174 and 16'767 tiles in the same comparisons (Figure 2b). In both time periods, we found more tiles losing (log2 FC < -0.6) than gaining (log2 FC > 0.6) H3K4me2 modifications (t5/t0: 11'260 and 8'358; t9/t5: 12'186 and 6'438, respectively). By contrast, we observed a higher number of tiles gaining than losing H3K27me3 modification in both time periods during differentiation (t5/t0: 7'914 and 6'260, t9/t5: 9'563 and 7'204, respectively). To address the occurrence of the dynamic programing of the histone modifications, we intersected tiles with changes in H3K4me2 and H3K27me3 modifications of both time frames with each other. We observed that genomic locations with alterations in of both histone modifications were preferentially losing H3K4me2 and gaining H3K27me3 modifications during the first five days of *in vitro* differentiation (90% of tiles) and also when comparing neutrophilic progenitors after nine and five days (75% of tiles) (Figure 2c, Supplementary Figure S6a). Following the individual H3K4me2 tiles throughout the nine days of differentiation, we determined that 6'689 tiles lost H3K4me2 during the first five days and also the following four days, while 1'866 tiles gained H3K4me2 in both stages during differentiation (Figure 2d). By contrast, we revealed 3'289 tiles with a gain of H3K27me3, while 1345 tiles lost H3K27me3 in both stages during differentiation. For instance, the *CD34* locus representing a pluripotency gene with an activated chromatin state with only H3K4me2 present in CD34+ cells (t0) is progressively losing H3K4me2 and accumulating the repressive H3K27me3 mark (Figure 2e, Supplementary Figure S6b,c). By contrast, the *ELANE* locus, a gene specific for the neutrophil lineage, is repressed in CD34+ cells and occupied by low amounts of H3K4me2 and high amounts of H3K27me3 marks. Consistently, a gain of H3K4me2 and a loss of H3K27me3 were observed during neutrophilic differentiation.

To investigate whether certain genomic features are preferentially associated with alterations of histone modifications in neutrophilic progenitors, we intersected differentially occupied genomic tiles with annotated gene promoters, exons, introns and intergenic regions (Figure 2f). In both time periods during differentiation, alterations in H3K4me2 modifications preferentially occurred at introns (t5/t0: 45% and t9/t5:42%) and less frequently in promoter regions (t5/t0: 18% and t9/t5: 30%), whereas changes in H3K27me3 are most prominent at intergenic regions (t5/t0: 40% and t9/t5: 38%) and promoters (t5/t0: 30% and t9/t5: 28%). Tiles with changes in H3K4me2 and H3K27me3 modifications are highly enriched at promoters in neutrophilic progenitors after five and nine days of differentiation (t5/t0: 48% and t9/t5: 52%). To investigate the functional role of these

genomic sites showing changes in histone modifications, we intersected them with the location of genes on the human genome (Figure 2g). The genes regulated by alterations in H3K4me2, H3K27me3 and both histone marks during granulopoiesis fell into the functional networks of related to the blood lineages, but were preferentially associated with different lineages than neutrophils. Overall, we conclude that the landscape of H3K4me2 and H3K27me3 reveal a fundamental chromatin reorganisation during *in vitro* neutrophilic granulopoiesis. Overall, we observed more tiles losing than gaining H3K4me2, while more genomic regions gain H3K27me3 than lost it. In particular, tiles with changes in both histone modifications preferentially lost H3K4me2 and gained H3K27me3. This implicates that these changes guiding the chromatin to a more compact state and allow for the establishment of cellular identity after lineage commitment of stem cells.

Genomic sites undergoing changes in DNA methylation and histone modifications are enriched for promoters and active enhancers.

We observed that the epigenetic code of histone modifications and DNA methylation undergoes the highest alterations at lineage commitment. To investigate whether histone and DNA methylation changes correlate, we intersected tiles with alterations of H3K4me2 and H3K27me3 with sites of DNA methylation changes between day 5 progenitors and CD34+ cells (Figure 3). Comparing tiles with H3K4me2 alterations, we observed that 10% are additional altered in H3K27me3, 3% in CpG sites and less than 1% where further changed in H3K27me3 and DNA methylation sites (Figure 3a). Tiles with H3K27me3 alterations were preferentially concomitant changed in H3K4me2 (17%), only 2% have DNA methylation changes and 1% were additionally altered in H3K4me2 and CpG methylation. Comparing sites with DNA methylation, 13% have alterations in H3K4me2 and 7% in H3K27me3, whereas 2% of all sites are additionally altered in H3K4me2 and H3K27me3 modifications.

To investigate whether sites with simultaneous changes in histone modifications and DNA methylation at lineage commitment are preferentially associated with certain genomic features, we intersected them with annotated gene promoters, exons, introns and intergenic regions, and calculated their distance to the nearest TSS (Figure 3b,c). In early neutrophilic progenitors, H3K4me2 modifications changes occurred to 20% at promoters, H3K27me3 changes to 30% and sites with changes in both histone modifications to 48% (Figure 2f). By contrast, genomic locations with changes in DNA methylation and histone modifications were enriched at promoters and less frequent at introns and intergenic regions (Figure 3b). We observed that genomic locations with changes in DNA methylation and H3K4me2 occurred to 28% at promoters, whereas sites with simultaneous changes in H3K27me3 and DNA methylation to 53% and sites with changes in all three features to 52%. Additionally, genomic locations with simultaneous changes in histone modifications and DNA

methylation are on average closer located to the nearest TSS than locations with only alterations of histone modifications (4'400 bp and 7'700 bp for H3K4me2, 850 bp and 6'800 bp for H3K27me3, and 920 bp and 1'100 bp for sites with changes in both histone modifications, respectively, Figure 3c).

Beside promoters, active and poised enhancers are important regulatory elements involved in cell-fate transitions and cell identity; they are marked by a unique signature of histone modifications and are enriched for DNase I hypersensitivity sites (Creyghton et al., 2010; Heintzman et al., 2007; Rada-Iglesias et al., 2011). To investigate the appearance of alterations in DNA methylation or histone modifications at enhancers, we intersected genomic locations with alterations in the epigenetic features with active (H3K4me1, deoxyribonuclease [DNase], H3K27acetylation [H3K27ac]) and poised enhancers (H3K4me1, DNase, no H3K27ac) in CD34+ cells (published data from Roadmap Epigenomics et al., 2015) (Figure 3d). We observe that genomic locations simultaneously changed in histone modifications and DNA methylation are significantly enriched at active enhancers compared to locations with only alterations in histone modifications (15% and 6% for H3K4me2, 17% and 4% for H3K27me3, and 15% and 5% for sites with changes in both histone modifications, respectively). The same comparisons with poised enhancers showed that genomic locations with changes in both histone modifications are less present at poised enhancers (9% and 12%) whereas H3K27me3 alteration are enriched at poised enhancers (17% and 8%), no significant difference observed at locations with H3K4me2 alterations (8% and 6%). Additionally, we determined the location of active and poised enhancers with alterations in the epigenetic features relative to the nearest TSS (Supplementary Figure S7). Regardless of DNA methylation changes, active and poised enhancers showing changes in H3K4me2 are further apart from the TSS, while active enhancer showing H3K27me3 alterations or changes in both histone modifications are closer to the TSS compared to sites with alterations in histone modifications but not located at enhancers. At poised enhancers, genomic locations showing changes in H3K27me3 are closer to the TSS, regardless of alterations in DNA methylation, while locations showing alteration in all three epigenetic features are further apart from the TSS compared to sites with alterations in histone modifications and DNA methylation but not located at enhancers.

Our data demonstrate that genomic locations undergoing epigenetic changes in histone modifications and DNA methylation are enriched at promoters and active enhancers, confirming their regulatory role during differentiation.

Most sites with coincident changes in histone modifications and DNA methylation change chromatin into a repressed state.

H3K4me2 is present at actively transcribed genes, whereas H3K27me3 as well as DNA methylation correlate with gene repression. During cell differentiation, active epigenetic features present at pluripotency genes change to a repressed state and repressed or poised epigenetic features of lineage-specific genes are activated, resulting in a global reorganisation of the epigenome (Boland et al., 2014; Hawkins et al., 2010; Kraushaar and Zhao, 2013). We observed a substantial reorganisation of histone modifications and DNA methylation during granulopoiesis and determined locations showing coordinated changes in both types of epigenetic features at lineage commitment. To address the directional interactions of these epigenetic changes at lineage commitment with each other, we compared relative alterations in histone modifications and DNA methylation at the same genomic locations (Figure 4). Genomic locations with changes in H3K4me2 and DNA methylation show either loss of H3K4me2 and gain of methylation at CpGs (393 sites) or gain of H3K4me2 and loss of methylation at CpGs (316 site, Figure 4a), indicating the negative correlation of these epigenetic marks. By contrast, sites with simultaneous alterations in H3K27me3 and DNA methylation are predominantly characterised by a gain of the H3K27me3 modification as well as of DNA methylation at CpGs (223 sites), while only a few sites lose H3K27me3 methylation (33 sites), indicating their preferred positive correlation. Moreover, locations with coincident alterations in H3K4me2, H3K27me3 and DNA methylation preferentially lose H3K4me2 and gain DNA methylation (143 sites, red), whereas the same sites preferentially gain H3K27me3 and DNA methylation (135 sites, blue; Figure 4a, right panel). These correlations between alterations in DNA methylation and active or repressive histone modifications are as well indicated in the % of simultaneous changes of each active and repressive epigenetic feature (Supplementary Figure S8).

We determined in total 150 genomic locations with significant alterations in H3K4me2, H3K27me3 as well as DNA methylation in early neutrophilic progenitors compared to CD34+ cells. Their pattern of changes can be divided in four different groups (Figure 4b). Six sites gain H3K4me2 modification, lose H3K27me3 as well as DNA methylation, indicating a transcriptional activation during differentiation (group 1). A loss of both histone modifications in combination with a gain of DNA methylation is observed at eight sites (group 2). One single site loses H3K4me2, gains H3K27me3 and loses DNA methylation (group 4). However, most locations (135 regions, group 3) lose H3K4me2 and gain H3K27me3 as well as DNA methylation, indicating a general transition towards a more repressed chromatin state. To investigate the functional role of these dynamic genomic locations, we intersected them with genes on the human genome (Figure 4c). We observed two genes associated with epigenetic alterations of group 1, indicating activation during differentiation. Both are cell type-

specific genes in neutrophils; *ELANE* is encoding a neutrophil elastase and *PRTN3* encodes for a neutrophil proteinase. By contrast, 57 genes are associated with group 3 changes, indicating gene repression (Supplementary Table 1). These are genes with a role in cellular development, particularly in blood development of multiple lineages beside granulocytes, including erythroid cells, leukocytes or natural killer cells (Figure 4c). Four genes are of the group 2 (*HSPB6*, *MARVELD2*, *RABL6)* and 4 (*MDM4)* type. They are silenced during differentiation and are not expressed in fully mature neutrophils (RNA-seq of Ronnerblad et al., 2014). From these results, we can conclude that key regulatory genes important for lineage specificity of neutrophils, haematopoietic stem cells or other blood lineages are activated or silenced after entering the granulocytic lineage with the help of alterations in histone modifications and DNA methylation.

Epigenetic repression occurs through H3K27me3 alone or together with *de novo* methylation of CpGs.

Genes important for development, morphogenesis and cell signalling are often associated with a poised chromatin state in pluripotent human embryonic stem cells, multipotent stem cells like HSCs or in progenitor cells. This provides a plasticity of a fast epigenetic adaptation during cell differentiation, resulting in the rapid activation or repression of genes (Bernstein et al., 2006; Boland et al.). To investigate the interplay of H3K27me3 and *de novo* DNA methylation in epigenetic repression of poised chromatin in CD34+ cells, we analysed their time-dependent change during differentiation (Figure 5). We first determined sites showing significant alterations in H3K4me2, H3K27me3 and DNA methylation during nine days of differentiation, and then associated these with locations occupied by poised chromatin in CD34+ cells and investigated sites with concomitant changes in H3K4me2, H3K27me3 and DNA methylation (Supplementary Figure S9). Finally, we analysed at which step during differentiation and through what epigenetic change repression occurred. A total of 35’489 and 23’396 tiles significantly (FDR-adjusted *P* value < 0.05, log2 FC > ±0.6) changed the levels of H3K4me2 and H3K27me3 modifications between CD34+ cells and neutrophilic progenitors after 9 days, respectively (Figure 5a). Additionally, we observe 11’026 and 7’196 significantly (FDR-adjusted *P* value < 0.05) changed CpGs losing (log2 FC < -0.6) and gaining (log2 FC > 0.6) DNA methylation, respectively (Figure 5b).

We observed in total 212 locations with a poised chromatin state in CD34+ cells and changing levels of H3K4me2, H3K27me3 and DNA methylation during nine days of neutrophilic differentiation. To address the time-dependency of these epigenetic changes during differentiation, we investigated the relative alterations of H3K4me2, H3K27me3 and DNA methylation of these sites in the first five days and in the following four days of differentiation (Figure 5c). We observed 197 locations that lost

H3K4me2 and gained H3K27me3 as well as CpG methylation during both time periods of differentiation, indicating a transition into a more repressed chromatin state, while only two locations gained H3K4me2 and lost H3K27me3 and DNA methylation, correlating with activated chromatin. By analysing the timing of epigenetic repression during differentiation at the identified 197 sites, we observed that more locations are significantly (FDR-adjusted *P* value < 0.05, log2 FC > 0.6) gaining H3K27me3 (t5/t0: 148 and t9/t5: 43) or DNA methylation (t5/t0: 88 and t9/t5: two) in the first part of differentiation than in the second one, H3K4me2 loss occurs preferentially in the second part of the differentiation (t5/t0: 89 and t9/t5: 164 tiles, Figure 5d). To address the first sequence of epigenetic events of epigenetic repression during nine days of differentiation, we clustered their changes in the same locations in each time period separately (Figure 5e). Significant loss of H3K4me2 modification occurred to equal parts in both time periods during differentiation, whereas *de novo* DNA methylation occurred only in the first part and gain of H3K27me3 modification preferentially in the first part but as well later on (Figure 5e, Supplementary Figure S9). 82 locations of the total 197 sites converted to a repressive state through gaining H3K27me3 with or without H3K4me2 loss in the first part of differentiation. 66 locations underwent repression in the first part of differentiation through gaining H3K27me3 modification with concomitant *de novo* DNA methylation. Only 8 locations were repressed through DNA methylation in the first part and gain of H3K27me3 in the second part of the differentiation, while 14 sites are repressed only through DNA methylation in the first part. These results suggest that during *in vitro* neutrophilic granulopoiesis, epigenetic repression of poised chromatin at HSCs occurs preferentially at lineage commitment through gaining of the H3K27me3 mark alone or in combination with DNA methylation, and occasionally only by DNA methylation alone. At some sites DNA methylation proceeds H3K27me3 modification.

Discussion

Aberrations of epigenetic modifications are a hallmark of cancer including acute myeloid leukaemia. However, to understand the potential perturbance of epigenetic programming during differentiation and its contribution to carcinogenesis, it is important to understand the physiological epigenetic pattern established during the differentiation process. Most previous studies investigating epigenetic features during myeloid development, including granulocytes were performed with isolated mouse or human progenitor cells or fully mature neutrophils (Bocker et al., 2011; Olins and Olins, 2005; Ronnerblad et al., 2014). To investigate the epigenetic programming during neutrophilic granulopoiesis, we performed genome-wide DNA methylation and histone modification (H3K4me2 and H3K27me3) analysis in *in vitro* differentiating CD34+ cells. We report that neutrophilic

granulopoiesis is accompanied by a global reorganisation of epigenetic modifications with the highest alterations occurring at the transition of CD34+ cells into the neutrophilic lineage, overall generating a more compact chromatin state. Additionally, lineage specific epigenetic activation occurred preferentially through DNA demethylation and repression through H3K27me3 and DNA methylation.

DNA methylation is dynamically regulated during granulopoiesis with more CpGs gaining methylation at the beginning, in progenitor cells after five and nine days, and more CpGs losing methylation in progenitors after 14 days compared to the earlier progenitor stages. In total, we observed more CpGs losing methylation than gaining it and this was most pronounced at the transition of CD34+ cells into the neutrophilic lineage. Recent work showed a loss of DNA methylation in mature neutrophils compared to HSCs, and between GMPs and promyelocytes as well as between promyelocytes and mature neutrophils (Alvarez-Errico et al., 2015; Bocker et al., 2011; Hodges et al., 2011; Ronnerblad et al., 2014). As day 5 progenitors of *in vitro* differentiation consist to 75% of promyelocytes, our results are consistent with these observed. Also, sites of DNA methylation changes at CGIs were preferentially gaining methylation in neutrophilic progenitors. CGIs are mainly non-methylated in neutrophilic progenitors as in most cell types (Smith and Meissner, 2013), therefore these results indicate that CpGs at CGIs undergo *de novo* methylation during *in vitro* differentiation. By contrast, sites with DNA methylation changes located in CGI shelves preferentially lose methylation in neutrophilic progenitors after five days, whereas CpGs with methylation changes located in CGI shores gaining or losing methylation. The preferred loss or gain of methylation at different CpGs is in agreement with the general DNA methylation pattern of these genomic locations. CGI shelves are enriched for methylated CpGs in neutrophilic progenitors or other cell types, negatively correlated with the preferred loss of methylation, whereas CGI shores show an overall bimodal pattern of methylation with methylated and non-methylated CpGs (Ronnerblad et al., 2014; Zhang et al., 2015). We observed the highest number of CpGs changing methylation in CGI shores or open sea, indicating that DNA methylation appears to be more dynamic outside of CGI during granulopoiesis as previously observed with differentiation systems (Meissner et al., 2008).

The active histone modification H3K4me2 and the repressive mark H3K27me3 revealed high alterations at lineage commitment and later during differentiation. In total, we observed more regions gaining H3K27me3 than losing it, while the H3K4me2 modification is preferentially lost. Additionally, genomic locations showing level changes in both histone modifications during differentiation preferentially lose H3K4me2 and gain H3K27me3 modification. Overall, the alterations of histone modifications guide the chromatin into a more compact structure in neutrophilic progenitors compared to CD34+ cells. This observation is in line with previous results reporting that human blood neutrophils are enriched for heterochromatin containing repressive

histone modifications as H3K9me3, H3K27me3 and low amounts of active histone modification, including H3K4me2 and H3K4me3 (Navakauskiene et al., 2014; Olins and Olins, 2005). We observed only a small fraction of genomic locations regulated through a gain of H3K4me2 and a loss of H3K27me3, generating an activated chromatin state. Previous studies indicated that neutrophil-specific genes are kept in a transcriptionally poised state in HSCs with high levels of H3K4me2, H3K27me3 and low H3K4me3 marks and get activated through a gain of H3K4me3, a loss of H3K27me3 and only a small increase of H3K4me2 (Attema et al., 2007; Orford et al., 2008; Tang et al., 2014). These results indicate that activation occurs mainly through H3K4me3 and that H3K4me2 is involved in maintenance of the activation potential required for differentiation and to prime loci for rapid activation by converting H3K4me2 to H3K4me3. This specific gene-priming mechanism may explain that we observe only a small amount of regions gaining H3K4me2 and losing H3K27me3 during neutrophilic granulopoiesis. Although both activating histone modifications, H3K4me2 and H3K4me3, are present at most genes, H3K4me3 is particularly highly enriched at promoters of active transcript genes (Bernstein et al., 2005; Sims and Reinberg, 2006). This indicates that a loss of H3K4me2 at gene promoters during neutrophilic granulopoiesis is not only associated with gene repression, but probably as well with gene activation through the conversion to H3K4me3.

Genomic locations with changes in H3K4me2, H3K27me3 and DNA methylation at lineage commitment are preferentially getting transcriptionally repressed. They are marked by a loss of H3K4me2 and a gain of H3K27me3 as well as DNA methylation, and are present at genes important for other blood lineages. Only two important neutrophil-specific genes are activated during differentiation with a gain of H3K4me2 and a loss of H3K27me3 as well as DNA methylation. These results indicate that the repression of important developmental or pluripotency genes is fulfilled by histone modifications in combination with DNA methylation to guide the chromatin into the right cell state. Additionally, we observed that epigenetic repression of poised chromatin states in HSCs occurs preferentially at lineage commitment through a gain of H3K27me3 alone or in combination with DNA methylation, but rarely with DNA methylation alone. These results indicate that H3K27me3 modification initiates the epigenetic repression before *de novo* DNA methylation at most of the observed locations. The delay of DNA methylation at poised genes that become repressed might illustrate that DNA methylation is not the primary operator of expression changes but has rather a role in stabilising gene repression or is involved in subsequent long term silencing (Rose and Klose, 2014; Vento-Tormo et al., 2015). Additionally, a previous study reported that the polycomb group protein EZH2 present at sites of H3K27me3 methylation is important for the recruitment of DNMT3a and DNMT3b, linking DNA methylation to sites of H3K27me3 modification (Vire et al., 2006). On the other side, myeloid-specific genes are repressed by DNA methylation in HSCs and undergo

programmed active demethylation initiating myeloid differentiation; *Dnmt1* deletion in HSCs resulted in an increase of myeloid progenitor cells, whereas *Tet2* depletion leads to an impaired myeloid differentiation (Cedar and Bergman, 2011; Ko et al., 2010; Trowbridge et al., 2009). During granulopoiesis, we observed a high amount of CpG sites losing methylation at the transition of HSCs into the neutrophilic lineage, particularly at neutrophil-specific genes, indicating their activation through DNA demethylation. Additionally, CpGs losing methylation in neutrophilic progenitors after five days of differentiation were preferentially not accompanied by a gain of H3K4me2 or changes of H3K27me3, indicating that DNA demethylation is the driver of gene activation at these neutrophil-specific genes. By contrast, lymphoid-specific genes are marked by the polycomb-mediated, repressive H3K27me3 modification in HSCs and get activated through removal of H3K27me3 (Oguro et al., 2010). We observed that some lymphoid-specific genes as well as pluripotency genes are regulated through a gain of H3K27me3, a loss of H3K4me2 and a gain of CpG methylation, indicating gene repression. Genomic locations that get activated with simultaneous alterations in DNA methylation and histone modifications H3K4me2 and H3K27me3 were rare. Additionally, we observe that only a few genomic locations with bivalent histone modifications in HSCs known to be present at developmental genes, are activated through the loss of the repressive H3K27me3 marks. Conclusively, our results indicate that neutrophil-specific genes are preferentially activated through DNA demethylation and not regulated through H3K4me2 and H3K27me3.

Overall, our study provides novel insight into the genome-wide dynamics of histone modifications and DNA methylation during human granulopoiesis. It illustrates that the highest epigenetic changes occur at lineage commitment. Our data indicate that epigenetic repression of genomic regions with a poised chromatin state at HSCs occurs through a gain of H3K27me3 mark alone or in combination with DNA methylation, but rarely with DNA methylation alone. Additionally, epigenetic activation of neutrophil-specific genes preferentially occurs through DNA demethylation without coincidental alterations in histone modifications H3K4me2 and H3K27me3.

Methods

Cell culture and neutrophilic differentiation.

CD34-positive cells isolated from human cord blood of mixed donors were obtained from AllCells (Alabama, United States). CD34+ cells were propagated in Stemline II medium expansion medium (Stemcell technology) supplemented with 100 ng/mL thrombopoietin, 100 ng/mL stem cell factor, 10 ng/mL Flt3-ligand (Peprotech), 5000 U/mL Penicillin and 5 mg/mL Streptomycin (Sigma-Aldrich)

for four days (De Bruyn et al., 2003). For the neutrophilic differentiation, expanded CD34+ cord blood cells were seeded at cell densities of 10^5 cells/mL in Stemline II medium supplemented with 100 ng/mL stem cell factor, 10 ng/mL Flt3-ligand, 100 ng/mL G-CSF (Peprotech), 5000 U/mL Penicillin and 5 mg/mL Streptomycin (Sigma-Aldrich) and cultured for 14 days. Every second day, fresh cell culture medium was added (1:2 dilution). During neutrophilic differentiation, cells were exposed to a powerline-simulating ELF-MF (50 Hz, 1 mT, 5' on/10' off), to the sham control (< 7 µT residual field) or not-exposed as descripted in Manser et al. (in preparation). The different exposure conditions were considered as replicates for the analysis of the differentiation dependent epigenetic reorganisation.

Identification of Cell Differentiation State by Flow Cytometry.

Maturation status of the differentiating neutrophilic cell population was analysed by flow cytometry detecting cell surface markers (CD34, CD11b, CD16b) by antibodies. After blocking the cells in Annexin-binding solution (Invitrogen) with 1% BSA on ice for 20 min, the cells were stained in 50 µL blocking buffer on ice for 20 min with the following combination of antibodies: PE mouse anti-human CD16b, APC mouse anti-human CD34 and APC-Cy7 mouse anti-human CD11b (all from BD Biosciences) and FITC-anti-Annexin V (Invitrogen) and washed three times with blocking buffer. As negative control, samples were stained with an unrelated isotype-matched antibody (BD Biosciences). Freshly isolated monocytes and granulocytes from human blood, separated by a Ficoll-plaque-plus density gradient (GE Healthcare), were used as positive controls. Cell samples were analysed by a FACSCanto II (BD Biosciences) and Flow cytometry data were determined with FlowJo software (TreeStar), with gating to exclude doublets and nonviable cells on the basis of pulse width and incorporation of DAPI in combination with Annexin V. The neutrophilic differentiation stages were identified by gating on subpopulations according to the expression of surface markers (Elghetany, 2002): CD34+ cells (CD34+, CD11b-, CD16b-), Promyelocytes (CD34-, CD11b-, CD16b-), Myelocytes (CD34-, CD11b+, CD16b-) and Metamyelocytes (CD36-, CD11b+, CD16b+). More details were described elsewhere (Manser et al., in preparation).

Base resolution DNA methylation analysis by Illumina Infinium HumanMethylation 450 array.

Genomic DNA was extracted from frozen cell pellets by QIAamp DNA mini kit (Qiagen) according to the manufacturer's instructions including an RNase-treatment step. 500 ng of genomic DNA was bisulfide converted using the EZ-96 DNA Methylation Kit (Zymo Research Corporation). Genome-wide assessment of DNA methylation was done on Illumina Infinium HumanMethylation 450 Beadchip arrays, interrogating methylation at 485'577 sites (Sandoval et al., 2014). Raw signal intensities were extracted by the Illumina GenomeStudio software and imported into R using the

methylumi package as a methylumi object. Data normalization was performed applying the dasen method as described previously (Touleimat, 2012). Briefly, probe-level signals for individual CpG sites were subjected to background adjustment, followed by quantile normalization of both typeI and typeII probes separately. Probes for CpG sites with signal intensities not significantly different (P<0.05) from background measurements in any data sets or mapping to regions with known germline polymorphisms, to multiple genomic loci (Price et al., 2013), or to either sex chromosome were removed, yielding a total of 412'940 CpG after filtering.

All computational and statistical analyses were performed using R and Bioconductor (Gentleman et al., 2004). All analyses for differential methylation were performed on M-values (M = log2 (methylated/unmethylated) as recommended (Du et al., 2010). Empirical Bayes methodology utilizing a moderated t-statistic available in limma was used to test for significant differences between the groups (Smyth, 2004). False-discovery rate (FDR)-adjusted *P* values for multiple comparisons were calculated using the Benjamini and Hochberg approach. Differentially methylated CpGs were defined as those with both a false discovery rate (FDR) adjusted *P* value < 0.05 and log2 fold change > 0.6. Promoter, exons, introns, intergenic regions and transcription start side were defined using the Bioconductor package TxDb.Hsapiens.UCSC.hg19.knownGene analysed by R/Bioconductor. Based on public datasets of DNA methylation profiles (Illumina Infinium HumanMethylation 450 Beadchip arrays) of human promyelocytes and CMPs, sites with DNA methylation changes (FDR adj. *P* value < 0.05 & delta b-value > 0.17) were calculated as descripted in publication (Ronnerblad et al., 2014). Gene annotations were defined using the Bioconductor package org.Hs.eg.db. The functional analyses were generated through the use of QIAGEN's Ingenuity Pathway Analysis (IPA®, QIAGEN Redwood City, www.qiagen.com/ingenuity).

Chromatin-Immunoprecipitation (ChIP).

Proteins bound to DNA were crosslinked by incubating cells with freshly prepared 1% methanol-free formaldehyde in PBS, pH 7.4 at room temperature under slow agitation for 10 min. Crosslinking was stopped by the addition of glycine to a final concentration of 125 mM. Cells were washed three times with ice-cold PBS, pelleted and snap-frozen. Cells were lysed in cold lysis buffer (1% SDS, 10 mM EDTA, 50 mM Tris-HCl pH 8 and 0.5% Triton-X100, 1 mM PMSF, 1x cOmplete™ Protease Inhibitor Cocktail [Roche]) on ice for 20 min while vortexing several times. To produce random chromatin fragments ranging from 250-400 base pairs in length, cell lysates were sonicated for 30 min (30 sec on, 30 sec off, power high) using a Bioruptor sonicator with a cooling system (diagenode) and cleared by centrifugation at 14'000 g at 4°C for 10 min. Chromatin concentration was estimated by measuring absorbance at 260 nm on a Nanodrop 1000 (Witec AG). For histone ChIPs, 20-30 µg

chromatin were diluted 10-fold in ChIP dilution buffer (0.01% SDS, 16.7 mM Tris-HCl pH 8.0, 1.2 mM EDTA, 167 mM NaCl, 1.055% Triton X-100, 1 mM PMSF, 1x cOmplete™), saving 1% of the volume for input analysis. Diluted chromatin was pre-cleared with 20 µL of magnetic Protein G beads (Invitrogen) and pre-blocked with 1 mg/mL BSA and 1 mg/mL tRNA or single-stranded salmon sperm DNA at 4°C for 1 h, prior to incubation with 1-2 µg of the respective antibody (H3K4me2: 07-030 Millipore; H3K27me3: 07-449 Millipore) overnight at 4°C under slow rotation. Histone-antibody-complexes were pulled down by incubation with 40 µL of pre-blocked magnetic Protein G beads at 4°C for 2 h, followed by serial washing with 500 µL ChIP wash buffer I (150 mM NaCl, 20 mM Tris-HCl pH 8.0, 2 mM EDTA, 0.1% SDS, 1% Triton X-100, 1 mM PMSF), 500 µL ChIP wash buffer II (500 mM NaCl, 20 mM Tris-HCl pH 8.0, 2 mM EDTA, 0.1% SDS, 1% TritonX-100, 1 mM PMSF) and 500 µL ChIP wash buffer III (250 mM LiCl, 1% NP40, 10 mM Tris-HCl pH 8.0, 1 mM EDTA, 1% sodium deoxycholate, 1 mM PMSF) at 4°C under rotation. After two additional washes with 500 µL TE buffer (10 mM Tris-HCl pH 8, 1 mM EDTA), bound complexes were eluted by two sequential incubations with 250 µL elution buffer (1% SDS, 0.1 M $NaHCO_3$) at 65°C for 10 min while shaking at 1'400 rpm. Reversal of crosslinking in eluates and input samples was done by incubation at 65°C for 4 h in the presence of 200 mM NaCl. After proteinase K digestion (50 µg/mL) in the presence of 10 mM EDTA and 40 mM Tris-HCl pH 6.5 at 45°C for 1 h, DNA was purified by phenol/chloroform extraction and NaCl/ethanol precipitation and resuspended in 10 mM Tris pH 8.0. QPCR with target specific primers (see Supplementary Table 2) was performed using Rotor-gene SYBR Green (Qiagen) with a Rotor-Gene Q thermocycler (Qiagen). Statistical analysis was performed on Graphpad Prism Software by unpaired Student's t-test.

Whole-Genome Analysis of Histone Modifications.

Single-end 50 bp reads sequencing of ChIP was performed at Genome Technology Access Center (GTAC) in St. Louis (Missouri, USA) using standard protocols for library generation for the Illumina HiSeq platform. In total 20 libraries were generated from H3K4me2 and H3K27me3 ChIP samples of the neutrophilic differentiation stages: two ChIP-seq replicates of CD34+ cells, five for progenitor cells after five days and three of progenitor cells after nine days for each histone modification (Manser et al., in preparation). Additionally, three input controls were included, one each for CD34+ cells, progenitors after five days and progenitors after nine days.

The analysis of ChIP-seq data was performed at the scientific computing core facility (sciCORE) of the University of Basel. For each library, sequence reads were aligned to the human reference genome assembly (hg19) using the Sequence Mapping and Alignment Tool (SMALT v 0.6.2). High quality alignments (bamtools filter-mapQuality ">30") were extracted. Center positions of ChIPped DNA

fragments were approximated based on average fragment lengths and orientations of read alignments (http://ccg.vital-it.ch/chipseq/chip_center.php). Fragment center-positions of each library were used to call genomic domains for H3K4me2 or H3K27me3 with increased read densities applying the program “chippart” (http://ccg.vital-it.ch/chipseq/). Global domain sets were assembled by combining domains less than 1 kb apart with the merge function of bedtools and being present in at least one of the samples. Merged domain sets were subdivided into tiles of uniform lengths of 500 and 1’000 bp. After random downsampling to about 26 million high quality alignments, the number of reads mapping within tiles (fragment center-positions) were extracted for each library. Tiles were further filtered for read counts above an arbitrary threshold above background (50 reads for H3K4me2, 30 for H3K27me3 per 500 bp tile and 100 reads for H3K4me2, 60 for H3K27me3 per 1’000 bp tile length) in at least one sample. As additional filtering criteria, 7 read counts above the corresponding input were applied. Read counts within genomic tiles were tested for differences between groups of samples applying a generalized linear model (GLM) likelihood ratio test as implemented in the EdgeR package, originally developed for differential gene expression data (Robinson et al., 2010). In brief, the dispersion parameter of the negative binomial model was estimated for each genomic interval. Tables with read counts resulting from the merging, normalization and filtering were used and the log2-fold changes and *P* values of the GLM likelihood ratio test were computed under the null hypothesis that the fitted coefficients of negative binomial GLMs of the compared groups are equal. Domains (500 bp and 1’000 bp) with significant alterations were defined as those with both a false discovery rate (FDR) adjusted *P* value < 0.05 and log2 fold change > ±0.6. If overlaying 500 and 1’000 bp tiles had significant alteration, 500 bp tile was selected. The integrative genomics viewer was used to visualize ChIP-seq reads (Robinson et al., 2011; Thorvaldsdottir et al., 2013).

Based on public datasets for primary haematopoietic stem cells from the Roadmap Epigenomics project (H3K4me1, E035-H3K4me1.narrowPeak; H3K27ac, E050-H3K27ac.narrowPeak; Dnase1, E051-DNase.all.peaks), active enhancers were determined by occupation of H3K4me1, DNase and H3K27ac, poised enhancers as H3K4me1 and DNase, but no H3K27ac present. Intersections between H3K4me2 and H3K27me3 ChIP-seq data in 500 bp tiles indicate sites with alterations in both histone modifications. Promoter, exons, introns, intergenic regions and transcription start side were defined using the Bioconductor package TxDb.Hsapiens.UCSC.hg19.knownGene analysed by R/Bioconductor. Gene annotations were defined using the Bioconductor package org.Hs.eg.db. The functional analyses were generated through the use of QIAGEN’s Ingenuity Pathway Analysis (IPA® , QIAGEN Redwood City, www.qiagen.com/ingenuity).

References

Alvarez-Errico, D., Vento-Tormo, R., Sieweke, M., and Ballestar, E. (2015). Epigenetic control of myeloid cell differentiation, identity and function. Nat Rev Immunol *15*, 7-17.

Amulic, B., Cazalet, C., Hayes, G.L., Metzler, K.D., and Zychlinsky, A. (2012). Neutrophil function: from mechanisms to disease. Annu Rev Immunol *30*, 459-489.

Attema, J.L., Papathanasiou, P., Forsberg, E.C., Xu, J., Smale, S.T., and Weissman, I.L. (2007). Epigenetic characterization of hematopoietic stem cell differentiation using miniChIP and bisulfite sequencing analysis. Proc Natl Acad Sci U S A *104*, 12371-12376.

Bernstein, B.E., Kamal, M., Lindblad-Toh, K., Bekiranov, S., Bailey, D.K., Huebert, D.J., McMahon, S., Karlsson, E.K., Kulbokas, E.J., 3rd, Gingeras, T.R*., et al.* (2005). Genomic maps and comparative analysis of histone modifications in human and mouse. Cell *120*, 169-181.

Bernstein, B.E., Meissner, A., and Lander, E.S. (2007). The mammalian epigenome. Cell *128*, 669-681.

Bocker, M.T., Hellwig, I., Breiling, A., Eckstein, V., Ho, A.D., and Lyko, F. (2011). Genome-wide promoter DNA methylation dynamics of human hematopoietic progenitor cells during differentiation and aging. Blood *117*, e182-189.

Boland, M.J., Nazor, K.L., and Loring, J.F. (2014). Epigenetic regulation of pluripotency and differentiation. Circ Res *115*, 311-324.

Borregaard, N. (2010). Neutrophils, from marrow to microbes. Immunity *33*, 657-670.

Cantone, I., and Fisher, A.G. (2013). Epigenetic programming and reprogramming during development. Nat Struct Mol Biol *20*, 282-289.

Cedar, H., and Bergman, Y. (2011). Epigenetics of haematopoietic cell development. Nat Rev Immunol *11*, 478-488.

Conway O'Brien, E., Prideaux, S., and Chevassut, T. (2014). The epigenetic landscape of acute myeloid leukemia. Adv Hematol *2014*, 103175.

Creyghton, M.P., Cheng, A.W., Welstead, G.G., Kooistra, T., Carey, B.W., Steine, E.J., Hanna, J., Lodato, M.A., Frampton, G.M., Sharp, P.A*., et al.* (2010). Histone H3K27ac separates active from poised enhancers and predicts developmental state. Proc Natl Acad Sci U S A *107*, 21931-21936.

Cui, K., Zang, C., Roh, T.Y., Schones, D.E., Childs, R.W., Peng, W., and Zhao, K. (2009). Chromatin signatures in multipotent human hematopoietic stem cells indicate the fate of bivalent genes during differentiation. Cell Stem Cell *4*, 80-93.

Dambacher, S., de Almeida, G.P., and Schotta, G. (2013). Dynamic changes of the epigenetic landscape during cellular differentiation. Epigenomics *5*, 701-713.

Dohner, K. (2002). Prognostic Significance of Partial Tandem Duplications of the MLL Gene in Adult Patients 16 to 60 Years Old With Acute Myeloid Leukemia and Normal Cytogenetics: A Study of the Acute Myeloid Leukemia Study Group Ulm. Journal of Clinical Oncology *20*, 3254-3261.

Doi, A., Park, I.H., Wen, B., Murakami, P., Aryee, M.J., Irizarry, R., Herb, B., Ladd-Acosta, C., Rho, J., Loewer, S*., et al.* (2009). Differential methylation of tissue- and cancer-specific CpG island shores

distinguishes human induced pluripotent stem cells, embryonic stem cells and fibroblasts. Nat Genet *41*, 1350-1353.

Elghetany, M.T. (2002). Surface antigen changes during normal neutrophilic development: a critical review. Blood Cells Mol Dis *28*, 260-274.

Ernst, T., Chase, A.J., Score, J., Hidalgo-Curtis, C.E., Bryant, C., Jones, A.V., Waghorn, K., Zoi, K., Ross, F.M., Reiter, A.*, et al.* (2010). Inactivating mutations of the histone methyltransferase gene EZH2 in myeloid disorders. Nat Genet *42*, 722-726.

Figueroa, M.E., Abdel-Wahab, O., Lu, C., Ward, P.S., Patel, J., Shih, A., Li, Y., Bhagwat, N., Vasanthakumar, A., Fernandez, H.F.*, et al.* (2010). Leukemic IDH1 and IDH2 mutations result in a hypermethylation phenotype, disrupt TET2 function, and impair hematopoietic differentiation. Cancer Cell *18*, 553-567.

Florean, C., Schnekenburger, M., Grandjenette, C., Dicato, M., and Diederich, M. (2011). Epigenomics of leukemia: from mechanisms to therapeutic applications. Epigenomics *3*, 581-609.

Greenblatt, S.M., and Nimer, S.D. (2014). Chromatin modifiers and the promise of epigenetic therapy in acute leukemia. Leukemia *28*, 1396-1406.

Hawkins, R.D., Hon, G.C., Lee, L.K., Ngo, Q., Lister, R., Pelizzola, M., Edsall, L.E., Kuan, S., Luu, Y., Klugman, S.*, et al.* (2010). Distinct epigenomic landscapes of pluripotent and lineage-committed human cells. Cell Stem Cell *6*, 479-491.

Heintzman, N.D., Stuart, R.K., Hon, G., Fu, Y., Ching, C.W., Hawkins, R.D., Barrera, L.O., Van Calcar, S., Qu, C., Ching, K.A.*, et al.* (2007). Distinct and predictive chromatin signatures of transcriptional promoters and enhancers in the human genome. Nat Genet *39*, 311-318.

Hodges, E., Molaro, A., Dos Santos, C.O., Thekkat, P., Song, Q., Uren, P.J., Park, J., Butler, J., Rafii, S., McCombie, W.R.*, et al.* (2011). Directional DNA methylation changes and complex intermediate states accompany lineage specificity in the adult hematopoietic compartment. Mol Cell *44*, 17-28.

Irizarry, R.A., Ladd-Acosta, C., Wen, B., Wu, Z., Montano, C., Onyango, P., Cui, H., Gabo, K., Rongione, M., Webster, M.*, et al.* (2009). The human colon cancer methylome shows similar hypo- and hypermethylation at conserved tissue-specific CpG island shores. Nat Genet *41*, 178-186.

Kelly, L.M., and Gilliland, D.G. (2002). Genetics of myeloid leukemias. Annu Rev Genomics Hum Genet *3*, 179-198.

Ko, M., Huang, Y., Jankowska, A.M., Pape, U.J., Tahiliani, M., Bandukwala, H.S., An, J., Lamperti, E.D., Koh, K.P., Ganetzky, R.*, et al.* (2010). Impaired hydroxylation of 5-methylcytosine in myeloid cancers with mutant TET2. Nature *468*, 839-843.

Kouzarides, T. (2007). Chromatin modifications and their function. Cell *128*, 693-705.

Kraushaar, D.C., and Zhao, K. (2013). The epigenomics of embryonic stem cell differentiation. Int J Biol Sci *9*, 1134-1144.

Ley, T.J., Ding, L., Walter, M.J., McLellan, M.D., Lamprecht, T., Larson, D.E., Kandoth, C., Payton, J.E., Baty, J., Welch, J.*, et al.* (2010). DNMT3A mutations in acute myeloid leukemia. N Engl J Med *363*, 2424-2433.

Manser, M., Sater, M., Schürmann, D., Murbach, M., Schmid, C., and Schär, P. (in preparation). ELF MF Exposure Affects Robustness of Epigenetic Programming during Granulopoiesis and in Leukaemic cells.

Martens, J.H., and Stunnenberg, H.G. (2010). The molecular signature of oncofusion proteins in acute myeloid leukemia. FEBS Lett *584*, 2662-2669.

Meissner, A., Mikkelsen, T.S., Gu, H., Wernig, M., Hanna, J., Sivachenko, A., Zhang, X., Bernstein, B.E., Nusbaum, C., Jaffe, D.B.*, et al.* (2008). Genome-scale DNA methylation maps of pluripotent and differentiated cells. Nature *454*, 766-770.

Mizuno, S.-i. (2001). Expression ofDNAmethyltransferases DNMT1, 3A, and 3B in normal hematopoiesis and in acute and chronic myelogenous leukemia. Blood *97*.

Navakauskiene, R., Borutinskaite, V.V., Treigyte, G., Savickiene, J., Matuzevicius, D., Navakauskas, D., and Magnusson, K.E. (2014). Epigenetic changes during hematopoietic cell granulocytic differentiation--comparative analysis of primary CD34+ cells, KG1 myeloid cells and mature neutrophils. BMC Cell Biol *15*, 4.

Nicholson, T.B., Veland, N., and Chen, T. (2015). Writers, Readers, and Erasers of Epigenetic Marks. 31-66.

Oguro, H., Yuan, J., Ichikawa, H., Ikawa, T., Yamazaki, S., Kawamoto, H., Nakauchi, H., and Iwama, A. (2010). Poised lineage specification in multipotential hematopoietic stem and progenitor cells by the polycomb protein Bmi1. Cell Stem Cell *6*, 279-286.

Olins, D.E., and Olins, A.L. (2005). Granulocyte heterochromatin: defining the epigenome. BMC Cell Biol *6*, 39.

Orford, K., Kharchenko, P., Lai, W., Dao, M.C., Worhunsky, D.J., Ferro, A., Janzen, V., Park, P.J., and Scadden, D.T. (2008). Differential H3K4 methylation identifies developmentally poised hematopoietic genes. Dev Cell *14*, 798-809.

Price, M.E., Cotton, A.M., Lam, L.L., Farre, P., Emberly, E., Brown, C.J., Robinson, W.P., and Kobor, M.S. (2013). Additional annotation enhances potential for biologically-relevant analysis of the Illumina Infinium HumanMethylation450 BeadChip array. Epigenetics Chromatin *6*, 4.

Rada-Iglesias, A., Bajpai, R., Swigut, T., Brugmann, S.A., Flynn, R.A., and Wysocka, J. (2011). A unique chromatin signature uncovers early developmental enhancers in humans. Nature *470*, 279-283.

Roadmap Epigenomics, C., Kundaje, A., Meuleman, W., Ernst, J., Bilenky, M., Yen, A., Heravi-Moussavi, A., Kheradpour, P., Zhang, Z., Wang, J.*, et al.* (2015). Integrative analysis of 111 reference human epigenomes. Nature *518*, 317-330.

Robinson, J.T., Thorvaldsdottir, H., Winckler, W., Guttman, M., Lander, E.S., Getz, G., and Mesirov, J.P. (2011). Integrative genomics viewer. Nat Biotechnol *29*, 24-26.

Robinson, M.D., McCarthy, D.J., and Smyth, G.K. (2010). edgeR: a Bioconductor package for differential expression analysis of digital gene expression data. Bioinformatics *26*, 139-140.

Ronnerblad, M., Andersson, R., Olofsson, T., Douagi, I., Karimi, M., Lehmann, S., Hoof, I., de Hoon, M., Itoh, M., Nagao-Sato, S.*, et al.* (2014). Analysis of the DNA methylome and transcriptome in granulopoiesis reveals timed changes and dynamic enhancer methylation. Blood *123*, e79-89.

Rose, N.R., and Klose, R.J. (2014). Understanding the relationship between DNA methylation and histone lysine methylation. Biochim Biophys Acta *1839*, 1362-1372.

Sandoval, J., Heyn, H., Moran, S., Serra-Musach, J., Pujana, M.A., Bibikova, M., and Esteller, M. (2014). Validation of a DNA methylation microarray for 450,000 CpG sites in the human genome. Epigenetics *6*, 692-702.

Seiter, K. (2016). Acute Myeloid Leukemia Staging retrieved July 31, 2016, from http://emedicinemedscapecom/article/2006750-overview.

Sims, R.J., 3rd, and Reinberg, D. (2006). Histone H3 Lys 4 methylation: caught in a bind? Genes Dev *20*, 2779-2786.

Smith, Z.D., and Meissner, A. (2013). DNA methylation: roles in mammalian development. Nat Rev Genet *14*, 204-220.

Tang, H., An, S., Zhen, H., and Chen, F. (2014). Characterization of combinatorial histone modifications on lineage-affiliated genes during hematopoietic stem cell myeloid commitment. Acta Biochim Biophys Sin (Shanghai) *46*, 894-901.

Thorvaldsdottir, H., Robinson, J.T., and Mesirov, J.P. (2013). Integrative Genomics Viewer (IGV): high-performance genomics data visualization and exploration. Brief Bioinform *14*, 178-192.

Touleimat, N. (2012). Complete pipeline for Infinium®Human Methylation 450K BeadChip data processing using subset quantile normalization for accurate DNA methylation estimation. Epigenomics.

Trowbridge, J.J., Snow, J.W., Kim, J., and Orkin, S.H. (2009). DNA methyltransferase 1 is essential for and uniquely regulates hematopoietic stem and progenitor cells. Cell Stem Cell *5*, 442-449.

Tura, O., Barclay, G.R., Roddie, H., Davies, J., and Turner, M.L. (2007). Optimal ex vivo expansion of neutrophils from PBSC CD34+ cells by a combination of SCF, Flt3-L and G-CSF and its inhibition by further addition of TPO. J Transl Med *5*, 53.

Vento-Tormo, R., Alvarez-Errico, D., Rodriguez-Ubreva, J., and Ballestar, E. (2015). Gains of DNA methylation in myeloid terminal differentiation are dispensable for gene silencing but influence the differentiated phenotype. FEBS J *282*, 1815-1825.

Vire, E., Brenner, C., Deplus, R., Blanchon, L., Fraga, M., Didelot, C., Morey, L., Van Eynde, A., Bernard, D., Vanderwinden, J.M.*, et al.* (2006). The Polycomb group protein EZH2 directly controls DNA methylation. Nature *439*, 871-874.

Zenhäusern, R., Zwicky, C., Solenthaler, M., Fey, M.F., and A., T. (2003). Akute Leukämien beim Erwachsenen. Schweiz Med Forum.

Zhang, W., Spector, T.D., Deloukas, P., Bell, J.T., and Engelhardt, B.E. (2015). Predicting genome-wide DNA methylation using methylation marks, genomic position, and DNA regulatory elements. Genome Biol *16*, 14.

Figures

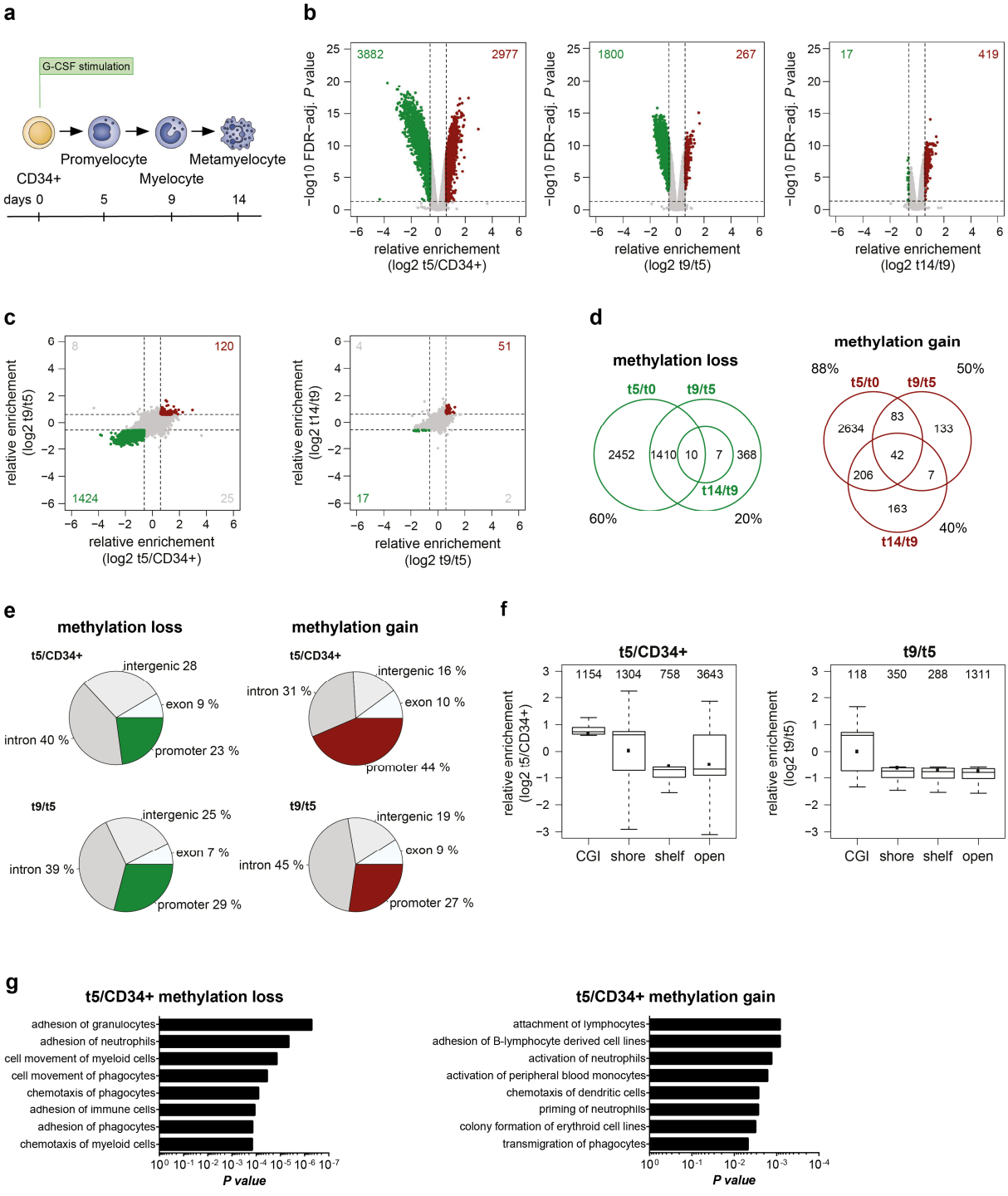

Figure 1: DNA methylation changes are most pronounced at the beginning of *in vitro* neutrophilic granulopoiesis. DNA methylation of CD34+ human cord blood cells (t0) and neutrophilic progenitors after five (t5), nine (t9) and 14 days (t14) of *in vitro* differentiation was analysed by Illumina Infinium HumanMethylation 450 array. (a) After the expansion of CD34+ human cord blood cells for four days, the CD34+ cell population was *in vitro* differentiated into neutrophilic lineage for 14 days by the addition of G-CSF. (b) Relative DNA methylation levels in log2-fold change (FC) on the x-axis are

plotted against the false discovery rate (FDR)-adjusted *P*-value (moderated *t*-statistic) on the y-axis for the comparison of neutrophilic progenitors after five days and CD34+ cells, neutrophilic progenitors after nine and five days, and progenitors after 14 and nine days. CpGs statistically significantly (FDR-adjusted $P < 0.05$) losing (FC < -0.6) and gaining (FC > 0.6) DNA methylation in these comparisons are indicated in green and dark red, respectively. (c) Comparing relative DNA methylation of log2-fold change (FC) between CD34+ and neutrophilic progenitor cells after five days (x-axis) with progenitors after five and nine days (y-axis) as well as between progenitors after five and nine days (x-axis) with progenitors after nine and 14 days (y-axis). Amount of CpG sites with significant alterations in both stages are indicated. (d) Intersections between CpGs gaining and losing methylation in the different neutrophilic progenitors after five, nine and 14 days, respectively. Illustrated is the number of CpGs in the corresponding category and the % of CpGs in only one category. (e) Relative occurrence of CpGs changing DNA methylation in different neutrophilic progenitors after five and nine days compared to earlier stages in gene promoters, exon, intron and intergenic regions. (f) Relative DNA methylation of log2-fold change (FC) in neutrophilic progenitors after five and nine days at CpG Islands (CGI), CGI shore (0-2 kb away from CGI), CGI shelf (2-4 kb away from *CGI*) and open sea. CpGs statistically significantly (FDR-adjusted $P < 0.05$, FC > ± 0.6) differently methylated at different features are indicated in black. (g) Functional analysis of CpGs gaining and losing DNA methylation by Ingenuity Pathway Analysis. Displayed are the top haematological system development and function features and their probability of overlain calculated by a right-tailed Fisher Exact Test.

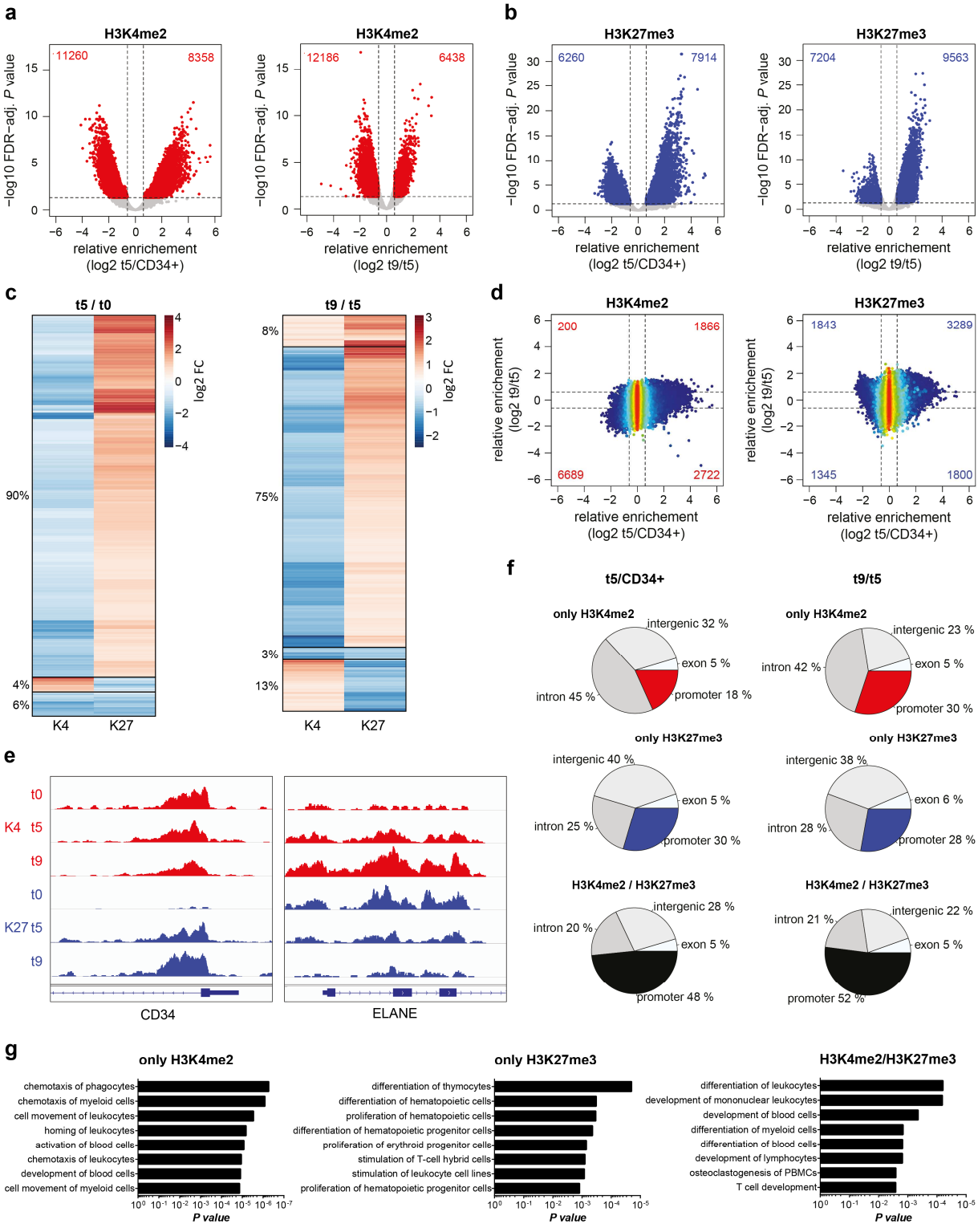

Figure 2: H3K4me2 and H3K27me3 modifications undergo fundamental changes during *in vitro* neutrophilic granulopoiesis. Human CD34+ cord blood cells were differentiated *in vitro* into the neutrophilic lineage for nine days. H3K4me2 and H3K27me3 profiles of CD34+ cells (t0) and neutrophilic progenitors after five (t5) and nine days (t9) were generated by ChIP-sequencing. Replicates (two replicates for t0, five for t5 and three for t9) were statistically analysed comparing

CD34+ and neutrophilic progenitor cells after five days or neutrophilic progenitors after five and nine days. Statistically significant (log2 fold change > ±0.6, FDR-adjusted $P < 0.05$) 500 and 1'000 bp tiles differentially occupied by H3K4me2 and H3K27me3 are highlighted in red and blue, respectively. Relative enrichments of H3K4me2 (a) and H3K27me3 (b) ChIP-seq reads in log2-fold change (FC) on the x-axis are plotted against false discovery rate (FDR)-adjusted *P*-value (likelihood ratio test) on the y-axis. (c) Tiles with significant alterations at both histone modifications. Indicated are the relative enrichments of log2 fold change with positive values in red and negative ones in blue. Tiles with the same epigenetic regulation are grouped and their relative occurrence is indicated. (d) Comparing relative enrichments of H3K4me2 and H3K27me3 ChIP-seq reads in log2-fold change (FC) between CD34+ and neutrophilic progenitor cells after five days (x-axis) and neutrophilic progenitors after five and nine days (y-axis). Number of tiles with significant alterations in both stages are indicated. (e) Profiles of H3K4me2 and H3K27me3 marks at the *ELANE* and *CD34* loci. (f) Relative occurrence of tiles significantly altered in H3K4me2 (red), H3K27me3 (blue) or both (black) epigenetic marks in gene promoters, exon, intron and intergenic regions. (g) Functional analysis of tiles with significant histone alterations by Ingenuity Pathway Analysis. Displayed are the top haematological system development and function features and their probability of overlain calculated by a right-tailed Fisher Exact Test.

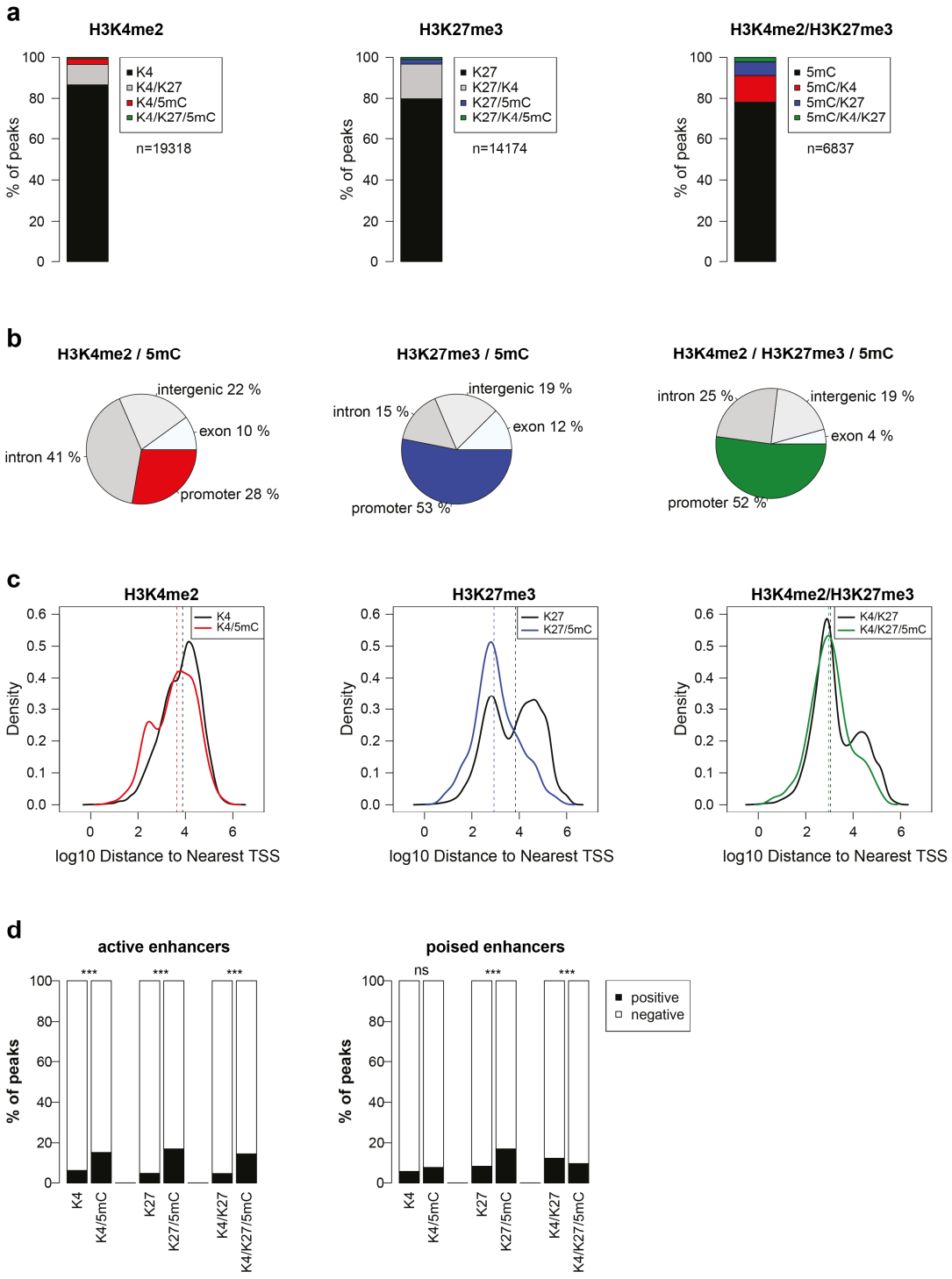

Figure 3: Genomic sites undergoing changes in DNA methylation and histone modifications are enriched for promoters and active enhancers. Intersections between sites with significant (log2 FC > ±0.6, FDR-adjusted *P* < 0.05) alterations in H3K4me2, H3K27me3 and DNA methylation between CD34+ cells and five day progenitors of *in vitro* differentiation were investigated. (a) Relative occurrence of sites significantly changed in H3K4me2, H3K27me3 or DNA methylation with coincident alterations in H3K4me2, H3K27me3 or DNA methylation. (b) Relative occurrence of tiles significantly altered in H3K4me2 (red), H3K27me3 (blue) or both (black) histone modifications in

combination with sites of DNA methylation changes in gene promoters, exon, intron and intergenic regions. (c) Distance to the nearest transcription start site (TSS) of sites significantly altered in histone modifications alone or in combination with DNA methylation. Distance is illustrated as log10 value (bp) on the x-axis and density on the y-axis. Dashed vertical lines illustrate median. (d) Relative occurrence of sites significantly altered in histone modifications alone or in combination with DNA methylation at active and poised enhancers in CD34+ cells (black). Data were statistically analysed by Fisher's exact test (*** $P < 0.001$, * $P < 0.05$).

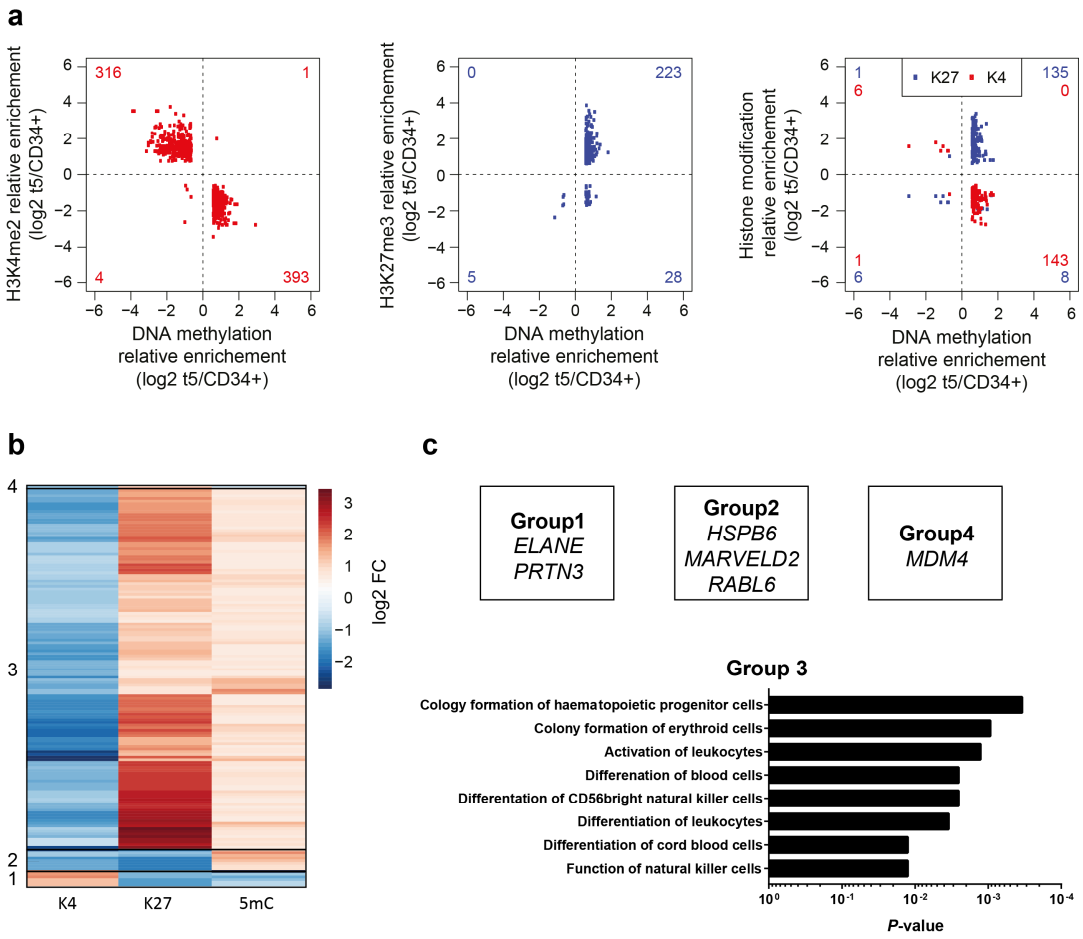

Figure 4: Most sites with coincident changes in histone modifications and DNA methylation change chromatin into a repressed state. Sites significantly altered in histone modifications (H3K4me2, 714 sites [red]; H3K27me3, 256 sites [blue] or in both, 150 sites) and DNA methylation between CD34+ cell and neutrophilic progenitors after five days of differentiation. (a) Relative differences of DNA methylation (x-axis) and histone modifications (y-axis) in log2 fold change. Number of sites with different modifications levels are indicated in red (H3K4me2) and blue (H3K27me3). (b) Comparison of relative enrichments of epigenetic modifications at sites showing level changing in H3K4me2, H3K27me3 and DNA methylation (150 sites) between CD34+ cells and neutrophilic progenitors after 5 days of differentiation. Indicated are log2 fold changes with positive (red) and negative values (blue). Four differently affected groups are indicated. (c) Genes in group 1 (H3K4me2 up, H3K27me3 down, 5mC down), 2 (H3K4me2 down, H3K27me3 down, 5mC up) and 4 (H3K4me2 down, H3K27me3 up, 5mC up) are shown in the upper panel. Genes in group 3 (H3K4me2 down, H3K27me3 up, 5mC up) and their ontology is shown in the lower panel. Indicated are the top haematological system development and function features and their probability of overlain calculated by a right-tailed Fisher Exact Test.

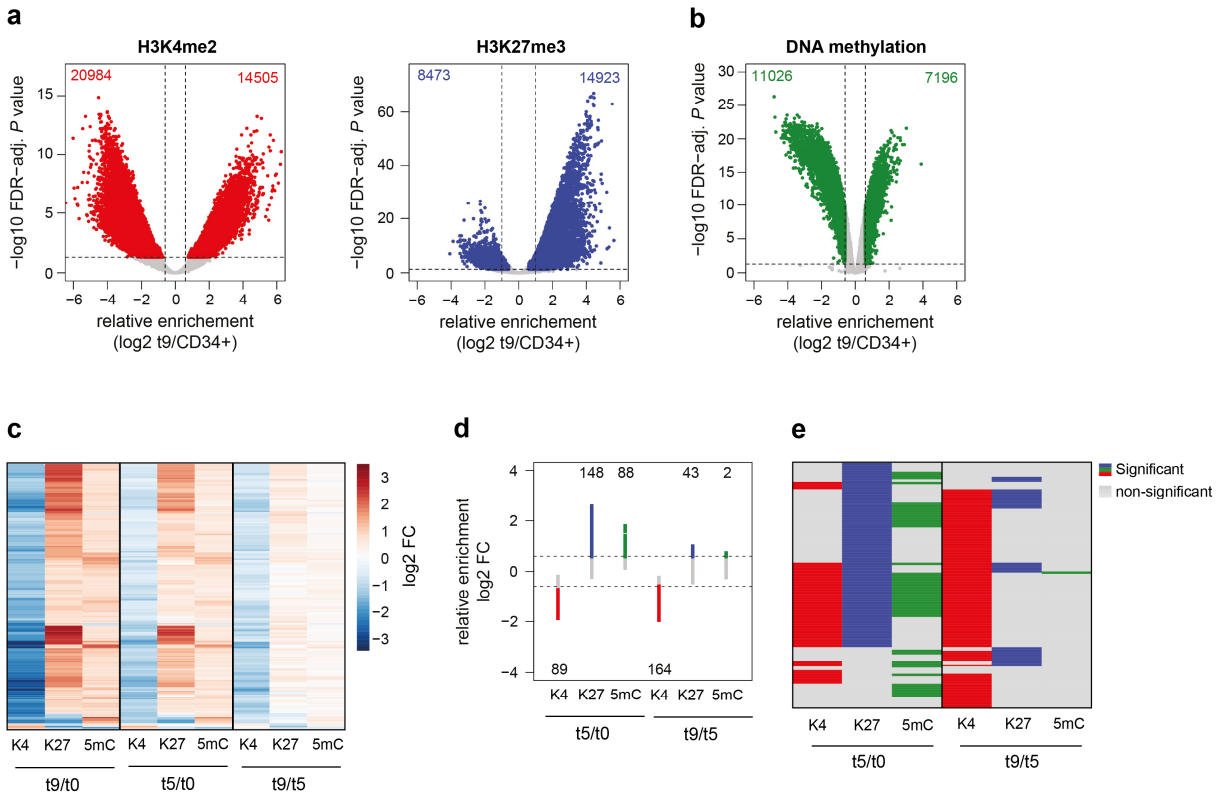

Figure 5: Epigenetic repression occurs through H3K27me3 alone or together with de novo methylation of CpGs. Sites of H3K4me2, H3K27me3 (two replicates for t0, three for t9) and DNA methylation (three replicates for t0, eight for t9) were statistically analysed comparing CD34+ cells and neutrophilic progenitor cells after nine days. (a) ChIP-seq reads within 500 and 1'000 bp genomic tiles in log2-fold change (FC) on the x-axis are plotted against false discovery rate (FDR)-adjusted *P*-value (likelihood ratio test) on the y-axis. Statistically significant (log2 fold change > ±0.6, FDR-adjusted $P < 0.05$) 500 and 1'000 bp tiles differentially occupied by H3K4me2 and H3K27me3 are highlighted in red and blue, respectively. (b) Relative DNA methylation levels in log2-fold change (FC) on the x-axis are plotted against the false discovery rate (FDR)-adjusted *P*-value (moderated *t*-statistic) on the y-axis. CpGs statistically significantly (FDR-adjusted $P < 0.05$) losing (FC < -0.6) and gaining (FC > 0.6) DNA methylation are indicated in green. (c) Sites (212 sites) with a poised chromatin state in CD34+ cells and changing levels of H3K4me2, H3K27me3 and DNA methylation between CD34+ cells and neutrophilic progenitors after nine days. The sites are correlated with the epigenetic changes of the same genomic sites between CD34+ cells and progenitors after five days or progenitors after five and nine days. Indicated are the relative enrichments of log2 fold change with positive values in red and negative ones in blue. (d, e) Sites (197 sites) significantly losing H3K4me2, gaining H3K27me3 modification and DNA methylation in neutrophilic progenitors after nine days compared to CD34+ cells. Shown are the relative enrichments of these sites off all three epigenetic features between progenitors after five days and CD34+ cells or progenitors after nine and five days

(d) and their correlation to each other (e). Significantly altered tiles (log2 fold change > ±0.6, FDR-adjusted $P < 0.05$) are indicated in red (H3K4me2), blue (H3K27me3) and green (DNA methylation), non-significant in grey.

Supplementary Material

Dynamics of Histone Modifications and DNA Methylation during *in vitro* Granulopoiesis

Melissa Manser[1], Mohamad R. Abdul Sater[2,3], Christoph D. Schmid[2,3], Faiza Noreen[1], David Schuermann[1], Primo Schär[1*]

[1] Department of Biomedicine, University of Basel, Mattenstrasse 28, Basel, CH-4058, Switzerland

[2] Swiss Tropical and Public Health Institute, Socinstrasse 57, Basel, CH-4002, Switzerland

[3] University of Basel, Petersplatz 1, Basel, CH-4001, Switzerland

Correspondence and requests for materials should be addressed to P.S. (email: primo.schaer@unibas.ch).

Key words: epigenetics, epigenetic landscape, DNA methylation, histone modification, H3K4me2, H3K27me3, granulopoiesis, differentiation, human haematopoietic progenitor cells

Supplementary Figures

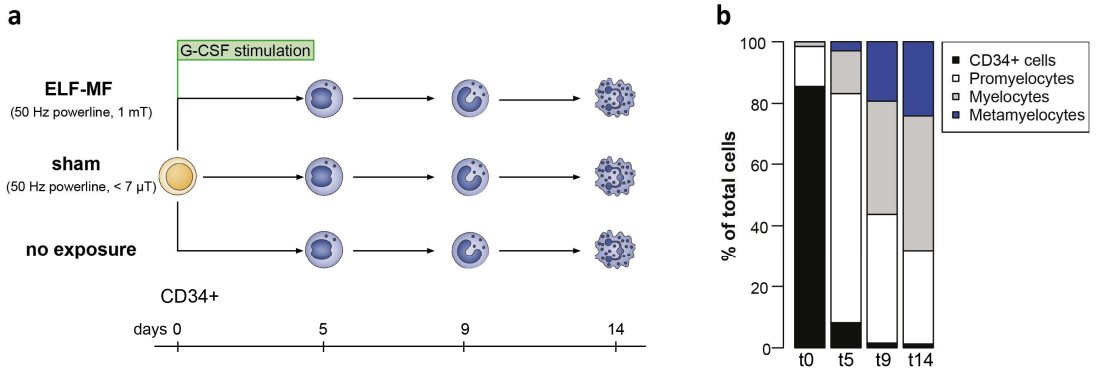

Supplementary Figure S1: *In vitro* neutrophilic differentiation procedure. (a) *In vitro* differentiation of CD34+ human cord blood cells into the neutrophilic lineage for 14 days under ELF-MF exposure and control conditions. After the expansion of CD34+ human cord blood cells for four days, the CD34+ cell population was split into three experimental groups before initiating the *in vitro* differentiation into neutrophilic lineage for 14 days by the addition of G-CSF. ELF-MF (50 Hz powerline, 1 mT, 5' on/10' off) or sham exposure was performed throughout the differentiation. (b) Proportion of alive cells in the population in distinct neutrophilic differentiation stages was analysed at the indicated time-points by flow cytometry, using the stem cell marker CD34 and the two neutrophilic markers CD11b and CD16b. Using the FlowJo software, the expression of these markers was used to discriminate between CD34+ cells (CD34+, CD11b-, CD16b-), promyelocytes (CD34-, CD11b-, CD16b-), myelocytes (CD34-, CD11b+, CD16b-) and metamyelocytes/neutrophils (CD36-, CD11b+, CD16b+). Shown are the means of eight replicates in total (ELF-MF: three, sham: three, no exposure: two).

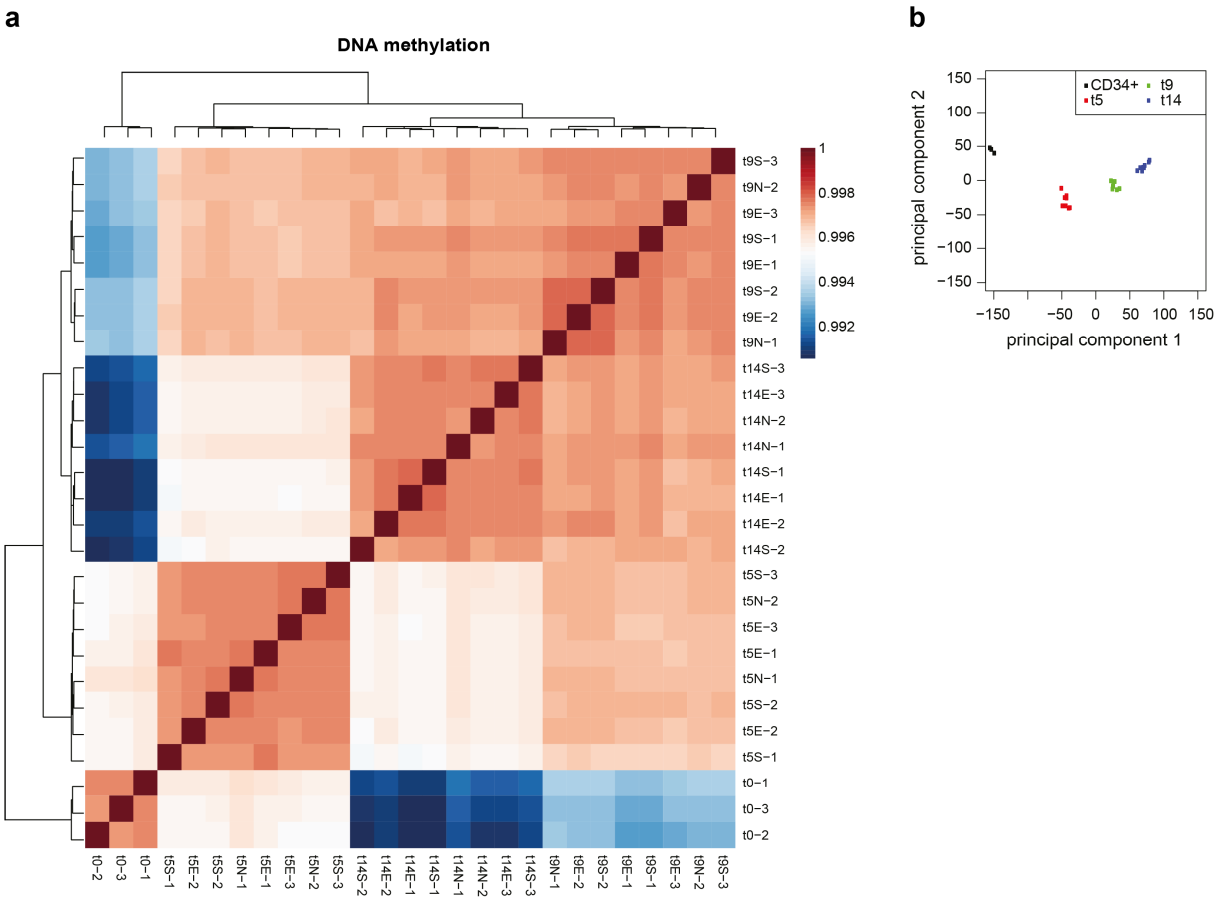

Supplementary Figure S2: Correlation of Cytosine methylation data of neutrophilic granulopoiesis. Global profiles of DNA methylation in CD34+ cord blood cells (t0, three replicates), neutrophilic progenitors after five (eight replicates) and nine days (eight replicates) of differentiation were generated by Illumina Infinium HumanMethylation 450 array. (a) The correlation of DNA methylation levels (β -values) between all replicates and experimental conditions is illustrated by a heatmap with euclidean clustering analysed by RStudio/Bioconductor. (b) Principal component analysis of all samples (M-values) analysed by RStudio/Bioconductor.

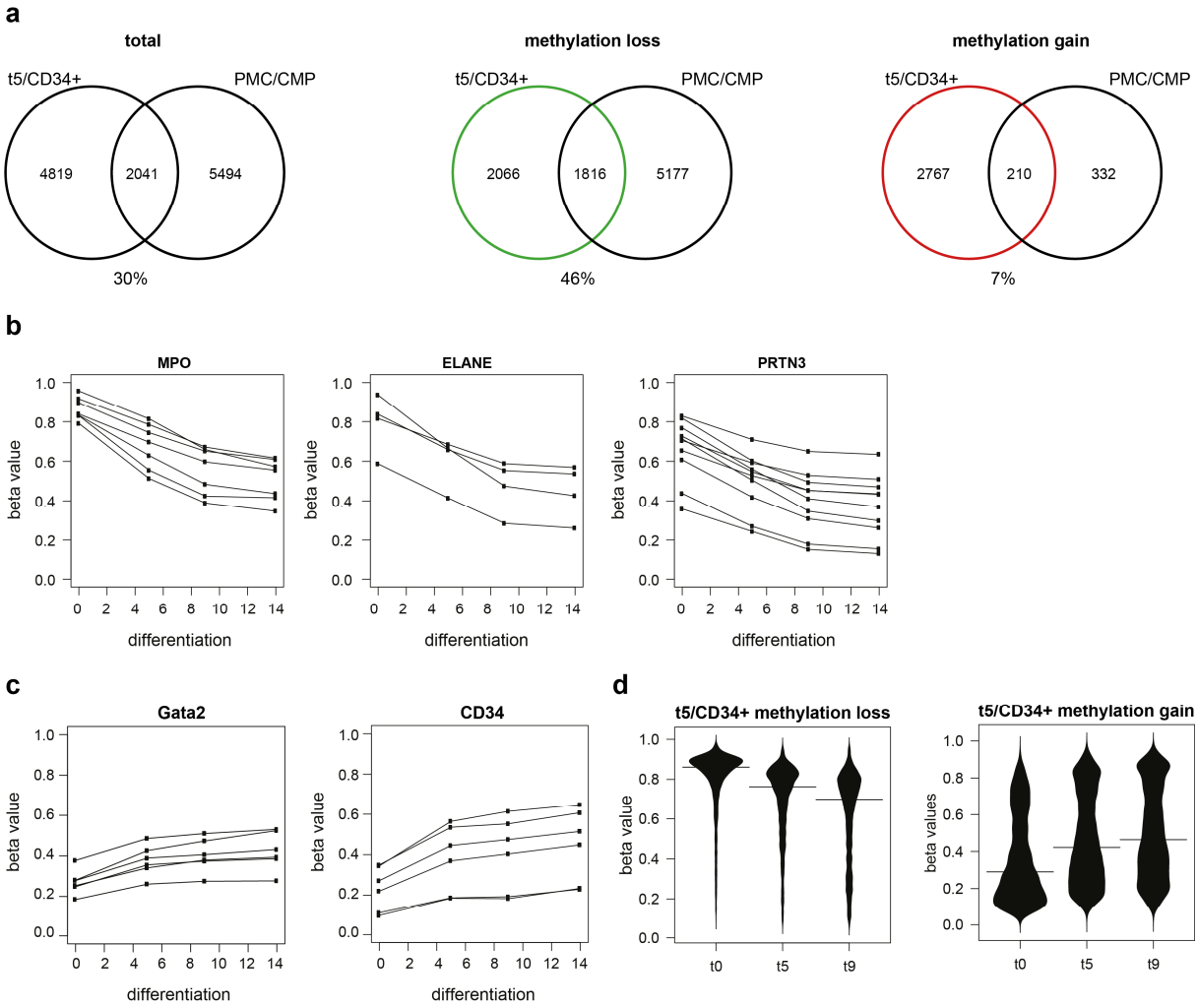

Supplementary Figure S3: Dynamic DNA methylation changes during neutrophilic granulopoiesis. (a) Intersections of differently methylated CpGs (FDR-adjusted $P < 0.05$, log2 FC < -0.6) between neutrophilic progenitors after five days and CD34+ cells with sites of DNA methylation changes between isolated promyelocytes and common myeloid progenitors from Ronnerblad et al. (2014). Indicated are overlays of all CpGs gaining or losing DNA methylation (b, c) DNA methylation changes at CpG sites at the *MPO, ELANE*, *PRTN3, Gata 2* and *CD34* locus. Indicated are the changes in beta-values of all CpGs with significant (FDR-adjusted $P < 0.05$, log2 FC < -0.6) methylation changes identified in each gene. Each dot represents one CpG. (d) Dynamic DNA methylation changes of CpGs with methylation changes in neutrophilic progenitors after five days compared to CD34+ cells. Illustrated are the distributions of the beta-values in CD34+ cells, progenitors after five and nine days of the CpGs. Horizontal line indicates median.

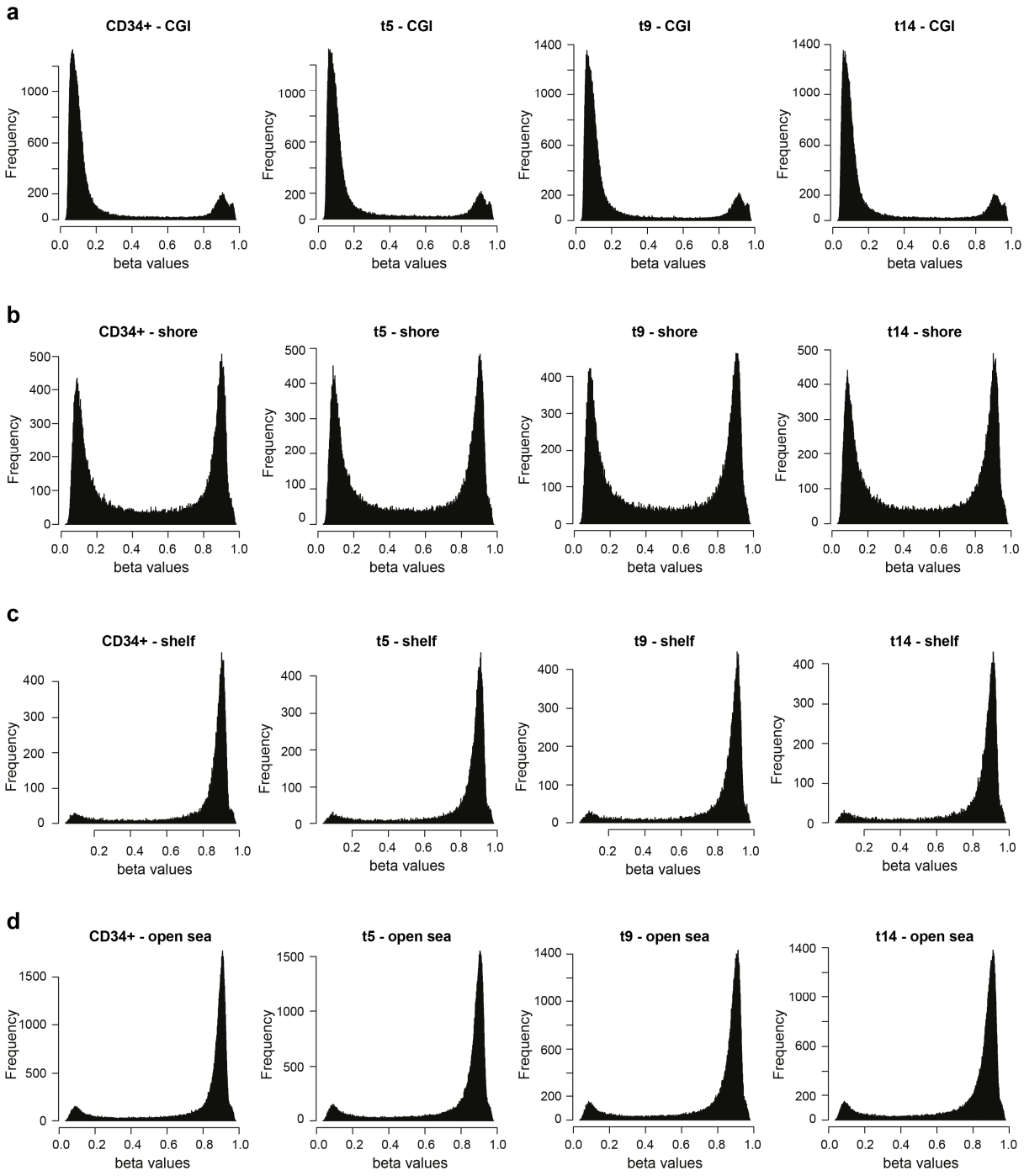

Supplementary Figure S4: Distribution of DNA methylation at CpG islands. Distribution of DNA methylation levels (beta values) at CpG island (CGI, a), CGI shores (0-2 kb away from CGI, b), CGI shelf (2-4 kb away from *CGI*, c) and open sea (d) in CD34+ cells and neutrophilic progenitors after five, nine and 14 days.

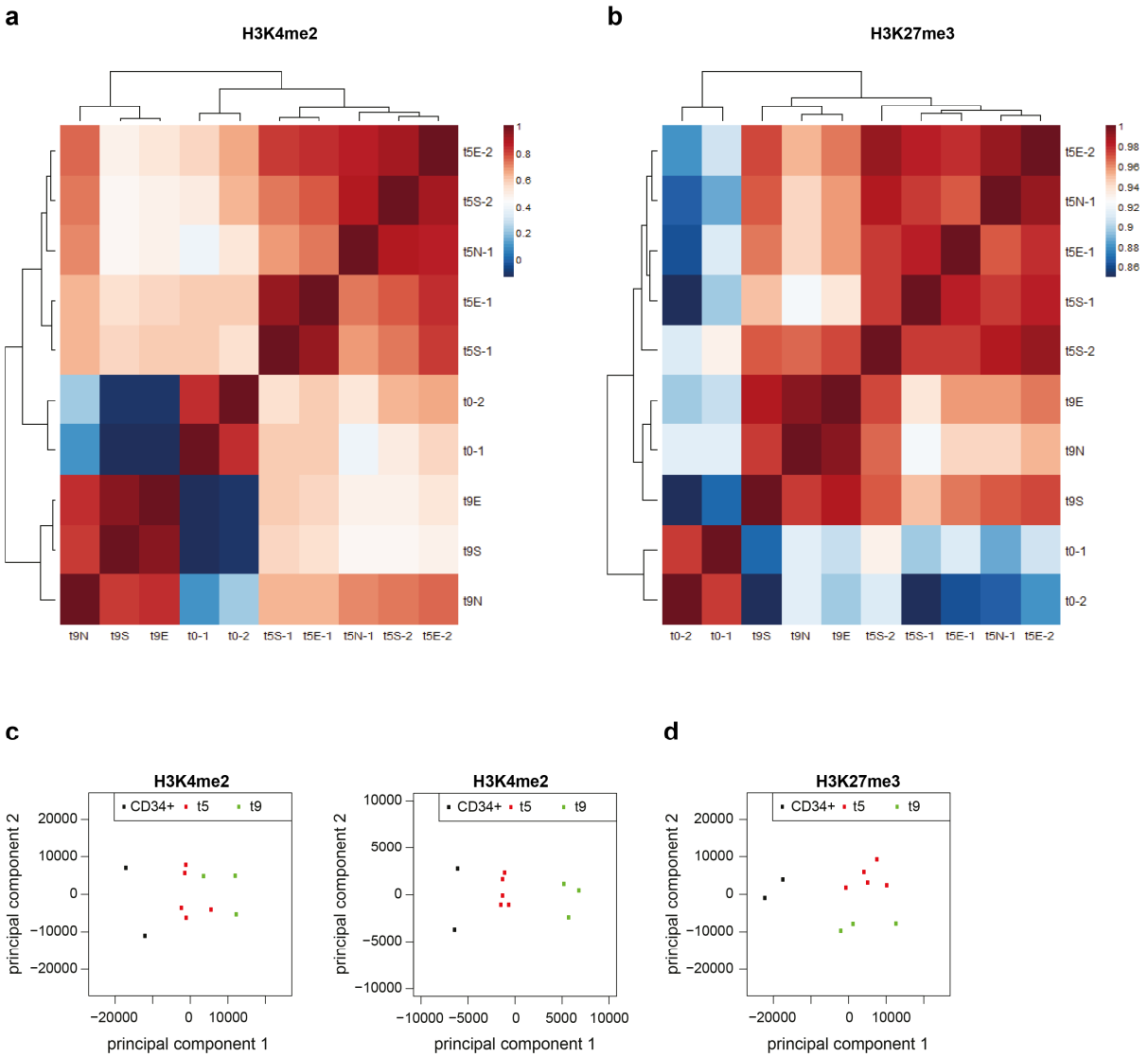

Supplementary Figure S5: Correlation between H3K4me2 or H3K27me3 ChIP samples of neutrophilic granulopoiesis. Global profiles of H3K4me2 and H3K27me3 histone modification of CD34+ cord blood cells (t0, 2 replicates), neutrophilic progenitors after five (t5, five replicates) and nine days (t9, 3 replicates) of differentiation were generated by ChIP-sequencing. Correlation of ChIP-seq reads in 500 bp tiles of all ChIP-seq replicates is illustrated as a heatmap with euclidean clustering. Included are statistically significant (log2 fold change > ±0.6, FDR-adjusted $P < 0.05$) 500 bp tiles differently occupied by H3K4me2 between progenitors after 5 days and CD34+ cells (a) and all observed H3K27me3 tiles (b). (c) Principal component analysis samples of all (left) and significant (t5 compared to t0, log2 fold change > ±0.6, FDR-adjusted $P < 0.05$, right) H3K4me2 ChIP-seq samples. (d) Principal component analysis samples of all H3K27me3 ChIP-seq samples. Data were analysed by RStudio/Bioconductor.

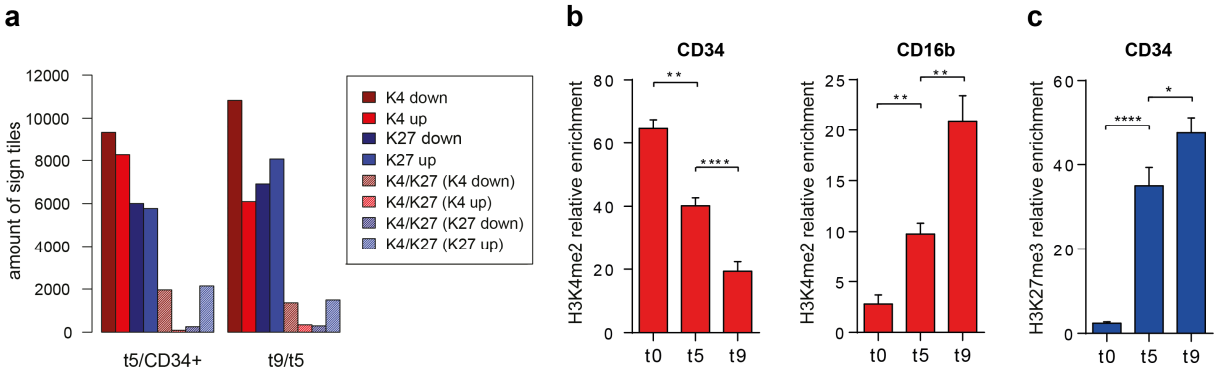

Supplementary Figure S6: Alterations in histone modifications during neutrophilic granulopoiesis. Human CD34+ cord blood cells were differentiated *in vitro* into the neutrophilic progenitor cells for nine days. (a) H3K4me2 and H3K27me3 profiles of CD34+ cells (t0) and neutrophilic progenitors after five (t5) and nine days (t9) were generated by ChIP-sequencing. Statistically significant (log2 fold change > ±0.6, FDR-adjusted $P < 0.05$) 500 and 1'000 bp tiles differentially occupied by H3K4me2 and H3K27me3 were investigated. Number of tiles with significant alteration in H3K4me2 (red) and H3K27me3 (blue) alone or in both histone modifications (colours with white stripes) are indicated with gain (dark red/dark blue) or loss of the epigenetic feature. ChIP-qPCR of H3K4me2 (b) and H3K27me3 (c) modifications in CD34+ cells and neutrophilic progenitors after five and nine days of *in vitro* differentiation for 3 biological replicates. Illustrated are the mean relative enrichment ($input_{target}$ [%]/$input_{control}$ [%]) with standard error. *Prdx3* and *GGA2* were used as normalizer. *P* values are according to unpaired Student's t- test (*** $P < 0.001$, ** $P < 0.01$).

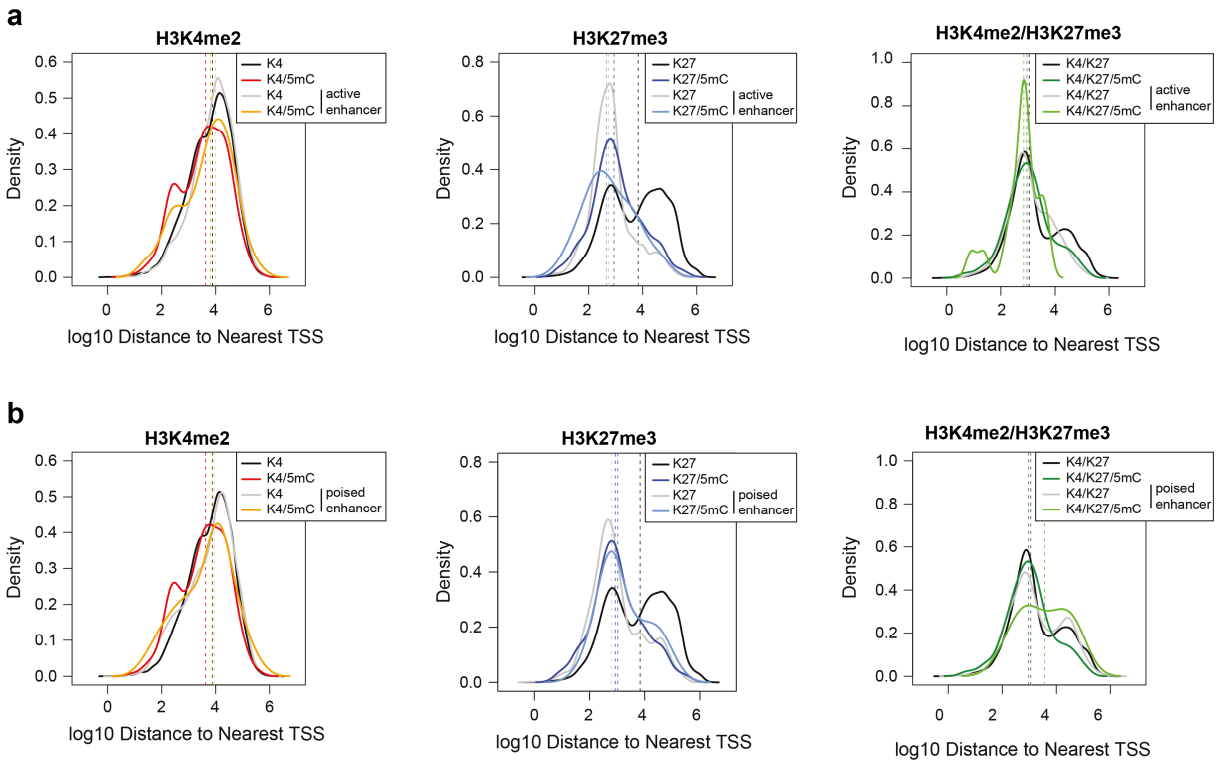

Supplementary Figure S7: Genomic location of enhancers occupied by epigenetic changes. Distance to the nearest transcription start site (TSS) of sites significantly changing histone modifications level alone or in combination with DNA methylation and located at active (a) or poised (b) enhancers in CD34+ cells or not. Distance is illustrated as log10 value (bp) on the x-axis and density on the y-axis. Dashed vertical lines illustrate median.

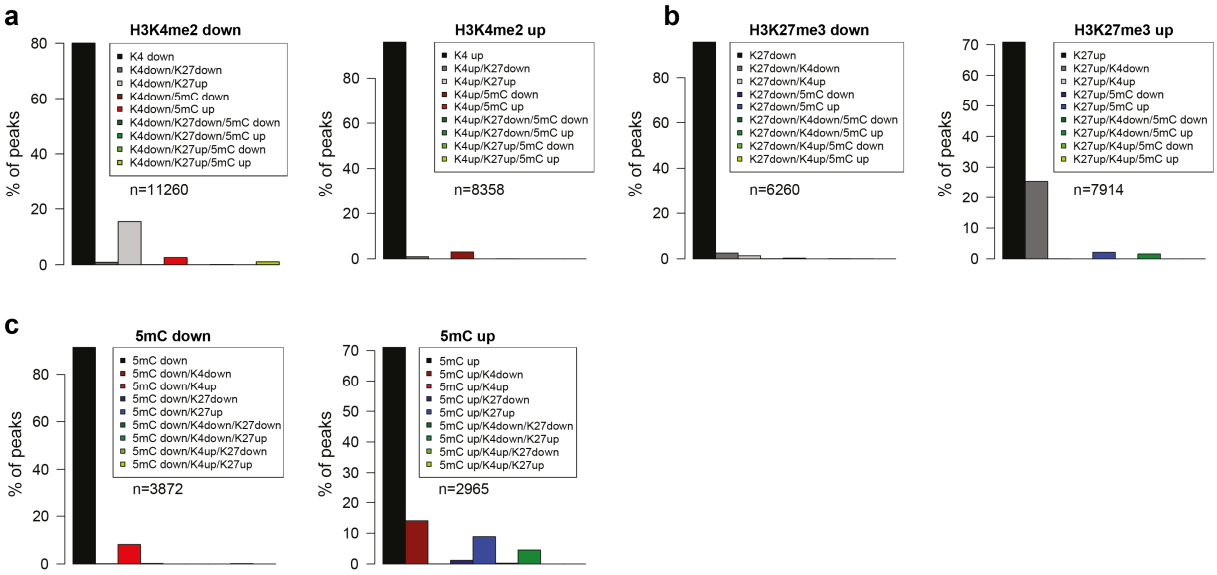

Supplementary Figure S8: Correlation of H3K4me2, H3K27me3 and DNA methylation changes. Intersections between sites with significant (log2 FC > ±0.6, FDR-adjusted *P* < 0.05) alterations in H3K4me2, H3K27me3 and DNA methylation levels between CD34+ cells and neutrophilic progenitors after five days of *in vitro* differentiation were investigated. Relative occurrence of sites significantly increased or decreased in H3K4me2 (a), H3K27me3 b) or DNA methylation (c) with coincident alterations in H3K4me2, H3K27me3 or DNA methylation.

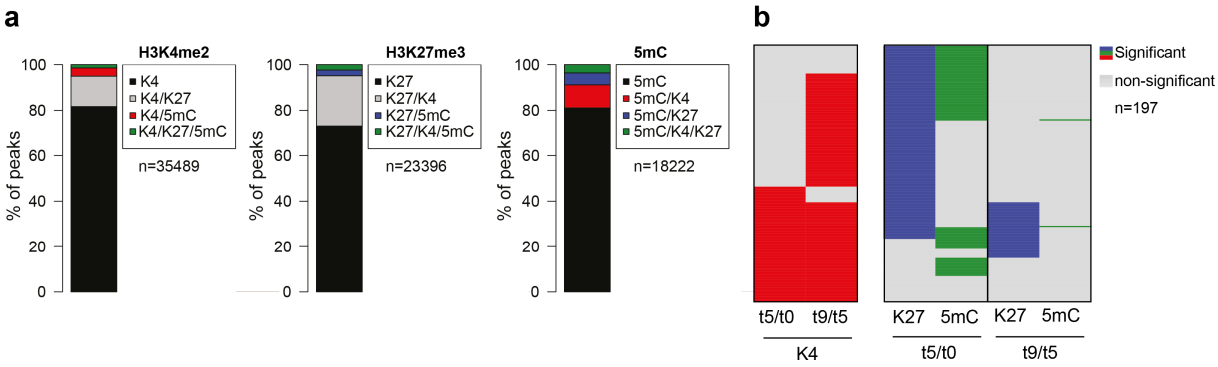

Supplementary Figure S9: Dynamics of epigenetic changes during neutrophilic granulopoiesis. Intersections between sites with significant (log2 FC > ±0.6, FDR-adjusted *P* < 0.05) alterations in H3K4me2, H3K27me3 as well as DNA methylation between CD34+ cells and neutrophilic progenitors after nine days of *in vitro* differentiation were investigated. (a) Relative occurrence of sites significantly changed in H3K4me2, H3K27me3 or DNA methylation with coincident alterations in H3K4me2, H3K27me3 or DNA methylation. (b) Sites (197) significantly losing H3K4me2, gaining H3K27me3 as well as DNA methylation in neutrophilic progenitors after nine days compared to CD34+ cells. Indicated are the relative enrichments off all three epigenetic features at these sites between progenitors after five days and CD34+ cells or progenitors after nine and five days. Clustered are the H3K4me2 or the H3K27me3 and DNA methylation changes. Significantly altered tiles (log2 fold change > ±0.6, FDR-adjusted *P* < 0.05) are indicated in red (H3K4me2), blue (H3K27me3) and green (DNA methylation), non-significant in grey.

Supplementary Tables

Supplementary Table 1: Genes occupied by group 3 epigenetic alterations in neutrophilic progenitor cells after five days of differentiation compared to CD34+ cells.

Genes occupied by H3K4me2 down / H3K27me3 up / 5mC up (group 3*)*				
ATP10A	*GAL3ST3*	*HOXB-AS3*	*PRKCH*	*TCAF1*
C7orf50	*GATA2*	*IFT140*	*PTRF*	*THRB-AS1*
CARD11	*GNG4*	*KCNJ12*	*RAI1*	*TMEM204*
CASC15	*HLCS*	*KIAA1217*	*REC8*	*TMEM25*
CD7	*HOXA10*	*LTBP3*	*ROBO3*	*WT1*
CLDN5	*HOXA10-AS*	*MDK*	*SCN1B*	*ZNF503-AS2*
DPF1	*HOXA10-HOXA9*	*MECOM*	*SDR42E1*	*ZNF662*
DPF1	*HOXA-AS3*	*MEIS1*	*SKIDA1*	*ZNRF3*
EGFL7	*HOXB3*	*MIB2*	*SOCS2*	*ZNRF3-AS1*
ESAM	*HOXB5*	*MOB2*	*ST3GAL4*	
EXD3	*HOXB6*	*NKX2-3*	*STIL*	
F2RL1	*HOXB-AS1*	*PLXNB2*	*TAL1*	

Supplementary Table 2: Primer used for ChIP-qPCR

Name	**Orientation**	**Sequence (5' – 3')**	**Length**
Prdx3_3'end_qPCR	Forward	CTAGCCAGCCACCAAGATGT	20
Prdx3_3'end_qPCR	Reverse	CCCATGTGTATCTGCACCTTC	21
GGA2_3'end_qPCR	Forward	CCTGGTCTTGGCAGATGATA	20
GGA2_3'end_qPCR	Reverse	ATGCCTCTGTCCCAATTCTG	20
pCD34_qPCR	Forward	GGTACTCACGCAGCAAACTC	20
pCD34_qPCR	Reverse	TCCTGGCCAAGCCGAGTA	18
pCD16b_qPCR	Forward	CCATCCCTTTGTGGGAGTCT	20
pCD16b_qPCR	Reverse	ACTCCAGTGTGGCATCATGT	20

Extremely low-frequency magnetic fields and the risk of childhood leukemia: a risk assessment by the ARIMMORA consortium

Joachim Schüz[1], Clemens Dasenbrock[2], Paolo Ravazzani[3], Martin Röösli[4], Primo Schär[5], Patricia L. Bounds[6], Friederike Erdmann[1], Arndt Borkhardt[7], César Cobaleda[8], Maren Fedrowitz[9], Yngve Hamnerius[10], Isidro Sanchez-Garcia[11], Rony Seger[12], Kjeld Schmiegelow[13], Gunde Ziegelberger[14], Myles Capstick[6], Melissa Manser[5], Meike Müller[2], Christoph D. Schmid[4], David Schürmann[5], Benjamin Struchen[4], Niels Kuster[6].

[1]International Agency for Research on Cancer (IARC), Section of Environment and Radiation, Lyon, France

[2]Fraunhofer ITEM, Hannover, Germany

[3]National Research Council of Italy, Institute of Electronics, Computer and Telecommunication Engineering, Milan, Italy

[4]University of Basel and Swiss Tropical and Public Health Institute, Basel, Switzerland

[5]Department of Biomedicine, University of Basel, Switzerland

[6]IT'IS: Foundation for Research on Information Technologies in Society, Zürich, Switzerland

[7]Department of Pediatric Oncology, Haematology and Clincial Immunology, Heinrich-Heine University, Düsseldorf, Germany

[8]Spanish National Research Council (CSIC), Centro de Biología Molecular Severo Ochoa, Madrid

[9]University of Veterinary Medicine, Hanover, Germany

[10]Chalmers University of Technology, Gothenburg, Sweden

[11]CSIC, Instituto de Biologia Molecular y Celular del Cancer, Salamanca, Spain

[12]Weizmann Institute of Science, Rehovat, Israel

[13]University Hospital, Copenhagen, Denmark

[14]German Federal Office for Radiation Protection, Neuherberg, Germany

Corresponding author

Joachim Schüz, Section of Environment and Radiation, International Agency for Research on Cancer (IARC), 150 cours Albert Thomas, F-69372 Lyon (e-mail: schuzj@iarc.fr)

Contribution: I planned and performed the *in vitro* exposure experiments in leukaemic cells as well as during a haematopoietic differentiation, determined histone modifications (H3K4me2 and H3K27me3) by ChIP, prepared the ChIP samples for next-generation sequencing and contributed to the bioinformatic analysis of the ChIP-seq data. Furthermore, attended at the ARIMMORA risk assessment meeting and was involved in the writing of the risk assessment.

Bioelectromagnetics

Comment

Extremely Low-Frequency Magnetic Fields and Risk of Childhood Leukemia: A Risk Assessment by the ARIMMORA Consortium

Joachim Schüz,[1]* Clemens Dasenbrock,[2] Paolo Ravazzani,[3] Martin Röösli,[4] Primo Schär,[5] Patricia L. Bounds,[6] Friederike Erdmann,[1] Arndt Borkhardt,[7] César Cobaleda,[8] Maren Fedrowitz,[9] Yngve Hamnerius,[10] Isidro Sanchez-Garcia,[11] Rony Seger,[12] Kjeld Schmiegelow,[13] Gunde Ziegelberger,[14] Myles Capstick,[6] Melissa Manser,[5] Meike Müller,[2] Christoph D. Schmid,[4] David Schürmann,[5] Benjamin Struchen,[4] and Niels Kuster[6]

[1]Section of Environment and Radiation, International Agency for Research on Cancer (IARC), Lyon, France
[2]Fraunhofer ITEM, Hanover, Germany
[3]National Research Council of Italy, Institute of Electronics, Computer and Telecommunication Engineering, Milan, Italy
[4]University of Basel and Swiss Tropical and Public Health Institute, Basel, Switzerland
[5]Department of Biomedicine, University of Basel, Basel, Switzerland
[6]ITIS: Foundation for Research on Information Technologies in Society, Zürich, Switzerland
[7]Medical Faculty, Department of Pediatric Oncology, Haematology and Clinical Immunology, Heinrich-Heine University, Düsseldorf, Germany
[8]Spanish National Research Council (CSIC), Centro de Biología Molecular Severo Ochoa, Madrid, Spain
[9]University of Veterinary Medicine, Hanover, Germany
[10]Chalmers University of Technology, Gothenburg, Sweden
[11]Spanish National Research Council (CSIC), Instituto de Biologia Molecular y Celular del Cancer, Salamanca, Spain
[12]Weizmann Institute of Science, Rehovat, Israel
[13]University Hospital, Copenhagen, Denmark
[14]German Federal Office for Radiation Protection, Neuherberg, Germany

Exposure to extremely low-frequency magnetic fields (ELF-MF) was evaluated in an International Agency for Research on Cancer (IARC) Monographs as "possibly carcinogenic to humans" in 2001, based on increased childhood leukemia risk observed in epidemiological studies. We conducted a hazard assessment using available scientific evidence published before March 2015, with inclusion of new research findings from the Advanced Research on Interaction Mechanisms of electroMagnetic exposures with Organisms for Risk Assessment (ARIMMORA) project. The

Grant sponsor: European Commission; grant number: 282891.

Conflicts of interest: Prof. Kuster and Dr. Capstick report ownership of public utility company shares. Dr. Capstick also declares that he consults on research questions with SPEAG. Prof. Hamnerius declares that he consults privately on problems concerning electromagnetic fields, such as measurements and calculations.

*Correspondence to: Joachim Schüz, Section of Environment and Radiation, International Agency for Research on Cancer (IARC), 150 Cours Albert Thomas, F-69372 Lyon, France. E-mail: schuzj@iarc.fr

Received for review 21 December 2015; Accepted 19 February 2016

DOI: 10.1002/bem.21963
Published online XX Month Year in Wiley Online Library (wileyonlinelibrary.com).

IARC Monograph evaluation scheme was applied to hazard identification. In ARIMMORA for the first time, a transgenic mouse model was used to mimic the most common childhood leukemia: new pathogenic mechanisms were indicated, but more data are needed to draw definitive conclusions. Although experiments in different animal strains showed exposure-related decreases of CD8+ T-cells, a role in carcinogenesis must be further established. No direct damage of DNA by exposure was observed. Overall in the literature, there is limited evidence of carcinogenicity in humans and inadequate evidence of carcinogenicity in experimental animals, with only weak supporting evidence from mechanistic studies. New exposure data from ARIMMORA confirmed that if the association is nevertheless causal, up to 2% of childhood leukemias in Europe, as previously estimated, may be attributable to ELF-MF. In summary, ARIMMORA concludes that the relationship between ELF-MF and childhood leukemia remains consistent with possible carcinogenicity in humans. While this scientific uncertainty is dissatisfactory for science and public health, new mechanistic insight from ARIMMORA experiments points to future research that could provide a step-change in future assessments. Bioelectromagnetics.

Key words: risk assessment; hazard identification; electromagnetic fields; adverse effects; children; leukemia

INTRODUCTION

Exposure to extremely low-frequency magnetic fields (ELF-MF), related to power transmission and electrical appliance use, was judged in 2001 by the International Agency for Research on Cancer (IARC) Monograph program on the evaluation of carcinogenic risks to humans [Cogliano et al., 2011] as possibly carcinogenic to humans (Group 2B), based on limited scientific evidence for childhood leukemia [IARC, 2002]. For other cancers in children or cancers in adults (including leukemia), evidence was judged inadequate [IARC, 2002]. No re-evaluation has been performed by the IARC since then, but other assessments have referred to it when updating literature reviews, notably those by the World Health Organization (WHO) in its Environmental Health Criteria series [WHO, 2007] and the European Commission's (EC) Scientific Committee on Emerging and Newly Identified Health Risks (SCENIHR) [2007, 2009, 2015]. All of those systematic assessments were in agreement with the previous IARC classification of possible carcinogenicity for childhood leukemia and inadequate evidence for other cancers. In particular, all assessments commonly pointed to lack of convincing mechanistic data and lack of appropriate animal models when addressing childhood leukemia [SCENIHR, 2007, 2009, 2015; WHO, 2007]. To overcome these limitations, the European Commission-funded project "Advanced Research on Interaction Mechanisms of electroMagnetic exposures with Organisms for Risk Assessment" (ARIMMORA), which started on October 1, 2011, embarked on a series of experiments. These were targeted to find possible pathways to explain the association between ELF-MF and childhood leukemia, given that in more than 20 epidemiological studies, such an association had been observed with relatively high consistency [Schüz, 2011].

To conclude the ARIMMORA project, a risk assessment was conducted on the basis of available scientific evidence published before March 9, 2015 and including new results from ARIMMORA experiments. This risk assessment included, first, a hazard identification informed by the IARC Monograph program evaluation scheme on the level of evidence regarding carcinogenicity to humans and, second, an estimation of how many diagnoses of leukemia in children would be attributable to the agent, assuming causality. This is a summary of the ARIMMORA [2015] risk assessment.

METHODS

Importantly, this hazard identification was not an evaluation within the IARC Monograph program, but the IARC evaluation scheme (Fig. 1) was strictly followed, as the scientific community would be familiar with the interpretation of the outcome [IARC, 2002; Cogliano et al., 2011]. According to the IARC, in a first step two distinct types of evidence, namely cancer in humans (epidemiology) and cancer in experimental animals (in vivo studies), are evaluated separately as to whether there is sufficient evidence of, limited evidence of, or inadequate evidence of carcinogenicity, or evidence suggesting lack of carcinogenicity. Mechanistic and other relevant data are classified into weak, moderate, or strong, if appropriate, and address whether the mechanism is likely to be operative in humans. From the combination of these three lines of evidence, the agent is classified into Group 1 (carcinogenic to humans), Group 2A (probably carcinogenic to humans), 2B (possibly carcinogenic to humans), Group 3 (not classifiable as to its carcinogenicity to humans), or Group 4 (probably not carcinogenic to humans), as outlined in the

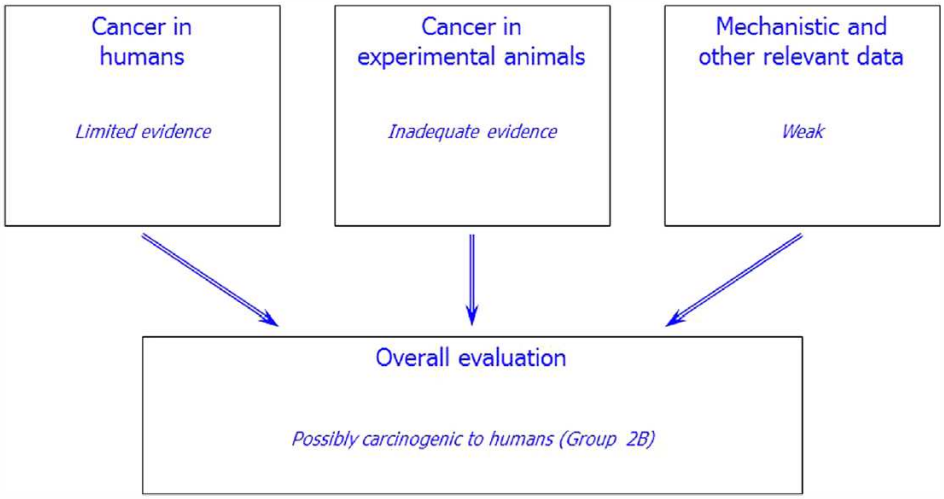

Fig. 1. ARIMMORA's evaluation of association between extremely low-frequency magnetic fields and risk of childhood leukemia according to the classification scheme of carcinogenicity from the IARC Monograph program on the evaluation of carcinogenic risks to humans.

preamble of the IARC Monographs program [2015]. In addition, and as in the IARC Monographs, human exposure data was reviewed.

The evidence base for the ARIMMORA risk assessment consisted of three sources. First, the SCENIHR [2015] update of their systematic literature review with collected evidence up to July 2014 was used to not duplicate other work commissioned by the EC; however, disagreements with this evaluation in terms of individual studies or conclusions would be noted [ARIMMORA, 2015]. Second, a review of individual studies published between July 2014 and March 9, 2015 was performed. Third, a review of outcomes from the ARIMMORA experiments, irrespective of whether they were accepted for publication at time of the risk assessment was performed [ARIMMORA, 2015].

RESULTS

Exposure

Measured typical daily mean personal exposure of children in Europe is below 0.1 μT, while only a small proportion (1–2% of children) are exposed to ELF-MF daily means >0.3 μT, corresponding to >60 μV/m induced fields. An association between ELF-MF and childhood leukemia risk has been observed mainly at daily mean levels >0.3 μT [Schüz, 2011]. New measurements of ELF-MF exposure of children in Italy and Switzerland within ARIMMORA confirmed those typical exposure levels of earlier studies, but highlighted the importance of child's behavior as a modifier of daily mean exposure levels, particularly for children living close to power lines [Struchen et al., 2015]. Nevertheless, measurements show good agreement between daily mean exposure levels from the child's bedroom and personal measurements, confirming that stationary bedroom measurements in epidemiological studies are good proxies of personal exposure.

Within ARIMMORA, measurements of household near-field sources showed that fields decay steeply with distance dropping to common household background levels <0.1 μT within centimeters to normally much less than a meter; most sources are used normally either relatively far from children or for only short periods of time, for example, fans and vacuum cleaners, and tend to act locally on the body in contrast to large sources such as power lines. The frequencies of fields emitted by devices with "universal" power supplies are intermediate frequency (IF) and not in ELF range, but whether IF exposure is relevant to leukemogenesis is unknown. Harmonic components of 50 Hz ELF-MF contribute somewhat to overall exposure, but although these contributions cannot be neglected, amplitudes are low, even in the worst-case scenarios. Measurement of ELF-MF at 50/60 Hz in bedrooms, as done in epidemiological studies, therefore appears to be an appropriate approach.

In addition, the ARIMMORA findings fill some gaps of knowledge about exposure assessment of pregnant women by means of a computational approach. For fetal ELF-MF exposure, the most exposed tissues in terms of maximum electric field have been found to be skin, fat, and subcutaneous adipose tissue across all gestational ages; and, in all tissues, induced electric field exposure increases with increase in gestational

age [Liorni et al., 2014]. Harmonic components also add some contributions to the overall level of electric fields induced in fetuses, but again are low, even in worst-case scenarios [Fiocchi et al., 2015].

Epidemiology

A positive association between residential exposure to ELF-MF and childhood leukemia has been observed in several epidemiological studies in various settings at different points in time. Combining those studies in pooled analysis showed relative risks of 1.5–2 at daily mean exposure levels exceeding 0.3/0.4 μT [Ahlbom et al., 2000; Kheifets et al., 2010; Schüz, 2011]. Despite data from more than 20 studies, there were small numbers of highly exposed children, hence, some uncertainty in risk estimates remained and precision to explore exposure-response relationships was limited. As an alternative to causal interpretation of epidemiological findings, methodological shortcomings such as information bias, selection bias, confounding, and publication bias are of concern, although no strong support for such alternative explanations had been obtained from either validation or simulation studies [IARC, 2002; Schüz, 2011; SCENIHR, 2015]. Results from more recent studies were broadly comparable with those from earlier studies [Ahlbom et al., 2000; Kheifets et al., 2010], but similar case-control designs and methods of exposure assessment were used, and it is therefore unclear whether consistency points to a consistent association or consistent underlying biases. Among the recent studies, one notable large register-based study from the United Kingdom indicates that observed association is present only in cases occurring before 1990 [Bunch et al., 2014] and suggests that factors other than ELF-MF may play a role.

While no epidemiological study was conducted within ARIMMORA, epidemiology played an influential role in hazard identification and risk assessment. It was consistency of epidemiological findings supporting evaluation of possible carcinogenicity in various previous hazard identification and risk assessments [IARC, 2002; SCENIHR, 2007, 2009, 2015; WHO, 2007]. However, doubts about methodological limitations remain, and bias and confounding cannot be ruled out with reasonable confidence. Therefore, the evaluation of the evidence was considered "limited" by the ARIMMORA consortium.

Experimental Animals

In the previous hazard identification and risk assessments by the IARC, the WHO, and the SCENIHR, evidence from studies in experimental animals was considered inadequate [IARC, 2002; SCENIHR, 2007, 2009, 2015; WHO 2007]. A major limitation was, however, that no human-based leukemia predisposed animal model was used.

One goal of ARIMMORA was therefore to study the possible role of ELF-MF in a transgenic mouse model in which the first genetic lesion associated with childhood precursor-B acute lymphoblastic leukemia (pB-ALL), namely *ETV6-RUNX1*, was constitutively expressed in the hematopoietic stem/progenitors compartment with potential to mimic initiation of human pB-ALL [Wiemels et al., 1999; ARIMMORA, 2015; Martín-Lorenzo et al., 2015]. Initially, 34 mice were exposed to 1.5 mT ELF-MF, while 27 were unexposed and monitored for a maximum of 24 months. Four exposed and two unexposed were found dead during the course of the experiment, but cause of death could not be determined. Excluding these dead animals at month 22, of a total of 30 exposed mice, one developed ETV6-RUNX1-positive pB-ALL at 14 months of age, while none of 25 non-exposed animals plus an independent cohort of 40 animals developed pB-ALL. It should be noted that this first experiment in which this transgenic mouse model was used was set up without any prior knowledge of frequency of leukemia development in mice and therefore provides data on the baseline leukemia rate in unexposed mice, to allow more informed statistical power calculations in future experiments.

The main outcome of animal studies within ARIMMORA is therefore that a new pB-ALL mouse model was successfully established and utilized for ELF-MF exposure studies. More data are required, as in this first experiment only one exposed mouse and no unexposed mice developed leukemia. Overall, from totality of the literature and new ARIMMORA results, evidence of carcinogenicity in experimental animals is considered "inadequate."

Mechanistic Data

Previous hazard identification and risk assessments describe lack of support from mechanistic data as a major weakness in causal interpretation of epidemiological findings that suggest an association between ELF-MF and childhood leukemia [IARC, 2002; SCENIHR, 2007, 2009, 2015; WHO 2007; Schmiedel and Blettner, 2010]. Without identification of relevant mechanisms of action, it is impossible to integrate all reported positive and negative experimental outcomes into a consistent picture [Santini et al., 2009]. Nevertheless, the body of evidence that ELF-MF can modulate cellular responses to chemical or physical agents is steadily increasing and, in some areas, gaining robustness, although underlying mechanisms, which are likely to be diverse and

complex, remain to be clarified [ARIMMORA, 2015]. These findings indicate that multiple cellular processes that depend on interactions of distinct molecular pathways may be affected in a similar fashion. In respect to neoplastic diseases, use of stem cells for mechanistic studies should provide better relevance for risk assessment, as non-terminally differentiated cells that escape control mechanisms are believed to be central to carcinogenesis. So far, studies in which stem cells were used are rather sparse [SCENIHR, 2015].

As one ARIMMORA goal on mechanisms, the impact of ELF-MF exposure on the immune system was analyzed for changes in hematopoiesis and gene expression profiles as well as for genotoxic and epigenetic effects [ARIMMORA, 2015]. Female CD-1 mice were exposed to 50 Hz ELF-MF at 10 μT, 1 mT, and 10 mT (controls were sham exposed), starting with pregnant dams and continuing to female offspring up to 90 days of age. Most importantly, on day 28 diminished numbers of CD8+ cytotoxic T-lymphocytes were seen in peripheral blood in all ELF-MF groups. Although the effect was moderate, it is statistically significant; however, the effect did not become stronger with increasing exposure level and was not observed after 60 and 90 days. Furthermore, number of B-lymphocytes was significantly increased in blood after 60 days of 1 mT and 10 mT exposure, and number of monocytes was diminished at exposure to 10 mT. Finally, no significant induction of micronuclei in peripheral blood erythrocyte fraction was observed, which would indicate profound and direct DNA-damaging potential of ELF-MF exposure.

Analysis of peripheral blood of ELF-MF-exposed transgenic mice from the experiment described above (see "Experimental Animals") showed a small, but statistically significant decrease in numbers of CD8+ T-cells in exposed mice at 2 months of age. There were no significant changes in populations of myeloid cells.

As another ARIMMORA goal on mechanisms, two well-known inbred rat strains, Lewis and Fischer 344 (F344), which are genetically related to the same background strain but differ in terms of sensitivity to stress, carcinogens, and ELF-MF exposure, were used to determine effects of in vivo ELF-MF exposure in blood, spleen, and bone marrow. Cell proliferation and apoptosis, cell cycle, cytokine secretion, and possible ELF-MF targets, expression and functionality of adrenergic receptor were investigated in animals exposed at 50 Hz 0.1 mT magnetic fields [ARIMMORA, 2015]. Effects of ELF-MF exposure on hematopoietic cell signaling were observed, and these confirmed differences between the two rat strains and sex. ELF-MF affected cellular regulation with distinct functional consequences. Apoptotic cascade and expression of cytokines related to cell death and cellular activation were altered in a strain- and sex-dependent manner and corresponded to alterations in peripheral blood and affected proliferative capacities after mitogen stimulation. Independent of rat strain and sex, the majority of cytokines altered by ELF-MF exposure impacted number of T-cells or were involved in T-cell functions.

In in vitro studies within ARIMMORA [2015], key regulatory mechanisms of carcinogenesis, namely signaling processes and epigenetic regulation were addressed. Pertinent findings indicated that ERK1/2 activation increases in response to ELF-MF in most cell lines tested. Notably, effects were detectable within minutes of exposure to low μT fields, comparable to residential levels. Additional data indicated possible involvement of the photoreceptor cryptochrome in the mechanism of ELF-MF perception. However, these effects were cell-line dependent, and signaling response level may not be sufficient to play a role in carcinogenesis.

Cell identity and fate is defined by the epigenetic landscape. As cells change their phenotype during carcinogenesis, the pattern of the chromatin modifications are dramatically altered. These aberrations are therefore a hallmark of cancer but may also be a driving force for carcinogenesis [Morgan and Shilatifard, 2015].

Examination of activating and inactivating histone modifications in exposed and sham exposed leukemic Jurkat cells at 50 Hz 1 mT did not reveal evidence for a significant disturbance of global epigenetic patterns but yielded some candidate regions for future investigation. Also, no effect on cell proliferation or induction of cell death was detected. Exposure of differentiating human hematopoietic stem cells revealed minor changes in apoptosis and cell cycle progression but not in lineage commitment. Activating and inactivating histone modifications were affected at a small number of loci in a differentiation-stage-dependent manner. These data establish a proof-of-concept that ELF-MF exposure can affect patterning of histone modifications. This appears to be particularly notable in differentiating hematopoietic cells undergoing differentiation but less so in leukemic cells, suggesting that ELF-MF affect programming rather than stability of epigenetic marks. Functional relevance and implication for carcinogenesis remain to be determined.

In summary, despite different exposure conditions, consistent T-cell immuno-alterations were identified in both mice and rats. However, biological

consequences of observed reductions of CD8+ T-cells remain to be determined. Finally, no direct genotoxic effects were observed in young and adult CD-1 mice. Some possible mechanistic effects on signaling processes and epigenetic regulation were observed, but their functional relevance and role in carcinogenicity is unclear at present.

Taken together with the body of evidence from outside ARIMMORA, no mechanism was identified from mechanistic studies to confirm epidemiological findings for childhood leukemia. Hence, overall, mechanistic evidence for specific cellular responses to ELF-MF exposure from the literature and ARIMMORA experiments can be considered moderate while evidence for contribution to carcinogenesis remains weak.

Potential Risk at Population Level

A recent estimate of incidence of childhood leukemia attributable to ELF-MF in Europe showed proportions of 0.30% (95% confidence interval (CI), −0.12% to 1.12%) for a categorical threshold exposure model, 1.53% (CI, −0.41% to 4.03%) for a categorical non-threshold model, and 1.86% (CI, −0.27% to 18.61%) for a continuous non-threshold model when the exposure-response relationship between ELF-MF and childhood leukemia risk was assessed, suggesting that, under an assumption of causality, up to 2% of childhood leukemia may be caused by ELF-MF exposure, which would correspond to 10–61 cases annually in the European Union (27 states at that time) [Grellier et al., 2014]. With confirmation of exposure levels from ARIMMORA, this estimate appears to be the most accurate and finds support from the ARIMMORA group.

DISCUSSION

The outcome of hazard identification within the ARIMMORA risk assessment is that the relationship between exposure to the agent ELF-MF and risk of childhood leukemia is considered consistent with "IARC Group 2B" classification of possibly carcinogenic to humans (Fig. 1). This category is the result of limited evidence of carcinogenicity in humans and inadequate evidence of carcinogenicity in experimental animals. There was only weak supporting evidence from mechanistic studies.

While overall interpretation has not changed compared to previous assessments by IARC [2002]; the WHO [2007]; and the SCENIHR [2007, 2009, 2015]. Opinion statements, the ARIMMORA project still adds important knowledge on the possible carcinogenicity of exposure to ELF-MF. Most importantly, a transgenic mouse model for predisposed childhood leukemia has been successfully established and utilized. This is considered a major step forward. In future experiments, larger numbers of animals should be used with a range of exposure levels. Some possible mechanistic effects were observed, the functional relevance and role in carcinogenicity of which are unclear at present. Findings related to the immune system have potential to provide future insight if a role in development of childhood leukemia is identified. ARIMMORA confirmed that exposure levels at which increased risks of childhood leukemia were observed in epidemiological studies are very uncommon in Europe, and it may be estimated that, under an assumption of causality, up to 2% of childhood leukemia may be caused by ELF-MF exposure in Europe.

In conclusion, the ARIMMORA risk assessment considers evidence on ELF-MF and childhood leukemia as being consistent with the classification of possibly carcinogenic to humans (IARC Group 2B). The continuing existence of major scientific uncertainty since 2001 is a dissatisfactory situation in terms of public health and prevention [Maslanyj et al., 2010] as well as for science, given the large number of studies and the large bulk of additional scientific data collected over the last decades. It highlights, however, the challenge of establishing convincing evidence for a presumably weak association between a rare exposure and rare disease as causal. Nevertheless, some notable progress has recently been made, such as establishment of an animal model that mimics the commonest form of childhood leukemia and findings of ELF-MF effects on the immune system.

Therefore, research on this topic needs to continue. Should the association observed in epidemiological studies turn out to be spurious, we could gain general methodological insight into limits of such studies in detecting small risks related to rare exposures. Should the association be causal, we could gain more insight into physiological pathways leading to childhood leukemia with preventive potential extending beyond ELF-MF, as there is at present little known about the etiology of childhood leukemia.

ACKNOWLEDGMENTS

We would like to thank colleagues who participated in the ARIMMORA consortium (and their studies), but not in risk assessment: Achim Bahr, Elena Campos-Sanchez, Mark Douglas, Serena Fiocchi, Yijian Gong, Roman Halter, Einat Kapri-Pardes, Sven Kühn, Geertje Lewin, Ilaria Liorni, Marta Para-

zzini, Davnah Payne, Katja Pokovic, Stella Reamon-Büttner, Mohamad Sater, Katharina Sewald, Carolina Vincente-Dueñas, Martin Wild, and Christina Ziemann. Special thanks to Iris Szankowski from IT'IS Foundation for her skillful support of ARIMMORA as project manager.

This risk assessment was part of the ARIMMORA project and therefore performed by those conducting the ARIMMORA experiments, with support of some external advisors. The task was to put new results from the ARIMMORA project into the context of overall scientific evidence. It is thereby inherent in the setup that results were used where scientific publications are still under way. All those participating in risk assessment had access to those results but risk assessment therefore reflects assessments made by the authors that were unanimous.

This risk assessment reflects the position of the authors (not representing their institutions) and is not an official report by the IARC and was not part of the IARC Monographs program on the evaluation of carcinogenic risks to humans.

ARIMMORA is a collaborative project funded by the European Commission within the 7th Framework Program (282891). The ARIMMORA Risk Assessment is fully supported within the collaborative project (Work Package 9 and additional travel resources for individual project partners).

REFERENCES

Ahlbom A, Day N, Feychting M, Roman E, Skinner J, Dockerty J, Linet M, McBride M, Michaelis J, Tynes T, Verkasalo PK. 2000. A pooled analysis of magnetic fields and childhood leukaemia. Br J Cancer 83:692–698.

ARIMMORA. 2015. Risk assessment: Extremely low-frequency magnetic fields and the risk of childhood leukaemia. A report by the ARIMMORA consortium. Lyon, France: Advanced research on interaction mechanisms of electro-Magnetic exposures with organisms for risk assessment. Available at: http://arimmora-fp7.eu/ (Last accessed 31 Jan 2016).

Bunch KJ, Keegan TJ, Swanson J, Vincent TJ, Murphy MF. 2014. Residential distance at birth from overhead high-voltage powerlines: Childhood cancer risk in Britain 1962–2008. Br J Cancer 110:1402–1408.

Cogliano VJ, Baan R, Straif K, Grosse Y, Lauby-Secretan B, El Ghissassi F, Bouvard V, Benbrahim-Tallaa L, Guha N, Freeman C, Galichet L, Wild CP. 2011. Preventable exposures associated with human cancers. J Natl Cancer Inst 1827–1839.

Fiocchi S, Liorni I, Parazzini M, Ravazzani P. 2015. Assessment of the foetal exposure to the homogeneous magnetic field harmonic spectrum generated by electricity transmission and distribution networks. Int J Env Res Publ Health 12:3667–3690.

Grellier J, Ravazzani P, Cardis E. 2014. Potential health impacts of residential exposures to extremely low frequency magnetic fields in Europe. Environ Int 62:55–63.

IARC. 2002. Non-ionizing radiation, Part 1: Static and extremely low-frequency (ELF) electric and magnetic fields. IARC Monographs on the evaluation of carcinogenic risks to humans. Lyon, France: IARC Press.

IARC. 2015. IARC Monographs program. Lyon, France: International Agency for Research on Cancer. http://monographs.iarc.fr/ENG/Preamble/index.php (Last accessed 1 March 2016).

Kheifets L, Ahlbom A, Crespi CM, Draper G, Hagihara J, Lowenthal RM, Mezei G, Oksuzyan S, Schüz J, Swanson J, Tittarelli A, Vinceti M, Wunsch Filho V. 2010. Pooled analysis of recent studies on magnetic fields and childhood leukaemia. Br J Cancer 103:1128–1135.

Liorni I, Parazzini M, Fiocchi S, Douglas M, Capstick M, Gosselin MC, Kuster N, Ravazzani P. 2014. Dosimetric study of fetal exposure to uniform magnetic fields at 50 Hz. Bioelectromagnetics 35:580–597.

Martín-Lorenzo A, Hauer J, Vicente-Dueñas C, Auer F, González-Herrero I, García-Ramírez I, Ginzel S, Thiele R, Constantinescu SN, Bartenhagen C, Dugas M, Gombert M, Schäfer D, Blanco O, Mayado A, Orfao A, Alonso-López D, Rivas Jde L, Cobaleda C, García-Cenador MB, García-Criado FJ, Sánchez-García I, Borkhardt A. 2015. Infection exposure is a causal factor in B-cell precursor acute lymphoblastic leukemia as a result of Pax5-inherited susceptibility. Cancer Discov 5:1328–1343.

Maslanyj M, Lightfoot T, Schüz J, Sienkiewicz Z, McKinlay A. 2010. A precautionary public health protection strategy for the possible risk of childhood leukaemia from exposure to power frequency magnetic fields. BMC Public Health 10:673.

Morgan MA, Shilatifard A. 2015. Chromatin signatures of cancer. Genes Dev 29:238–249.

Santini MT, Rainaldi G, Indovina PL. 2009. Cellular effects of extremely low frequency (ELF) electromagnetic fields. Int J Radiat Biol 85:294–313.

Schmiedel S, Blettner M. 2010. The association between extremely low-frequency electromagnetic fields and childhood leukaemia in epidemiology: Enough is enough? Br J Cancer 103:931–932.

Scientific Committee on Emerging and Newly Identified Health Risks (SCENIHR). 2007. Possible effects of electromagnetic fields (EMF) on human health. Brussels, Belgium: European Commission.

Scientific Committee on Emerging and Newly Identified Health Risks (SCENIHR). 2009. Health effects of exposure to EMF. Brussels, Belgium: European Commission.

Scientific Committee on Emerging and Newly Identified Health Risks (SCENIHR). 2015. Potential health effects of exposure to electromagnetic fields (EMF). Luxembourg: European Commission.

Schüz J. 2011. Exposure to extremely low-frequency magnetic fields and the risk of childhood cancer: Update of the epidemiological evidence. Prog Biophys Mol Biol 107:339–342.

Struchen B, Liorni I, Parazzini M, Gaengler S, Ravazzani P, Röösli M. 2015. Analysis of children's personal and bedroom exposure to ELF-MF in Italy and Switzerland. J Expo Sci Environ Epidemiol; epub ahead of print December 2015.

WHO. 2007. Environmental health criteria 238. Extremely low frequency (ELF) fields. Geneva, Switzerland: World Health Organization.

Wiemels JL, Cazzaniga G, Daniotti M, Eden OB, Addison GM, Masera G, Saha V, Biondi A, Greaves MF. 1999. Prenatal origin of acute lymphoblastic leukaemia in children. Lancet 354:1499–1503.